Functional characterisation of Hfq and identification of Hfq-dependent sRNAs in *Pantoea ananatis*

By

Gi Yoon Shin

Submitted in partial fulfilment of the requirements for the degree

Philosophiae Doctor (Microbiology)

In the Faculty of Natural & Agricultural Sciences

University of Pretoria

Pretoria

2020, 10 February

SUPERVISORY COMMITTEE

Professor Teresa A. Coutinho Department of Biochemistry, Genetics and Microbiology

Forestry and Agricultural Biotechnology Institute (FABI)

Centre for Microbial Ecology and Genomis (CMEG)

University of Pretoria

Pretoria

0028

South Africa

Professor Lucy N. Moleleki Department of Biochemistry, Genetics and Microbiology

Forestry and Agricultural Biotechnology Institute (FABI)
University of Pretoria

Pretoria

0028

South Africa

Doctor Divine Y. Shyntum Department of Biochemistry, Genetics and Microbiology

Forestry and Agricultural Biotechnology Institute (FABI)
University of Pretoria

Pretoria

0028

South Africa

DECLARATION

I, the undersigned, hereby declare that the thesis submitted herewith for the degree Philosophiae Doctor to the University of Pretoria, contains my own independent work and has hitherto not been submitted by me for a degree at this or any other tertiary institution.

Gi Yoon Shin

10 February 2020

ACKNOWLEDGMENTS

"The Lord thy God in the midst of thee is mighty; He will save, He will rejoice over thee with joy; He will rest in His love, He will joy over thee with singing" (Zephaniah 3: 17)

I would like to express my deepest gratitude to my supervisor (a second mom) Professor Teresa Coutinho for her unceasing faith in me. Without your optimism, support and coffees, this work would not have been possible.

To my co-supervisors Professor Lucy Moleleki and Doctor Divine Shyntum, I am grateful for your valuable guidance and warm welcome to my abrupt visits for 'occasional' random chat.

A special thanks to Professor George Sundin for receiving me in his lab for the research visit. Michigan spring felt like winter but I stayed warm in your kind hospitality.

Acknowledgment would be incomplete without extending my sincere gratitude to my beloved family: Mom, Dad, Maeyong the cat, Gihea & Isaac and a new addition to the family, Juahn. Your unconditional love and encouragement kept me sane, I mean, happy.

I would like to send my love to my parents-in-law for their continuous support and prayers. Thank you very much for all you do for us.

Dearest Lee, my better-half. I am utterly indebted to you for your selflessness act of cooking on behalf of me despite it was my turn countless times. Thank you for never giving up on us. Can we have something other than noodles now?

To my sisters from other moms: Ilkadim, Ilkser and Vou. We cried and laughed together through our ups and downs. I am very fortunate to have you 'life-mentors' as pillars of strength in my life.

I owe big thanks to all my past and present lab-mates (Sundin Lab, FABI and CMEG) and students: Rosa, Zanele and Charmaine. You made me feel extremely special when you came to ask me for my autoclaved 1.5 ml tubes (and advice). Thank you for doing the night-shift in the lab with me and scaring me at the other end of the dark corridor (Max).

PREFACE

Pantoea ananatis is a bacterium that is widely spread in varied ecological niches, exhibiting an array of lifestyles as a beneficial, commensal or pathogenic bacterium in association with both weed and crop plants. The success of *P. ananatis* as a ubiquitous plant pathogen could be attributed to its rapid adaptive response to changing environments. The post-transcriptional regulatory roles of *trans*-encoded small RNAs (sRNAs) and their chaperone protein Hfq (host factor need for replication of bacteriophage Qβ) in modulating global cellular functions of bacteria have been a key in deciphering bacteria's adaptive response to their surrounding. Therefore, the research presented in this thesis aims to identify *trans*-encoded sRNAs that are dependent on Hfq and to characterize the functional roles of Hfq in acylated homoserine lactone production, biofilm formation, motility and pathogenicity of *P. ananatis*.

Chapter 1 is an introductory chapter that introduces sRNA and Hfq and their molecular interaction leading to different modes of target (mRNA) regulation. Furthermore, based on the available literature, the current understanding of sRNA/Hfq-mediated regulation of bacterial physiologies such as stress responses, respiration, motility, quorum-sensing and virulence will be discussed in detail with a special focus on the Gram-negative bacterial pathogens. The chapter ends off with a brief overview of the virulence factors of phytopathogen *P. ananatis* and the importance of coordinate expression of these factors in the fitness of this bacterium.

Chapter 2 is the research chapter of the thesis and presents the effect of *hfq* deletion mutation on the virulence factors of *P. ananantis* LMG 2665^{T}. Moreover, a list of Hfq-dependent sRNA candidates found in *P. ananatis* was identified using a differential sRNA expression analysis based on the data generated from stranded-sRNA deep sequencing. Expression and nucleotide sequences of a subset of Hfq-dependent sRNAs were further experimentally validated. The findings of this chapter have been published: Shin, G.Y., Schachterle, J.K., Shyntum, D.Y., Moleleki, L.N., Coutinho, T.A. and Sundin, G.W. (2019) Functional Characterization of a Global Virulence Regulator Hfq and Identification of Hfq-Dependent sRNAs in the Plant Pathogen *Pantoea ananatis*. *Front. Microbiol,* 10:2075. (doi: 10.3389/fmicb.2019.02075).

Chapter 3 summarizes the findings of this study, highlighting the significance of Hfq as a global virulence regulator of *P. ananatis*. Future works and perspectives with respect to current research findings are suggested in this chapter.

TABLE OF CONTENTS

LIST OF TABLES

LIST OF FIGURES

SUPPORTING INFORMATION

LIST OF SUPPLEMENTARY TABLES

LIST OF SUPPLEMENTARY FIGURES

LIST OF ABBREVIATIONS

AHL Acylated homoserine lactone

AMP Adenosine monophosphate

ANOVA Analysis of variance

ATP Adenosine triphosphate

bp Basepairs

c-di-GMP Cyclic dimeric guanosine monophosphate

cDNA Complementary DNA

CFU Colony forming unit

CLASH Cross-linking, ligation and sequencing of the hybrids

CLIP-seq Cross-linking immunoprecipitation sequencing

Cm Chloroamphenicol

CRP Cylic AMP receptor protein

C-terminus Carboxyl-terminus

DNA Deoxyribonucleic acid

dpi Days post inoculation

EPS Exopolysaccharide

ESR Envelope stress response

Fe Iron

Fe-S Iron-Sulphur

Fur Ferric uptake regulator

GC Guanine-Cytosine

Gm Gentamicin

Grad-seq Gradient-based sequencing

GRIL-seq Global small non-coding RNA target identification by ligation and sequencing

GSP Gene specific PCR

H_2O_2 Hydrogen peroxide

Hfq Host factor need for replication of bacteriophage Qβ RNA binding protein

HGT Horizontal gene transfer

HK Histidine kinase

IGR Intergenic region

IM inner membrane

Kan Kanamycin

kb Kilo-basepairs

kDa Kilodalton

LB Luria-Bertani

LPP Lipoprotein

LPS Lipopolysaccharides

MAP-seq Multiplexed analysis of projections by sequencing

miRNA MicroRNA

MMR Mismatch repair

mRNA Messenger RNA

nt Nucleotides

OD Optical density

OM Outer membrane

OMP Outer membrane protein

ORF Open reading frame

OVR Onion virulence region

PAPI Poly(A) polymerase I

PBS Phosphate buffered saline

PCR Polymerase chain reaction

PCWDE Plant cell wall degrading enzyme

PG Peptidoglycan

PNPase 3'-5' exoribonulease polynucleotide phosphorylase

qRT-PCR Quantitative real time PCR

QS Quorum sensing

RACE Rapid amplification of cDNA ends

RBP RNA binding protein

RBS Ribosome binding site

RIL-seq RNA interaction by ligation and sequencing

RIP-seq RNA immunoprecipitation sequencing

RIT Rho-independent terminator

RNA Ribonucleic acid

RNase E Endoribonuclease E

RNA-seq RNA-sequencing

ROS Reactive oxygen species

RppH RNA 5' pyrophosphohydrolase

RR Response regulator

rut Rho-utilization site

SAM Sequence alignment map

SD Shine-Dalgarno

SE Standard error

Sm Streptomycin

SOD Superoxide dismutase

SPI-1 *Salmonella* pathogenicity island 1

SPI-2 *Salmonella* pathogenicity island 2

sRNA Small RNA

T2SS Type 2 secretion system

T3SS Type 3 secretion system

T6SS Type 6 secretion system

TCA Tricarboxylic cycle

TCS Two-component signal transduction system

TF Transcriptional factor

UA-rich Uridine-Adenine rich

U-rich Uridine-rich

UTR Untranslated region

w/v Weight/Volume

WT Wild-type

Xcv *Xanthomonas campestris* pathovar *vesicatoria*

Xoo *Xanthomonas oryzae* pathovar *oryzae*

σ^{38} RpoS

σ^{54} RpoN

σ^{70} RpoD

σ^{E} RpoE

σ^{F} FliA

CHAPTER ONE

1. INTRODUCTION

Bacteria inhabit a wide range of ecological niches and survive harsh environments that constantly change. To survive, bacteria rely on rapidly regulated gene expression that results in adequate phenotypes in response to environmental cues. Conventionally, gene expression regulation has been mostly attributed to transcriptional modulation of genes exercised by transcriptional factors. However, with the advent of whole genome and ribonucleic acid (RNA) sequencing technology, the regulatory roles of RNA molecules in gene regulation have been noted and are presently widely recognised.

The RNA regulators consist of a group of heterogeneous, small RNA molecules that have different structures and mechanisms of action. They are largely divided into two classes, namely, *cis* and *trans* depending on how close their encoding positions are with respect to their target transcripts. RNA thermometers and riboswitches represent *cis*-acting RNA structural elements and are present in the 5' untranslated region (UTR) of the messenger RNA (mRNA). In both cases, conformational alterations caused by temperature fluctuations or binding of small molecules, respectively, lead to the regulation of downstream gene expression (Mandal and Breaker, 2004; Henkin, 2008).

Antisense RNAs constitute a substantial proportion of *cis*-acting RNAs and are transcribed from the opposite strand of the target gene, thus *cis*-encoded (Sharma *et al*., 2010). Due to the extensive sequence complementarity shared between antisense RNA and the target transcript, base-pairing between the two RNA molecules readily takes place, leading to a translation regulation of the bound transcript. Previously, it was thought that antisense RNAs were only expressed from mobile elements such as phage, plasmids, and transposons for the regulation of their copy numbers (Brantl, 2007), but chromosomally encoded antisense RNAs are more common than initially thought (Georg and Hess, 2011). In fact, antisense RNAs modulate their target genes at both transcriptional and translational levels, serving as repressors of genes associated with toxin synthesis (Fozo *et a*l., 2010).

The *trans*-encoded small RNAs (sRNA) represent the largest group of RNA regulators that are associated with post-transcriptional regulation in both the Gram-negative and positive bacteria. As they are encoded at a distant location from their target mRNAs, base-pairing between the two RNAs is partial and requires the concerted action of RNA chaperone proteins such as Hfq for stability, interaction and regulation thereof. The *trans*-encoded sRNA mediated Hfq

regulation is extensive and comprised of interconnected networks that modulate bacterial growth, metabolism, motility, stress response, quorum sensing, and virulence (Majdalani *et al*., 2005; De Lay and Gottesman, 2012; Papenfort and Vogel, 2014; Holmqvist and Wagner, 2017; Papenfort and Bassler, 2016)

In the present review, the molecular mechanisms and the roles of Hfq and Hfq-dependent sRNAs in the regulation of stress response and virulence in Gram-negative bacteria will be discussed.

1.1 Trans-encoded small regulatory RNAs

1.1.1 Where are they found?

Trans-encoded sRNAs are, typically, ~ 50 to 500 nucleotides (nt) long non-coding single-stranded RNAs (Figure 1.1) that are functionally analogous to microRNAs (miRNAs) of eukaryotes, (Aiba, 2007). Bacterial *trans*-encoded sRNAs share a set of features that are useful for their identification. Such features are an environmentally-sensitive promoter, a Rho-independent terminator, an unstructured seed/mRNA base-pairing and structured (loop) double-stranded regions (Updegrove *et al*., 2015). However, the nucleotide sequences of *trans*-encoded sRNAs are rather poorly conserved at both the inter- and intra-species levels, (Hoeppner *et al*., 2012) and this lack of sequence conservation and fast evolution (Gottesman and Storz, 2011) pose a challenge in determining the origins of sRNA. Currently, the origins of most sRNAs are unknown but there is evidence that they originated via horizontal gene transfer (HGT) (Ochman *et al*., 2000), duplication events (Zhang, 2003) and, *de novo* emergence (Schlötterer, 2015).

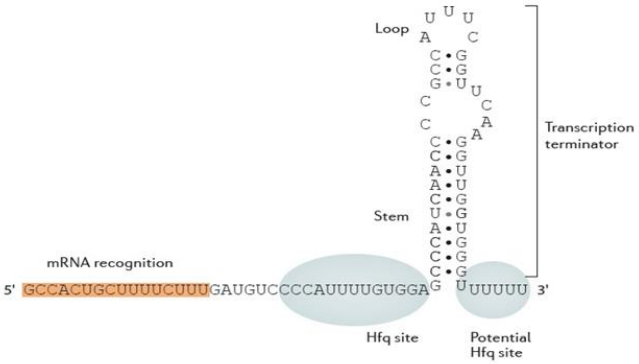

Figure 1.1 A typical structure of trans-encoded sRNA comprised of mRNA recognition (seed) region, Hfq binding site followed by a hairpin and poly-uridine tail (Vogel and Luisi, 2011).

In bacteria, *trans*-encoded sRNAs are transcribed from the intergenic regions (IGRs) of a chromosome as free-standing transcripts (Argaman *et al*., 2001). However, recent studies showed that trans-encoded sRNAs are not only limited to IGRs but are also derived from the 3' UTR of parent mRNA. For example, the sRNA, CpxQ, is synthesized from the 3' processing of the *cpxP* mRNA, whose product (a protein) is involved in an inner membrane stress response (Miyakoshi *et al*., 2015). This means that *cpxQ* shares a promoter with *cpxP* and its transcription is dependent on the transcription of its parental mRNA *cpxP*. Once, 58-nt long CpxQ is cleaved from *cpxP* by endoribonuclease E (RNase E) thereafter downregulates the expression of other mRNAs whose products alleviate the inner membrane stress. In this way, inner membrane homeostasis is achieved by the cooperative action of CpxQ and CpxP.

Similarly, a *Salmonella enterica typhimurium* specific sRNA, DapZ, is derived from the 3' UTR of *dapB* mRNA but, in this case, DapZ shares a transcription terminator with *dapB*, not a promoter (Chao *et al*., 2012). Another 3' UTR associated sRNA MicL's promoter was found embedded in the coding region of an adjacent gene *cutC* (Guo *et al*., 2014). The primary transcript of MicL is 308-nt long and is further processed to an 80-nt form that targets *lpp*, an outer membrane lipoprotein encoding mRNA. Although the promoter of sRNA is found within the open reading frame (ORF) of *cutC* gene, the transcription of *micL* is co-regulated with *lpp* by the transcription factor σ^E (RpoE), rather than with *cutC*. This is becuase sRNA MicL and Lpp, together form a σ^E–dependent regulatory loop that maintains the outer membrane homeostasis (expanded in the section 1.4.1 Envelope stress response).

1.1.2 Coding or Non-coding?

A majority of small regulatory RNAs, known to date, lack ORF and are therefore non-coding. Only a few sRNAs are an exception to this definition and execute "dual function" as a base-pairing regulatory RNA and a peptide encoding transcript. According to Gimpel and Brantl (2017), there are approximately ten dual-functioning sRNAs found across Gram-negative and positive bacteria but only half have known functions for the peptide they encode. The five dual-function sRNAs include SgrS from *Escherichia coli* (Vanderpool and Gottesman, 2004), *Staphylococcus aureus* Psm-mec and RNAIII (Morfeldt *et al*., 1995; Kaito *et al*., 2011), Pel RNA of *Streptococcus pyogenes* (Mangold *et al*., 2004) and SR1 from *Bacillus subtilis* (Gimpel *et al*., 2010). Their regulatory mechanisms of dual-function sRNAs are reviewed in-depth by Gimpel and Brantl (2017). In most cases, both the sRNA and its peptide function in the same

pathway, resulting in the cooperative regulation of physiological processes such as metabolism and virulence in bacteria.

Recently, the non-coding nature of sRNAs has been questioned as most methods used for computational prediction of ORFs are not optimized for short genes like sRNAs. Friedman *et al*. (2017) devised a new computational method called 'discovery of sRNA coding ORFs in bacteria (DiSCO-Bac)' that incorporates sRNA sequence features (GC content and Shine-Dalgarno-sequence motifs frequency and strength) and comparative genomics (multiple genomes of phylogenetically closely related species) to comprehensively identify coding sequences of sRNA. Using DiSCO-Bac, Friedman and colleagues found that at least 10 % of the annotated sRNAs from numerous bacterial species were predicted to possess an ORF. This finding was further confirmed by ribosome profiling and mass spectrometry which validated the translation of sRNAs that were predicted to have ORFs by DiSCO-Bac. It is possible that dual-functioning sRNAs are more common than anticipated, as it is the case in eukaryotes (Bardou *et al*., 2011).

1.2 RNA binding protein Hfq

1.2.1 Discovery

Although extensive sRNA-Hfq mediated post-transcriptional gene regulation has become evident in the past two decades, the discovery of Hfq dates back to 1968. Because of Hfq's affinity for single-stranded RNA molecules, it was initially identified as an *E. coli* host factor required for the replication of bacteriophage Qβ (Franze de Fernandez *et al*., 1968, 1972). Only in the 1990s, was the role of Hfq in the physiology of bacteria demonstrated by the pleiotropic phenotypes displayed by an *hfq*-null *E. coli* mutant (Tsui *et al*., 1994). Presently, Hfq is recognised as a key component of the sRNA-mediated post-transcriptional regulation by providing sRNAs with structural stability and mediating short and imperfect base-pairing between the sRNA and mRNA (Vogel and Luisi, 2011).

1.2.2 Structure of Hfq

Hfq is a hexameric protein in which the monomers are arranged in a ring-like structure. The size of the monomer ranges between 8 to 11 kilodalton (kDa) across bacterial species but contains two phylogenetically conserved Sm motifs in the N-terminal region of the peptide

namely; Sm1 and Sm2. These motifs mediate the folding of Hfq monomers in an Sm-like (LSm) protein fashion (Møller *et al*., 2002; Zhang *et al*., 2002). This multimeric, quaternary protein that resembles a 'doughnut' is characteristic of the proteins belonging to the Sm-LSm family that is found, not only in bacteria but also, in archaea and eukaryotes (Mura *et al*., 2003). The eukaryotic counterpart of Hfq, Sm-LSm proteins are RNA binders of ribosomal RNAs and are involved in mRNA splicing as a component of the spliceosome (Kambach *et al*., 1999; Wilusz and Wilusz, 2013).

There are four RNA binding surfaces present on Hfq: the proximal and distal faces, the lateral rim, and, the C-terminal tail (Figure 1.2). The proximal face has a strong affinity for uridine-rich (U-rich) sequences thus binds the 3' poly-uridine tail of sRNA at its Rho-independent terminator (Otaka *et al*., 2011; Sauer and Weichenrieder, 2011). As mentioned above, this is the typical feature of Hfq-dependent trans-encoded sRNAs that allows voluntary binding of sRNAs to Hfq. In contrast, the distal face preferentially binds adenine-rich (AAN)n motifs, in which A is adenine and N means any nucleotide, that is found in the 5' UTR of sRNA-targeted mRNAs (Mikulecky *et al*., 2004; Link *et al*., 2009). In this way, multiple sRNAs and mRNAs are bound on a single Hfq protein and are brought into proximity for interaction and regulation. Between the two faces, the proximal face is suggested to be an ancient domain as its specificity for U-rich sequences at the 3' of sRNA is conserved across bacterial species as well as in archaea (Sauer and Weichenrieder, 2011). However, the distal face of archaeal Hfq no longer recognizes the adenine rich sequences, therefore, the affinity for adenine rich sequence could be an exclusive feature of bacterial Hfq (Nikulin *et al*., 2017). The rim of Hfq is an additional UA-rich sequence binding surface that stabilizes sRNA and promotes annealing between the sRNA and mRNA pair (Sauer *et al*., 2012; Panja *et al*., 2013). The presence of arginine patches on the rim is crucial for the chaperone activity of Hfq as a mutation in these patches resulted in disrupted nucleation of sRNA-mRNA in *E. coli* (Panja *et al*., 2013).

While the proximal, distal and rim contact surfaces constitute a stable domain of Hfq, C-termini of the hexamer are disordered and form protruding tails out of the protein rim (Vecerek *et al*., 2008). Due to this flexible architecture, C-terminal tails interact with RNAs either by stabilizing or occluding RNAs' binding to Hfq. The contribution of these tails in riboregulation has been controversial (Vecerek *et al*., 2008; Olsen *et al*., 2010) but recent studies showed that these tails might help to displace the bound transcript (Santiago-Frangos *et al*., 2016) thereby promoting active and rapid cycling of RNAs on Hfq (Fender *et al*., 2010; Santiago-Frangos and Woodson, 2018). Santiago-Frangos *et al*. (2017) further demonstrated that these C-

terminal tails may bring about Hfq's auto-regulation of RNAs by transiently regulating access to active sites of the protein.

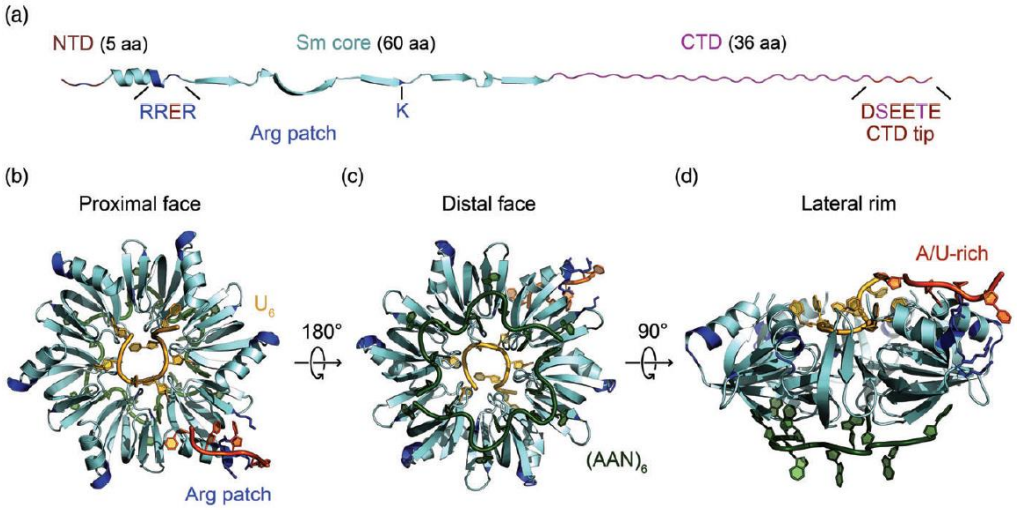

Figure 1.2 Structure of Hfq. (a) A secondary structure of Hfq monomer of *E. coli*. A tertiary structure of Hfq showing RNA binding surfaces: (b) proximal face, (c) distal face and (d) lateral rim (Santiago-Frangos and Woodson, 2018).

1.2.3 Hfq-sRNA interaction

The sRNAs are grouped into two classes based on their mechanisms of binding to Hfq (Schu *et al*., 2015). The Class I sRNA, using its U-rich Rho-independent terminator, attaches to the proximal pocket of Hfq and also interacts with the protein rim by means of its single-stranded UA-rich region of the sRNA. This leaves the distal pocket available for binding of mRNAs, particularly, those that possess (AAN)n motifs. The base-pairing between Class I sRNA and their cognate mRNAs is then catalyzed by the active sites of Hfq (Figure 1.3 right top panel), leading to regulation (degradation) of the transcript. The second class of sRNA (Class II) occupies the proximal and the distal faces of Hfq through the utilization of its U-rich tail and A-rich motifs. The corresponding mRNAs wrap Hfq around the rim and are annealed to Class II sRNAs by Hfq (Figure 1.3 right bottom panel). The resulting regulation is less likely to involve degradation of the duplex formed (Schu *et al*., 2015).

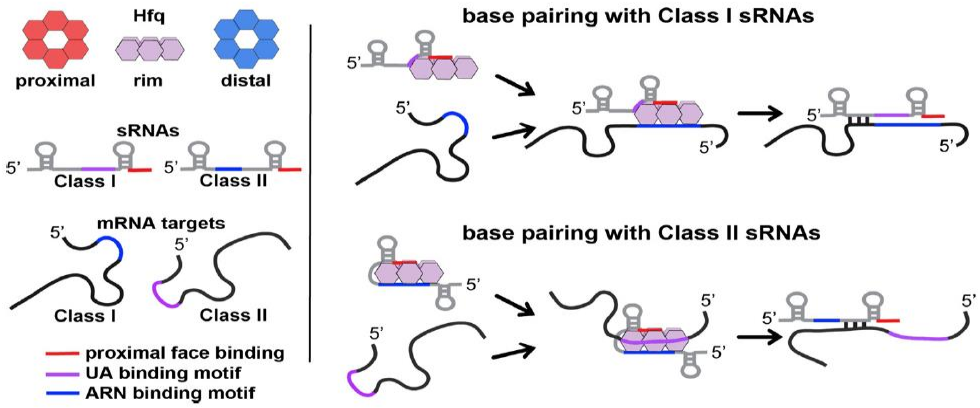

Figure 1.3 Hfq binding modes of Class I and II sRNAs. (Left) Motifs present on small and messenger RNAs: Rho-independent terminator (red), UA motif (purple) and ARN motif (blue). (Right) Hfq binding models of Class I and II sRNAs (Schu *et al*., 2015).

1.2.4 sRNA cycling on Hfq

Multiple RNA contact surfaces of Hfq accommodate the binding of RNAs that are of vastly different sequences and structures. In fact, Hfq simultaneously interacts with a great number of sRNAs as well as more than thousands of mRNAs at a time (Sittka *et al*., 2008). There are three major benefits for regulatory sRNAs to be associated with Hfq. Firstly, sRNAs are stabilized by Hfq and are less prone to endoribonuclease E (RNase E) degradation as Hfq and RNase E share the same binding site (AU-rich sequences) on the sRNA. Once bound to Hfq, the 3' terminal of sRNA becomes inaccessible for RNase E degradation (Chao *et al*., 2012). Secondly, sRNAs are brought into proximity with mRNAs, increasing their chances of finding cognate transcripts. Lastly, Hfq aids in the restructuring of sRNAs and mRNAs that are bound to it (Updegrove and Wartell, 2011; Bordeau and Felden, 2014), exposing the seed and the target regions to one another for annealing, thus the RNA helix formation.

In *E. coli*, the number of Hfq hexamers is estimated to range from 1500 to 10 000 during the course of its growth (Moon and Gottesman, 2011) and they are normally surrounded by a large pool of RNAs including sRNAs, mRNAs as well as other free RNA substrates. The levels of RNA transcripts are in excess compared to that of Hfq which ensures their saturation on the hexamer that is further intensified by the four different binding surfaces available on Hfq. This competition of sRNAs on Hfq ensures the active cycling of sRNAs, (Figure 1.4) where free sRNAs continuously displace the ones that are already bound to the protein (Wagner, 2013).

In this way, a slow Hfq-RNA dissociation rate is overcome and the regulatory or cognate ternary complex is rapidly found and formed (Fender *et al*., 2010; Hussein and Lim, 2011).

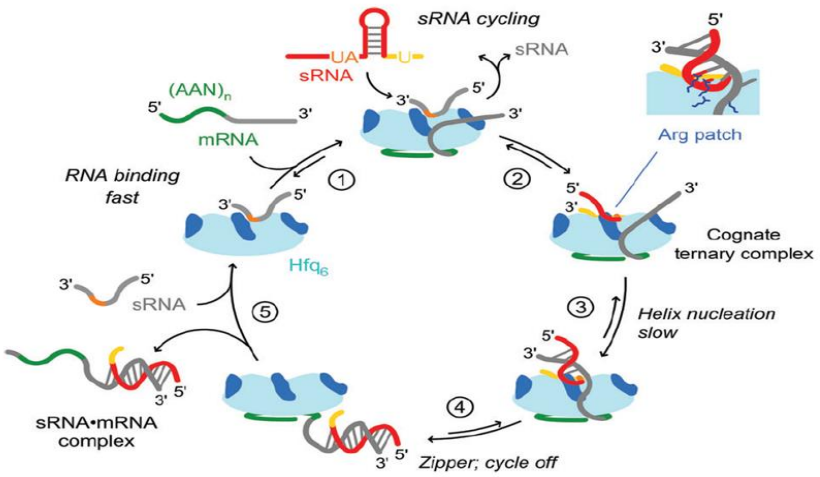

Figure 1.4 sRNA cycling on Hfq. (1) sRNA (red) and mRNA (green/gray) simultaneously bind Hfq, leading to (2) formation of the cognate ternary complex (sRNA-mRNA-Hfq). (3) Annealing of sRNA and mRNA is facilitated by arginine patch of Hfq. (4) RNA duplex is release or further regulated by RNaseE. (5) Recruitment of new small- and mRNAs, continuing RNA cycling (Santiago-Frangos and Woodson, 2018).

1.3 Mechanisms of regulation

The formation of cognate Hfq-RNA complex modulates the expression of a bound mRNA by affecting its translation efficiency (Kavita *et al*., 2018). The increase or decrease in translation efficiency is achieved by altering accessibility to ribosome binding site (RBS) (Waters and Storz, 2009; Battesti *et al*., 2011), or by recruiting or interacting with other proteins that affect the stability of the RNAs (De Lay *et al*., 2013). The outcomes of the Hfq-sRNA regulation benefit the host cell greatly by reducing the energy and resource loss caused by unnecessary translation of the mRNAs as well as rapidly increasing the production of metabolites or proteins that are required by the bacterial cell to withstand a stressful environment (Fröhlich and Vogel, 2009).

1.3.1 Translational activation

For translation of mRNA to occur, the 30S ribosomal subunit needs to bind mRNA at a patch of sequence called Shine-Dalgarno (SD) contained in the RBS and assemble into a 70S ribosome. Once assembled, the ribosome occupies SD and up to 20 nt SD flanking sequences that are collectively recognized as the ribosome binding or interacting site. However, an intrinsic secondary inhibitory structure may occur in this region, masking the RBS from the ribosome for translation inhibition. The melting of this structure occurs when the Hfq-facilitated base-pairing between the mRNA and sRNA takes place in proximity to the SD sequence or RBS. The remodelling of the secondary structure uncovers RBS of the mRNA to a ribosome to initiate the translation (Prévost *et al*., 2007; Urban and Vogel, 2007). Although less known, there are a number of sRNAs such as ArcZ, DsrA and RprA that positively regulate the translation of their target mRNA this way and such target include *rpoS*, a stationary phase sigma factor (Battesti *et al*., 2011).

1.3.2 Translational repression

The seed region or mRNA recognition site of a sRNA primarily sequesters RBS of mRNA. The pairing between the two RNA strands is discontinuously formed across approximately 10 to 25 bp. With the help of Hfq, sRNA is able to target multiple mRNAs with limited complementarity and this annealing to RBS blocks the binding of the ribosome, thereby repressing the translation of mRNA (Waters and Storz, 2009). However, repression of translation can still be achieved by a sRNA pairing with mRNA region that is more than 50 nt upstream of the RBS (Sharma *et al*., 2007) or near the start codon of the transcript (Bouvier *et al*., 2008). Moreover, a sRNA, MicC has been found to base-pair with *omp*D mRNA (encoding the outer membrane porin protein) within the open reading frame (ORF) to repress the translation of the transcript (Pfeiffer *et al*., 2009). The ribosome-free mRNAs then become prone to decay by enzymes that are already present in the cytoplasm or recruited by the Hfq.

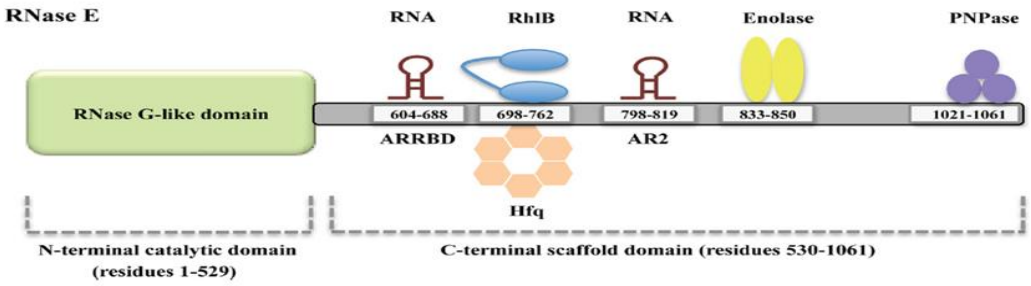

Figure 1.5 RNA degradosome model in *E. coli*. N-terminus is a ribonucleolytic domain and C-terminus provides binding sites for auxiliary proteins involved in mRNA decay (De Lay *et al*., 2013).

Not only Hfq does facilitate sRNA-mRNA helix formation but it also serves as a platform for recruitment and interaction of other proteins that affect the stability of the RNA molecules. Co-immunoprecipitation studies of Hfq revealed a number of proteins that may act on Hfq bound RNAs. They are poly-(A) polymerase I (PAPI) and 3'–5' exoribonuclease polynucleotide phosphorylase (PNPase) that destabilize the RNAs (Mohanty *et al*., 2004) and contributes to sRNA activity and turnover (De Lay and Gottesman, 2011). In fact, the formation of a multiprotein complex 'degradosome' (Figure 1.5) initiates mRNA decay and/or sRNA-mRNA coupled degradation (De Lay *et al*., 2013). Several auxiliary proteins such as PNPase, ATP-dependent RNA helicase RhlB and glycolytic enolase adhere to the C-terminal domain of the RNase E, performing additional functions besides the N-terminal endoribonucleolytic domain of the RNase E (Morita *et al*., 2005; Ikeda *et al*., 2011). The degradosome thus degrades structured and single-stranded small and messenger RNAs (Massé *et al*., 2003; Carpousis *et al*, 2009).

1.3.3 Regulation of transcription termination

Post-transcriptional modulation of gene expression can be further achieved by regulating transcription elongation. In bacteria, transcription elongation is terminated in either a factor-dependent or independent (intrinsic) manner. This factor refers to the RNA binding helicase, Rho that binds newly forming mRNA at the Rho utilization site (*rut*). Then Rho moves towards the 3' end of the RNA molecule and displaces RNA polymerase from the DNA template, thus terminating the transcription (Santangelo and Artsimovitch, 2011). Meanwhile, a factor-independent transcription termination relies on the intrinsic terminator sequences and the formation of secondary structures resulting from the sequence.

The sRNA-Hfq interaction with cognate mRNAs has been found to influence transcriptional termination of associated mRNAs. For example, the loading of *S. typhimurium* sRNA ChiX and Hfq complex onto the RBS of the *chiPQ* mRNA was found to reinforce the Rho-dependent transcription termination of the *chiPQ* operon (Bossi *et al*., 2012). The reinforcement was brought about the formation of ChiX and Hfq complex on RBS of *chiPO* mRNA which reveals the *rut* sites of transcript thereby, allowing Rho to access the transcript and terminate the transcription elongation. In contrast, *E. coli* sRNAs ArcZ, DsrA and RprA positively regulate the transcription of *rpoS* by masking the *rut* sites to Rho to inhibit Rho-dependent transcriptional termination (Battesti *et al*., 2011; Sedlyarova *et al*., 2016).

1.3.4 Regulation of sRNA by sRNA decoy and sponge

Abundance or availability of sRNAs is important for regulation as it directly affects the levels of mRNAs that are being regulated. A study by Schu *et al*. (2015) showed that the mode of sRNA binding to Hfq directs the fate of sRNAs as not all sRNAs would decay after pairing with mRNA but can get reused. However, reusable sRNAs would then need to be actively degraded when their regulation is no longer needed. For the sRNA ChiX, a 'decoy' or non-target RNA resulting from the intercistronic region of *chb* operon (encoding for enzymes needed for chitooligosaccharide metabolism) is induced to pair and destabilize ChiX, (Figueroa-Bossi *et al*., 2009).

Similarly, sRNA sponges (endogenous sRNA competitors) pair and inactivate sRNAs, (Bossi and Figueroa-Bossi, 2016). These sponges are RNA fragments originating from different RNA sources such as bacteriophage elements, mRNAs (Overgaard *et al*., 2009), and tRNA precursors and they sequester sRNAs to abolish their regulatory functions. For example, a previously thought non-functional tRNA precursor fragment 3' ETS^{leuZ} (3' external transcribed spacer of glyWcysTleuZ polycistronic tRNA precursor) acts as a sponge for RyhB, a sRNA induced when iron is scarce (Lalaouna *et al*., 2015). An amino acid metabolism regulator sRNA GcvB has two sponges namely, bacteriophage-derived AgvB and *gltIJKL*-derived SroC (Tree *et al*., 2014; Miyakoshi *et al*., 2015).

1.4 Hfq-sRNA regulation of physiological processes

1.4.1 Envelope stress response

The cellular content of the Gram-negative bacteria is enclosed by two concentric membranes, namely, the inner- and outer membrane. The former consists of a symmetrical phospholipid bilayer that separates cytoplasm from periplasm whereas the latter composes of an asymmetrical bilayer of phospholipids and surface-exposed lipopolysaccharides (LPS) (Nikaido and Nakae, 1980; Beveridge, 1999). In both membranes, integrated proteins play an important role in transporting molecules into and out of the cell as well as in perceiving and transducing of the environmental signals. The integrity of these cell envelope structure and composition is tightly regulated (Grabowics and Silhavy, 2017). Upon perturbation, the envelope stress response (ESR) is triggered and is co-ordinated by the transcriptional sigma factor RpoE (σ^E), two-component signal transduction systems (TCS) like Cpx, EnvZ/OmpR, and Rcs in conjunction with sRNAs to alleviate the membrane stress (Fröhlich and Gottesman, 2018).

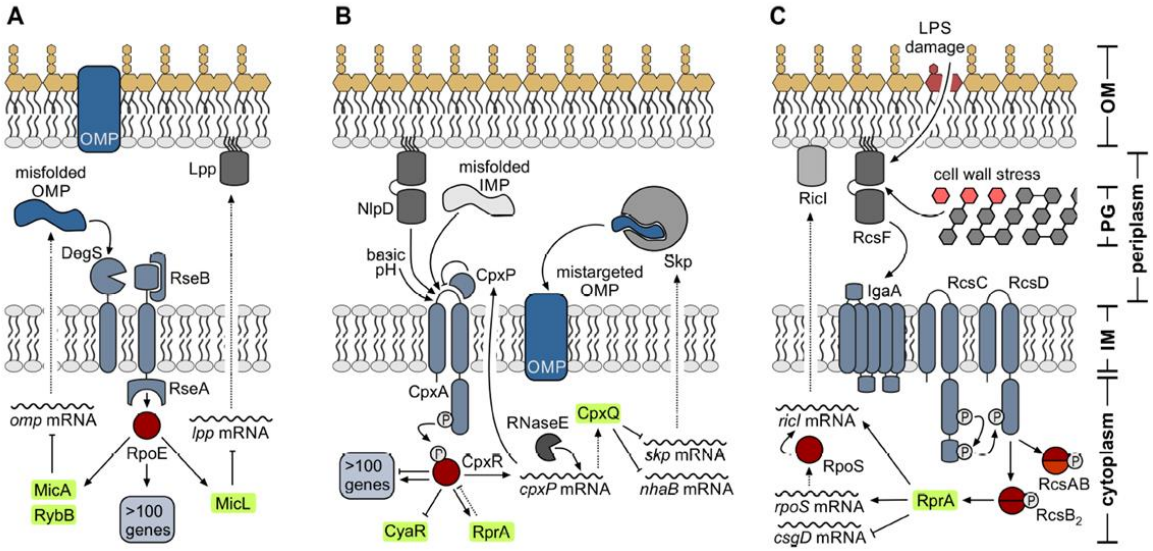

Figure 1.6 sRNAs involved in envelope stress response pathways. (A) RpoE-mediated outer membrane homeostasis. Maintenance of (B) inner membrane by Cpx TCS and (C) lipopolysaccharides by Rcs TCS (Fröhlich and Gottesman, 2018).

In the absence of membrane stress, σ^E is maintained in a sequestered state by the anti-sigma factor, RseA. The release of σ^E is initiated by the protease DegS that recognizes misfolded outer membrane proteins (OMPs) or mislocalized LPS (Lima *et al*., 2013). This recognition

sets off a protease cascade, leading to the degradation of RseA, (Figure 1.6A) (Chaba *et al*., 2011). The free σ^E then activates expression of approximately 100 genes under its regulon that are typically required for the synthesis, assembly and transport of the OMPs and LPS to the outer membrane (OM) (Rhodius *et al*., 2006; Skovierova *et al*., 2006). However, overexpression of these genes from the σ^E burst is undesired as it increases the chances of generating misfolded OMPs. Thus, Hfq-dependent sRNAs RybB and MicA serve as the repressive arm of σ^E–mediated ESR, providing immediate relief of this overexpression by degrading transcripts encoding for OMPs, lipoproteins (LPPs) and OM transporters, (Gogol *et al*., 2011). An additional sRNA, MicL also represses the translation of *lpp* mRNA in order to salvage phospholipid precursors and prevent Lpp build-up toxicity. This sRNA also negatively regulates the *rpoE* mRNA, providing negative feedback control of σ^E (Guo *et al*., 2014).

Besides RpoE, the maintenance of OM is also complemented by another regulatory pathway such as EnvZ/OmpR TCS, (Figure not shown). This TCS controls the expression of major OMPs upon activation by acidic pH, increased temperature and osmolarity, (Pratt *et al*., 1996). The activated or phosphorylated sensor histidine kinase (HK) EnvZ transfers its phosphoryl-group to the cognate response regulator (RR) OmpR that conversely regulates the expression of OmpC and OmpF outer membrane proteins (Guillier and Gottesman, 2006). This opposite regulation is brought about by OmpR-P differentially regulating the expression of two sRNAs, namely, MicF and MicC. As a transcriptional factor, OmpR activates the expression of MicF while repressing the MicC expression. The targets of the two sRNAs are *ompF* and *ompC* mRNAs, respectively, where, in both cases, the targets are negatively regulated by the sRNAs (Chen *et al*., 2004; Vogt *et al*., 2014). The expression of two additional sRNAs, OmrA and OmrB, is under positive control of OmpR. These sRNAs, together with OmpR, reinforce the repression of TonB-dependent receptors, OM protease OmpT and transcriptional factor of curli fimbriae *csgD* as well as *envZ* and *ompR* mRNAs for autoregulation (Guillier and Gottesman, 2006; Holmqvist *et al*., 2010; Brosse *et al*., 2016).

The integrity of the inner membrane (IM) is maintained by a CpxA-CpxR TCS, (Figure 1.6B). For example, protein defects in the periplasm and peptidoglycan (PG), stress factors such as hyperosmolarity and high pH trigger autophosphorylation of the IM-embedded HK CpxA, (Raivio *et al*., 1999). The CpxA phospho-transfer to CpxR, the RR, activates the transcription of the genes belonging to the Cpx regulon. However, in the absence of a stress signal, phosphoryl-group of CpxR is actively removed by the phosphatase CpxA, leading to the inactivation of the RR (Raivio and Silhavy, 1997). Unlike the σ^E, CpxR can serve both as an

activator or repressor of the genes under its transcriptional control. The products of the up-regulated genes are periplasmic protein chaperones and proteases that help to correct protein defects and maintain homeostatic IM composition. The transcription of *cpxP* is also highly fostered by the Cpx response. The resulting protein, CpxP, assists in the degradation of misfolded proteins in periplasmic space by guiding them to the protease DegP. Furthermore, it provides negative feedback control of Cpx response by directly masking the sensory domain of the CpxA, (Raivio *et al*., 1999). In contrast to enhanced expression of the proteases and chaperones, genes that encode structural components of a cellular appendage such as pilus, are down-regulated by the Cpx transcriptional control (Vogt *et al*., 2010).

The repressive arm of the Cpx response is enhanced by sRNA regulation of the mRNA targets. The Hfq-dependent sRNA CpxQ, as mentioned above (Section 1.1), is processed from the 3' UTR of the *cpxR* transcript by RNase E (Chao and Vogel, 2016). CpxQ represses the translation of *nhaB* (sodium-proton antiporter) and *skp* (periplasmic OMP chaperone) mRNAs. This repression stabilises the polarization of IM resulting from the loss of proton motive force (PMF) during the IM stress (Chao and Vogel, 2016) and minimizes the risk of OMP insertion into IM by Skp chaperone (Grabowicz *et al*., 2016). Furthermore, CpxQ may link different stress response pathways by positively regulating the expression of sRNAs MicF, RprA, OmrA, and OmrB and negatively regulating sRNA CyaR.

Indeed, ESR induced by Cpx is linked to that of the Rcs by the sRNA RprA, (Figure 1.6C). In addition to Cpx regulon, RprA is also positively regulated by the Rcs response that is triggered by LPS damage and disrupted peptidoglycan (PG) biosynthesis (Laubacher and Ades, 2008). The stress signal is perceived by the surface-exposed lipoprotein RcsF and upon degradation of the repressor IgaA, a phosphorelay is initiated from the IM-bound RcsC to RcsD. The transfer of phosphoryl group to the transcriptional factor RcsB ultimately leads to the expression of Rcs regulon. Interestingly, RcsB binds to *rprA* gene promoter as a homodimer but acts on another promoter of *cps* genes (encoding colanic acid and capsular polysaccharide) as a heterodimer with RcsA (Ebel and Trempy, 1999; Majdalani and Gottesman, 2005). The sRNA RprA has two known targets that it down-regulates: *csgD* (transcriptional factor of curli fimbriae/cellulose) and *ydaM* (diguanylate cyclase, a transcriptional activator for *csgD* (Mika *et al*., 2012; Bordeau and Felden, 2014). Repression of these two genes prevents the cell from over-expressing curli fimbriae under envelope stress. On the contrary, RprA positively modulates the expression of *rpoS*, a stationary sigma factor (Majdalani *et al*., 2001) which allows the bacterial cell to activate a global stress response. Furthermore, in response to LPS

damage, RpoS and Rcs TCS elicit OM stress response by activating the transcription of the *rpoE* (Klein and Raina, 2015).

1.4.2 Aerobic and anaerobic respiration

Among Gram-negatives, species of enterobacteria are known as facultative anaerobes due to their ability to produce adenosine triphosphate (ATP) from both the aerobic respiration and fermentation, (Unden *et al*., 1994). The switch from the oxidative to fermentative respiration requires a major shift in gene expression which is coordinately regulated by transcriptional regulators such as ArcA and FNR (Georgellis *et al*., 2001; Constantinidou *et al*., 2006). The oxygen sensor ArcB is the HK of TCS ArcA/ArcB (anoxic redox control) that is autophosphorylated under anaerobic conditions. The ArcB phosphotransfers to ArcA, the cytosolic RR, and the extent of ArcA phosphorylation (ArcA-P levels) in the cellular environment determine the repression or induction of genes involved in either aerobic or anaerobic metabolism (Liu and De Wulf, 2004). The ArcA/ArcB system is modulated by the sRNA ArcZ regulatory feedback loop in which the level of *arcB* is directly manipulated by ArcZ in response to oxygen availability, (Mandin and Gottesman, 2010). During aerobic growth, highly abundant ArcZ down-regulates expression of the *arcB* mRNAs which, as a result, prevents ArcA from being activated by ArcB. Conversely, during anaerobic growth, activated ArcZ down-regulates the expression of *arcZ*, allowing *arcB* expression to ensure its own activation.

FNR (fumarate and nitrate reductase) encoded by the gene *fnr* is a transcriptional regulator responsible for transitioning cellular respiration from aerobic to anaerobic respiration by repressing the expression of 'aerobic' genes but activating the 'anaerobic' genes (Salmon *et al*., 2003; Kang *et al*., 2005). As FNR is a direct sensor of oxygen through its surface exposed Fe-S cluster, it rapidly reprograms the bacterial respiration mode (Unden and Schirawski, 1997). The expression of FNR-dependent sRNA FnrS is anaerobically induced and negatively regulates the 'aerobic' and energy metabolism genes to assist with FNR-mediated gene regulation (Boysen *et al*., 2010; Durand and Storz, 2010).

1.4.3 Quorum sensing

Quorum sensing (QS) is a bacterial signal-response system in which the signal molecules called autoinducers are produced in a population density manner. The production and sensing of these molecules allow a cell to cell communication at inter- and/or intraspecies level, eliciting a collective gene expression change in the members of the QS bacterial community. Examples of QS-mediated phenotypes include biofilm formation, bioluminescence, HGT, sporulation, and virulence (Waters and Bassler, 2005). Such phenomena take place in high cell density state, allowing QS bacterial community to survive the stressful environment. During the transition from low to high cell density state, QS is meticulously regulated by sRNAs that modulate information fed into the QS circuits.

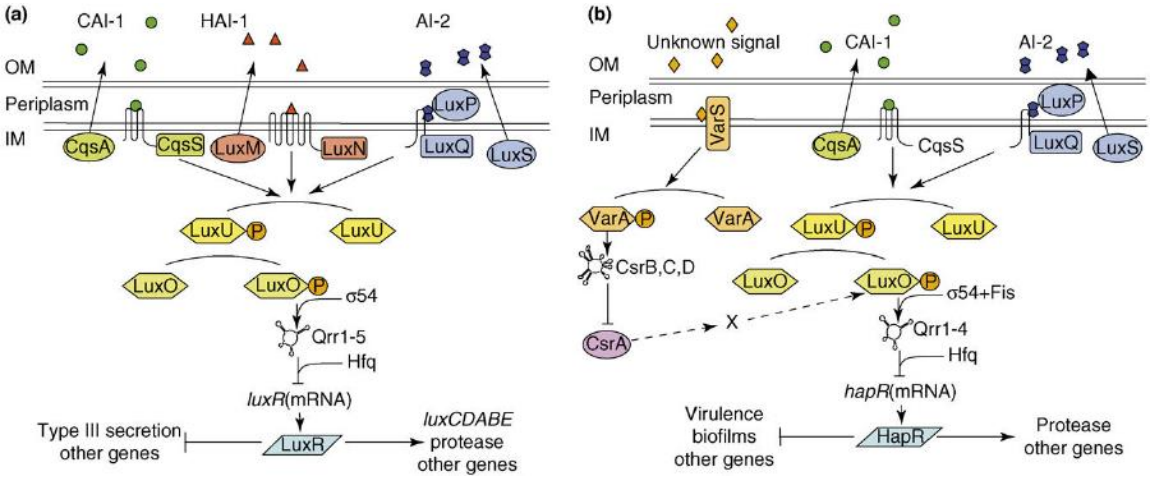

Figure 1.7 Quorum sensing signal transduction systems of (a) *Vibrio harveyi* and (b) *V. cholerae*, (Bejerano-Sagie and Xavier, 2007).

In *Vibro harveyi* (Figure 1.7a) and *V. cholerae* (Figure 1.7b), acylated homoserine lactone (AHL) autoinducer molecules are synthesized by three *luxI* homologs which are perceived by membrane-bound sensors/receptors that set phosphorelay cascade in motion (Reviewed in Papenport and Bassler, 2016). At low cell density, the signals from the receptors converge at LuxU, a phosphorelay protein that transfers its phosphate to a DNA-binding RR LuxO. Together with σ^{54}, the LuxO-P transcriptionally activates Hfq-dependent quorum regulatory sRNAs Qrrs that negatively regulate the mRNAs of a QS master regulator *luxR* (*V. harveyi*) or *hapR* (*V. cholerae*) (Lenz, 2004). This, in turn, represses the expression of genes under LuxR/HapR's control. Such examples include *vca0939* and *aphA* of *V. cholerae* whose products stimulate the formation of biofilm and expression of virulence genes, respectively

(Hammer and Bassler, 2007; Rutherford *et al*., 2011). Interestingly, *V. cholerae* has four Qrrs that are functionally redundant and are speculated to work as an 'ultra-sensitive switch' that intricately transitions bacterial state from a low cell density to a high density (Bardill *et al*., 2011). On the contrary, *V. harveyi* possesses five Qrrs that function in an additive manner. Four of the five Qrrs of *V. harveyi* repress *luxR* to varying degrees, resulting in gradient levels of *luxR* to achieve a differential regulation of genes belonging to the QS regulon (Tu and Bassler, 2007).

At high cell density, extensive binding of autoinducers at receptors allow the sensors to function as phosphatases to reverse the phosphorelay. The phosphate is now removed from LuxU, making it inactive and unable to phosphorylate LuxO. Both LuxU and LuxO thus remain dephophorylated and transcription of *qrrs* no longer takes place. This relieves Qrr-repression of *luxR* or *hapR* hence the expression of QS controlled genes needed for biofilm formation and virulence resumes. This transition from planktonic and motile lifestyle to 'sessile' biofilm community is further assisted by an additional pathway, VarS HK/VarA RR TCS that directly channels QS information to LuxO (Lenz *et al*., 2005). The expression of sRNA CsrB, CsrC and CsrD is triggered by VarS/VarA system to inhibit CsrA activity. CsrA is a RNA-binding post-transcriptional regulator protein that up-regulates the expression of *flhDC* (a master regulator of flagellar biosynthesis) but down-regulates the expression of the *pga* operon (biofilm matrix component poly N-acetyl-D-glucosamine) and genes encoding enzymes involved in cyclic-di-GMP production (Mika and Hengge, 2013). This activity of CsrA is abolished by CsrB, CsrC and CsrD sequestration of the CsrA protein thereby promoting the biofilm formation and 'sessile' lifestyle of the QS bacterial community. The homologs of VarS/VarA system called GacS/GacA is widely used in species of Gram-negative bacteria like *Pseudomonas aeruginosa* and *Pectobacterium carotovorum* (Kay *et al*., 2006; Cui *et al*., 2005). The formation of the biofilms confers protection to bacterial community from antibiotics, desiccation and host immune response. Moreover, expression of the virulence genes such as proteases and toxins helps to acquire new nutrient sources from the host cell or environment.

1.4.4 Motility

$FlhD_2C_2$ (a heterotetramer of homodimer FlhD and FlhC) is a master regulator of flagellar biosynthesis operon in *E. coli* whose expression is up-regulated in the late-exponential growth. The regulator activates the genes that encode flagellar basal body, hook and a sigma factor FliA

(σ^F) that further initiates the expression of genes involved in the making of flagellar cap and filament (Soutourina and Bertin, 2003). The expression of flagella permits the bacterial cells to exhibit motility that increases their access to nutrients (Zhao *et al*., 2007). The mRNA *flhDC* is a direct target of many post-transcriptional regulatory sRNAs that respond to an array of environmental cues. This involvement of multiple sRNAs in the *flhDC* regulatory cascade ensures monitoring and integration of environmental and intracellular conditions so that the formation of flagella (involving more than 60 genes) is beneficial to the bacterium which should also take place at an appropriate growth stage or cell state.

De Lay and Gottesman (2012) characterized five sRNAs that regulate flagellar synthesis at the *flhDC* level. The four sRNAs, namely, ArcZ, OmrA, OmrB, and OxyS negatively regulated the expression of *flhDC* while the sRNA MicA promotes motility through an unknown mechanism that is independent of *flhDC*. In addition, Thomson *et al*. (2012) described an additional sRNA McaS (multi-cellular adhesive sRNA under CRP, cyclic AMP receptor protein, regulon) that positively regulates the expression of *flhDC*. Surprisingly, a region upstream of the RBS in the *flhD* leader sequence was shared between the ArcZ and McaS for binding. The binding of ArcZ-Hfq complex led to ribosome occlusion hence repression of *flhD* translation but the pairing of McaS with the *flhD* leader caused structural remodelling of the secondary structure that allowed the ribosome access. Notably, the above-mentioned sRNAs are part of regulons that modulate various cellular responses such as, oxygen availability (ArcZ), membrane stress (MicA and OmrAB) and oxidative stress (OxyS). The cross-talk between different regulatory circuits connected by sRNAs allows integration of environmental signals into regulating motility which is likely to ensure that benefits of flagella expression coincides with given environmental condition.

1.4.5 Iron homeostasis

Iron (Fe) is an essential element in bacterial life which is used as an indispensable co-factor in many enzymes. Ferrous iron (Fe^{2+}) is the main bioactive form found in the proteins that are involved in important cellular processes such as aerobic and anaerobic respiration, DNA biogenesis, nitrogen fixation, photosynthesis, and the tricarboxylic acid (TCA) cycle. Although indispensable, the level of Fe in a bacterial cell is carefully monitored due to its toxicity arising from its insoluble form as ferric iron (Fe^{3+}) as well as from the formation of reactive oxygen species (ROS) by reacting with a by-product of aerobic respiration, H_2O_2 (Imlay, 2013).

Therefore, bacterial have developed intracellular Fe homeostasis mechanisms that coordinate the acquisition of essential Fe and removal of excess free Fe.

In both Gram-positive and negative bacteria, the ferric uptake regulator, Fur, has been associated with Fe homeostasis (Hantke, 2001). This transcriptional factor (TF) is a metalloprotein that requires Fe^{2+} as a co-factor to bind Fur boxes in DNA during iron abundance. The bound Fur^{Fe2+} complex has been shown to represses the transcription of up to 100 genes involved in iron assimilation (Beauchene *et al*., 2015). At low concentration of iron, the Fur^{Fe2+} complex dissociates from the Fur boxes and allows expression of the previously repressed genes, including a small RNA RyhB, to relieve Fe starvation. The regulatory sRNA RyhB plays a key role in Fe homeostasis by exhibiting a 'Fe sparing response' which helps the cell to cope with the Fe scarcity by redirecting the usage of intracellular Fe stores as well as increasing a Fe import into the cell.

The 'targetome' of RyhB comprises approximately 56 mRNAs whose expression is mostly repressed by RyhB (Massé *et al*., 2005; Chareyre and Mandin, 2018). These mRNAs encode Fe-containing proteins that are involved in the biogenesis of iron-sulphur (Fe-S) cluster, respiration, TCA cycle, and siderophore biosynthesis. Under Fe limiting conditions, genes encoding 'essential' Fe-containing proteins and non-Fe utilizing proteins are expressed while repressing expression of genes encoding 'non-essential' Fe-containing proteins. For example, RyhB negatively regulates the translation of *sodB* that encodes the Fe-containing superoxide dismutase (SOD) but not *sodA*, a manganese-utilizing SOD (Massé and Gottesman, 2002). In contrast to *sod* genes, the expression of the mRNAs *cirA* (TonB-dependent transporter of siderophore) and *shiA* (a transporter of shikimate, a precursor in siderophore production) have been found to be activated by RyhB (Prévost *et al*., 2007; Salvail *et al*., 2013). The activation of these genes promotes the production of Fe^{3+} chelating compound (siderophore) and its import into the cell. Lastly, the usage of Fe is further redirected from the housekeeping Isc Fe-S biogenesis system to a stress-induced, Fe-sparing Suf system. The transition is indirect and involves partial RyhB-degradation of the mRNA resulting from an *iscRSUA* operon. During Fe shortage, RyhB binds at the *iscS* gene to degrade *iscSUA* but leaving *iscR* intact in the 5' region of the mRNA. The resulting short transcript containing *iscR* is then translated into the transcriptional regulator IscR (Fe-S containing holo-protein at Fe sufficiency) which in its apo-form activates the *suf* promoter (Desnoyers *et al*., 2009; Mettert and Kiley, 2015).

1.4.6 Oxidative stress

ROS such as peroxide and superoxide are naturally produced from the metabolism of oxygen in a bacterial cell. However, increased levels of ROS results in oxidative stress where DNA, enzymes, and membranes are exposed to excess ROS and are damaged. The oxidative stress is counteracted by RpoS (σ^{38}) and OxyR activation of stress-relieving and genes encoding antioxidants, such as *kat* genes encoding catalases that decompose harmful H_2O_2 to water and oxygen. Although the mechanism of action is less well understood, the Hfq-dependent sRNA, OxyS, also plays an important role in detoxifying oxidative stress (Zhang *et al*., 1998).

The role of OxyS in oxygen homeostasis first came to light when *oxyS* deletion mutant of *E. coli* accumulated a higher intracellular ROS level than the wild type (Altuvia *et al*., 1997). The studies have shown that OxyS represses the expression of genes that encode metal co-factor using enzymes such as *fhlA* (transcription activator of formate-hydrogen lyase complexes) and *hyp* operon (Nickel-Iron hydrogenase enzyme) and provide protection of DNA from H_2O_2-induced spontaneous mutations (Altuvia *et al*., 1998; González-Flecha and Demple, 1999). Surprisingly, another target that is negatively regulated by OxyS is *rpoS*, (Zhang *et al*., 1998). This action has been speculated to promote RpoD (σ^{70})-dependent OxyR oxidative response over RpoS (σ^{38}) stress response that competes for the same RNA polymerase.

Interestingly, one of the down-regulated genes of OxyS is *nusG*, encoding the RNA polymerase regulator that, together with Rho, silences the transcription of horizontally transferred genes, (Ray-Soni *et al*., 2016). Down-regulation of *nusG* may enable transcription of a laterally acquired novel gene in the host bacterial cell (Wang *et al*., 2011). Similarly, Hfq, independent of sRNAs, has been shown to promote bacterial genome evolution by negatively regulating *mutS* of the DNA mismatch repair (MMR) system (Chen and Gottesman, 2017). MutS is a dimer protein that binds DNA at a mismatched base and initiates MMR (Li, 2008). Repression of *mutS* inevitably permits the adoption of mismatched or erroneous insertion of bases in the bacterial genome that may be deleterious or beneficial.

1.4.7 Virulence

1.4.7.1 sRNA regulation of virulence in animal pathogen

Species of *Salmonella* represent important pathogens that cause gastrointestinal salmonellosis and sepsis (para- / typhoid fever) in humans. The type 3 secretion system (T3SS) and its effector molecules are essential virulence factors that enable adhesion and invasion of

Salmonella into the host's intestinal epithelial cells or macrophages (Eriksson *et al*., 2003). These virulence factors are encoded within the horizontally acquired *Salmonella* Pathogenicity Island 1 (SPI-1) (Galan, 2001; Lostroh and Lee, 2001; Srikumar *et al*., 2015). Under host invasion, the pathogen's transcriptional regulators HilC, HilD and RtsA of the pathogen activate the expression of *hilA*, whose protein product initiates transcription of the T3SS apparatus and effector genes (Bajaj *et al*., 1995; Eichelberg and Galan, 1999). The sRNA, InvR, is co-expressed with *hilA* alongside the genes found on SPI-1 (Pfeiffer *et al*., 2007) but post-transcriptionally acts on the genes unrelated to SPI-1, (Figure 1.8A). A notable target of InvR is *ompD*, encoding outer membrane porin, whose translation is repressed by the sRNA to prevent the overexpression of porins that may destabilize the outer membrane integrity and the structure of T3SS apparatus, hinging on the membrane for stability (Pfeiffer *et al*., 2007).

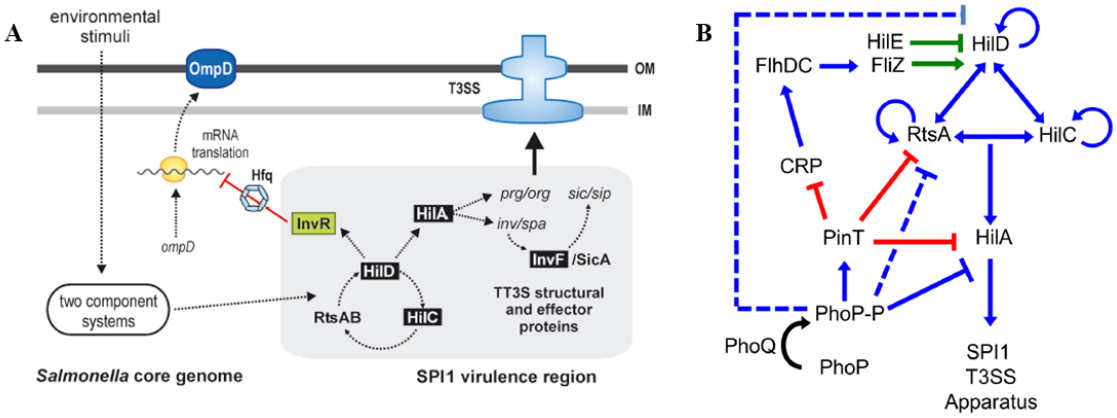

Figure 1.8 sRNA-regulation of the *Salmonella* pathogenicity island (SPI-1) encoded type 3 secretion system (T3SS) expression in *Salmonella*. (A) The sRNA InvR encoded from SPI-1 negatively regulates ompD for the stabilization of outer membrane during T3SS expression. (B) The sRNA PinT shuts down T3SS expression by repressing *hilD* and *hilA*, transcriptional regulators of SPI-1 encoded genes (Vogel, 2009; Kim *et al*., 2019).

Once the pathogen is phagocytised by the host cell, the expression of SPI-1 is no longer needed and is switched off by the PhoP/PhoQ TCS–dependent sRNA PinT (Kim *et al*., 2019). PinT directly represses the translation of *hilD* and *hilA* SPI-1 transcriptional regulators thereby shutting down the expression of T3SS and effector molecules to transition the state of *Salmonella* from invasion to intracellular survival, (Figure 1.8B).

1.4.7.2 Role of sRNAs in virulence regulation of plant pathogenic bacteria

Overall, functional roles and regulatory pathways of sRNAs are less well understood in plant pathogenic bacteria than in animal bacterial pathogens. This is largely due to the latter's importance as human pathogens and the diseases caused by them that directly affect human lives. However, with the increasing importance of sRNAs as global regulators, investigative efforts are being made in the field of plant pathology to elucidate the functional roles of sRNAs present in the plant pathogenic bacteria. A number of studies have been conducted on representative plant pathogens of agricultural and economic importance including, *Dickeya dadantii* (Yuan *et al*., 2019), *Erwinia amylovora* (Zeng *et al*., 2013; Zeng and Sundin, 2014; Lee and Zhao, 2016; Schachterle *et al*., 2019), *Pectobacterium carotovorum* (Wang *et al*., 2018) and *Xanthomonas* species, (Schmidtke *et al*., 2013; Abendroth *et al*., 2014; Hu *et al*., 2018).

D. dadantii and *P. carotovorum* are pathogens of potato and vegetables which deploy plant cell wall degrading enzymes (PCWDEs) to exhibit soft rot symptom on the host plants. In *D. dadantii,* a LysR-type transcriptional regulator PecT negatively modulates the expression of T3SS, *pel* (pectate lyase) and Hfq-independent sRNA *rsmB* (Hérault *et al*., 2014). This repression is lifted by ArcZ which negatively regulates *pecT* at the translational level in an Hfq-dependent manner. RsmB is a sRNA which together with another global post-transcriptional regulator called RsmA (homolog CsrA) represses translation of the genes associated with expression of T3SS and production of pectate lyase production. By ArcZ saving RsmB from PecT-mediated repression, RsmB is able to antagonize the activity of RsmA by sequestration, allowing the expression of virulence genes in *D. dadantii* (Yuan *et al*., 2019). It is possible that the virulence of *P. carotovorum* is regulated by ArcZ and CsrB (homolog RsmB) in a similar manner as their counterparts in *D. dadantii*, demonstrated by the loss of pathogenicity in *arcZ* and *csrB* deletion mutants of *P. carotovorum* (Wang *et al*., 2018).

A knockout mutation of *arcZ* also affects the flagellar motility in *D. dadantii* (Yuan *et al*., 2019) and *E. amylovora*, (Zeng *et al*., 2013; Zeng and Sundin, 2014). Interestingly, the loss of *arcZ* in *D. dadantii* resulted in hypermotility while reduced motility was displayed by the *arcZ* mutant strain of *E. amylovora* compared to that of the wild-type. The hypermotility observed in *D. dadantii arcZ* mutant is in agreement with the finding of De Lay and Gottesman (2012) that ArcZ directly represses the translation of *flhD* (flagellar master regulator, See section 4.4). Therefore, in the absence of ArcZ, overexpression of *flhD* is likely to take place, leading to increased motility in the *arcZ* deletion mutant. On the contrary, it has been suggested that the reduced motility in the *arcZ* mutant strain of *E. amylovora* is may be due to an additional

regulatory pathway of ArcZ specific to *E. amylovora*. In fact, the ArcZ of *E. amylovora* not only regulates *flhD* post-transcriptionally (repression) but also transcriptionally (activation), resulting in conflicting regulatory outputs (Schachterle *et al*., 2019). However, overall motility promotion through ArcZ-pathway is likely to have been achieved by co-operative and indirect activation of *flhD* by additional sRNA RmaA whose transcriptional target remains to be elucidated (Schachterle *et al*., 2019).

Virulence expression in the species of *Xathomonas* is regulated by sRNAs that act independently of Hfq. The sRNA, sX13, in *Xanthomonas campestris* pathovar *vesicatoria* (Xcv) was found to regulate Xcv's growth and virulence (Schmidtke *et al*., 2013). Similarly, two sRNAs namely, trans217 and trans3287 in *X. oryzae* pathovar *oryzae* (Xoo) were found responsible for Xoo pathogenicity in rice and hypersensitivity response in tobacco by promoting translation of *hrpG* (transcriptional regulator of *hrpX* and *hrp*-encoded T3SS genes) and *hrpX*, whose translations are crucial for the expression of a functional T3SS machinery (Hu *et al*., 2018). Although the regulatory mechanisms and pathways of sX13 in Xcv remain to be elucidated, RNA sequencing analysis showed that sX13 affects the abundances of more than 60 genes involved in motility, signalling, and virulence (Abendroth *et al*., 2014). Among those, the transcript level of *hrpX* (hypersensitive response and pathogenicity) gene that encodes AraC-type transcriptional regulator of T3SS was positively affected by sX13, while *hfq* mRNAs were negatively regulated (Abendroth *et al*., 2014). The loss of the *hfq* gene did not cause any visible phenotype in Xcv but inactivation of *rsmA* (*csrA*) resulted in pleiotropic effects in Xcv, causing reduced EPS production, QS activity as well as virulence. The regulatory role of RsmA in various cellular processes has been previously characterized for the species of *Xanthomonas* (Chao *et al*., 2008; Zhu *et al*., 2011) and it will be interesting to determine if sX13, trans217, and trans3287 act on their targets in RsmA-dependent pathways.

Hfq-dependent, virulence regulating sRNAs are largely unknown in *Pseuodomonas syringae*. A deletion mutation of *hfq* gene in *P. syringae* pv. tomato DC3000 was found lethal subsequently posing a challenge in comprehensively understanding the role of Hfq and Hfq-dependent sRNAs in this pathogen (Park *et al*., 2013). However, a number of Hfq-associated sRNAs have been characterised to date which include P16/RgsA (Park *et al*., 2013), Spf (Park *et al*., 2014), CrcZ and CrcX (Filiatrault *et al*., 2013). Among these, a sRNA Spf is most closely associated with virulence by affecting the expression of *alg8* (encoding glycosyltransferase) thereby regulating the alginate biosynthesis, while P16 and Crc sRNAs modulate oxidative stress and carbon catabolite repression, respectively. Recently, two GacA-dependent sRNAs

RsmX and RsmY have been described to have a population density dependent expression in strains of *P. syringae* (Nakatsu *et al*., 2019). Their expression was highly activated during high cell density condition regardless of *P. syringae* strains' ability to produce AHL molecules. The authors suggested potential existence of uncharacterized quorum chemicals that regulate the expression of RsmX and RsmY. The GacS/A TCS, RsmA (homolog CsrA) and Rsm sRNAs are known regulators of virulence expression in many bactetrial pathogen (See section 1.4.3). Such is true for *P. aeruginosa* whose T3SS, T6SS, type IV pili, biofilm formation and quorum sensing phenotypes are modulated by RsmA, GacS/A and sRNA RsmY and RsmZ pathway, (Vakulskas *et al*., 2015). Similarly, in *P. syringae* pv. tomato DC3000, RsmA protein alters expressions of alginate synthesis, growth, motility and virulence (Ferreiro *et al*., 2018). The acticity of RsmA protein is inhibited by Rsm sRNAs by a sequestering mechanisms, (Sonnleitner and Haas, 2011). In *P. aruginosa* and *P. fluorescens* CHA0, the transcription of Rsm sRNAs are activated by GacA RR and this is likely to be also true for *P. syringae* pv. tomato DC3000 RsmX and RsmY which is demonstrasted by the abolished and reduced expressions of RsmX and RsmY, respectively, in the absence of *gacA* (Nakatsu *et al*., 2019).

Table 1 A summary of sRNAs and their regulatory roles in various cellular processes

sRNA	Main targets	Regulation
Dual function sRNA		
SgrS	*ptsG, manXYZ, yigL, sopD*	Encodes SgrT that represses PtsG (glucose transporter) activity
RNAIII	*spa, coa, hla*	Encodes Hld, δ-haemolysin haemolysis
Psm-mec	*agrA*	Encodes PSM protein, biofilm formation
Pel	*emm, speB*	Encodes SLS streptococcal β-haemolysin Regulates transcription of virulence factors
Envelope stress response		
RybB	*omp, lpp*	Represses translation of outermembrane proteins
MicL	*lpp, rpoE*	Represses translation of lipoproteins Negative feedback control of σ^E
MicC	*ompC, ompF*	Represses translation of major outermembrane proteins
MicF	*ompC, ompF*	Represses translation of major outermembrane proteins
OmrA/B	*envZ, ompR, csgD, ompT, tonB*	Repress translation of outermembrane proteins, curli fimbriae transcription factor, tonB-dependent receptor Autoregulation of EnvZ and OmpR
CpxQ	*nhaB, skp*	Represses translation of sodium-proton antiporter and periplasmic omp chaperone

		Stabilises polarization of inner membrane
RprA	*csgD, ydaM, rpoS*	Represses translation of curli fimbriae transcription factor, diaguanylate cyclase Enhances translation of *rpoS*, stationary sigma factor
Aerobic and anaerobic respiration		
ArcZ	*arcB*	Inhibits ArcA RR by repressing translation of *arcB* HK under aerobic condition
FnrS	*sodB, maeA, gpmA, folEX*	Represses translation of transcripts encoding enzymes for energy metabolisim under anaerobic condition
Quorum sensing		
Qrr1-4/5	*aphA* (*hapR*), *vca0939*	Repress expression of transcripts encoding virulence factors that stimulate biofilm formation Facilitate transitioning bacterial state from low to high cell density
CsrB,**C**,**D**	CrsA	Sequestrate CsrA protein to inhibit CsrA activity in promoting flagellar biosynthesis and down-regulating pga operon (biofilm matrix) Promote biofilm formation and 'sessile' lifestyle
Motility		
ArcZ, **OmrAB**, **OxyS**	*flhDC*	Repress translation of *flhDC* master regulator of flagellar biosynthesis
MicA	*flhDC*	Promotes translation of *flhDC*
McaS	*flhDC, csrA, pga*	Promotes translation of *flhDC* and *csrA* Represses translation of *pga* operon
Iron homeostasis		
RyhB	*sodB, cirA, shiA, iscRSUA*	Fe-sparing response Represses translation of mRNAs encoding non-essential iron-binding enzymes Promotes translation of mRNAs encoding proteins needed for siderophore production Promotes degradation of *iscRSUA* mRNA to *iscR* to activate Fe-sparing Suf system
Oxidative stress		
OxyS	*rpoS, fhlA, hyp*	Anti-mutator Represses translation *fhlA* and *hyp* operon transcripts that encode metal co-factor using enzymes Represses translation of *rpoS* to promote RpoD-dependent OxyR oxidative response
Virulence		
InvR	*ompD*	Represses translation of outer membrane porin transcript Stabilizes outer membrane integrity

PinT	*hilD, hilA*	Represses translation of *hilD* and *hilA* transcriptional regulators of *Salmonella* Pathogenicity Island encoded T3SS Facilitates *Salmonella* from invasion to intracellular survival state
ArcZ	*pecT*	Represses translation of *pecT* transcriptional regulator that down-regulates expression of T3SS and *rsmB* in *Dickeya dadantii*
RsmB/CsrB	RsmA/CsrA	Sequesterates RsmA/CrsA to inhibit its activity to allow virulence gene expression
sX13	unknown	Regulates growth and virulence in *Xanthomonas campestris* pv. *vesicatoria*
trans217, trans3287	*hrpG*	Promote translation of transcriptional regulator *hrpG* that modulates expression of *hrp*-encoded T3SS in *Xanthomonas oryzae* pv. *oryzae*
P16/RgsA		Oxidative stress response in *Pseudomonas syringae*
Spf	*alg8*	Promotes translation of alg8 glycosyltransferase enzyme Promotes alginate biosynthesis in *Pseudomonas syringae*
CrcZ, X	Crc	Sequestrate Crc to ihibit its activity in the absence of preferred growth substrates Carbon catabolite repression controlling sRNAs in *Pseudomonas syringae*

1.5 sRNA interactome discovery

Trans-acting sRNAs represent a large group of post-transcriptional regulators of bacterial genes by affecting the stability, abundance and translation efficiency of their mRNAs. The interaction is direct, forming a base-pairing between the regulator and the cognate RNA pair (Storz *et al*., 2004; Kavita *et al*., 2018). The global transcriptional state shaped by the sRNAs can be captured by a high-throughput transcriptome analysis or RNA-sequencing (RNA-seq) where RNAs are converted to complementary DNAs (cDNA) and sequenced in-depth, allowing the genome-wide discovery of sRNAs and the transcriptional changes thereof. The specializations of the standard RNA-seq method have been an on-going task for researchers to improve the specificity of sRNA interaction not only with its target mRNAs but also with the protein molecules, such as RNA-binding chaperones and ribonuclease RNaseE that are functionally related to the sRNA-mediated regulations (Bilusic *et al*., 2014; Han *et al*., 2016; Holmqvist *et al*., 2016; Smirnov *et al*., 2016; Waters *et al*., 2017) The RNA-seq technologies and their potentials in capturing 'sRNA-induced interactome' are comprehensively reviewed by Barquist and Vogel (2015) and Saliba *et al*., (2017). In this section, some of these specialized

RNA-seq approaches and their applications in sRNA and its interactome discovery will be discussed, (Figure 1.9).

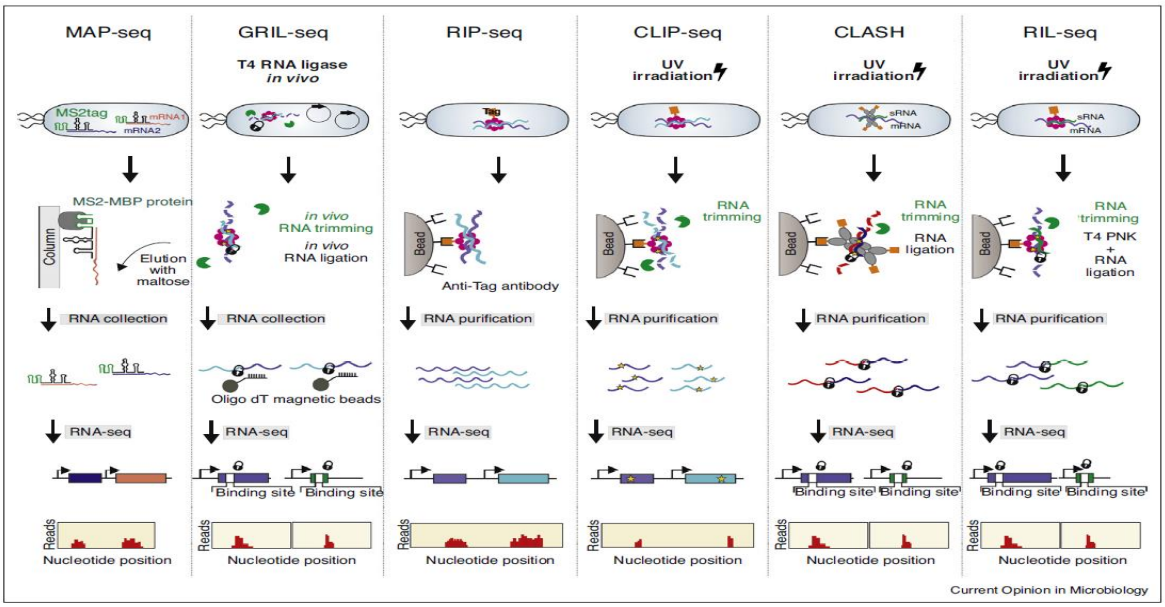

Figure 1.9 RNA-sequencing based methods for discovery of sRNA interactome (Saliba *et al*., 2017).

Earlier methods used to identify sRNAs targets relied on the microarray-based RNA-seq method called MAP-seq. This technique relies on the ability of the target transcripts to hybridize to MS2-tagged sRNAs which are then co-purified and sequenced (Lalaouna *et al*., 2015). This method led to the discovery of a tRNA precursor, 3'EST^{leuZ}, as the sRNA sponge in *E. coli*, (See section 3.5). However, as many of these trans-acting sRNAs act on their targets with the help of RBP such as Hfq, a new approach to interactome identification was devised. One of those approaches, called RIP-seq (RNA immunoprecipitation sequencing) captures populations of RNAs bound to Hfq by co-immunoprecipitation using antibody detection of the epitope-tagged RBP (Bilusic *et al*., 2014). As an example of its application, the Hfq-associated RNA profiles of different growth stages/conditions of *Salmonella* were obtained using RIP-seq, leading discovery of novel sRNAs, including DapZ whose expression was controlled by HilD, a master regulator of virulence in *Salmonella* (Chao *et al*., 2012).

In order to determine the nucleotide bases at which the RNAs interact with the RBP, a UV treatment step was introduced in CLIP-seq (Cross-linking immunoprecipitation sequencing). The UV treatment enabled a covalent linking of RNAs to the proteins, allowing a stringent

downstream purification to reduce the rate of yielding false positives. Furthermore, direct RNA-protein contact bases could be identified by the mutations caused in the cross-linked sites during reverse transcription, (Holmqvist *et al*., 2016). The CLIP-seq study of *Salmonella* identified the preferential RBP (Hfq and CsrA) binding sites present on s- and mRNAs, contributing to understanding the role of RBPs in facilitating sRNA-mRNA interactions. The CLIP protocol can be further advanced to the CLASH (cross-linking, ligation and sequencing of the hybrids) method in which the sRNA:mRNA interactions are captured in the form of RNA chimeras. CLASH-seq works on the same principle as CLIP-seq but an additional RNA modification step is introduced in which the UV cross-linked RNA pairs immobilized on the RBP are partially trimmed and their proximal ends are ligated together, (Waters *et al*., 2017). The RNA hybrids result in chimeric cDNAs that are used to determine *bona fide* sRNA:mRNA interaction site (or seed region) at the nucleotide level.

Similarly, RIL-seq (RNA interaction by ligation and sequencing) and GRIL-seq (global small non-coding RNA target identification by ligation and sequencing) produce chimeric cDNA sequences that are further computationally analyzed to accurately map sRNA:mRNA interacting sites (Melamed *et al*., 2016; Han *et al*., 2016). In GRIL-seq, the ligation of chimeric RNA takes place *in vivo*, allowing for the detection of sRNA:mRNA pairs that are independent of Hfq, (Han *et al*., 2016) whereas, in RIL-seq, RNA hybrids immobilized on Hfq are isolated by enzymatically digesting the protein. Using RIL-seq, more than 2800 Hfq-associated RNA pairs were identified, expanding the sRNA interactome of *E. coli* by 44% (56% of the pairs belonged to the known interactions (Melamed *et al*., 2016). Not only, have both the RIL- and GRIL-seq contributed to identifying direct targets of sRNAs but have they also facilitated our understanding of novel regulatory roles of sRNAs in bacterial pathogens.

In addition, a new global RBP ProQ was unveiled by Grad-seq in *Salmonella* (Smirnov *et al*., 2016). Grad-seq is a gradient-based sequencing in which the cellular contents of the bacterium are fractioned on a density gradient, (Figure 1.10A). Each fraction comprises of coding and non-coding transcripts with their shared proteins, enabling biochemical or functional partitioning of the cellular RNAs and proteins. In this way, a new post-transcriptional regulator ProQ and ProQ-associated sRNAs were identified. Furthermore, Grad-seq was able to differentiate the classes of sRNAs associated with different RBPs such as Hfq, CsrA, and ProQ, revealing previously unknown post-transcriptional sRNA landscapes, (Figure 1.10B). The addition of the ProQ post-transcriptional hub will unlock novel regulatory roles of ProQ-associated sRNAs in modulating bacterial physiology.

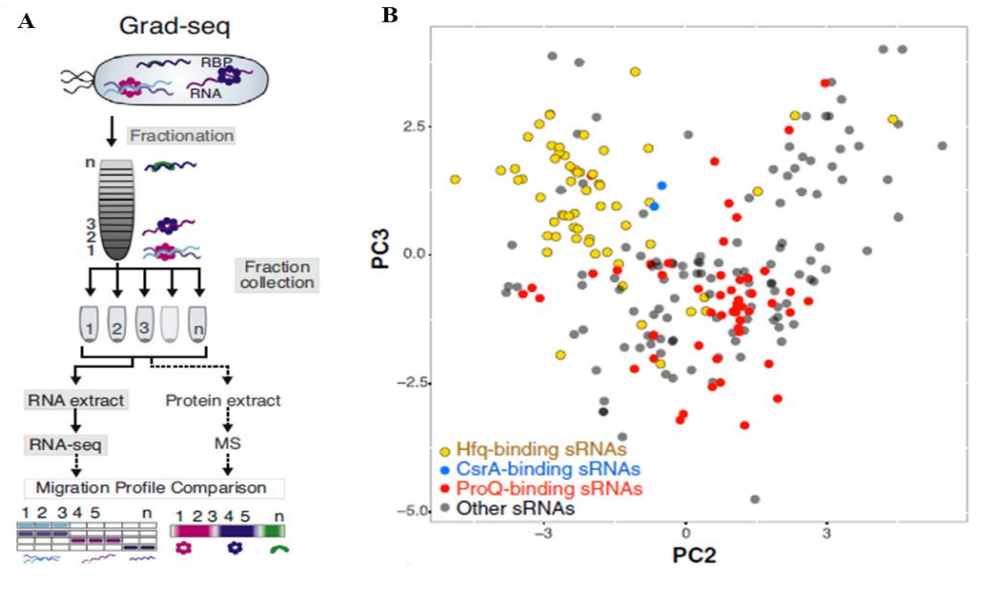

Figure 1.10 (A) Schematic diagram showing methodological steps in the gradient fractionation-based RNA-sequencing (Grad-seq) method. (B) The use of Grad-seq in Salmonella led to the discovery of new RNA-binding protein (RBP) ProQ and the existence of sRNA classes based on their RBP (Smirnov *et al*., 2016; Saliba *et al*., 2017).

1.6 Plant pathogen *Pantoea ananatis*

Pantoea ananatis is a Gram-negative, rod-shaped, motile bacterium, belonging to the versatile genus *Pantoea* within the family *Enterobacteriaceae*, (Mergaert *et al*., 1993). Members of this genus are represented by both environmental and pathogenic bacteria of humans and plants, (Coutinho and Venter, 2009; Walterson and Stavrinides, 2015). *P. ananatis* is an unusual bacterium belonging to this group that is ubiquitously found in aquatic and terrestrial habitats in commensal associations with plants and insects (Gitaitis *et al*., 2002, Brady *et al*., 2008, Dutta *et al*., 2014) but *P. ananatis* is also a plant pathogen of many agriculturally and economically important plant hosts such as rice (Cother *et al*., 2004), maize (Paccola-Meirelles *et al*., 2001; Goszczynska *et al*., 2007; Pérez-y-Terrón *et al*., 2009), onion (Gitaitis and Gay, 1997) , melons (Kido *et al*., 2008) and *Eucalyptus* (Coutinho *et al*., 2002). Yet, genetic determinants for *P. ananatis*' pathogenicity in a wide range of plant hosts are somewhat elusive.

Unlike its sister taxa *P. agglomerans* and *P. stwewartii*, *P. ananatis* lacks major virulence determinants such as T2SS and T3SS (De Maayer *et al*., 2014). Instead, it uses T6SS for an intra-and interspecies competition, facilitating *P. ananatis* in niche colonization and fitness

(Shyntum *et al*., 2014; Shyntum *et al*., 2015), however, the role of T6SS in different susceptible host plants remains largely unknown. Motility and QS were shown contribute to virulence of *P. ananatis* in onion plants by aiding in pathogen's attachment to the plant surface and activating population-density dependent phenotype such as production of biofilm and EPS, respectively (Weller-Stuart *et al*., 2016; Morohoshi *et al*., 2007; Sibanda *et al*., 2016, 2018). Furthermore, plasmid-borne 'Onion Virulence Region' (OVR) and chromosomally encoded 'HiVir' virulence gene cluster were identified in onion pathogenic strains of *P. ananatis*. The former comprised of genes encoding putative PCWDEs, sulphur-reducing enzymes and transporters that are likely needed for manipulation of the host environment so that *P. ananatis* strains are able to survive under harsh plant immunity-induced conditions (Stice *et al*., 2018) whereas the latter, HiVir encoded genes involved in phosphonate biosynthesis (Asselin *et al*., 2018). However, phosphonates' mode of action in plant-pathogen interaction remains to be elucidated. It will be interesting to determine whether OVRs and HiVir are specific to onion-associated *P. ananatis* strains or widely distributed within the *P. ananatis* clade, moreover within the genus *Pantoea*.

Since the aforementioned genes or systems vastly affect the pathogenicity and fitness of *P. ananatis*, a collective regulation of these genes is surely a key to successful infection and survival of *P. ananatis* in the plant host. As reviewed in this chapter, the rapid adaptive response of numerous Gram-negative bacterial pathogens is accomplished by the post-transcriptional regulators namely, Hfq and sRNAs. Thus, investigating the functional role of Hfq in regulating different virulence factors and identification of Hfq-dependent sRNAs in *P. ananatis* will be of critical importance.

1.7 RESEARCH AIMS AND OBJECTIVES

The overall aims of the current study are to characterize the functional roles of Hfq and to identify Hfq-dependent sRNAs that are present in a phytopathogen *Pantoea ananatis* LMG 2665^{T}. To achieve these aims, an *hfq* deletion mutant strain of *P. ananatis* was created and its phenotypes were characterized in comparison to that of the wild type and *hfq*-complementing *P. ananatis* strains. Secondly, a strand-specific sRNA sequencing was conducted for the *hfq* mutant and the wild type *P. ananatis* strains at two-time points (lag and exponential phase) to identify the total pool of putative sRNAs and to further characterize selected Hfq-dependent sRNAs that are differentially regulated at the two-time points.

The specific objectives are:

i. To determine the role of Hfq in *P. ananatis*' *in vitro* and *in planta* growths, biofilm formation, motility, pathogenicity and production of quorum sensing inducer molecule.

ii. To generate sRNA expression data of *P. ananatis* by conducting stranded-sRNA sequencing of the *hfq* mutant and wild type strains of *P. ananatis* at low and high cell density conditions and resulting sequence data will be computationally filtered and screened for sRNA candidates.

iii. To identify Hfq-regulated sRNAs by bioinformatically profiling differential sRNA expression between the *hfq* mutant and wild type.

iv. To experimentally characterize and validate the expression of selected Hfq-dependent sRNAs by performing 5' rapid amplification of cDNA ends (RACE) and quantitative PCR analyses.

v. To computationally predict structures and putative targets of a subset of *P. ananatis* sRNAs.

The outcome of this study will contribute to elucidating the diversity of Hfq-dependent post-transcriptional sRNA regulators found in the plant pathogen *P. ananatis* LMG 2665^{T} that may play indispensable roles in coordinating the expression of virulence and adaptive response genes to allow survival and fitness of *P. ananatis* in constantly changing environments.

1.8 REFERENCES

Abendroth, U., Schmidtke, C. and Bonas, U. (2014) Small non-coding RNAs in plant-pathogenic *Xanthomonas* spp. *RNA Biol*, 11, 457–463. doi: 10.4161/rna.28240

Aiba, H. (2007) Mechanism of RNA silencing by Hfq-binding small RNAs. *Curr. Opin. Microbiol*, 10, 134–139. doi: 10.1016/j.mib.2007.03.010

Altuvia, S., Weinstein-Fischer, D., Zhang, A., Postow, L. and Storz, G. (1997) A small, stable RNA induced by oxidative stress: role as a pleiotropic regulator and antimutator. *Cell*, 90, 43–53. doi: 10.1016/S0092-8674(00)80312-8

Altuvia, S., Zhang, A., Argaman, L., Tiwari, A. and Storz, G. (1998) The *Escherichia coli* OxyS regulatory RNA represses *fhlA* translation by blocking ribosome binding. *EMBO J*, 17, 6069–6075. doi: 10.1093/emboj/17.20.6069

Argaman, L., Hershberg, R., Vogel, J., Bejerano, G., Wagner, E.G.H., Margalit, H. and Altuvia, S. (2001) Novel small RNA-encoding genes in the intergenic regions of *Escherichia coli*. *Curr. Biol,* 11, 941–950. doi: 10.1016/S0960-9822(01)00270-6

Asselin, J.E., Bonasera, J.M. and Beer, S.V. (2018) Center rot of onion (*Allium cepa*) caused by *Pantoea ananatis* requires *pepM*, a predicted phosphonate-related gene. *Mol. Plant Microbe-Interact,* doi: 10.1094/MPMI-04-18-0077-R.

Bajaj, V., Hwang, C. and Lee, C.A. (1995) *hilA* is a novel *ompR/toxR* family member that activates the expression of *Salmonella typhimurium* invasion genes. *Mol. Microbiol*, 18, 715-27. doi: 10.1111/j.1365-2958.1995.mmi_18040715.x

Bardill, J.P., Zhao, X. and Hammer, B.K. (2011) The *Vibrio cholerae* quorum sensing response is mediated by Hfq-dependent sRNA/mRNA base pairing interactions. *Mol. Microbiol*, 80, 1381–1394. doi: 10.1111/j.1365-2958.2011.07655.x

Bardou, F., Merchan, F., Ariel, F. and Crespi, M. (2011) Dual RNAs in plants. *Biochimie*, 93, 1950–1954. doi: 10.1016/j.biochi.2011.07.028

Barquist, L. and Vogel, J. (2015) Accelerating discovery and functional analysis of small RNAs with new technologies. *Annu. Rev. Genet*, 49, 367-394. doi: 10.1146/annurev-genet-112414-054804

Battesti, A., Majdalani, N. and Gottesman, S. (2011) The RpoS-mediated general stress response in *Escherichia coli*. *Annu. Rev. Microbiol*, 65, 189–213. doi: 10.1146/annurev-micro-090110-102946

Beauchene, N.A., Myers, K.S., Chung, D., Park, D.M., Weisnicht, A.M., Keleş, S. and Kiley, P.J. (2015) Impact of anaerobiosis on expression of the iron responsive Fur and RyhB regulons. *mBio*, 6:e01947–e15. doi: 10.1128 /mBio.01947-15.

Bejerano-sagie, M. and Xavier, K.B (2007) The role of small RNAs in quorum sensing The role of small RNAs in quorum sensing, *Curr. Opin. Microbiol*, 10, 189-198. doi: 10.1016/j.mib.2007.03.009.

Beveridge, T.J. (1999) Structures of Gram-negative cell walls and their derived membrane vesicles. *J. Bacteriol*, 181, 4725-4733.

Bilusic, I., Popitsch, N., Rescheneder, P., Schroeder, R. and Lybecker, M. (2014) Revisiting the coding potential of the *E. coli* genome through Hfq co-immunoprecipitation. *RNA Biol*, 11, 641-654. doi: 10.4161/rna.29299

Bordeau, V. and Felden, B. (2014) Curli synthesis and biofilm formation in enteric bacteria are controlled by a dynamic small RNA module made up of a pseudoknot assisted by an RNA chaperone. *Nucleic Acids Res*, 42, 4682–4696. doi: 10.1093/nar/gku098

Bossi, L. and Figueroa-Bossi, N. (2016) Competing endogenous RNAs: a target-centric view of small RNA regulation in bacteria. *Nat. Rev. Microbiol*, 14, 775–84. doi: 10.1038/nrmicro.2016.129

Bossi, L., Schwartz, A., Guillemardet, B., Boudvillain, M. and Figueroa-Bossi, N. (2012) A role for Rho-dependent polarity in gene regulation by a noncoding small RNA. *Genes Dev*, 26, 1864–1873. doi: 10.1101/gad.195412.112

Bouvier, M., Sharma, C. M., Mika, F., Nierhaus, K. H. and Vogel, J. (2008) Small RNA binding to 5' mRNA coding region inhibits translational initiation. *Mol. Cell*, 32, 827–837. doi: 10.1016/j.molcel.2008.10.027

Boysen, A., Møller-Jensen, J., Kallipolitis, B., Valentin-Hansen, P. and Overgaard, M. (2010) Translational regulation of gene expression by an anaerobically induced small non-coding RNA in *Escherichia coli*. *J. Biol. Chem*, 285, 10690–10702. doi: 10.1074/jbc.M109.089755

Brady, C., Cleenwerck, I., Venter, S., Vancanneyt, M., Swings, J. and Coutinho, T. (2008) Phylogeny and identification of *Pantoea* species associated with plants, humans and the natural environment based on multilocus sequence analysis (MLSA). *Syst. Appl. Microbiol,* 31, 447–460. doi: 10.1016/j.syapm.2008.09.004

Brantl, S. (2007) Regulatory mechanisms employed by cis-encoded antisense RNAs. *Curr. Opin. Microbiol,* 10, 102–9. doi: 10.1016/j.mib.2007.03.012

Brosse, A., Korobeinikova, A., Gottesman, S. and Guillier, M. (2016) Unexpected properties of sRNA promoters allow feedback control via regulation of a two-component system. *Nucleic Acids Res,* 44, 9650–9666. doi: 10.1093/nar/gkw642

Carpousis, A.J., Luisi, B.F. and McDowall, K.J. (2009) Endonucleolytic initiation of mRNA decay in *Escherichia coli*. *Prog. Mol. Biol. Transl. Sci,* 85, 91–135. doi: 10.1016/s0079-6603(08)00803-9

Chaba, R., Alba, B.M. Guo, M.S. Sohn, J. Ahuja, N. Sauer, R.T. and Gross, C.A. (2011) Signal integration by DegS and RseB governs the σ E-mediated envelope stress response in *Escherichia coli*. *Proc. Natl. Acad. Sci. USA,* 108, 2106–2111. doi: 10.1073/pnas.1019277108

Chao, N-X., Wei, K., Chen, Q., Meng, Q-L., Tang, D-J., He, Y-Q., Lu, G-T., Jiang, B-L., Liang, X-X., Feng, J-X., Chen, B. and Tang, J-L. (2008) The *rsmA*-like gene *rsmA(Xcc*) of *Xanthomonas campestris* pv. *campestris* is involved in the control of various cellular processes, including pathogenesis. *Mol. Plant Microbe-Interact,* 21, 411-23. doi: 10.1094/MPMI-21-4-0411

Chao, Y. and Vogel, J. (2016) A 3′ UTR-derived small RNA provides the regulatory noncoding arm of the inner membrane stress response. *Mol. Cell,* 61, 352–363. doi: 10.1016/j.molcel.2015.12.023

Chao, Y., Papenfort, K., Reinhardt, R., Scharma, C.M. and Vogel, J. (2012) An atlas of Hfq-bound transcripts reveals 3' UTRs as a genomic reservoir of regulatory small RNAs. *EMBO J,* 31, 4005–4019. doi: 10.1038/emboj.2012.229

Chareyre, S. and Mandin, P. (2018) Bacterial iron homeostasis regulation by sRNAs. *Microbiol. Spectrum* 6, RWR-0010-2017. doi:10.1128/microbiolspec.RWR-0010-2017.

Chen, J. and Gottesman, S. (2017) Hfq links translation repression to stress induced mutagenesis in *E. coli*. *Genes Dev,* 31, 1382–1395. doi: 10.1101/gad.302547.117

Chen, S., Zhang, A., Blyn, L.B. and Storz, G. (2004) MicC, a second small-RNA regulator of Omp protein expression in *Escherichia coli*. *J. Bacteriol*, 186, 6689–6697. doi: 10.1128/JB.186.20.6689-6697.2004

Constantinidou, C., Hobman, J.L., Griffiths, L., Patel, M.D., Penn, C.W., Cole, J.A. and Overton, T.W. (2006) A reassessment of the FNR regulon and transcriptomic analysis of the effects of nitrate, nitrite, NarXL, and NarQP as *Escherichia coli* K12 adapts from aerobic to anaerobic growth. *J. Biol. Chem*, 281, 4802–4815. doi: 10.1074/jbc.M512312200

Cother, E.J., Reinke, R., McKenzie, C., Lanoiselet, V.M. and Noble, D.H. (2004) An unusual stem necrosis of rice caused by *Pantoea ananas* and the first record of this pathogen on rice in Australia. *Australas. Plant Pathol*, 33, 495-503. doi: 10.1071/AP04053

Coutinho, T.A. and Venter, S.N. (2009) *Pantoea ananatis*: an unconventional plant pathogen. *Mol. Plant Pathol*, 10, 325-335. doi: 10.1111/j.1364-3703.2009.00542.x

Coutinho, T.A., Preisig, O., Mergaert, J., Cnockaert, M.C., Riedel, K-H., Swings, J. and Wingfield, M.J. (2002) Bacterial blight and die-back of *Eucalyptus* species, hybrids and clones in South Africa. *Plant Dis*, 86, 20-25. doi: 10.1094/PDIS.2002.86.1.20

Cui, Y., Chatterjee, A., Hasegawa, H., Dixit, V., Leigh, N. and Chatterjee, A.K: (2005) ExpR, a LuxR homolog of *Erwinia carotovora* subsp. *carotovora*, activates transcription of *rsmA*, which specifies a global regulatory RNA-binding protein. *J. Bacteriol*, 187, 4792-4803. doi: 10.1128/JB.187.14.4792-4803.2005

De Lay, N. and Gottesman, S. (2011) Role of polynucleotide phosphorylase in sRNA function in *Escherichia coli*. *RNA*, 17, 1172–1189. doi: 10.1261/rna.2531211

De Lay, N. and Gottesman, S. (2012) A complex network of small non-coding RNAs regulate motility in *Escherichia coli*. *Mol. Microbiol*, 86, 524–538. doi: 10.1111/j.1365-2958.2012.08209.x. doi: 10.1111/j.1365-2958.2012.08209.x

De Lay, N., Schu, D.J. and Gottesman, S. (2013) Bacterial small RNA-based negative regulation : Hfq and its accomplices. *J. Biol. Chem*, 288, 7996–8003. doi: 10.1074/jbc.R112.441386

De Maayer, P., Chan, W.Y, Rubagotti, Venter, S.N., Toth, I.K., Birch, P.R.J. and Coutinho, T.A. (2014) Analysis of the *Pantoea ananatis* pan-genome reveals factors underlying its ability

to colonize and interact with plant, insect and vertebrate hosts. *BMC Genomics*, 15,404. doi: 10.1186/1471-2164-15-404

Desnoyers, G., Morissette, A., Prévost, K. and Massé, E. (2009) Small RNA induced differential degradation of the polycistronic mRNA *iscRSUA*. *EMBO J*, 28, 1551–1561. doi: 10.1038/emboj.2009.116

Durand, S. and Storz, G. (2010) Reprogramming of anaerobic metabolism by the FnrS small RNA. *Mol. Microbiol*, 75, 1215–1231. doi: 10.1111/j.1365-2958.2010.07044.x

Dutta, B., Barman, A.K., Srinivasan, R., Avci, U., Ullman, D.E., Langston, D.B. and Gitaitis, R.D. (2014) Transmission of *Pantoea ananatis* and *P. agglomerans*, causal agents of center rot of onion (*Allium cepa*), by onion thrips (*Thrips tabaci*) through feces. *Phytopathology*, 104,812-819. doi: 10.1094/PHYTO-07-13-0199-R

Ebel, W. and Trempy, J.E. (1999) *Escherichia coli* RcsA, a positive activator of colanic Acid capsular polysaccharide synthesis, functions to Activate its own expression. *J. Bacteriol*, 181, 577-584.

Eichelberg, K. and Galan, J.E. (1999) Differential regulation of *Salmonella typhimurium* type III secreted proteins by pathogenicity island 1 (SPI-1)-encoded transcriptional activators InvF and HilA. *Infect. Immun*, 67, 4099-105.

Eriksson, S., Lucchini, S., Thompson, A., Rhen, M. and Hinton, J.C. (2003) Unravelling the biology of macrophage infection by gene expression profiling of intracellular *Salmonella enterica*. *Mol. Microbiol*, 47, 103–118. doi: 10.1046/j.1365-2958.2003.03313.x

Fender, A., Elf, J., Hampel, K., Zimmermann, B. and Wagner, E.G. (2010) RNAs actively cycle on the Sm-like protein Hfq. *Genes Dev*, 24, 2621–2626. doi: 10.1101/gad.591310

Ferreiro, M-D., Nogales, J., Farias, G.A., Olmedilla, A., Sanjuan, J., Gallegos, M.T. (2018) Multiple CsrA proteins control key virulence traits in *Pseudomonas syringae* pv. *tomato*DC3000. *Mol. Plant Microbe-Interact*, 31, 525–536. doi: 10.1094/MPMI-09-17-0232-R.

Figueroa-Bossi, N., Valentini, M., Malleret, L. and Bossi, L. (2009) Caught at its own game: regulatory small RNA inactivated by an inducible transcript mimicking its target. *Genes Dev*, 23, 2004–2015. doi: 10.1101/gad.541609

Filiatrault, M.J., Stodghill, P.V., Wilson, J., Butcher, B.G., Chen, H., Myers, C.R. and Cartinhour, S.W. (2013). CrcZ and CrcX regulate carbon source utilization in Pseudomonas syringae pathovar tomato strain DC3000. *RNA Biol*, 10, 245–255. doi: 10.4161/rna.23019

Fozo, E.M., Makarova, K.S., Shabalina, S.A., Yutin, N., Koonin, E.V. and Storz, G. (2010) Abundance of type I toxin-antitoxin systems in bacteria: searches for new candidates and discovery of novel families. *Nucleic Acids Res,* 38, 3743–59. doi: 0.1093/nar/gkq054

Franze de Fernandez, M.T., Eoyang, L. and August, J.T. (1968). Factor fraction required for the synthesis of bacteriophage Qβ-RNA. *Nature*, 219, 588–590. doi: 10.1038/219588a0

Franze de Fernandez, M.T., Hayward, W.S. and August, J.T. (1972). Bacterial proteins required for replication of phage Q ribonucleic acid. Purification and properties of host factor I, a ribonucleic acid binding protein. *J. Biol. Chem*, 247, 824–831

Friedman, R.C., Kalkhof, S., Doppelt-Azeroua, O., Mueller, S.A., Chovancová, M., von Bergen, M. and Schwikowski, B. (2017) Common and phylogenetically widespread coding for peptides by bacterial small RNAs. *BMC Genomics*, 18, 553. doi: 10.1186/s12864-017-3932-y

Fröhlich, K. S. and Vogel, J. (2009) Activation of gene expression by small RNA. *Curr. Opin. Microbiol*, 12, 674–682. doi: 10.1016/j.mib.2009.09.009

Fröhlich, K.S. and Gottesman, S. (2018) Small Regulatory RNAs in the Enterobacterial Response to Envelope Damage and Oxidative Stress. Regulating with RNA in Bacteria and Archaea, 213–228. Available at: http://dx.doi.org/10.1128/microbiolspec.rwr-0022-2018

Galan, J.E. (2001) *Salmonella* interactions with host cells: type III secretion at work. *Annu. Rev. Cell Dev. Biol*, 17, 53-86. doi: 10.1146/annurev.cellbio.17.1.53

Georg, J. and Hess, W.R. (2011) cis-Antisense RNA, another level of gene regulation in bacteria. *Microbiol. Mol. Biol. Rev*, 75, 286–300. doi: 10.1128/MMBR.00032-10

Georgellis, D., Kwon, O. and Lin, E.C. (2001) Quinones as the redox signal for the Arc two-component system of bacteria. *Science*, 292, 2314–2316. doi: 10.1126/science.1059361

Gimpel, M. and Brantl, S. (2017) Dual-function small regulatory RNAs in bacteria. *Mol. Microbiol*, 103, 387–397. doi: 10.1111/mmi.13558

Gimpel, M., Heidrich, N., Mäder, U., Krügel, H. and Brantl, S. (2010) A dual-function sRNA from *B. subtilis*: SR1 acts as peptide encoding mRNA on the *gapA* operon. *Mol. Microbiol*, 76, 990–1009. doi: 10.1111/j.1365-2958.2010.07158.x

Gitaitis, R., Walcott, R., Culpepper, S., Sanders, H., Zolobowska, L. and Langston, D. (2002) Recovery of *Pantoea annatis*, causal agent of center rot of onion, from weeds and crops in Georgia, USA *Crop Protect*, 21, 983-989. doi: 10.1016/S0261-2194(02)00078-9

Gitaitis, R.D. and Gay, J D. (1997) First report of leaf blight, seed stalk rot, and bulb decay of onion by *Pantoea ananas* in Georgia. *Plant Dis*, 81, 1096. doi: 10.1094/PDIS.1997.81.9.1096C

Gogol, E.B., Rhodius, V.A., Papenfort, K., Vogel, J. and Gross, C.A. (2011) Small RNAs endow a transcriptional activator with essential repressor functions for single-tier control of a global stress regulon. *Proc. Natl. Acad. Sci. USA*, 108, 12875–12880. doi: 10.1073/pnas.1109379108

González-Flecha, B. and Demple, B. (1999) Role for the *oxyS* gene in regulation of intracellular hydrogen peroxide in *Escherichia coli*. *J. Bacteriol*, 181, 3833–3836.

Goszczynska, T., Venter, S.N. and Coutinho, T.A. (2007). Isolation and identification of the causal agent of brown stalk rot, a new disease of corn in South Africa. *Plant Dis*, 91, 711-718. doi: 10.1094/PDIS-91-6-0711

Gottesman, S. and Storz, G. (2011) Bacterial small RNA regulators: versatile roles and rapidly evolving variations. *RNA*, 21, 511-512. doi: 10.1261/rna.050047.115

Grabowicz, M. and Silhavy, T.J. (2017) Envelope stress responses: an interconnected safety net. *Trends Cell Biol*, 42, 232–242. doi: 10.1016/j.tibs.2016.10.002

Grabowicz, M., Koren, D. and Silhavy, T.J. (2016) The CpxQ sRNA negatively regulates Skp to prevent mistargeting of β-barrel outer membrane proteins into the cytoplasmic membrane. *mBio*, 7:e00312-16. doi:10.1128/mBio.00312-16. doi: 10.1128/mBio.00312-16

Guillier, M. and Gottesman, S. (2006) Remodelling of the *Escherichia coli* outer membrane by two small regulatory RNAs. *Mol. Microbiol*, 59, 231–247. doi: 10.1111/j.1365-2958.2005.04929.x

Guo, M.S., Updegrove, T.B., Gogol, E.B., Shabalina, S.A., Gross, C.A. and Storz, G. (2014) MicL, a new σ^E-dependent sRNA, combats envelope stress by repressing synthesis of Lpp, the major outer membrane lipoprotein. *Genes Dev*, 28, 1620-1634. doi: 10.1101/gad.243485.114

Hammer, B.K. and Bassler, B.L. (2007) Regulatory small RNAs circumvent the conventional quorum sensing pathway in pandemic *Vibrio cholerae*. *Proc. Natl. Acad. Sci. USA*, 104, 11145–11149. doi: 10.1073/pnas.0703860104

Han, K., Tjaden, B. and Lory, S. (2016) GRIL-Seq: a method for identifying direct targets of bacterial small regulatory RNA by *in vivo* proximity ligation. *Nat. Microbiol*, 2, 16239. doi: 10.1038/nmicrobiol.2016.239.

Hantke, K. (2001) Iron and metal regulation in bacteria. *Curr. Opin. Microbiol*, 4, 172–177. doi: 10.1016/S1369-5274(00)00184-3

Henkin, T.M. (2008) Riboswitch RNAs: using RNA to sense cellular metabolism. *Genes Dev*, 22, 3383–3390. doi: 10.1101/gad.1747308

Hérault, E., Reverchon, S., and Nasser, W. (2014) Role of the LysR-type transcriptional regulator PecT and DNA supercoiling in the thermoregulation of pel genes, the major virulence factors in *Dickeya dadantii*. *Environ. Microbiol*, 16, 734–745. doi: 10.1111/1462-2920.12198

Hoeppner, M.P. Gardner, P.P. and Poole, A.M. (2012) Comparative analysis of RNA families reveals distinct repertoires for each domain of life. *PLoS Comput. Biol*, 8, e1002752. doi: 10.1371/journal.pcbi.1002752

Holmqvist, E. and Wagner, E.G.H. (2017) Impact of bacterial sRNAs in stress responses. *Biochem. Soc. T*, 45, 1203-1212. doi: 10.1042/BST20160363

Holmqvist, E., Reimegård, J., Sterk, M., Grantcharova, N., Römling, U. and Wagner, E.G. (2010) Two antisense RNAs target the transcriptional regulator CsgD to inhibit curli synthesis. *EMBO J*, 29, 1840–1850. doi: 10.1038/emboj.2010.73

Holmqvist, E., Wright, P.R., Li, L.; Bischler, T., Barquist, L., Reinhardt, R., Backofen, R. and Vogel, J. (2016) Global RNA recognition patterns of post-transcriptional regulators Hfq and CsrA revealed by UV crosslinking *in vivo*. *EMBO J*, 35, 991–1011. doi: 10.15252/embj.201593360

Hu, Y., Zhang, L., Wang, X., Sun, F., Kong, X., Dong, H. and Xu, H. (2018) Two virulent sRNAs identified by genomic sequencing target the type III secretion system in rice bacterial blight pathogen. *BMC Plant Biol*, 18, 237 doi: 10.1186/s12870-018-1470-7

Hussein, R. and Lim, H.N. (2011) Disruption of small RNA signaling caused by competition for Hfq. *Proc. Natl. Acad. Sci. USA*, 108, 1110–1115. doi: 10.1073/pnas.1010082108

Ikeda, Y., Yagi, M., Morita, T. and Aiba, H. (2011) Hfq binding at RhlB recognition region of RNase E is crucial for the rapid degradation of mRNAs mediated by sRNAs in *Escherichia coli*. *Mol. Microbiol,* 79, 419-432. doi: 10.1111/j.1365-2958.2010.07454.x

Imlay, J.A. (2013) The molecular mechanisms and physiological consequences of oxidative stress: lessons from a model bacterium. *Nat. Rev. Microbiol*, 11, 443–454. doi: 10.1038/nrmicro3032

Kaito, C., Saito, Y., Nagano, G., Ikuo, M., Omae, Y., Hanada, Y., Han, X., Kuwahara-Arai, K., Hishinuma, T., Baba, T., Ito, T., Hiramatsu, K. and Sekimizu, K. (2011) Transcription and translation products of the cytolysin gene psm-mec on the mobile genetic element SCCmec regulate *Staphylococcus aureus virulence*. *PLoS Pathog,* 7, e1001267. doi: 10.1371/journal.ppat.1001267

Kambach, C., Walke, S., Young, R., Avis, J.M., de la Fortelle, E., Raker, V.A., Lührmann, R., Li, J. and Nagai, K. (1999) Crystal structures of two Sm protein complexes and their implications for the assembly of the spliceosomal snRNPs. *Cell*; 96, 375-87. doi: 10.1016/S0092-8674(00)80550-4

Kang, Y., Weber, K.D., Qiu, Y., Kiley, P.J. and Blattner, F.R. (2005) Genome-wide expression analysis indicates that FNR of *Escherichia coli* K-12 regulates a large number of genes of unknown function. *J. Bacteriol,* 187, 1135–1160. doi: 10.1128/JB.187.3.1135-1160.2005

Kavita, K., de Mets, F. and Gottesman, S. (2018) New aspects of RNA-based regulation by Hfq and its partner sRNAs. *Curr. Opin. Microbiol,* 42, 53–61. doi: 10.1016/j.mib.2017.10.014

Kay, E., Humair, B., Denervaud, V., Riedel, K., Spahr, S., Eberl, L., Valverde, C. and Haas, D. (2006) Two GacA-dependent small RNAs modulate the quorum-sensing response in *Pseudomonas aeruginosa*. *J. Bacteriol*, 188, 6026-6033. doi: 10.1128/JB.00409-06

Kido, K., Adachi, R., Hasegawa, M., Yano, K., Hikichi, Y., Takeuchi, S., Atsuchi, T. and Takikawa, Y. (2008) Internal fruit rot of netted melon caused by *Pantoea ananatis* (=*Erwinia ananas*) in Japan. *J. Gen. Plant Pathol*, 74, 302–312. doi: 10.1007/s10327-008-0107-3

Kim, K. Palmer, A.D. Vanderpool, C.K. and Slauch, J.M. (2019) The Small RNA PinT Contributes to PhoP-Mediated Regulation of the *Salmonella* Pathogenicity Island 1 Type III Secretion System in *Salmonella enterica* Serovar Typhimurium. *J. Bacteriol,* 201, e00312-19. doi: 10.1128/JB.00312-19

Klein, G. and Raina, S. (2015). Regulated control of the assembly and diversity of LPS by noncoding sRNAs. *Biomed. Res. Int*, 2015:153561. doi: 10.1155/2015/153561

Lalaouna, D., Carrier, M-C., Semsey, S., Brouard, J-S.,Wang, J., Wade, J.T. and Massé, E. (2015) A 3' external transcribed spacer in a tRNA transcript acts as a sponge for small RNAs to prevent transcriptional noise. *Mol. Cell*, 58, 393–405. doi: 10.1016/j.molcel.2015.03.013

Laubacher, M.E. and Ades, S.E. (2008) The Rcs phosphorelay is a cell envelope stress response activated by peptidoglycan stress and contributes to intrinsic antibiotic resistance. *J. Bacteriol*, 190, 2065–2074. doi: 10.1128/JB.01740-07

Lee, J-H. and Zhao, Y. (2016) Integration host factor is required for RpoN-dependent *hrpL* gene expression and controls motility by positively regulating *rsmB* sRNA in *Erwinia amylovora*. *Phytopathology*, 106, 29-36. doi: 10.1094/PHYTO-07-15-0170-R

Lenz, D.H., Miller, M.B., Zhu, J, Kulkarni, R.V. and Bassler, B.L. (2005) CsrA and three redundant small RNAs regulate quorum sensing in *Vibrio cholerae*. *Mol. Microbiol*, 58, 1186-1202. doi: 10.1111/j.1365-2958.2005.04902.x

Lenz, D.H., Mok, K.C., Lilley, B.N., Kulkarni, R.V., Wingreen, N.S. and Bassler, B.L: (2004) The small RNA chaperone Hfq and multiple small RNAs control quorum sensing in *Vibrio harveyi* and *Vibrio cholerae*. *Cell*, 118, 69-82. doi: 10.1016/j.cell.2004.06.009

Li, G.M. (2008) Mechanisms and functions of DNA mismatch repair. *Cell Res*, 18, 85–98. doi: 10.1038/cr.2007.115

Lima, S., Guo, M.S., Chaba, R., Gross, C.A. and Sauer, R.T. (2013) Dual molecular signals mediate the bacterial response to outer-membrane stress. *Science*, 340, 837–841. doi: 10.1126/science.1235358

Link, T.M., Valentin-Hansen, P. and Brennan, R.G. (2009) Structure of *Escherichia coli* Hfq bound to polyriboadenylate RNA. *Proc. Natl. Acad. Sci. USA*, 106, 19292-7. doi: 10.1073/ pnas.0908744106

Liu, X. and De Wulf, P. (2004) Probing the ArcA-P modulon of *Escherichia coli* by whole genome transcriptional analysis and sequence recognition profiling. *J. Biol. Chem*, 279, 12588–12597. doi: 10.1074/jbc.M313454200

Lostroh, C.P. and Lee, C.A (2001) The *Salmonella* Pathogenicity Island 1 type III secretion system. *Microb. Infect*, 3, 14-15. doi: 10.1016/S1286-4579(01)01488-5

Majdalani, N. and Gottesman, S. (2005) The Rcs phosphorelay: a complex signal transduction system. *Annu. Rev. Microbiol*, 59, 379–405. doi: 10.1146/annurev.micro.59.050405.101230

Majdalani, N. Vanderpool, C.K. and Gottesman, S. (2005) Bacterial small RNA regulators. *Crit. Rev. Biochem. Mol. Biol*, 40, 93-113, doi: 10.1080/10409230590918702

Majdalani, N., Chen, S., Murrow, J., St John, K. and Gottesman, S. (2001) Regulation of RpoS by a novel small RNA: the characterization of RprA. *Mol. Microbiol*, 39, 1382–1394. doi: 10.1111/j.1365-2958.2001.02329.x

Mandal, M. and Breaker, R. R. (2004) Gene regulation by riboswitches. *Nat. Rev. Mol. Cell Biol*, 5, 451-463. doi: 10.1038/nrm1403

Mandin, P. and Gottesman, S. (2010) Integrating anaerobic/aerobic sensing and the general stress response through the ArcZ small RNA. *EMBO J*, 29, 3094–3107. doi: 10.1038/emboj.2010.179

Mangold, M., Siller, M., Roppenser, B., Vlaminck, B.J.,Penfound, T.A., Klein, R., Novak, R., Novick, R.P. and Charpentier, E. (2004) Synthesis of group A streptococcal virulence factors is controlled by a regulatory RNA molecule. *Mol. Microbiol*, 53, 1515–1527. doi: 10.1111/j.1365-2958.2004.04222.x

Massé, E. and Gottesman, S. (2002) A small RNA regulates the expression of genes involved in iron metabolism in *Escherichia coli*. *Proc. Natl. Acad. Sci. USA*, 99:4620–4625. doi: 10.1073/pnas.032066599

Massé, E., Escorcia, F.E. and Gottesman, S. (2003) Coupled degradation of a small regulatory RNA and its mRNA targets in *Escherichia coli*. *Genes Dev*, 17, 2374–238. doi: 10.1101/gad.1127103

Massé, E., Vanderpool, C.K. and Gottesman, S. (2005) Effect of RyhB small RNA on global iron use in *Escherichia coli*. *J. Bacteriol*, 187, 6962–6971. doi: 10.1128/JB.187.20.6962-6971.2005

Melamed, S., Peer, A., Faigenbaum-Romm, R., Gatt, Y.E., Reiss, N., Bar, A., Altuvia, Y., Argaman, L. and Margalit, H. (2016) Global mapping of small RNA–target interactions in bacteria. *Mol. Cell*, 63, 884-897. doi: 10.1016/j.molcel.2016.07.026

Mergaert, J., Verdonck, L. and Kersters, K. (1993) Transfer of *Erwinia ananas* (synonym, *Erwinia uredovora*) and *Erwinia stewartii* to genus *Pantoea* emend. as *Pantoea ananas*

(Serrano 1928) comb. nov. and *Pantoea stewartii* (Smith 1898) comb. nov., respectively, and description of *Pantoea stewartii* subsp. *indologenes* subsp. nov. *Int. J. Sys. Bacteriol*, 43, 162-173. doi: 10.1099/00207713-43-1-162

Mettert, E.L. and Kiley, P.J. (2015) How is Fe-S cluster formation regulated? *Annu. Rev. Microbiol*, 69, 505–526. doi: 10.1146/annurev-micro-091014-104457

Mika, F. and Hengge, R. (2013) Small regulatory RNAs in the control of motility and biofilm formation in *E. coli* and *Salmonella*. *Int. J. Mol. Sci*, 14, 4560–4579. doi: 10.3390/ijms14034560

Mika, F., Busse, S., Possling, A., Berkholz, J., Tschowri, N., Sommerfeldt, N., Pruteanu, M. and Hengge, R. (2012) Targeting of *csgD* by the small regulatory RNA RprA links stationary phase, biofilm formation and cell envelope stress in *Escherichia coli*. *Mol. Microbiol*, 84, 51–65. doi: 10.1111/j.1365-2958.2012.08002.x

Mikulecky, P.J., Kaw, M.K., Brescia, C.C., Takach, J.C., Sledjeski, D.D. and Feig, A.L. (2004) *Escherichia coli* Hfq has distinct interaction surfaces for DsrA, rpoS and poly(A) RNAs. *Nat. Struct. Mol. Biol;* 11:1206-14. doi: 10.1038/nsmb858

Miyakoshi, M., Chao, Y. and Vogel, J. (2015) Cross talk between ABC transporter mRNAs via a target mRNA derived sponge of the GcvB small RNA. *EMBO J*, 34, 1478–92. doi: 10.15252/embj.201490546

Miyakoshi, M., Chao, Y. and Vogel, J. (2015) Regulatory small RNAs from the 3’ regions of bacterial mRNAs. *Curr. Opin. Microbiol,* 24, 132–139. doi: 10.1016/j.mib.2015.01.013

Mohanty, B. K., Maples, V. F. and Kushner, S. R. (2004) The Sm-like protein Hfq regulates polyadenylation-dependent mRNA decay in *Escherichia coli*. *Mol. Microbiol,* 54, 905–920. doi: 10.1111/j.1365-2958.2004.04337.x

Møller, T., Franch, T., Højrup, P., Keene, D.R., Bächinger, H.P., Brennan, R.G. and Valentin-Hansen, P. (2002). Hfq: a bacterial Sm-like protein that mediates RNA-RNA interaction. *Mol. Cell*, 9, 23–30. doi: 10.1016/s1097-2765(01)00436-1

Moon, K. and Gottesman, S. (2011) Competition among Hfq-binding small RNAs in *Escherichia coli*. *Mol. Microbiol,* 82, 1545–1562. doi: 10.1111/j.1365-2958.2011.07907.x

Morfeldt, E., Taylor, D., von Gabain, A. and Arvidson, S. (1995) Activation of alpha-toxin translation in *Staphylococcus aureus* by the trans-encoded antisense RNA, RNAIII. *EMBO J,* 14, 4569–4577. doi: 10.1002/j.1460-2075.1995.tb00136.x

Morita, T., Maki, K. and Aiba, H. (2005) RNase E-based ribonucleoprotein complexes: mechanical basis of mRNA destabilization mediated by bacterial noncoding RNAs. *Genes Dev,* 19, 2176–2186. doi: 10.1101/gad.1330405

Morohoshi, T., Nakamura, Y., Yamazaki, G., Ishida, A., Kato, N. and Ikeda, T. (2007) The plant pathogen *Pantoea ananatis* produces N-acylhomoserine lactone and causes center rot disease of onion by quorum sensing. *J. Bacteriol*, 189, 8333-8338. doi: 10.1128/JB.01054-07

Mura, C., Phillips, M., Kozhukhovsky, A. and Eisenberg, D. (2003) Structure and assembly of an augmented Sm-like archaeal protein 14-mer. *Proc. Natl. Acad. Sci. USA*, 100, 4539-44. doi: 10.1073/pnas.0538042100

Nakatsu, Y., Matsui, H., Yamamoto, M., Noutoshi, Y., Toyoda, K. (2019) Quorum-dependent expression of *rsmX* and *rsmY*, small non-coding RNAs, in *Pseudomonas syringae*. *Microbiol. Res*, 223-225, 72-78. doi: 10.1016/j.micres.2019.04.004

Nikaido, H. and Nakae, T. (1980).The outer membrane of Gram-negative bacteria. *Adv. Microb. Physiol*, 20, 163–250. doi:10.1016/s0065-2911(08)60208-8

Nikulin, A., Mikhailina, A., Lekontseva, N., Balobanov, V., Nikonova, E. and Tishchenko, S. (2017) Characterization of RNA-binding properties of the archaeal Hfq-like protein from *Methanococcus jannaschii*. *J. Biomol. Struct. Dyn*, 35, 1615–1628. doi: 10.1080/07391102.2016.1189849

Ochman, H., Lawrence, J. G. and Groisman, E. (2000) Lateral gene transfer and the nature of bacterial innovation, *Nature*, 405, 299–304. doi: 10.1038/35012500

Olsen, A.S., Moller-Jensen, J., Brennan, R.G. and Valentin-Hansen, P. (2010) C-terminally truncated derivatives of *Escherichia coli* Hfq are proficient in riboregulation. *J. Mol. Biol*, 404, 173–182. doi: 10.1016/j.jmb.2010.09.038

Otaka, H., Ishikawa, H., Morita, T. and Aiba, H. (2011) PolyU tail of rho-independent terminator of bacterial small RNAs is essential for Hfq action. *Proc. Natl. Acad. Sci. USA*, 108, 13059-64.doi: 10.1073/pnas.1107050108

Overgaard, M., Johansen, J., Møller-Jensen, J. and Valentin-Hansen, P. (2009) Switching off small RNA regulation with trap-mRNA. *Mol. Microbiol,* 73, 790–800. doi: 10.1111/j.1365-2958.2009.06807.x

Paccola-Meirelles, L.D., Ferreira, A.S., Meirelles, W.F., Marriel, I.E. and Casela, C.R. (2001) Detection of a bacterium associated with a leaf spot disease of maize in Brazil. *J. Phytopathol,* 149, 275-279. doi: 10.1046/j.1439-0434.2001.00614.x

Panja, S., Schu, D. J. and Woodson, S.A. (2013) Conserved arginines on the rim of Hfq catalyze base pair formation and exchange. *Nucleic Acids Res,* 41, 7536–7546. doi: 10.1093/nar/gkt521

Papenfort, K. and Bassler, B. L. (2016) Quorum sensing signal – response systems in Gram-negative bacteria. *Nat. Rev. Microbiol*, 14, 576–588. doi: 10.1038/nrmicro.2016.89

Papenfort, K. and Vogel, J. (2014) Small RNA functions in carbon metabolism and virulence of enteric pathogens. *Front. Cell. Infec. Microbiol,* 4, 1–12. doi: 10.3389/fcimb.2014.00091

Park, S.H., Bao, Z., Butcher, B.G., D'Amico, K., Xu, Y., Stodghill, P., Schneider, D.J., Cartinhour, S. and Filiatrault, M.J. (2014) Analysis of the small RNA *spf* in the plant pathogen *Pseudomonas syringae* pv. tomato strain DC3000. *Microbiol*, 160, 941-953. doi: 10.1099/mic.0.076497-0

Park, S.H., Butcher, B.G., Anderson, Z., Pellegrini, N., Bao, Z., D'Amicol, K. and Filiatrault, M.J. (2013) Analysis of the small RNA *P16/RgsA* in the plant pathogen *Pseudomonas syringae* pv. tomato strain DC3000. *Microbiol*, 159, 296-306. doi: 10.1099/mic.0.063826-0

Pérez-y-Terrón, R., Villegas, M.C., Cuellar, A., Muñoz-Rojas, J., Castañeda-Lucio, M., Hernández-Lucas, I., Bustillos-Cristales, R., Bautista-Sosa, L., Munive, J.A., Caicedo-Rivas, R. and Fuentes-Ramírez, L.E. (2009). Detection of *Pantoea ananatis*, causal agent of leaf spot disease of maize, in Mexico. *Australas. Plant Dis. Notes*, 4, 96–99.

Pfeiffer, V., Papenfort, K., Lucchini, S., Hinton, J. C. and Vogel, J. (2009). Coding sequence targeting by MicC RNA reveals bacterial mRNA silencing downstream of translational initiation. *Nat. Struct. Mol. Biol*, 16, 840–846. doi: 10.1038/nsmb.1631

Pfeiffer, V., Sittka, A., Tomer, R., Tedin, K., Brinkmann, V. and Vogel, J. (2007) A small non-coding RNA of the invasion gene island (SPI-1) represses outer membrane protein synthesis from the *Salmonella* core genome. *Mol Microbiol* 66, 1174–1191. doi: 10.1111/j.1365-2958.2007.05991.x

Pratt, L.A., Hsing, W. Gibson, K.E. and Silhavy, T.J. (1996) From acids to *osmZ*: multiple factors influence synthesis of the OmpF and OmpC porins in *Escherichia coli*. *Mol. Microbiol,* 20, 911–917. doi: 10.1111/j.1365-2958.1996.tb02532.x

Prévost, K., Salvail, H., Desnoyers, G., Jacques, J.F., Phaneuf, E. and Massé, E. (2007) The small RNA RyhB activates the translation of *shiA* mRNA encoding a permease of shikimate, a compound involved in siderophore synthesis. *Mol. Microbiol*, 64, 1260–1273. doi: 10.1111/j.1365-2958.2007.05733.x

Raivio, T.L. and Silhavy, T.J. (1997) Transduction of envelope stress in *Escherichia coli* by the Cpx two-component system. *J. Bacteriol*, 179, 7724–7733. doi: 10.1128/jb.179.24.7724-7733.1997

Raivio, T.L. Popkin, D.L. and Silhavy, T.J. (1999) The Cpx envelope stress response is controlled by amplification and feedback inhibition. *J. Bacteriol*, 181, 5263–5272.

Ray-Soni, A., Bellecourt, M.J. and Landick, R. (2016) Mechanisms of bacterial transcription termination: all good things must end. *Annu. Rev. Biochem*, 85, 319–347. doi: 10.1146/annurev-biochem-060815-014844

Rhodius, V.A., Suh, W.C., Nonaka, G., West, J. and Gross, C.A. (2006) Conserved and variable functions of the σ^E stress response in related genomes. *PLoS Biol*, 4:e2. doi: 10.1371/journal.pbio.0040002. doi: 10.1371/journal.pbio.0040002

Rutherford, S.T., van Kessel, J.C., Shao, Y. and Bassler, B.L. (2011) AphA and LuxR/HapR reciprocally control quorum sensing in vibrios. *Genes Dev*, 25, 397–408. doi: 10.1101/gad.2015011

Saliba, A-E., Santos, C.S. and Vogel, J. (2017) New RNA-seq approaches for the study of bacterial pathogens. *Curr. Opin. Microbiol*, 35, 78–87. doi: 10.1016/j.mib.2017.01.001.

Salmon, K., Hung, S.P., Mekjian, K., Baldi, P., Hatfield, G.W. and Gunsalus, R.P. (2003) Global gene expression profiling in *Escherichia coli* K12. The effects of oxygen availability and FNR. *J. Biol. Chem*, 278, 29837–29855. doi: 10.1074/jbc.M213060200

Salvail, H., Caron, M-P., Bélanger, J. and Massé, E. (2013) Antagonistic functions between the RNA chaperone Hfq and an sRNA regulate sensitivity to the antibiotic colicin. *EMBO J*, 32, 2764–2778. doi: 10.1038/emboj.2013.205

Santagelo, T.J. and Artsimovitch, I. (2011) Termination and antitermination: RNA polymerase runs a stop sign. *Nat. Rev. Microbiol*, 9, 319-329. doi: 10.1038/nrmicro2560

Santiago-Frangos, A. and Woodson, S.A. (2018) Hfq chaperone brings speed dating to bacterial sRNA, *Wiley Interdiscip. Rev. RNA*, 9, 1–16. doi: 10.1002/wrna.1475

Santiago-Frangos, A., Jeliazkov, J.R., Gray, J.J. and Woodson, S.A. (2017) Acidic C-terminal domains autoregulate the RNA chaperone Hfq. *eLife*, 6. doi: 10.7554/eLife.27049

Santiago-Frangos, A., Kavita, K., Schu, D.J., Gottesman, S. and Woodson, S.A. (2016) C-terminal domain of the RNA chaperone Hfq drives sRNA competition and release of target RNA. *Proc. Natl. Acad. Sci. USA*, 113(41), E6096. doi: 10.1073/pnas.1613053113

Sauer, E. and Weichenrieder, O. (2011) Structural basis for RNA 3'-end recognition by Hfq. *Proc. Natl. Acad. Sci. USA*, 108, 13065-70. doi: 10.1073/pnas.1103420108

Sauer, E., Schmidt, S. and Weichenrieder, O. (2012) Small RNA binding to the lateral surface of Hfq hexamers and structural rearrangements upon mRNA target recognition. *Proc. Natl. Acad. Sci. USA*, 109:9396-401. doi: 10.1073/pnas.1202521109

Schachterle, J.K., Zeng, Q. and Sundin, G.W. (2019) Three Hfq-dependent small RNAs regulate flagellar motility in the fire blight pathogen *Erwinia amylovora*. *Mol. Microbiol*, 111, 1476-1492. doi: 10.1111/mmi.14232

Schlötterer, C. (2015) Genes from scratch - the evolutionary fate of *de novo* genes. *Trends Genet*, 31, 215–219. doi: 10.1016/j.tig.2015.02.007

Schmidtke, C., Abendroth, U., Brock, J., Serrania, J., Becker, A. and Bonas, U. (2013) Small RNA sX13: A multifaceted regulator of virulence in the plant pathogen *Xanthomonas*. *PLoS Pathog*, 9, e1003626. doi: 10.1371/journal.ppat.1003626

Schu, D.J., Zhang, A., Gottesman, S. and Storz, G. (2015) Alternative Hfq-sRNA interaction modes dictate alternative mRNA recognition. *EMBO J*, 34, 2557–2573. doi: 10.15252/embj.201591569

Sedlyarova, N., Shamovsky, I., Bharati, B.K., Epshtein, V., Chen, J., Gottesman, S., Schroeder, R. and Nudler, E. (2016) sRNA-mediated control of transcription termination in *E. coli*. *Cell*, 167, 111–21.e13. doi: 10.1016/j.cell.2016.09.004

Sharma, C.M., Darfeuille, F., Plantinga, T.H. and Vogel, J. (2007) A small RNA regulates multiple ABC transporter mRNAs by targeting C/A-rich elements inside and upstream of ribosome-binding sites. *Genes Dev*, 21, 2804–17. doi: 10.1101/gad.447207

Sharma, C.M., Hoffmann, S., Darfeuille, F., Reignier, J., Findeiß, S., Sittka, A., Chabas, S., Reiche, K., Hackermüller, J., Reinhardt, R., Stadler, P.F. and Vogel, J. (2010) The primary transcriptome of the major human pathogen *Helicobacter pylori*. *Nature*, 464, 250–255. doi: 10.1038/nature08756

Shyntum, D.Y., Theron, J., Venter, S.N., Moleleki, L.N., Toth, I. K. and Coutinho, T. A. (2015) *Pantoea ananatis* utilizes a type VI secretion system for pathogenesis and bacterial competition. *Mol. Plant-Microbe Interact*, 28, 420-431. doi: 10.1094/MPMI-07-14-0219-R

Shyntum, D.Y., Venter, S.N., Moleleki, L.N., Toth, I. and Coutinho, T.A. (2014) Comparative genomics of type VI secretion systems in strains of *Pantoea ananatis* from different environments. *BMC Genomics* 15, 163–178. doi: 10.1186/1471-2164-15-163

Sibanda, S., Kwenda, S., Tanui, C.K., Shyntum, D.Y., Coutinho, T.A. and Moleleki, L.N. (2018) Transcriptome profiling reveals the EanI/R quorum sensing regulon in *Pantoea ananatis* LMG 2665^{T}. *Genes*, 9, 1–17. doi: 10.3390/genes9030148

Sibanda, S., Theron, J., Shyntum, D.Y., Moleleki, L.N. and Coutinho, T.A. (2016) Characterization of two LuxI/R homologs in *Pantoea ananatis* LMG 2665^{T}. *Can. J. Microbiol*, 62, 893-903. doi: 10.1139/cjm-2016-0143

Sittka, A., Lucchini, S., Papenfort, K., Sharma, C.M., Rolle, K., Binnewies, T.T., Hinton, J.C.D. and Vogel, J. (2008) Deep sequencing analysis of small noncoding RNA and mRNA targets of the global post-transcriptional regulator, Hfq. *PLoS Genet*, 4, e1000163. doi: 10.1371/journal.pgen.1000163

Skovierova, H., Rowley, G., Rezuchova, B., Homerova, D., Lewis, C., Roberts, M. and Kormanec, J. (2006) Identification of the σ^{E} regulon of *Salmonella enterica* serovar *Typhimurium*. *Microbiol*, 152, 1347–1359. doi: 10.1099/mic.0.28744-0

Smirnov, A., Forstner, K.U., Holmqvist, E., Otto, A., Gunster, R., Becher, D., Reinhardt, R. and Vogel, J. (2016) Grad-seq guides the discovery of ProQ as a major small RNA-binding protein. *Proc. Natl. Acad. Sci. USA*, 113, 11591-11596. doi: 10.1073/pnas.1609981113

Sonnleitner, E. and Haas, D. (2011) Small RNAs as regulators of primary and secondary metabolism in *Pseudomonas* species. *Appl. Microbiol. Biotechnol*, 91, 63-79. doi: 10.1007/s00253-011-3332-1.

Soutourina, O.A. and Bertin, P.N. (2003) Regulation cascade of flagellar expression in Gram-negative bacteria. *FEMS Microbiol. Rev*, 27, 505–523. doi: 10.1016/S0168-6445(03)00064-0

Srikumar, S., Kroger, C., Hebrard, M., Colgan, A., Owen, S.V., Sivasankaran, S.K., Cameron, A.D., Hokamp, K. and Hinton, J.C. (2015) RNA-seq brings new insights to the intra-macrophage transcriptome of *Salmonella Typhimurium. PLoS Pathog*, 11:e1005262. doi: 10.1371/journal.ppat.1005262.

Stice, S.P., Stumpf, D.S., Gitaitis, R.D. Kvitko, B.H. and Dutta, B. (2018) *Pantoea ananatis* genetic diversity analysis reveals limited genomic diversity as well as accessory genes correlated with onion pathogenicity. *Front. Microbiol*, 9, 1–18. doi: 10.3389/fmicb.2018.00184

Storz, G., Opdyke, J.A. and Zhang, A. (2004) Controlling mRNA stability and translation with small, noncoding RNAs. *Curr. Opin. Microbiol*, 7, 140–144. doi: 10.1016/j.mib.2004.02.015

Thomason, M.K., Fontaine, F., De Lay, N. and Storz, G. (2012) A small RNA that regulates motility and biofilm formation in response to changes in nutrient availability in *Escherichia coli*. *Mol. Microbiol*, 84, 17–35. doi: 10.1111/j.1365-2958.2012.07965.x

Tree, J.J., Granneman, S., McAteer, S.P., Tollervey, D. and Gally, D.L. (2014) Identification of bacteriophage encoded anti-sRNAs in pathogenic *Escherichia coli*. *Mol. Cell*, 55, 199–213. doi: 10.1016/j.molcel.2014.05.006

Tsui, H.C., Leung, H.C. and Winkler, M.E. (1994). Characterization of broadly pleiotropic phenotypes caused by an *hfq* insertion mutation in *Escherichia coli* K-12. *Mol. Microbiol*, 13, 35–49. doi: 10.1111/j.1365-2958.1994.tb00400.x

Tu, K.C. and Bassler, B.L. (2007) Multiple small RNAs act additively to integrate sensory information and control quorum sensing in *Vibrio harveyi*. *Genes Dev*, 21, 221-233. doi: 10.1101/gad.1502407

Unden, G. and Schirawski, J. (1997) The oxygen-responsive transcriptional regulator FNR of *Escherichia coli* : the search for signals and reactions. *Mol. Microbiol*, 25, 205–210. doi: 10.1046/j.1365-2958.1997.4731841.x

Unden, G., Becker, S., Bongaerts, J., Schirawski, J. and Six, S. (1994) Oxygen regulated gene expression in facultatively anaerobic bacteria. *Ant. van Leeuwen*, 66**:** 3–23. doi: 10.1007/BF00871629

Updegrove, T.B. and Wartell, R.M. (2011) The influence of *Escherichia coli* Hfq mutations on RNA binding and sRNA*mRNA duplex formation in *rpoS* riboregulation. *Biochim. Biophys. Acta*, 1809, 532–540. doi: 10.1016/j.bbagrm.2011.08.006

Updegrove, T.B., Shabalina, S.A. and Storz, G. (2015) How do base-pairing small RNAs evolve? *FEMS Microbiol. Rev*, 39, 379-391. doi: 10.1093/femsre/fuv014

Urban, J. H. and Vogel, J. (2007) Translational control and target recognition by *Escherichia* coli small RNAs *in vivo*. *Nucleic Acids Res*, 35, 1018–1037. doi: 10.1093/nar/gkl1040

Vakulskas, C.A., Potts, A.H., Babitzke, P., Ahmer, B.M.M. and Romeo, T. (2015) Regulation of bacterial virulence by Csr (Rsm) Systems. *Microbiol. Mol. Biol. Rev*, 79, 193-223. doi: 10.1128/MMBR.00052-14

Vanderpool, C.K. and Gottesman, S. (2004) Involvement of a novel transcriptional activator and small RNA in post-transcriptional regulation of the glucose phosphoenolpyruvate phosphotransferase system. *Mol. Microbiol*, 54, 1076–1089. doi: 10.1111/j.1365-2958.2004.04348.x

Vecerek, B., Rajkowitsch, L., Sonnleitner, E., Schroeder, R. and Bläsi, U. (2008) The C-terminal domain of *Escherichia coli* Hfq is required for regulation. *Nucleic Acids Res*, 36, 133-43. doi: 10.1093/nar/gkm985

Vogel, J. (2009) A rough guide to the non-coding RNA world of *Salmonella*. *Mol. Microbiol*, 71, 1-11. doi: /10.1111/j.1365-2958.2008.06505.x.

Vogel, J. and Luisi, B.F. (2011) Hfq and its constellation of RNA. *Nat. Rev. Microbiol, 9*, 578. doi: 10.1038/nrmicro2615

Vogt, S.L., Evans, A.D., Guest, R.L. and Raivio, T.L. (2014) The Cpx envelope stress response regulates and is regulated by small noncoding RNAs. *J. Bacteriol*, 196, 4229–4238. doi: 10.1128/JB.02138-14

Vogt, S.L., Nevesinjac, A.Z., Humphries, R.M., Donnenberg, M.S., Armstrong, G.D. and Raivio, T.L. (2010) The Cpx envelope stress response both facilitates and inhibits elaboration

of the enteropathogenic *Escherichia coli* bundle-forming pilus. *Mol. Microbiol*, 76, 1095–1110. doi: 10.1111/j.1365-2958.2010.07145.x

Wagner, E.G. (2013) Cycling of RNAs on Hfq. *RNA Biol*, 10, 619–626. doi: 10.4161/rna.24044

Walterson, A.M. and Stavrinides, J. (2015) *Pantoea*: insights into a highly versatile and diverse genus within the *Enterobacteriaceae*. *FEMS Microbiol. Rev*, 39, 968-984. doi: 10.1093/femsre/fuv027.

Wang, C., Pu, T., Lou, W., Wang, Y., Gao, Z., Hu, B. and Fan, J. (2018) Hfq, a RNA chaperone, contributes to virulence by regulating plant cell wall–degrading enzyme production, type VI secretion system expression, bacterial competition, and suppressing host defense response in *Pectobacterium carotovorum*. *Mol*. *Plant-Microbe Interact.* doi: 10.1094/MPMI-12-17-0303-R.

Wang, L. Wang, F-F. and Qian, W. (2011) Evolutionary rewiring and reprogramming of bacterial transcription regulation. *J. Genet. Genomics*, 38, 279-288. doi: 10.1016/j.jgg.2011.06.001

Waters, C.M. and Bassler, B.L. (2005) Quorum sensing: cell-to-cell communication in bacteria. *Annu. Rev. Cell Dev. Biol*, 21, 319–346. doi: 10.1146/annurev.cellbio.21.012704.131001

Waters, L.S. and Storz, G. (2009) Regulatory RNAs in bacteria. *Cell*, 136, 615–628. doi: 10.1016/j.cell.2009.01.043

Waters, S.A., McAteer, S.P., Kudla, G., Pang, I., Deshpande, N.P., Amos, T.G., Leong, K.W., Wilkins, M.R., Strugnell, R., Gally, D.L., Tollervey, D. and Tree, J.J. (2017) Small RNA interactome of pathogenic *E. coli* revealed through crosslinking of RNase E. *EMBO J*, 36, 374-387. doi: 10.15252/embj.201694639.

Weller-Stuart, T., Toth, I., De Maayer, P. and Coutinho, T.A. (2016) Swimming and twitching motility are essential for attachment and virulence of *Pantoea ananatis* in onion seedlings. *Mol*. *Plant Pathol*, 18, 734-745. doi: 10.1111/mpp.12432

Wilusz, C.J. and Wilusz, J. (2013) Lsm proteins and Hfq. *RNA Biol*, 10, 592-601. doi: 10.4161/rna.23695

Yuan, X., Zeng, Q., Khokhani, D., Tian, F., Severin, G.B., Waters, C.M., Xu, J., Zhou, X., Sundin, G.W., Ibekwe, A.M., Liu, F., Yang, C.H. (2019) A feed-forward signalling circuit

controls bacterial virulence through linking cyclic-di-GMP and two mechanistically distinct sRNAs; ArcZ and RsmB. *Environ. Microbiol*, doi: 10.1111/1462-2920.14603

Zeng, Q. and Sundin, G.W. (2014) Genome-wide identification of Hfq-regulated small RNAs in the fire blight pathogen *Erwinia amylovora* discovered small RNAs with virulence regulatory function. *BMC Genomics*, 15, 414. doi: 10.1186/1471-2164-15-414

Zeng, Q., McNally, R. R. and Sundin, G. W. (2013) Global small RNA chaperone Hfq and regulatory small RNAs are important virulence regulators in *Erwinia amylovora. J. Bacteriol*, 195, 1706-1717. doi: 10.1128/JB.02056-12

Zhang, A., Altuvia, S., Tiwari, A., Argaman, L., Hengge-Aronis, R. and Storz, G. (1998) The OxyS regulatory RNA represses *rpoS* translation and binds the Hfq (HF-I) protein. *EMBO J*, 17, 6061–6068. doi: 10.1093/emboj/17.20.6061

Zhang, A., Wassarman, K.M., Ortega, J., Steven, A.C. and Storz, G. (2002). The Sm-like Hfq protein increases OxyS RNA interaction with target mRNAs. *Mol. Cell*, 9, 11–22. doi: 10.1016/s1097-2765(01)00437-3

Zhang, J. (2003) Evolution by gene duplication: an update. *Trends Ecol. Evol*, 18, 292-298. doi: 10.1016/S0169-5347(03)00033-8

Zhao, K., Liu, M. and Burgess, R.R. (2007) Adaptation in bacterial flagellar and motility systems: from regulon members to 'foraging'-like behavior in *E. coli*. *Nucleic Acids Res*, 35, 4441–4452. doi: 10.1093/nar/gkm456

Zhu, P.L., Zhao, S., Tang, .J.L. and Feng, J.X. (2011) The *rsmA* like gene *rsmA(Xoo*) of *Xanthomonas oryzae* pv. *oryzae* regulates bacterial virulence and production of diffusible signal factor. *Mol. Plant. Pathol*, 12, 227-37. doi: 10.1111/j.1364-3703.2010.00661.x

CHAPTER TWO

Functional Characterization of a Global Virulence Regulator Hfq and Identification of Hfq-dependent sRNAs in the Plant Pathogen *Pantoea ananatis*

Gi Yoon Shin[1, 2], Jeffrey K. Schachterle[3], Divine Y. Shyntum[2], Lucy N. Moleleki[2], Teresa A. Coutinho[1, 2]* and George W. Sundin[3]

[1]Centre for Microbial Ecology and Genomics, Forestry and Agricultural Biotechnology Institute, Department of Biochemistry, Genetics and Microbiology, University of Pretoria, Pretoria, Gauteng, Republic of South Africa

[2]Forestry and Agricultural Biotechnology Institute, Department of Biochemistry, Genetics and Microbiology, University of Pretoria, Pretoria, Gauteng, Republic of South Africa

[3]Department of Plant, Soil and Microbial Sciences, Michigan State University, East Lansing, MI, United States of America

This chapter has been prepared in the format of a manuscript that has been published in the peer-reviewed journal Frontiers in Microbiology and can be accessed under doi: 10.3389/fmicb.2019.02075.

2.1 ABSTRACT

To successfully infect plant hosts, the collective regulation of virulence factors in a bacterial pathogen is crucial. Hfq is an RNA chaperone protein that facilitates the small RNA (sRNA) regulation of global gene expression at the post-transcriptional level. In this study, the functional role of Hfq in a broad host range phytopathogen *Pantoea ananatis* was determined. Inactivation of the *hfq* gene in *P. ananatis* LMG 2665^{T} resulted in the loss of pathogenicity and motility. In addition, there was a significant reduction of quorum sensing signal molecule acyl-homoserine lactone (AHL) production and biofilm formation. Differential sRNA expression analysis between the *hfq* mutant and wild-type strains of *P. ananatis* revealed 276 sRNAs affected in their abundance by the loss of *hfq* at low (OD_{600} = 0.2) and high cell (OD_{600} = 0.6) densities. Further analysis identified 25 Hfq-dependent sRNAs, all showing a predicted Rho-independent terminator of transcription and mapping within intergenic regions of the *P. ananatis* genome. These included known sRNAs such as ArcZ, FnrS, GlmZ, RprA, RyeB, RyhB, RyhB2, Spot42, SsrA and 16 novel *P. ananatis* sRNAs. The current study demonstrated that Hfq is an important component of the collective regulation of virulence factors and sets a foundation for understanding Hfq-sRNA mediated regulation in the phytopathogen *P. ananatis*.

2.2 INTRODUCTION

Pantoea ananatis, formerly described as the pineapple pathogen *Erwinia ananas* (Serrano, 1928), is a gram-negative bacterium belonging to the family *Enterobacteriaceae*. To date, the occurrence of *P. ananatis* has been reported from various ecological niches spanning both the aquatic and terrestrial environments, including fresh (Morohoshi et al., 2007) and marine water (Jatt et al., 2014) as well as the rhizosphere of crop plants (Oliveira et al., 2008; Marquez-Santacruz et al., 2010). The bacterium exhibits ecologically-diverse roles in association with its environment. For example, *P. ananatis* can be found as an epiphyte of crop and weed plants (Gitatitis et al., 2002) or as an endophyte in maize kernels (Rijavec et al., 2007) and rice seeds (Okunishi et al., 2005). Moreover, the ability of *P. ananatis* to solubilize phosphate, and produce indole-acetic acid and siderophores, makes the bacterium an ideal plant growth-promoting agent in the production of pepper (Kang et al., 2007), soybean (Kuklinsky-Sobral et al., 2004) and sugarcane (da Silva et al., 2015).

Pantoea ananatis is better known as a phytopathogen affecting the yield of many economically-important plant species that causes blight and dieback of *Eucalyptus* (Coutinho et al., 2002), maize leaf spot disease and brown stalk rot (Goszczynska et al., 2006; Pérez-y-Terrón et al., 2009; Alippi and Lopez, 2010; Krawczyk et al., 2010), leaf blight and bulb rot of onion (Gitatitis and Gay, 1997; Schwartz and Otto, 2000; Goszczynska et al., 2007), palea browning and stem necrosis of rice (Azegami et al., 1983, Cother et al., 2004, Cortesi and Pizzatti, 2007), and fruit rot of netted melon (Kido et al., 2008). *P. ananatis* has also been considered an emerging plant pathogen due to increasing reports of disease outbreaks in the previously undescribed host and geographical regions (Coutinho and Venter, 2009). This emergence is likely to have resulted from the persistent nature of *P. ananatis* in diverse environments through its association with a wide range of non-host plants and even insect vectors (Gitaitis et al., 2003; Dutta et al., 2014).

The virulence factors that have been identified as necessary for the pathogenesis of *P. ananatis* in onion are motility for attachment (Weller-Stuart et al., 2016) and quorum sensing (QS) for production of biofilm and exopolysaccharide (EPS) (Morohoshi et al., 2007). In addition, genomic regions named ‘HiVir’ (Asselin et al., 2018) and ‘Onion Virulence Region’ (Stice et al., 2018), encoding enzymes catalysing phosphonate biosynthetic pathway and cell wall degradation, respectively, have been characterized in the onion pathogenic strains of *P. ananatis*. For successful infection by *P. ananatis*, rapid and collective expression of these

virulence genes in response to the surrounding environment is critical as it results in the modulation of cellular pathways that predisposes the pathogen for infection, pathogenesis and survival in the host.

Hfq is an RNA binding protein that constitutes a key component of post-transcriptional gene regulation exhibited by small non-coding regulatory RNAs (sRNAs) (Vogel and Luisi, 2011). Hfq is a ring-like homohexameric protein that was initially identified as a host factor needed for the replication of RNA bacteriophage Qβ (Franza de Fernandez et al., 1968). It is now known that the chaperone Hfq is essential for the structural stabilization of the class of *trans*-acting sRNAs whose regulatory mechanisms are dependent on Hfq (Updegrove et al., 2016). The chaperone facilitates imperfect base-pairing between the sRNA and its cognate messenger RNA (mRNA), forming an Hfq-sRNA-mRNA complex that determines the fate of target mRNA translation (Gottesman and Storz, 2011; Storz et al., 2011). Suppression of the protein synthesis is achieved by the formation of a sRNA-mRNA duplex at the 5' untranslated region (UTR) of the transcript by occlusion of ribosome binding and/or by recruiting ribonucleases for mRNA degradation (De Lay et al., 2013). Conversely, translation of the mRNA is enhanced by Hfq-sRNA complexes that alter the 5' secondary inhibitory structure of an mRNA, making it more accessible for initiation of translation.

Hfq-dependent sRNAs are typically 50 to 300 nucleotides in length and are *trans*-encoded from their cognate mRNAs. They are mostly found in, but not limited to, the intergenic regions of bacterial chromosomes (Argaman et al., 2001, Chao et al., 2012; Guo et al., 2014), and are characterized by often possessing a Rho-independent terminator at the 3' end, resulting in a poly-uridine tail of sRNA that are recognized by Hfq (Otaka et al., 2011). The cellular functions modulated by Hfq-sRNAs are diverse, ranging from cell membrane integrity, acquisition, and metabolism of nutrients, motility, secretion systems, stress response and virulence (Chao and Vogel, 2010). Their role in virulence regulation has been extensively studied in bacterial pathogens of animals. For example, in *Salmonella typhimurium*, motility and expression of the T3SS encoded within *Salmonella* pathogenicity island SPI-1 and SPI-2 are dependent on Hfq and contribute significantly to the adhesion and invasion of *Salmonella* into the host cells (Sittka et al., 2007, 2008) whereas in *Vibrio cholera*, Hfq and its *trans* acting sRNAs *Qrr* 1- 4 regulate cholera toxin (CT) biosynthesis (Bardill and Hammer, 2012) and QS as an ultrasensitive switch to transition *V. cholerae* from low to high cell density mode for colonization and disease development (Lenz et al., 2004).

Despite the growing evidence of Hfq and Hfq-dependent sRNAs as a global post-transcriptional gene regulatory complex, the functionality of Hfq and its *trans* acting sRNAs in plant pathogenic bacteria has only been investigated in a few bacterial species to date, namely in *Agrobacterium tumefaciens* (Wilms et al., 2012a, b), *Burkholderia glumae* (Kim et al., 2018), *Dickeya dadantii* (Yuan et al., 2019), *Erwinia amylovora* (Zeng et al., 2013, Zeng and Sundin, 2014), *Pectobacterium carotovorum* (Wang et al., 2018), and *Xanthomonas* spp. (Schmidtke et al., 2013). Consequently, the functional role of Hfq and the diversity of Hfq-dependent sRNAs in phytopathogens remains largely elusive. We hypothesized that Hfq and Hfq-dependent sRNAs would play a critical role in *P. ananatis* pathogenesis, through direct regulation of specific virulence traits and through regulation of QS system. In this study, we functionally characterized the role of Hfq as a regulator in the production of acyl-homoserine lactones (AHLs), biofilm development, motility, and virulence, and identified the Hfq-dependent sRNAs that are potentially implicated in the regulation of the virulence traits of the ubiquitous plant pathogen *P. ananatis*.

2.3 MATERIALS AND METHODS

2.3.1 Bacterial strains and growth conditions

The bacterial strains and plasmids used in this study are listed in Table 2.1. *Pantoea ananatis* LMG2665^T and *Escherichia coli* DH5α strains were cultured in Luria-Bertani (LB) broth (1% [w/v] NaCl, 1% [w/v] tryptone, 0.5% [w/v] yeast extract; pH 7.2) or on LB agar plates (LB broth amended with 1.5% [w/v] agar; pH 7.2) at 28℃ and 37℃, respectively. The growth medium was supplemented with either ampicillin (100 µg/ml), chloramphenicol (50 µg/ml), gentamicin (20 µg/ml), or kanamycin (50 µg/ml) for plasmid DNA selection and maintenance.

2.3.2 Generation of a *P. ananatis hfq* mutant and complemented strains

A mutant strain with chromosomal deletion of a single copy gene *hfq* (locus tag: PANA_RS17940) was constructed as previously described (Katashkina et al., 2009; Shyntum et al., 2015). The modification was made in the preparation of the knockout cassette which was amplified from the pKD13 plasmid using the Kan-F and Kan-R primers (Table 2.2) consisting of 50 bp homologous sequences of *hfq* flanking regions and 20 bp of kanamycin resistance gene priming sequences. The insertion of the kanamycin resistance gene was verified by Southern blotting, PCR amplification, and sequencing of the *hfq* region.

The promoter sequence of *hfq* determined in *E. coli* K12 MG1655 by Kim et al., (2012) was searched against the upstream sequence of the *hfq* start codon in *P. ananatis* LMG2665^T. An amplicon (1038 bp) containing the *hfq* gene (315 bp), its native promoter (58 bp) and flanking sequences (662 bp) were cloned into a pBBR1MCS-5_START vector (Obranić et al., 2013) restricted with SmaI and BamHI enzymes. Electrocompetent *hfq* deletion mutant *P. ananatis* was transformed with *hfq* complementing plasmid, pBBR1MCS::*hfq* and the resulting transformants were selected on the gentamicin amended LB agar. The integrity of the *hfq* complementation was determined by plasmid extraction, PCR and sequencing using Test-F and Test-R primers (Table 2.2).

2.3.3 *In vitro* and *in planta* growth assay

The growth of wild-type *P. ananatis* with an empty pBBR1MCS-5_START vector (WT), *hfq* deletion mutant with an empty pBBR1MCS-5_START vector (Δ*hfq*) and *hfq* complementing

pBBR1MCS-5_START::*hfq* (pBBR1MCS::*hfq*) strains of *P. ananatis* was monitored both *in vitro* and *in planta* conditions.

P. ananatis strains grown overnight in LB broth were normalized to an OD_{600nm} reading of 0.5. For *in vitro* growth assay, the normalized cultures were diluted 100 fold in fresh LB medium and incubated with shaking at 200 rpm. The absorbency of each culture was periodically measured. There were three replicates for each culture and the experiment was repeated twice.

The previously described red onion scale assay (Stice et al., 2018) was adapted for quantifying *in planta* growth of *P. ananatis* between the WT, Δ*hfq,* and *hfq* complementing strains. In summary, sliced red onion (*Allium cepa* L) scales of approximately 9 cm^2 in area were surface sterilized in 3% bleach solution for 1 min and were rinsed twice in distilled water. Each scale was inoculated with 1 µl of bacterial cells (1 X 10^7 CFU/ml) suspended in 1 X PBS (0.8% [w/v] NaCl, 0.02% [w/v] KCl, 0.144% [w/v] $NaHPO_4$, 0.024% KH_2PO_4; pH 7.4) using a sterile pipette tip. Inoculated scales were placed on moistened paper towels in a surface-sterilized container and were incubated at room temperature for 5 days. To quantify growth, three onion scales per strain were harvested at 24 h intervals. Each scale was macerated in 1 ml of 1 X PBS and the extract was serially diluted and cells were enumerated on LB supplemented with gentamicin. Experiments were repeated in triplicate, and the results were presented as CFU/g of onion tissue. Sterile water was used as a negative control.

2.3.4 Virulence assay

Virulence assay was performed as previously described for *in planta* growth assay. The vertical diameter of the water-soaked lesion on onion scales inoculated with WT, Δ*hfq* and *hfq* complementing *P. ananatis* strains was measured at three days post inoculation (dpi). The virulence assay was repeated twice, and there were three technical replicates for each *P. ananatis* strains.

2.3.5 Motility assay

Overnight cultures of *P. ananatis* strains (WT, Δ*hfq* and pBBR1MCS::*hfq*) were normalized to OD_{600nm} = 0.5 and 1 µl of each culture was inoculated in the centre of the soft agar (0.5% [w/v] NaCl, 1% [w/v] tyrptone and 0.3% [w/v] agar; pH 7.2). The inoculated plates were incubated at 28℃, and swimming motility was determined after 24 hr. Negative control plates were

inoculated with sterile water. The swimming motility experiment was repeated three times with three biological replicates in each experiment.

2.3.6 Bioassay detection of acyl-homoserine lactones (AHLs)

Formation of AHL by WT, Δ*hfq,* and *hfq* complementing strains of *P. ananatis* was determined using experimental procedures adapted from McClean et al., (1997). An aliquot (0.5 ml) of AHL reporter strain *Chromobacterium violaceum* (*C. violaceum* 026) grown in LB overnight was spread plated on LB agar plates and air-dried. Thereafter, three wells were (three replicates) created on each plate by puncturing the agar with a sterile cork-borer and inoculated with 100 µl of cell-free filtrate of *P. ananatis* WT, Δ*hfq* and *hfq* complementing strains overnight cultures. The inoculated plates were incubated at 28℃ for 48 h. The formation of violacein (purple halo) by CV026, around the inoculated wells was indicative of AHL production. The assay was repeated twice and carried out in three technical replicates.

2.3.7 Biofilm quantification

The biofilm of WT, Δ*hfq,* and *hfq* complementing strains of *P. ananatis* was quantified as previously described by Santander and Biosca, (2017) with slight modifications. An aliquot of 160 µl broth culture diluted to an OD_{600nm} of 0.5 in half-strength LB (0.5% [w/v] NaCl, 0.5% [w/v] tryptone, 0.25% [w/v] yeast extract; pH 7.2) was made into each well of a polystyrene 96-well microplate (Nunc™ MicroWell™, Thermo Scientific; Waltham, MA, USA) and incubated for 24 h under static conditions. Eight replicates per *P. ananatis* strain were included in each experiment with sterile half-strength LB broth serving as a negative control. Thereafter, the inoculated 96-well plates were inverted to remove the excess LB broth, air-dried and incubated at 60℃ for 40 min to heat-fix the biofilms. The biofilms were stained with 1% crystal violet (220 µl) for 15 min before being rinsed with distilled water. After rinsing and invert-air-drying the microplate, 220 µl of ethanol: acetone in 8:2 ratio was added to the wells to solubilize the crystal violet dye for 20 min at room temperature. The solubilized biofilm was measured at OD_{600} using Safire Microplate Reader (Tecan, Research Triangle Park, NC, USA), and this assay was repeated three times.

2.3.8 RNA extraction and transcriptomic analysis

Total RNA of *P. ananatis* WT and Δ*hfq* strains grown in LB broth was extracted at OD_{600nm} readings of 0.2 (T1 = low cell density) and 0.6 (T2 = high cell density) using the miRNeasy Mini kit (Qiagen; Hilden, Germany). Genomic DNA was removed by including an on-column DNase digestion step during the RNA extraction. The purity (A260/A280) of extracted RNA was measured by Nanodrop2000 (Thermo Scientific, Sugarland, TX, USA) and RNA integrity was determined by Agilent2100 Bioanalyzer (Agilent Technologies, Santa Clara, CA, USA). Illumina Truseq Small RNA Library (Illumina; San Diego, CA, USA) preparation was performed on the RNA samples, and deep sequencing of the library was conducted on Illumina HiSeq2500 platform (single-end, 1 X 50 bp) by Macrogen (South Korea).

2.3.9 Bioinformatic analysis and sRNA identification

Raw sequencing reads (BioProject accession number: PRJNA550544) were stringently trimmed and filtered using Trimmomatic (Bolger et al., 2014) to remove adapter sequences and low quality reads. Following adapter trimming and filtering, quality was verified using FastQC (Andrews, 2010) and reads were mapped to the *Pantoea ananatis* LMG20103 genome (De Maayer et al., 2010) using Bowtie2 (Langmead and Salzberg, 2012), as the genome of LMG 20103 was the only *P. ananatis* genome with a complete annotation at the time of analysis. For sRNA identification, a custom python script (script.pdf, see section genic_filter.py in supplementary material) was compiled to remove reads that mapped to coding sequences, ribosomal RNA and transfer RNA or within 120 bases upstream or downstream of these features from the resulting sequence alignment map (SAM) files. The purpose of the 120 base buffer was to reduce the number of sRNAs identified that originated from extended 5' or 3' UTR regions. All wild-type sequencing replicates from the same sampling time point were merged into a single gene-filtered SAM file for sRNA identification.

To identify putative sRNAs from gene-filtered SAM files, a custom python script (script.pdf, see section peak_ID.py in supplementary material) was used to calculate per base depth relative to the genome-wide per-base sequencing depth by replicate, which was also normalized to library size. A threshold of 10-fold increased abundance above background with a minimum length of 10 nucleotides was chosen for sRNA identification. Using the script, putative sRNAs at the low cell density and high cell density sampling time points were identified and the lists of sRNAs were merged using a custom python script (script.pdf, see section mergeList.py in

supplementary material), combining any overlapping identified sRNAs into a single sRNA to generate a single list of putative *P. ananatis* sRNAs (pPARs sRNA).

2.3.10 Computational prediction of Rho-independent terminators

Following established criteria (Zeng and Sundin, 2014), Rho-independent terminators were searched in the *P. ananatis* LMG20103 genome using a custom python script (script.pdf, see section RI_term.py in supplementary material). Briefly, the search was conducted in an effort to detect poly-T regions with at least six continuous T's and for those that had at least 4 GC base pairs in the last 6 bases before the poly-T stretch. Of these, those that had at least 50% GC content in the last 25 bases before the poly-T were considered to be putative Rho-independent terminators.

2.3.11 Differential sRNA expression in *P. ananatis* LMG 2665 WT vs Δ*hfq*

Using the genomic coordinates from the BLAST+ search of the pPAR sRNAs against the *P. ananatis* LMG2665 genome (Adam et al., 2014), a gene format file (.gff) for all the pPAR sRNAs was generated. The sRNA sequencing reads that had been trimmed and filtered were mapped to the LMG2665 genome using Bowtie2 (Langmead and Salzberg, 2012). The mapped reads were sorted using SAMtools (Li et al., 2009) and the number of reads mapping to pPAR sRNAs in the LMG2665 genome was counted using HTSeq (Anders et al., 2015). Read counts tables were analyzed for statistically-significant differential expression of pPAR sRNAs between WT and Δ*hfq* mutant samples at corresponding time points using the DESeq R package which utilizes a negative binomial distribution model (Anders and Huber, 2010; R Core Team 2013). Resulting genes with a false-discovery rate of 0.05 were considered differentially expressed.

2.3.12 sRNA conservation analysis

The bacterial genomes were downloaded from NCBI and searched using BLAST+ (Camacho et al., 2009) with all pPAR sRNA sequences as queries. Because BLAST uses local alignment, the global percent identity to pPAR sRNAs was calculated by multiplying the percent identity by the length of the BLAST alignment and dividing by the length of the pPAR sRNA.

Heatmaps showing percent identity of sRNA by genome were generated using ClustVis (Metsalu and Vilo, 2015).

2.3.13 qRT-PCR validation of sRNA expression

To validate the expression of putative sRNAs identified, a quantitative RT-PCR was conducted on a subset of sRNAs. The 2 µg of total RNA extracted from the two-time points (low and high cell density) was converted to cDNA using random primers using the High-Capacity cDNA Synthesis Kit (Applied Biosystems, Carlsbad, CA, USA). Subsequently, PowerUP™ SYBR™ Green Master Mix (Applied Biosystems) was used to quantify expression levels of the selected sRNAs real-time in QuantStudio 12K Flex Real-Time PCR System (Applied Biosystems). The list of primers used for qRT-PCR is found in Table 2.2. The relative expression of sRNA was calculated using $2^{-\Delta\Delta CT}$ method (Livak and Schimittgen 2001) with the gene *ffh* encoding a signal recognition particle protein, serving as an endogenous mRNA control (Takle et al., 2007; Sibanda et al., 2018).

2.3.14 5' Rapid Amplification cDNA Ends (RACE) analysis

The 5' RACE analysis was conducted on the selected putative sRNAs to capture their transcription start sites (TSS). Total RNA (up to 15 µg) of *P. ananatis* strains grown to high density (OD_{600} = 0.6), was extracted as above mentioned (See RNA extraction). The resulting RNA was ligated to 300 pmol of RNA linker: GACGAGCACGAGGACACUGACAUGGAGGAGGGAGUAGAAA in the presence of RNA 5' pyrophosphohydrolase (RppH) (New England BioLabs, Ipswich, MA, USA) and T4 RNA ligase (New England BioLabs) at 37 ℃ for 4 hr. The linker-ligated RNA was purified using Trizol-chloroform (2:1) extraction method, as described by Rio et al., (2010). The resulting RNA was ethanol precipitated and suspended in 10 µl of RNase-free water. The cDNA of linker-ligated RNA was synthesized as previously described (See qRT-PCR validation of sRNA expression) and Gene Specific PCR (GSP) was performed using nested linker and sRNA specific PCR primers (Table 2.2). The GSP using genomic DNA was used as a control and resulting bands from 5' RACE were gel-purified and cloned into pJET1.2 blunt (Thermo Scientific) prior to sequencing.

2.3.15 Secondary Structure and mRNA target Prediction

The secondary structures of sRNAs, of which their TSS have been determined by 5' RACE analysis, were predicted *in silico* using RNAfold web server (Hofacker, 2003 available at http://rna.tbi.univie.ac.at). The putative target mRNAs of novel sRNAs pPAR237, pPAR238 and pPAR395 and their putative interacting domains were computationally predicted using CopraRNA and IntaRNA (Wright et al., 2014 available at http://rna.informatik.uni-freiburg.de). The above information is presented in Supplementary Figure 2.6 and Supplementary Table 2.4, respectively.

2.3.16 Image and Statistical analysis

Images resulting from motility, AHL detection, and virulence assays were analysed in ImageJ (Schneider et al., 2012) for the measurement of halos and lesion diameter. Statistical analyses are performed with R 3.2.6 (R Core Team, 2013) and significance of the data ($P < 0.05$) was determined by Analysis of variance (ANOVA) and Tukey's Honestly Significantly Difference (HSD) tests. Except where otherwise mentioned, all data shown in this study represent mean values and error bars represent standard error (SE) of the samples.

2.4 RESULTS

2.4.1 *hfq* mutation negatively affects growth

To investigate the functional role of Hfq in the pathogenesis of *P. ananatis*, an *hfq* deletion mutant (Δ*hfq*) was constructed by replacing the *hfq* gene with a kanamycin resistance marker (Materials and Method). Southern blotting (Supplementary Figure 2.1) and PCR amplification of the *hfq* region (Supplementary Figure 2.2) verified a single insertion of the antibiotic marker in the *hfq* mutant strain. For the construction of the *hfq*-complementing plasmid, *hfq* promoter sequence of *E. coli* K12 was used to search for *hfq* promoter in *P. ananatis* and a highly conserved *hfq* promoter sequence (93 % nucleotide identity) of *P. ananatis* compared to that of *E. coli* K12 was found overlapping in the coding region of the adjacent gene *miaA*.

In vitro growth analyses of *P. ananatis* WT, Δ*hfq* and *hfq* complementing strains cultured in LB medium showed that the *hfq* mutation affected the growth of *P. ananatis*. The *hfq* mutant exhibited a slower growth rate relative to the WT and *hfq*-complementing strains, but similar cell density was reached at a stationary phase as both strains (Supplementary Figure 2.3). Similarly, i*n planta* growth curves at 12 hr showed that WT, Δ*hfq* and *hfq* complementing strains of *P. ananatis* exhibited comparable cell densities to one another (Supplementary Figure 2.4B) which were at sufficient levels for the onset of symptoms by 3 dpi (Supplementary Figure 2.4A).

2.4.2 Loss of Hfq attenuates virulence in *P. ananatis*

Virulence assay on red onion scales demonstrated clearing of the red pigment and formation of a water-soaked lesion in the onion scales inoculated with WT *P. ananatis* while no disease symptoms were observed on the scales infected with the *P. ananatis* Δ*hfq* mutant (Figure 2.1). The impaired virulence of the *P. ananatis* Δ*hfq* mutant was restored to the wild-type levels by *trans* expression of *hfq* gene on the plasmid pBBR1MCS-5_START::*hfq*. The finding that the *P. ananatis* Δ*hfq* mutant strain was able to attain *in planta* population densities equivalent to WT (Supplementary Figure 2.4), suggests that the lack of disease symptoms is not associated with a growth defect, and that *hfq* is required for virulence of this strain when inoculated into the red onion.

2.4.3 Hfq regulates motility, AHL production and biofilm formation

To determine whether the *P. ananatis* Hfq regulates virulence traits, swimming motility, production of AHL molecules and biofilm were quantified in WT, Δ*hfq* and *hfq*-complementing strains of *P. ananatis*. The results show that *P. ananatis hfq* mutant was impaired in swimming motility relative to the wild type strain, as determined by the size of the halo that formed on the soft agar (Figure 2.2). In addition, AHL production, as determined by the production of the purple pigment violacein by the *C. violaceum* 026 biosensor demonstrated a statistically significant reduction in the size of the purple halo formed by the *hfq* mutant strain relative to the wild type, indicating a significant reduction in AHL production by the mutant strain (Figure 2.3). Furthermore, a 3-fold reduction ($P < 0.05$) in the biofilms formed by the *hfq* mutant strain relative to the WT *P. ananatis* was also observed (Figure 2.4). These findings are consistent with previous studies that showed that AHL molecules are needed as a signal for QS to regulate biofilm formation in *P. ananatis* (Morohoshi et al., 2007; Sibanda et al., 2016). The phenotypic defects resulting from loss of *hfq,* which were restored to wild-type levels by *trans*-complementation of *hfq,* suggest that Hfq regulates the production of multiple virulence traits in *P. ananatis*.

2.4.4 Identification of putative sRNAs

Due to impaired motility, AHL production, biofilm formation and virulence caused by the loss of Hfq in *P. ananatis* LMG 2665, a sRNA sequencing analysis were conducted to identify the regulatory sRNAs that are dependent on Hfq for stability and function. Deep sequencing of the sRNA transcriptomes of WT and Δ*hfq* mutant *P. ananatis* strains at low (OD_{600} = 0.2) and high cell density (OD_{600} = 0.6) time points resulted in a total of 172.03 million reads. Following trimming of adapters and filtering for high-quality reads (Phred score≥ 30), 66.74 million reads were retained, of which 83.2% mapped uniquely to the *P. ananatis* LMG20103 genome. Following removal of the reads that mapped to protein-coding genes, rRNAs, or tRNAs, 9.72 million reads remained for the sRNA identification and analysis. The distribution of reads across the WT and Δ*hfq* mutant *P. ananatis* strains, each with three technical replicates at low and high cell density time points, are included in Supplementary Table 2.1.

For identification of sRNAs in the transcriptome dataset, the WT sequencing data was utilized and calculated for the per-base depth across the genome relative to the genome-wide average

per-base depth. To select a threshold that would allow for sensitive detection of sRNAs while also filtering out noise in the sequencing data, the number of putative sRNAs identified across a broad range of signal-to-noise thresholds was calculated. A strong linear relationship (R^2= 0.9981) between Log_{10} (Threshold) and Log_{10} (# sRNAs identified) was found (Supplementary Figure 2.5), and a signal-to-noise threshold ratio of 10 was selected for calling of putative sRNAs from the sequencing data. Using this threshold, a total of 615 putative *P. ananatis* sRNAs (pPARs) were identified. Of these, 425 pPARs were identified in both time points, 90 were identified only in the low cell density time point and 100 only in the high cell density time point in *P. ananatis* LMG2665.

2.4.5 Characterization of pPAR sRNAs

The 615 identified pPARs were further classified as intergenic, antisense, or overlapping. The classification resulted in 249 intergenic pPAR sRNAs, 302 antisense pPAR sRNAs, and 64 overlapping pPAR sRNAs (Figure 2.5A). The mean length of pPAR sRNAs was 66.4 bases with a median of 42 bases (Figure 2.5B) and the mean GC content of pPAR SRNAs was 52.3% with a median of 52.2% (Figure 2.5C). Both of these are quite close to the genome average of 53.7% GC bases (De Maayer et al., 2010). Of note, seven pPAR sRNAs had GC content below 30%, and 14 pPAR sRNAs had GC content above 70%, suggesting the potential horizontal acquisition of the genomic regions containing these sRNAs.

In addition, we performed a genome-wide computational search for putative Rho-independent terminators that are associated with the transcription termination of Hfq-dependent sRNAs (Otaka et al., 2011). The results revealed that there were 5,002 poly-T stretches with at least 6 continuous Ts and 2,437 of these had four or more GC base pairs in the last 6 bases before the poly-T. A total of 1,842 of poly-T stretches had approximately 50% GC content in the final 25 bases before the poly-T, meeting the established criteria of Rho-independent terminators (Zeng and Sundin, 2014). Based on these criteria, only 569 were associated with protein-coding genes and 69 were associated with the identified pPAR sRNAs. The key features of select pPAR sRNAs are presented in Table 2.3 and for full data, including genomic coordinates and sRNA sequences, refer to Supplementary Table 2.2 in the supplementary materials.

2.4.6 Identification of Hfq-dependent sRNAs

Because *trans* encoded sRNAs have been shown to depend on RNA chaperone proteins such as Hfq for stability and activity (Vogel and Luisi, 2011), an *hfq* mutant was included in the sRNA sequencing experiment in order to determine pPAR sRNAs that are dependent on or influenced by the loss of *hfq.* The analysis of *hfq* to WT samples from both low cell density and high cell density samples identified a total of 276 pPAR sRNAs affected in abundance by Hfq. Sixty-four pPAR sRNAs were affected in abundance by loss of *hfq* in both cell density samples, 58 pPAR sRNAs in low cell density samples, and 154 pPAR sRNAs only in high cell density samples (Figure 2.6). Of all the Hfq-dependent pPAR sRNAs, 145 had decreased abundance and 131 had increased abundance in the *hfq* mutant relative to wild-type. Overall, results indicate that Hfq affects the abundances of numerous pPAR sRNAs either positively and/or negatively. Supplementary Table 2.3 lists all pPAR sRNAs affected in abundance by loss of *hfq* as well as corresponding fold changes in both low and high cell densities.

Of the pPAR sRNAs affected by the loss of *hfq,* 41 have predicted Rho-independent terminators. Of these, 25 are intergenic and 16 are antisense, consistent with the classical model that Hfq-dependent sRNAs are frequently intergenic (Vogel and Luisi, 2011). Among the sRNAs detected in intergenic regions and Hfq-dependent with Rho-independent terminator, 9 known sRNAs and 16 novel sRNAs were identified. The known sRNAs included ArcZ, FnrS, GlmZ, RprA, RyeB/SdsR, RyhB, RyhB2, Spot42, and SsrA. The depth plots for a number of selected known and novel pPAR sRNAs of interest were generated, showing per-base sequencing depth across the length of the sRNA (Figure 2.7). Several pPAR sRNAs have certain regions with far greater sequencing depth than the rest of the sRNA which suggests that mechanisms such as post-transcriptional processing (Davis and Waldor, 2007; Chao et al., 2017) might be active in *P. ananatis,* playing a role in sRNA maturation and/or processing.

2.4.7 Conservation of identified sRNAs

To visualize the degree of conservation of the identified pPAR sRNAs, a genome-wide analysis was performed to identify sequences similar to those of the pPAR sRNAs for several bacterial species both within and outside the genus *Pantoea* were conducted. Nearly all of the pPAR sRNAs are highly conserved within the *P. ananatis* strains, and a large portion of sRNAs was also well conserved within the genus *Pantoea* (Figure 2.8A). As some *P. ananatis* genomes are in draft form, it is possible that some sRNAs have not yet been assembled, accounting for

low levels of conservation within the species. However, it will be interesting to determine experimentally if some sRNAs are specific within *P. ananatis* or within the genus *Pantoea* as far fewer pPAR sRNAs are conserved across different enterobacterial species (Figure 2.8B).

2.4.8 Experimental validation and characterization of individual sRNAs

Expression of the *arc*Z, *fnr*S, *glm*Z, *rpr*A, *rye*B, *ryh*B2, *pPAR*237, *pPAR*238, and *pPAR*395 sRNA genes was quantified in the *P. ananatis hfq* mutant strain relative to WT using qRT-PCR (Figure 2.9). The resulting expression profile of the aforementioned sRNA transcript levels (except *glmZ* and *ryhB2*) was decreased in the absence of *hfq*, which was in agreement with the depth plots analysis (Figure 2.7). In WT *P. ananatis*, *glmZ* expression is likely repressed at low cell density (OD_{600} = 0.2) and increased at high cell density (OD_{600} = 0.6) in a Hfq-dependent manner as the opposite expression levels were observed in *hfq* mutant *P. ananatis* where abundances of *glmZ* transcripts were detected at low cell density but not at high cell density condition. Similarly, Hfq may negatively affect *ryhB2* expression, as the abundances of *ryhB2* transcript in WT at low and high cell density conditions were both low relative to the *hfq* mutant *ryhB2* levels. The transcription start site of FnrS, GlmZ, pPAR237, pPAR238, and pPAR395 was determined by 5' RACE analysis. Their predicted structures, sequence, and targets are reported in Supplementary Figure 2.6 and Supplementary Table 2.4.

2.5 DISCUSSION

In the present study, we investigated the functional role of Hfq in the pathogenesis of the Gram-negative phytopathogen *P. ananatis* and demonstrated that Hfq is important for motility, AHL and biofilm formation, and virulence of the pathogen. We also identified several putative sRNAs, which include known and novel sRNAs that are Hfq-dependent for their abundances in *P. ananatis*. The pleiotropic phenotypes caused by *hfq* mutation is due to global post-transcriptional gene regulation operated by Hfq and Hfq-dependent sRNAs that modulate stress response and virulence of numerous bacterial pathogens (Chao and Vogel, 2010). The ability of *P. ananatis* to survive in diverse ecological niches and to successfully infect susceptible plant hosts requires a timely and collective regulation of cellular functions in response to environmental conditions.

Inactivation of *hfq* in bacteria generally results in pleiotropic effects, of which growth retardation is common. Decreased growth rate has been reported in *hfq*-attenuated bacteria such as *Acinetobacter baumannii* (Kuo et al., 2017), *Haemophilus influenzae* (Hempel et al., 2013), *Yersinia enterocolitica* (Kakoschke et al., 2016) and the plant pathogens *A. tumefaciens* (Wilms et al., 2012) and *P. carotovorum* (Wang et al., 2018). This phenotype was consistent with the *P. ananatis hfq* deletion mutant growing *in vitro*, however, this alteration did not prevent *P. ananatis* from entering the logarithmic growth phase and eventually reaching the wild-type cell density at a stationary phase which was also observed *in planta* (Supplementary Figure 2.4). Unlike the *E. amylovora hfq* mutant (Zeng et al., 2013), which exhibited reduced growth in an immature pear fruit infection model, the *P. ananatis hfq* mutant strain was able to reach a population density comparable to that of the wild-type strain when inoculated into onion, indicating that the abolishment of virulence in the *hfq* mutant *P. ananatis* was not due to a growth defect.

The loss of *hfq* gives rise to impairment of important virulence determinants such as motility in bacterial pathogens. Impaired motility affects the overall fitness of a bacterium as a pathogen as it disables attachment and dispersal of the pathogen in the host. This, in turn, results in diminished invasion, colonization and hence virulence (Sittka et al., 2007; Kulesus et al., 2008). In enterobacterial pathogens, Hfq and Hfq-dependent sRNAs control flagellar based motility. For example, in *E. coli*, multiple sRNAs including ArcZ, OmrAB, OxyS and RyeB/SdsR have been shown to modulate the expression and/or translation of *flhDC*, the master regulator of flagellar biosynthesis (De Lay and Gottesman, 2012). In the phytopathogen, *E. amylovora*, the

sRNAs ArcZ, OmrAB, and RmaA have been found to regulate *flhDC* at both transcriptional and post-transcriptional levels (Schachterle et al., 2019; Schachterle and Sundin, 2019). In this way, the integration of different environmental cues is achieved through several sRNAs, allowing fine-tuning of flagellar expression and production.

The lack of swimming motility displayed by the *P. ananatis hfq* mutant clearly demonstrates the role of Hfq in regulating flagellar motility. In a previous study by Weller-Stuart et al., (2016), a *P. ananatis flg*K mutant deficient in flagellar assembly enzyme, FlgK, was abolished in swimming motility and pathogenicity in onion seedlings. Together with the current study, these findings suggest that flagellar motility is required for the virulence of *P. ananatis*, and this trait is regulated by functional Hfq. Similarly, in *P. carotovorum* (Wang et al., 2018) and *Serratia* sp. ATCC 39006 (Wilf et al., 2013, Hampton et al., 2016), attenuation of flagellar motility was observed in *hfq*-deletion mutant strains, as an expression of the *flhD*C genes was dependent on Hfq. Given that sRNAs namely, ArcZ, OmrAB and RyeB/SdsR, were also identified in our sRNA sequencing data (Supplementary Table 2.2), and that their wild-type transcript levels are dependent on the functional copy of *hfq* (Figure 2.9), we hypothesize that Hfq, in conjunction with the identified sRNAs, may regulate the flagellar motility of *P. ananatis* in a similar manner as the other enterobacterial species.

In addition to impaired motility, disruption of *hfq* in Gram-negative pathogens often results in reduced biofilm formation (Kulesus et al., 2008; Monteiro et al., 2012; Zeng et al., 2013; Wang et al., 2018). One possible explanation for this phenotype is an effect on quorum sensing-mediated regulation of motility and biofilm formation. As biofilm formation is a developmental and co-operative process, the process necessitates cell to cell communication that enables perception of the signals generated from the community. The signal or information is packaged in the form of autoinducer molecules, acylated homoserine lactones (AHLs), or may be communicated to the QS circuit by secondary signalling molecule such as cyclic dimeric guanosine monophosphate (c-di-GMP) (Castiblanco and Sundin, 2015). Through protein phospho-relay, signals resulting from high cell density reach Hfq-dependent sRNAs which initiate the expression of genes required for the extracellular matrix synthesis and maturation of biofilm (Lenz et al., 2004; Kay et al., 2006; Tu and Bassler, 2007).

Consistent with the findings that in some bacteria, Hfq positively regulates biofilm production, a significantly reduced amount of biofilm was formed by the *P. ananatis* strain lacking an *hfq* gene. Interestingly, a decreased level of extracellular AHLs diffused in the supernatant of an

hfq mutant overnight culture was detected by the CV026 biosensor, suggesting a potential role of Hfq in the positive regulation of AHL synthesis. According to Pomini et al., (2006), the main *P. ananatis* derived AHL molecule is N-hexaonoyl-L-homoserine lactone (C6-HSL) and is synthesized by the LuxI homolog EanI, while LuxR homolog EanR is a transcriptional regulator that down-regulates the expression of *ean*IR operon in the absence of AHL (Morohoshi et al., 2007). Functional characterization further demonstrated that *eanI* or AHL synthase was required for the formation of biofilm, EPS and pathogenicity of *P. ananatis* (Morohoshi et al., 2007; Sibanda et al., 2016). Thus, decreased production of AHL in the *hfq* mutant strain of *P. ananatis* would mean down-regulation of *ean*I, virulence-related genes, as well as the genes within the QS regulon (Sibanda et al., 2018).

In the present study, two putative novel Hfq-dependent sRNAs were identified in the vicinity of the *ean*IR genes namely, pPAR237 and pPAR238 (Supplementary Figure 2.7A). These sRNAs are partially antisense to each other and are abundantly present in the low cell density condition but are drastically reduced in abundance at high cell density (Figure 2.9). In contrast to the wild-type expression levels, expression of pPAR237 and pPAR238 was almost non-existent in the two cell density conditions in the *P. ananatis hfq* mutant strain (Figure 2.9). The decreased transcript levels of pPAR237 and pPAR238 in *hfq* mutant relative to WT *P. ananatis* were validated experimentally by qRT-PCR, reinforcing the idea that the expression of these sRNAs is dependent on cell density and Hfq. Potential pairing sites of pPAR237 and pPAR238 to *ean*I and *ean*R were predicted *in silico* using IntaRNA (Supplementary Figure 2.7B, 2.7C, 2.7D). Further experimental confirmation of their interaction will indicate the role of pPAR237 and pPAR238 in QS through modulation of AHL synthesis in *P. ananatis*. Moreover, it will be also interesting to determine whether there are other upstream and downstream transcriptional or translational regulators of putative sRNAs pPAR237 and pPAR238. This is the case in *V. cholera* and *Pseudomonas aeruginosa* whose Hfq-dependent sRNA Qrr 1,2,3 and 4 and RsmY are transcriptionally activated by LuxO and GacA, respectively, and are used to repress transcription of *hapR* or sequester translational regulator RsmA (Lenz et al., 2004; Kay et al., 2006; Tu and Bassler, 2007; Brencic et al., 2009).

To date, factors that contribute to the pathogenicity of *P. ananatis* have been characterized, resulting in an expansion in our understanding of virulence mechanisms of this pathogen. A collective regulation of all virulence traits seems likely for the success and persistence of *P. ananatis* in hostile environments, and this can be achieved through Hfq and its global regulatory networks constituted by Hfq-dependent sRNAs. Overall, this study provided

valuable insights into the essential role of Hfq in regulating different virulence traits of *P. ananatis*. A total of 276 sRNAs were identified that are affected in abundance by Hfq at low and high cell density conditions. These sRNAs include those that are well characterized as well as novel putative sRNAs that may possess novel function involved in the QS of *P. ananatis*.

2.6 REFERENCES

Adam, Z., Tambong, J. T., Lewis, C. T., Lévesque, C. A., Chen, W., Bromfield, E.S.P., Khan, I.U.H. and Xu, R. (2014) Draft genome sequence of *Pantoea ananatis* strain LMG 2665^{T}, a bacterial pathogen of pineapple fruitlets. *Genome Announc*, 2, e00489-14. doi: 10.1128/genomeA.00489-14

Alippi A.M. and López A.C. (2010) First report of leaf spot disease of maize caused by *Pantoea ananatis* in Argentina. *Plant Dis*, 94, 487. doi: 10.1094/PDIS-94-4-0487A

Anders, S. and Huber, W. (2010). Differential expression analysis for sequence count data. *Genome Biol*, 11, R106. doi: 10.1186/gb-2010-11-10-r106

Anders, S., Pyl, P. T. and Huber, W. (2015) HTSeq—a Python framework to work with high-throughput sequencing data. *Bioinformatics*, *31*, 166-169. doi: 10.1093/bioinformatics/btu638

Andrews, S. (2010) FastQC: a quality control tool for high throughput sequence data. Available online at: http://www.bioinformatics.babraham.ac.uk/projects/fastqc.

Argaman, L., Hershberg, R., Vogel, J., Bejerano, G., Wagner, E.G., Margalit, H. and Altuvia, S. (2001) Novel small RNA-encoding genes in the intergenic regions of *Escherichia coli*. *Curr. Biol.*, 11, 941–950. doi: 10.1016/S0960-9822(01)00270-6

Asselin, J.E., Bonasera, J.M. and Beer, S.V. (2018) Center rot of onion (*Allium cepa*) caused by *Pantoea ananatis* requires *pepM*, a predicted phosphonate-related gene. *Mol. Plant Microbe-Interact.* doi: 10.1094/MPMI-04-18-0077-R.

Azegami, K., Ozaki, K., Matsuda, A. and Ohata, K. (1983) Bacterial palea browning, a new disease of rice caused by *Erwinia herbicola* (in Japanese with English summary). *Bull. Natl. Inst. Agric. Sci. Ser. C*, 37, 1–12.

Bardill, J.P. and Hammer, B.K. (2012) Non-coding sRNAs regulate virulence in the bacterial pathogen *Vibrio cholerae*. *RNA Biol*, 9, 392-401. doi: 10.4161/rna.19975

Bolger, A.M., Lohse, M. and Usadel, B. (2014) Trimmomatic: a flexible trimmer for Illumina sequence data. *Bioinformatics*, *30*, 2114-2120. doi: 10.1093/bioinformatics/btu170

Brencic, A., McFarland, K.A., McManus, H.R., Castang, S., Mogno, I., Dove, S.L. and Lory, S. (2009) The GacS/GacA signal transduction system of *Pseudomonas aeruginosa* acts

exclusively through its control over the transcription of the RsmY and RsmZ regulatory small RNAs. *Mol. Microbiol*, 73, 434-445. doi: 10.1111/j.1365-2958.2009.06782.x

Camacho, C., Coulouris, G., Avagyan, V., Ma, N., Papadopoulos, J., Bealer, K. and Madden, T.L. (2009) BLAST+: architecture and applications. *BMC Bioinformatics*, 10, 421. doi: 10.1186/1471-2105-10-421

Castiblanco, L.F. and Sundin, G.W. (2015) New insights on molecular regulation of biofilm formation in plant-associated bacteria. *J. Integr. Plant Biol*, 58, 362-372. doi: 10.1111/jipb.12428

Chao, Y. and Vogel, J. (2010) The role of Hfq in bacterial pathogens. *Curr. Opin. Microbiol*, 13, 24–33. doi: 10.1016/j.mib.2010.01.001

Chao, Y., Li, L., Girodat, D., Förstner, K. U., Said, N., Corcoran, C., Śmiga, M., Papenfort, K., Reinhardt, R., Wieden, H-J., Luisi, B.F. and Vogel, J. (2017) *In vivo* cleavage map illuminates the central role of RNase E in coding and non-coding RNA pathways. *Mol. Cell*, 65, 39-51. doi: 10.1016/j.molcel.2016.11.002

Chao, Y., Papenfort, K., Reinhardt, R., Scharma, C.M. and Vogel, J. (2012) An atlas of Hfq-bound transcripts reveals 3' UTRs as a genomic reservoir of regulatory small RNAs. *EMBO J*, 31, 4005–4019. doi: 10.1038/emboj.2012.229

Cortesi P. and Pizzatti C. (2007) Palea browning, a new disease of rice in Italy caused by *Pantoea ananatis*. *J. Plant Pathol*, 89, S76.

Cother, E.J., Reinke, R., McKenzie, C., Lanoiselet, V.M. and Noble, D.H. (2004) An unusual stem necrosis of rice caused by *Pantoea ananas* and the first record of this pathogen on rice in Australia. *Australas. Plant Pathol*, 33, 495-503. doi: 10.1071/AP04053

Coutinho, T.A. and Venter, S.N. (2009) *Pantoea ananatis*: an unconventional plant pathogen. *Mol. Plant Pathol*, 10, 325-335. doi: 10.1111/j.1364-3703.2009.00542.x

Coutinho, T.A., Preisig, O., Mergaert, J., Cnockaert, M.C., Riedel, K-H., Swings, J. and Wingfield, M. J. (2002) Bacterial blight and die-back of *Eucalyptus* species, hybrids and clones in South Africa. *Plant Dis*, 86, 20-25. doi: 10.1094/PDIS.2002.86.1.20

da Silva, J. F. Barbosa, R.R., de Souza, A.N., da Motta, O.V., Teixeira, G.N., Carvalho, V.S., de Souza, A.L.S.R. and de Souza Filho, G.A. (2015) Isolation of *Pantoea ananatis* from

sugarcane and characterization of its potential for plant growth promotion. *Genet. Mol. Res*, 14, 15301–15311. doi: 10.4238/2015.November.30.6

Datsenko, K.A. and Wanner, B.L. (2000) One-step inactivation of chromosomal genes in *Escherichia coli* K-12 using PCR products. *Proc. Natl. Acad. Sci. U.S.A*, 97, 6640-6645. doi: 10.1073/pnas.120163297

Davis, B.M. and Waldor, M.K. (2007) RNase E-dependent processing stabilizes MicX, a *Vibrio cholerae* sRNA. *Mol. Microbiol*, 65, 373-385. doi: 10.1111/j.1365-2958.2007.05796.x

De Lay, N. and Gottesman, S. (2012) A complex network of small non-coding RNAs regulate motility in *Escherichia coli*. *Mol. Microbiol*, 86, 524–538. doi: 10.1111/j.1365-2958.2012.08209.x. doi: 10.1111/j.1365-2958.2012.08209.x

De Lay, N., Schu, D.J. and Gottesman, S. (2013) Bacterial small RNA-based negative regulation : Hfq and its accomplices. *J. Biol. Chem*, 288, 7996–8003. doi: 10.1074/jbc.R112.441386

De Maayer, P., Chan, W.Y., Venter, S.N., Toth, I.K., Birch, P.R., Joubert, F. and Coutinho, T.A. (2010) Genome sequence of *Pantoea ananatis* LMG20103, the causative agent of *Eucalyptus* blight and dieback. *J. Bacteriol*, 192, 2936-2937. doi: 10.1128/JB.00060-10

Dutta, B., Barman, A.K., Srinivasan, R., Avci, U., Ullman, D.E., Langston, D.B. and Gitaitis, R.D. (2014) Transmission of *Pantoea ananatis* and *P. agglomerans*, causal agents of center rot of onion (*Allium cepa*), by onion thrips (*Thrips tabaci*) through feces. *Phytopathology*, 104, 812-819. doi: 10.1094/PHYTO-07-13-0199-R

Franze de Fernandez, M.T., Eoyang, L. and August, J.T. (1968) Factor fraction required for the synthesis of bacteriophage Qβ-RNA. *Nature*, 219, 588–590. doi: 10.1038/219588a0

Gitaitis, R., Walcott, R., Culpepper, S., Sanders, H., Zolobowska, L. and Langston, D. (2002) Recovery of *Pantoea annatis*, causal agent of center rot of onion, from weeds and crops in Georgia, USA. *Crop Protect*, 21, 983-989. doi: 10.1016/S0261-2194(02)00078-9

Gitaitis, R.D. and Gay, J D. (1997) First report of leaf blight, seed stalk rot, and bulb decay of onion by *Pantoea ananas* in Georgia. *Plant Dis*, 81, 1096. doi: 10.1094/PDIS.1997.81.9.1096C

Gitaitis, R.D., Walcott, R.R., Wells, M.L., Diaz Perez, J.C. and Sanders, F.H. (2003) Transmission of *Pantoea ananatis*, causal agent of center rot of onion, by tobacco thrips, *Frankliniella fusca*. *Plant Dis*, 87,675-678. doi: 10.1094/PDIS.2003.87.6.675

Goszczynska, T., Moloto, V.M., Venter, S.N. and Coutinho, T.A. (2006). Isolation and identification of *Pantoea ananatis* from onion seed in South Africa. *Seed. Sci. Technol*, 34, 655-668. doi: 10.15258/sst.2006.34.3.12

Goszczynska, T., Venter, S.N. and Coutinho, T.A. (2007). Isolation and identification of the causal agent of brown stalk rot, a new disease of corn in South Africa. *Plant Dis*, 91, 711-718. doi: 10.1094/PDIS-91-6-0711

Gottesman, S. and Storz, G. (2011) Bacterial small RNA regulators: versatile roles and rapidly evolving variations. *RNA*, 21, 511-512. doi: 10.1261/rna.050047.115

Guo, M.S., Updegrove, T.B., Gogol, E.B., Shabalina, S.A., Gross, C.A. and Storz, G. (2014) MicL, a new σ^E –dependent sRNA, combats envelope stress by repressing synthesis of Lpp, the major outer membrane lipoprotein. *Genes Dev*, 28, 1620-1634. doi: 10.1101/gad.243485.114

Hampton, H.G., McNeil, M.B., Paterson, T.J., Ney, B., Williamson, N.R., Easingwood, R.A., Bostina, M., Salmond, G.P. and Fineran, P.C. (2016) CRISPR-Cas gene-editing reveals RsmA and RsmC act through FlhDC to repress the SdhE flavinylation factor and control motility and prodigiosin production in *Serratia*. *Microbiology*, 162, 1047-1058. doi: 10.1099/mic.0.000283

Hempel, R.J., Morton, D.J., Seale, T.W., Whitby, P.W. and Stull, T.L. (2013) The role of the RNA chaperone Hfq in *Haemophilus influenzae* pathogenesis. *BMC Microbiol*, 13, 134. doi: 10.1186/1471-2180-13-134

Hofacker, I.L. (2003) Vienna RNA secondary structure server. *Nucleic Acids. Res*, 31, 3429–3431. doi: 10.1093/nar/gkg599

Jatt, A.B., Tang, K., Liu, J., Zhang, Z. and Zhang, X-H. (2014) Quorum sensing in marine snow and its possible influence on production of extracellular hydrolytic enzymes in marine snow bacterium *Pantoea ananatis* B9. *FEMS Microbiol. Ecol*, 91, 1-13. doi: 10.1093/femsec/fiu030

Kakoschke, T.K., Kakoschke, S.C., Zeuzem, C., Bouabe, H., Adler, K., Heesemann, K. and Rossier, O. (2016) The RNA chaperone Hfq is essential for virulence and modulates the expression of four adhesins in *Yersinia enterocolitica*. *Sci. Rep.* 6, 29275. doi: 10.1038/srep29275

Kang, S.H., Cho, H-S., Cheong, H., Ryu, C-M., Kim, J.F. and Park, S-H. (2007) Two bacterial endophytes eliciting both plant growth promotion and plant defense on pepper (*Capsicum annuum* L.). *J. Microbiol. Biotechnol*, 17, 96-103.

Katashkina, J.I., Hara, Y., Golubeva, L.I., Andreeva, I.G., Kuvaeva, T.M. and Mashko, S.V. (2009) Use of the λ Red-recombineering method for genetic engineering of *Pantoea ananatis*. *BMC Mol*. *Biol*, 10, 34-45. doi: 10.1186/1471-2199-10-34

Kay, E., Humair, B., Denervaud, B., Riedel, K., Spahr, S., Eberl, L., Valverde, C. and Haas, D. (2006) Two GacA-dependent small RNAs modulate the quorum-sensing response in *Pseudomonas aeruginosa*. *J. Bacteriol*, 188, 6026-6033. doi: 10.1128/JB.00409-06

Kido, K., Adachi, R., Hasegawa, M., Yano, K., Hikichi, Y., Takeuchi, S., Atsuchi, T. and Takikawa, Y. (2008) Internal fruit rot of netted melon caused by *Pantoea ananatis* (=*Erwinia ananas*) in Japan. *J. Gen*. *Plant Pathol*, 74, 302–312. doi: 10.1007/s10327-008-0107-3

Kim, D., Hong, J.S., Qui, Y., Nagarajan, H., Seo, J-H., Cho, B-K., Tsai, S-F. and Palsson, B.Ø. (2012) Comparative analysis of regulatory elements between *Escherichia coli* and *Klebsiella pneumoniae* by genome-wide transcription start site profiling. *PLoS Genet*, 8, e1002867. doi: 10.1371/journal.pgen.1002867

Kim, J., Mannaa, M., Kim, N., Lee, C., Kim, J., Park, J., Lee, H-H., Seo, Y-S. (2018). The roles of two *hfq* genes in the virulence and stress resistance of *Burkholderia glumae*. *Plant Pathol J.* 34, 412-425.

Krawczyk, K., Kamasa, J., Zwolinska, A. and Pospieszny, H. (2010). First report of *Pantoea ananatis* associated with white leaf spot disease of maize in Poland. *J. Plant Pathol*. 92, 807-811.

Kuklinsky-Sobral, J., Araújo, W.L., Mendes, R., Geraldi, I.O., Pizzirani-Klelner, A.A. and Azevedo, J.L. (2004) Isolation and characterization of soybean-associated bacteria and their potential for plant growth promotion. *Environ*. *Microbiol*, 6, 1244-1251. doi: 10.1111/j.1462-2920.2004.00658.x

Kulesus, R.R., Diaz-Perez, K., Slechta, E.S., Eto, D.S. and Mulvey, M.A. (2008) Impact of the RNA chaperone Hfq on the fitness and virulence potential of uropathogenic *Escherichia coli*. *Infect. Immun*, 76, 3019–3026. doi: 10.1128/IAI.00022-08

Kuo, H-Y., Chao, H-H., Liao, P-C., Hsu, L., Chang, K-C., Tung, C-H., Chen, C-H. and Liou, M-L. (2017) Functional characterization of *Acinetobacter baumannii* lacking the RNA chaperone Hfq. *Front. Microbiol*, 8, 1–12. doi: 10.3389/fmicb.2017.02068

Langmead, B. and Salzberg, S.L. (2012) Fast gapped-read alignment with Bowtie 2. *Nat. Methods*, 9, 357. doi: 10.1038/nmeth.1923

Lenz, D.H., Mok, K.C., Lilley, B.N., Kulkarni, R.V., Wingreen, N.S. and Bassler, B.L. (2004) The small RNA chaperone Hfq and multiple small RNAs control quorum sensing in *Vibrio harveyi* and *Vibrio cholerae*. *Cell*, 118, 69–82. doi: 10.1016/j.cell.2004.06.009

Li, H., Handsaker, B., Wysoker, A., Fennell, T., Ruan, J., Homer, N., Marth, G., Abecasis, G. and Durbin, R. (2009) The sequence alignment/map format and SAMtools. *Bioinformatics*, 25, 2078-2079. doi:10.1093/bioinformatics/btp352

Livak, K.J. and Schmittgen, T.D. (2001) Analysis of relative gene expression data using real-time quantitative PCR and the $2^{-\Delta\Delta CT}$ method, *Methods*, 25, 402–408. doi: 10.1006/meth.2001.1262

Marquez-Santacruz, H.A., Hernandez-Leon, R., Orozco-Mosqueda, M.C., Velazquez-Sepulvedal, I. and Santoyo, G. (2010) Diversity of bacterial endophytes in roots of Mexican husk tomato plants (*Physalis ixocarpa*) and their detection in the rhizosphere. *Genet. Mol. Res*, 9, 2372-2390. doi: 10.4238/vol9-4gmr921

McClean, K.H.; Winson, M.K.; Fish, L.; Taylor, A.; Chhabra, S.R.; Camara, M.; Daykin, M.; Lamb, J.H.; Swift, S. and Bycroft, B.W. (1997) Quorum sensing and *Chromobacterium violaceum*: Exploitation of violacein production and inhibition for the detection of N-acylhomoserine lactones. *Microbiology*, 143, 3703–3711. doi: 10.1099/00221287-143-12-3703

Metsalu, T. and Vilo, J. (2015) ClustVis: a web tool for visualizing clustering of multivariate data using principal component analysis and heatmap. *Nucleic Acids Res*, 43, W566-W570. doi: 10.1093/nar/gkv468

Monteiro, C, Papenfort, K., Hentrich, K., Ahmad, I., Le Guyon, S., Reimann, R. and Grantcharova, N. (2012) Hfq and Hfq-dependent small RNAs are major contributors to multicellular development in *Salmonella enterica* serovar *typhimurium*. *RNA Biol*, 9, 489–502. doi: 10.4161/rna.19682

Morohoshi, T., Nakamura, Y., Yamazaki, G., Ishida, A., Kato, N. and Ikeda, T. (2007) The plant pathogen *Pantoea ananatis* produces N-acylhomoserine lactone and causes center rot disease of onion by quorum sensing. *J. Bacteriol*, 189, 8333-8338. doi: 10.1128/JB.01054-07

Obranić, S., Babić, F. and Maravić-Vlahoviček, G. (2013) Improvement of pBBR1MCS plasmids, a very useful series of broad-host-range cloning vectors. *Plasmid*, 70, 263–267. doi: 10.1016/j.plasmid.2013.04.001

Okunishi, S., Sako, K., Mano, H., Imamura, A. and Morisaki, H. (2005) Bacterial flora of endophytes in the maturing seed of cultivated rice (*Oryza sativa*). *Microbes Environ*, 20, 168-177. doi: 10.1264/jsme2.20.168

Oliveira, C.A., Alves, V.M.C., Marriel, I.E., Gomes, E.A., Scotii, M.R., Carneiro, N.P., Guimara˜es, C.T., Schaffert, R.E. and Sa´, N.M.H. (2008) Phosphate solubilizing microorganisms isolated from rhizosphere of maize cultivated in an oxisol of the Brazilian Cerrado Biome. *Soil Biol. Biochem.* 41, 1782-1787. doi: 10.1016/j.soilbio.2008.01.012

Otaka, H., Ishikawa, H., Morita, T. and Aiba, H. (2011) PolyU tail of rho-independent terminator of bacterial small RNAs is essential for Hfq action. *Proc. Natl. Acad. Sci. USA*, 108, 13059–13064. doi: 10.1073/pnas.1107050108

Pérez-y-Terrón, R., Villegas, M.C., Cuellar, A., Muñoz-Rojas, J., Castañeda-Lucio, M., Hernández-Lucas, I., Bustillos-Cristales, R., Bautista-Sosa, L., Munive, J.A., Caicedo-Rivas, R. and Fuentes-Ramírez, L.E. (2009). Detection of *Pantoea ananatis*, causal agent of leaf spot disease of maize, in Mexico. *Australas. Plant Dis. Notes*, 4, 96–99.

Pomini, A.M., Araújo, W.L., and Marsaioli, A.J. (2006) Structural elucidation and biological activity of acyl-homoserine lactones from the phytopathogen *Pantoea ananatis* Serrano 1928. *J. Chem. Ecol*, 32, 1769–1778. doi: 10.1007/s10886-006-9108-x

R Core Team (2013) R: A language and environment for statistical computing. R Foundation for Statistical Computing, Vienna, Austria. Available at http://www.R-project.org/.

Rijavec, T., Lapanje, A., Dermastia, M. and Rupnik, M. (2007) Isolation of bacterial endophytes from germinated maize kernels. *Can. J. Microbiol*, 53, 802-808. doi: 10.1139/W07-048

Rio, D. C., Ares, M. Jr., Hannon, G. J. and Nilsen, T. W. (2010). Purification of RNA using TRIzol (TRI reagent). Cold Spring Harb. Protoc. 6:pdb.prot5439. doi: 10.1101/pdb.prot5439

Santander, R.D. and Biosca, E.G. (2017) *Erwinia amylovora* psychrotrophic adaptations: evidence of pathogenic potential and survival at temperate and low environmental temperatures. *PeerJ*, 5, e3931. doi: 10.7717/peerj.3931

Schachterle, J.K. and Sundin, G.W. (2019) The leucine-responsive regulatory protein participates in virulence regulation downstream of small RNA ArcZ in *Erwinia amylovora*. *mBio*, 10:e00757-19. doi: 10.1128/mBio.00757-19

Schachterle, J.K., Zeng, Q. and Sundin, G.W. (2019) Three Hfq-dependent small RNAs regulate flagellar motility in the fire blight pathogen *Erwinia amylovora*. *Mol. Microbiol*, 111, 1476-1492. doi: 10.1111/mmi.14232.

Schmidtke, C., Abendroth, U., Brock, J., Serrania, J., Becker, A. and Bonas, U. (2013) Small RNA sX13: A multifaceted regulator of virulence in the plant pathogen *Xanthomonas*. *PLoS Pathog*, 9, e1003626. doi: 10.1371/journal.ppat.1003626

Schneider, C.A., Rasband, W.S. and Eliceiri, K.W. (2012) NIH Image to ImageJ: 25 years of image analysis. *Nat. Methods*, 9, 671-675. doi: 10.1038/nmeth.2089

Schwartz, H. F. and Otto, K. (2000) First report of a leaf blight and bulb decay of onion by *Pantoea ananatis* in Colorado. *Plant Dis*, 84,808. doi: 10.1094/PDIS.2000.84.7.808A

Serrano, F.B. (1928) Bacterial fruitlet brown-rot of pineapple in the Philippines. *Philippines J. Sci*, 36, 271-324.

Shyntum, D.Y., Theron, J., Venter, S.N., Moleleki, L.N., Toth, I. K. and Coutinho, T. A. (2015). *Pantoea ananatis* utilizes a type VI secretion system for pathogenesis and bacterial competition. *Mol. Plant-Microbe Interact*, 28, 420-431. doi: 10.1094/MPMI-07-14-0219-R

Sibanda, S., Kwenda, S., Tanui, C.K., Shyntum, D.Y., Coutinho, T.A. and Moleleki, L.N. (2018) Transcriptome profiling reveals the EanI/R quorum sensing regulon in *Pantoea ananatis* LMG 2665^{T}. *Genes*, 9, 1–17. doi: 10.3390/genes9030148

Sibanda, S., Theron, J., Shyntum, D.Y., Moleleki, L.N. and Coutinho, T.A. (2016) Characterization of two LuxI/R homologs in *Pantoea ananatis* LMG 2665^{T}. *Can. J. Microbiol*, 62, 893-903. doi: 10.1139/cjm-2016-0143

Sittka, A., Lucchini, S., Papenfort, K., Sharma, C.M., Rolle, K., Binnewies, T.T., Hinton, J.C.D. and Vogel, J. (2008) Deep sequencing analysis of small noncoding RNA and mRNA targets of

the global post-transcriptional regulator, Hfq. *PLoS Genet,* 4, e1000163. doi: 10.1371/journal.pgen.1000163

Sittka, A., Pfeiffer, V., Tedin, K. and Vogel, J: (2007) The RNA chaperone Hfq is essential for the virulence of *Salmonella typhimurium*. *Mol. Microbiol*, 63, 193-217. doi: 10.1111/j.1365-2958.2006.05489.x

Stice, S.P., Stumpf, D.S., Gitaitis, R.D. Kvitko, B.H. and Dutta, B. (2018) *Pantoea ananatis* genetic diversity analysis reveals limited genomic diversity as well as accessory genes correlated with onion pathogenicity. *Front*. *Microbiol*, 9, 1–18. doi: 10.3389/fmicb.2018.00184

Storz, G., Vogel, J. and Wassarman, K.M. (2011) Regulation by small RNAs in bacteria. Expanding frontiers. *Mol*. *Cell*, 43, 880-891. doi: 10.1016/j.molcel.2011.08.022

Takle, G.W.; Toth, I.K.; Brurberg, M.B. (2007) Evaluation of reference genes for real-time RT-PCR expression studies in the plant pathogen *Pectobacterium atrosepticum*. *BMC Plant Biol*, 7, 50. doi: 10.1186/1471-2229-7-50

Tu, K.C. and Bassler, B.L. (2007) Multiple small RNAs act additively to integrate sensory information and control quorum sensing in *Vibrio harveyi*. *Genes Dev*, 21, 221-233. doi: 10.1101/gad.1502407

Updegrove, T.B. Zhang, A. and Storz, G. (2016) Hfq: the flexible RNA matchmaker. *Curr*. *Opin*. *Microbiol*, 30, 133-138. doi: 10.1016/j.mib.2016.02.003

Vogel, J. and Luisi, B.F. (2011) Hfq and its constellation of RNA. *Nat*. *Rev*. *Microbiol*, *9*, 578. doi: 10.1038/nrmicro2615

Wang, C., Pu, T., Lou, W., Wang, Y., Gao, Z., Hu, B. and Fan, J. (2018) Hfq, a RNA chaperone, contributes to virulence by regulating plant cell wall–degrading enzyme production, type VI secretion system expression, bacterial competition, and suppressing host defense response in *Pectobacterium carotovorum*. *Mol*. *Plant-Microbe Interact.* doi: 10.1094/MPMI-12-17-0303-R.

Weller-Stuart, T., Toth, I., De Maayer, P. and Coutinho, T.A. (2016) Swimming and twitching motility are essential for attachment and virulence of *Pantoea ananatis* in onion seedlings. *Mol*. *Plant Pathol*, 18, 734-745. doi: 10.1111/mpp.12432

Wilf, N.M., Reid, A.J., Ramsay, J.P., Williamson, N.R., Croucher, N.J., Gatto, L., Hester, S.S., Goulding, D., Barquist, L., Lilley, K.S., Kingsley, R.A., Dougan, G. and Salmond, G.P.C. (2013) RNA-seq reveals the RNA binding proteins, Hfq and RsmA, play various roles in virulence, antibiotic production and genomic flux in *Serratia* sp. ATCC 39006. *BMC Genomics* 14, 822. doi: 10.1186/1471-2164-14-822

Wilms, I., Möller, P., Stock, A., Gurski, R., Lai, E. and Naberhaus, F. (2012a) Hfq influences multiple transport systems and virulence in the plant pathogen *Agrobacterium tumefaciens*, *J. Bacteriol*, 194, 5209–5217. doi: 10.1128/JB.00510-12

Wilms, I., Overlöper, A., Nowrousian, M., Sharma, C.M. and Narberhaus, F. (2012b) Deep sequencing uncovers numerous small RNAs on all four replicons of the plant pathogen *Agrobacterium tumefaciens*. *RNA Biology*, 9, 446–457. doi: 10.4161/rna.17212

Wright, P.R., Georg, J., Mann, M., Sorescu, D.A., Richter, A.S., Lott, S., Kleinkauf, R.(2014) CopraRNA and IntaRNA: predicting small RNA targets, networks and interaction domains. *Nucleic Acids Res*, 42, 119-123. doi: 10.1093/nar/gku359

Yuan, X., Zeng, Q., Khokhani, D., Tian, F., Severin, G.B., Waters, C.M., Xu, J., Zhou, X., Sundin, G.W., Ibekwe, A.M., Liu, F., Yang, C.H. (2019) A feed-forward signalling circuit controls bacterial virulence through linking cyclic-di-GMP and two mechanistically distinct sRNAs; ArcZ and RsmB. *Environ. Microbiol.* doi: 10.1111/1462-2920.14603.

Zeng, Q. and Sundin, G.W. (2014) Genome-wide identification of Hfq-regulated small RNAs in the fire blight pathogen *Erwinia amylovora* discovered small RNAs with virulence regulatory function. *BMC Genomics*, 15, 414. doi: 10.1186/1471-2164-15-414

Zeng, Q., McNally, R. R. and Sundin, G. W. (2013). Global small RNA chaperone Hfq and regulatory small RNAs are important virulence regulators in *Erwinia amylovora. J. Bacteriol*, 195, 1706-1717. doi: 10.1128/JB.02056-12

Table 2.1 A list of strains for plasmids used in this study

Strain or Plasmid		Characteristics[a]	Source
Strains			
Escherichia coli DH5α		F$^-$ φ80*lac*ZΔM15 Δ(*lac*ZYA-*arg*F)U169 *rec*A1 *end*A1 *hsd*R17(r_K^-, m_K^+) *pho*A *sup*E44 λ$^-$ *thi*-1 *gyr*A96 *rel*A1	Invitrogen
Chromobacterium violaceum CV026		ATCC 31532 derivative, *cviI*::Tn*5xylE*; Km^r, Sm^r	McClean *et al*., 1997
Pantoea ananatis			
	LMG 2665^T	Wild-type	Serrano, 1928
	LMG 2665^T (pRSFredTER)	LMG 2665^T transformed with pRSFredTER, Cm^r	This study
	LMG 2665^T (pBBR1MCS-START-5)	LMG 2665^T transformed with pBBR1MCS-START-5, Gm^r	This study
	LMG 2665^T Δ*hfq*	*hfq* deletion mutant, Km^R	This study
	LMG 2665^T Δ*hfq*-pBBR1MCS-5_START::*hfq*	LMG 2665^T Δ*hfq* transformed with pBBR1MCS-START-5::*hfq*, Km^r, Gm^r	This study
Plasmids			
	pKD13	Broad-host range vector, mutagenesis cassette template, Km^r	Datsenko and Wanner 2000
	pRSFredTER	Broad-host range vector, expresses bacteriophage λ red recombinase (*bet*, *exo*, *gam*) and *sacB*, Cm^r	Katashkina *et al*., 2009
	pBBR1MCS-START-5	Broad-host range vector, promoterless, Gm^r	Obranić *et al*., 2013
	pBBR1MCS-START-5::*hfq*	pBBR1MCS-START-5 containing *hfq* and 613 bp upstream region (native promoter) cloned as SmaI and BamHI, Gm^r	This study

[a] Cm^r, Gm^r, Km^r and Sm^r represent chloramphenicol, gentamicin, kanamycin and streptomycin resistance, respectively.

Table 2.2 A list of primers used in this study

Primer name	Sequence (5'-3')	Length (nt)
Mutagenesis		
Kan-F	ACGTCGCTTATATAAAAAGACCAGGATGGAA AACCTGACGCTTTCCGATGCGATTGTGTAGGC TGGAGCT	70
Kan-R	TTACGCAGTTTTTTTCAGAACCACTGTGTTCTA CAAGCAACAAACAACAAATTCCGGGGATCCG TCGACC	70
Test-F	TAGTGCGAAGCATGGGTG	18
Test-R	TGCTCACCGGCATCATAACGG	21
Southernblot-F	GCGATTGTGTAGGCTGGAGCT	21
Southernblot-R	TCGGATGGAAGCCGGTCTTGTCG	23
Complementation		
Comp-F	AAAAGGATCCGAGGCTGGGAGCTTTACATCG	31
Comp-R	CGGTCAAACAAGCTATAACCTCG	23
qRT-PCR		
ffh-F	CATTGAGATCAAAACCGTCG	20
ffh-R	TGGGCGACGTGCTGTCGCT	19
ArcZ-F	GCAAGTGTTAACCAATACCC	20
ArcZ-R	GGGTGCGCTAATACTGC	17
FnrS-F	GGTGAATGCAACGTCAA	17
FnrS-R	GTTAGCCGGCGTATTTC	17
GlmZ-F	CATAAACCTGGGAATGACG	19
GlmZ-R	AGCAGGTGTAAGATCAGG	18
RprA-F	TACCATGTTTCCTATGTTGG	20
RprA-R	GATGGGCAAAGACTACAC	18

RyhB2-F	TCGCGTGTCATCGACACGG	19
RyhB2-R	GGCTGGCTAAATAATACTGGAAGC	24
RyeB-F	CGAAAGCCTCTTATTAATGCC	20
RyeB-R	AGACCGAACACGATTCC	17
pPAR237-F	GTGGGAAAGCGAAGGTA	17
pPAR237-R	CTTTCCGGCCAGACTTC	17
pPAR238-F	CTGAAACAGCCAACACC	17
pPAR238-R	GGATGTTACTCTGAGTGTCC	20
pPAR395-F	TGGCGACAATTCAGATGG	18
pPAR395-R	CCGCACCTCGTTAAAGG	17

5' RACE		
Linker nested-F	GAGGACACTGACATGGAGG	19
FnrS-R	GTTAGCCGGCGTATTTC	17
FnrS-nR	AGACAATATGGAGCGCAACG	20
GlmZ-R	AGCAGGTGTAAGATCAGG	18
GlmZ-nR	CGAGAGGTACCCGACTCAACGTG	23
pPAR237-R	ACTTTCCGGCCAGACTTCACA	21
pPAR237-nR	GGGACACTCAGAGTAACATCC	21
pPAR238-R	TGAGTGTCCCGGCCAGCATCACT	23
pPAR238-nR	TCCCTGGTGTTGGCTGTTTC	20
pPAR395-R	CCGCACCTCGTTAAAGG	17
pPAR395-nR	CCTAAATGACTTCCAAACAGCG	22

Table 2.3 A list of selected *Pantoea ananatis* LMG2665^{T} pPAR sRNAs

sRNA Locus_ID	sRNA name	Strand[a]	Start[a]	End[a]	Length (nt)	Classification	RI-terminator[b]	Hfq-dependent
pPAR009	-	+	97939	98052	113	Intergenic	Yes	Yes
pPAR026	glmZ	+	183885	184074	189	Intergenic	Yes	Yes
pPAR035	-	-	241229	241262	33	Antisense	Yes	No
pPAR052	-	+	318391	318427	36	Intergenic	Yes	Yes
pPAR063	arcZ	-	497228	497409	181	Intergenic	Yes	Yes
pPAR069	-	+	518137	518185	48	Overlapping	Yes	Yes
pPAR091	-	+	758889	758998	109	Intergenic	Yes	No
pPAR143	-	+	1192217	1192317	100	Overlapping	Yes	Yes
pPAR155	-	+	1306802	1306953	151	Antisense	Yes	Yes
pPAR165	-	-	1480479	1480511	32	Intergenic	Yes	No
pPAR184	-	-	1706868	1706902	34	Antisense	Yes	No
pPAR204	-	-	1900966	1901000	34	Antisense	Yes	No
pPAR205	rprA	-	1918007	1918133	126	Intergenic	Yes	Yes
pPAR237	-	-	2187335	2187526	191	Intergenic	Yes	Yes
pPAR241	-	-	2226977	2227034	57	Intergenic	Yes	Yes
pPAR245	fnrS	-	2254671	2254792	121	Intergenic	Yes	Yes
pPAR246	ryhB	-	2267249	2267331	82	Intergenic	Yes	Yes

pPAR263	-	+	2451765	2451968	203	Antisense	Yes	No
pPAR287	-	+	2750610	2750660	50	Intergenic	Yes	Yes
pPAR307	-	+	2914323	2914402	79	Intergenic	Yes	Yes
pPAR330	-	-	3095161	3095223	62	Intergenic	Yes	No
pPAR332	-	-	3146708	3146885	177	Intergenic	Yes	Yes
pPAR337	-	-	3235861	3235937	76	Antisense	Yes	Yes
pPAR343	ssrA	+	3274707	3274936	229	Intergenic	Yes	Yes
pPAR345	-	+	3335859	3335962	103	Overlapping	Yes	Yes
pPAR364	-	+	3475041	3475225	184	Intergenic	Yes	No
pPAR367	-	-	3505014	3505042	28	Antisense	Yes	No
pPAR388	-	+	3747994	3748044	50	Antisense	Yes	No
pPAR394	-	-	3822243	3822284	41	Intergenic	Yes	Yes
pPAR395	-	-	3822866	3822977	111	Intergenic	Yes	Yes
pPAR404	-	+	3929664	3929700	36	Antisense	Yes	No
pPAR418	-	+	4001816	4001864	48	Overlapping	Yes	No
pPAR433	ryhB	-	4105322	4105419	97	Intergenic	Yes	Yes
pPAR442	-	-	4239633	4239719	86	Intergenic	Yes	No
pPAR447	-	+	4256795	4256882	87	Intergenic	Yes	No
pPAR457	-	-	4330842	4330892	50	Overlapping	Yes	Yes
pPAR463	-	-	4372873	4372966	93	Intergenic	Yes	No
pPAR464	spf	-	4373881	4373992	111	Intergenic	Yes	Yes

pPAR470	-	-	4388229	4388352	123	Overlapping	Yes	Yes
pPAR479	-	-	4457282	4457307	25	Intergenic	Yes	Yes
pPAR509	-	+	122956	123006	50	Intergenic	Yes	No
pPAR511	-	-	132823	132844	21	Antisense	Yes	Yes
pPAR521	-	+	392904	392975	71	Antisense	Yes	No
pPAR525	-	-	477597	477633	36	Intergenic	Yes	No
pPAR535	-	+	809520	809548	28	Antisense	Yes	Yes
pPAR544	-	+	900462	900550	88	Antisense	Yes	No
pPAR582	-	+	2552244	2552278	34	Intergenic	Yes	No
pPAR590	-	-	2886291	2886321	30	Antisense	Yes	Yes
pPAR608	-	+	3962774	3962823	49	Antisense	Yes	Yes
pPAR626	-	+	4293304	4293392	88	Intergenic	Yes	No
pPAR632	-	+	4459587	4459632	45	Antisense	Yes	No
pPAR638	-	+	58679	58728	49	Intergenic	Yes	Yes
pPAR642	-	-	116116	116179	63	Overlapping	Yes	No
pPAR667	-	+	812084	812142	58	Overlapping	Yes	Yes
pPAR679	-	+	1035446	1035471	25	Intergenic	Yes	Yes
pPAR699	-	-	1501874	1501915	41	Antisense	Yes	Yes
pPAR714	-	-	2049786	2049816	30	Antisense	Yes	Yes
pPAR719	-	-	2171734	2171781	47	Intergenic	Yes	Yes
pPAR724	-	+	2341919	2341964	45	Antisense	Yes	Yes

pPAR726	-	-	2353498	2353521	23	Intergenic	Yes	Yes
pPAR732	sdsR/ryeA	-	2435078	2435148	70	Intergenic	Yes	Yes
pPAR765	-	-	3763787	3763821	34	Antisense	Yes	Yes
pPAR793	-	-	4420191	4420213	22	Intergenic	Yes	Yes
pPAR796	-	-	4502685	4502709	24	Intergenic	Yes	Yes

[a]Based on location and position in the genome of strain LMG 20103 (LMG 2665 co-ordinates are found in Table S2.2).

[b]RI terminator indicates the presence of a Rho-independent terminator sequence downstream of the sRNA sequence.

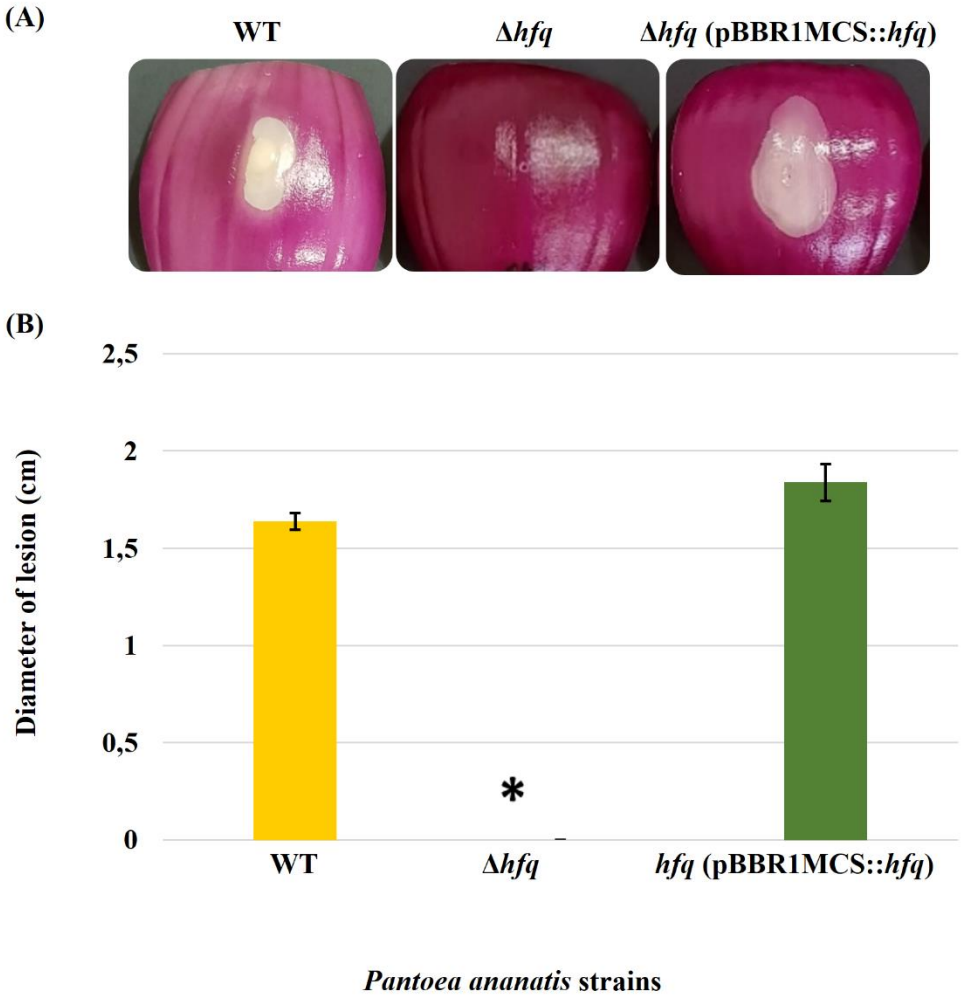

Figure 2.1 Effect of deletion of *hfq* on the virulence of *P. ananatis.* (A) Water-soaked lesion caused by the wild-type (WT), *hfq* mutant (Δ*hfq*) and *hfq* complementing (Δ*hfq* (pBBR1MCS::*hfq*)) strains of *P. ananatis* LMG 2665^{T} in red onion scales at 3 days post inoculation (dpi). (B) The diameter of the lesion caused by the WT, Δ*hfq*, and Δ*hfq* (pBBR1MCS::*hfq*) strains was measured at 3 dpi from three replicates for each strain. Mean lesion length from two independent assays is plotted. An asterisk denotes significance differences (P<0.05) in the lesion size caused by Δ*hfq* relative to WT *P. ananatis*.

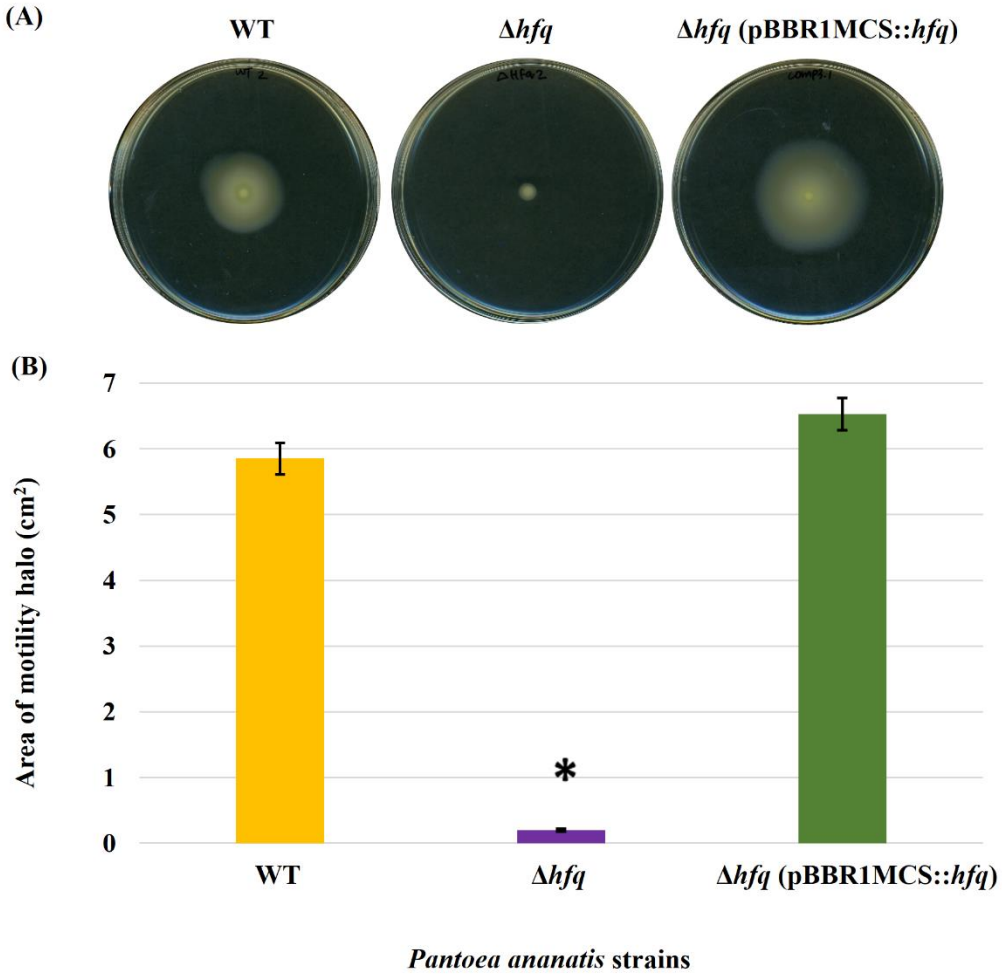

Figure 2.2 Effect of deletion of *hfq* on the motility of *P. ananatis*. (A) Motility of wild-type (WT), *hfq* mutant (Δ*hfq*) and *hfq* complementing (Δ*hfq* pBBR1MCS::*hfq*) strains of *P. ananatis* LMG 2665^{T} after 24 h on 0.3% swimming agar plates. (B) Motility area of WT, Δ*hfq*, and Δ*hfq* (pBBR1MCS::*hfq*) strains was measured at 24 hpi. An asterisk denotes significant differences (P<0.05) in the motility of Δ*hfq* relative to WT *P. ananatis*.

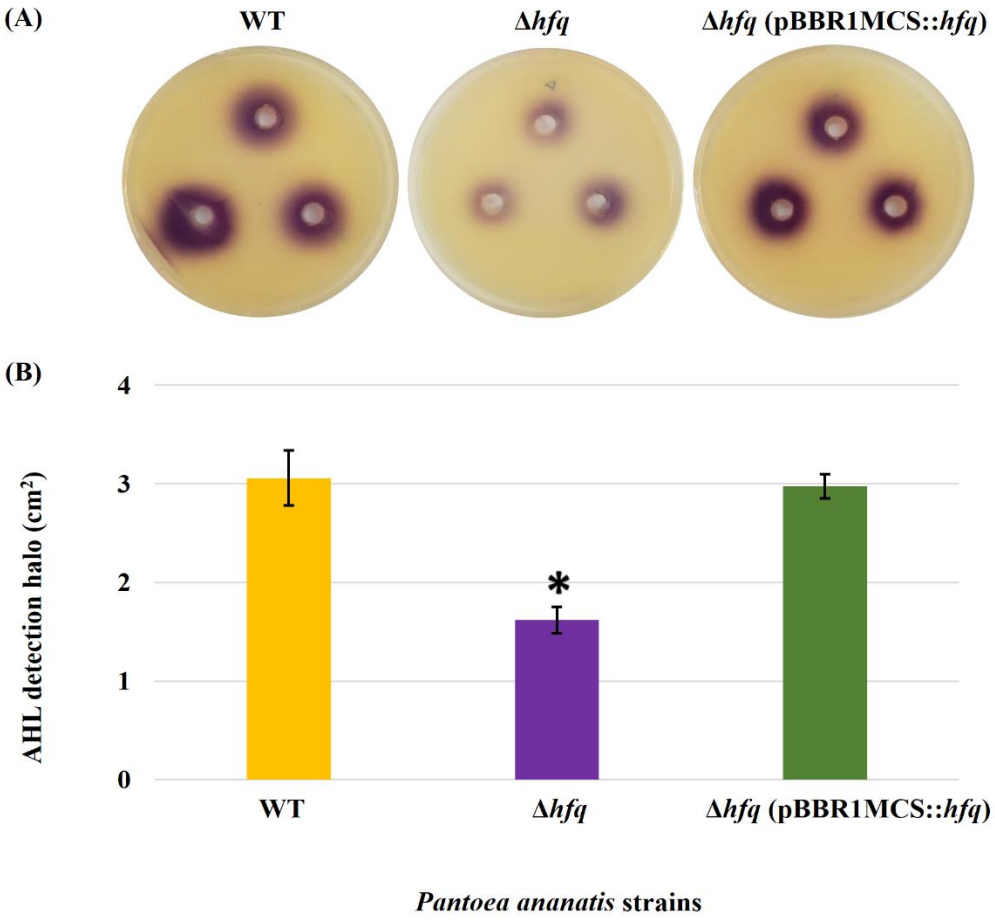

Figure 2.3 AHL detection bioassay. (A) Detection of AHLs produced by the wild-type (WT), *hfq* mutant (Δ*hfq*) and *hfq* complementing (Δ*hfq* (pBBR1MCS::*hfq*)) strains of *P. ananatis* LMG 2665^{T} by biosensor *Chromobacter violaceum* CV026 in the form of a purple (violacein) halo after 48 h. (B) Mean areas of the violacein halo (excluding the area of the well) from two independent experiments were measured for the WT, Δ*hfq*, and Δ*hfq* (pBBR1MCS::*hfq*) strains. Each plate contained three replicates. An asterisk denotes significant differences (P<0.05) in the size of violacein halo of Δ*hfq* relative to WT *P. ananatis.*

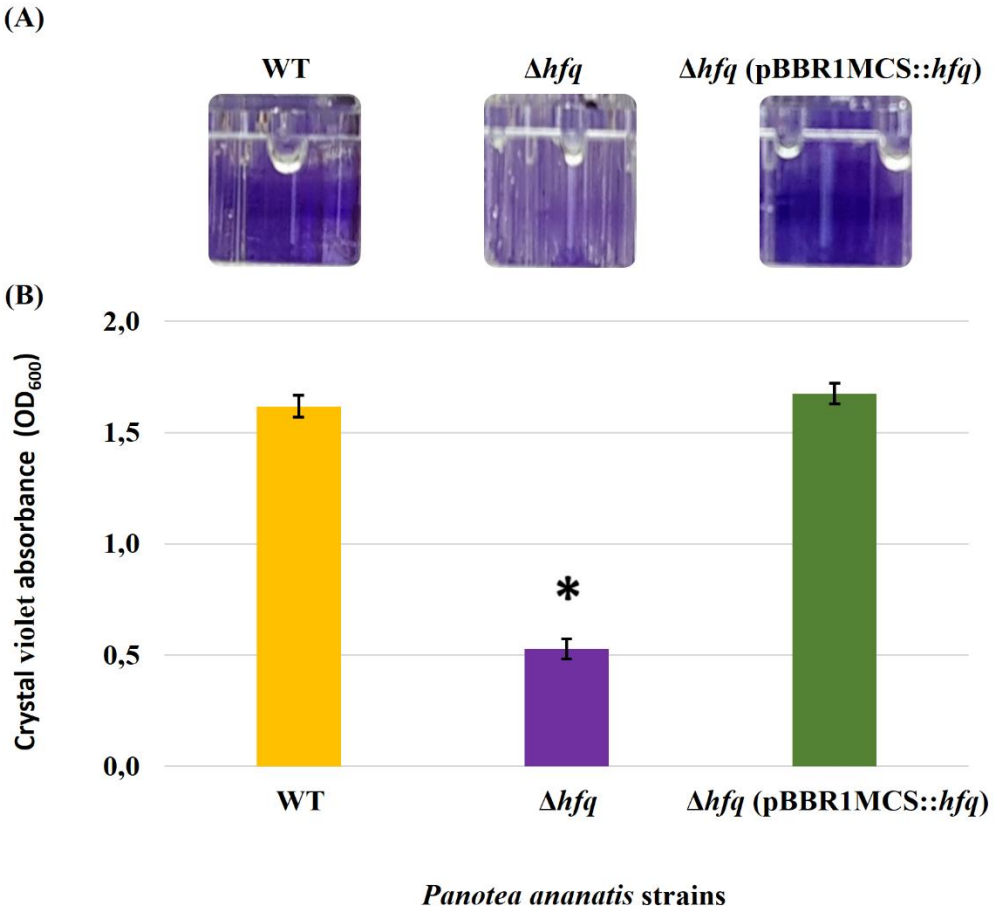

Figure 2.4 Effect of deletion of *hfq* on the biofilm-forming ability of *P. ananatis.* (A) Biofilms formed by the wild-type (WT), *hfq* mutant (Δ*hfq*) and *hfq* complementing (Δ*hfq* (pBBR1MCS::*hfq*)) strains of *P. ananatis* LMG 2665^{T} in 96-well microtitre plate after 24 h incubation under static conditions. (B) Quantification of the biofilms formed by the (WT), Δ*hfq* and Δ*hfq* (pBBR1MCS::*hfq*) strains after 24 h using crystal violet (1%) staining method. The absorbance of solubilized biofilms stained with crystal violet was measured at an optical density wavelength of 600 nm. An asterisk denotes significance differences (P<0.05) in the amount of biofilm formed by Δ*hfq* relative to WT *P. ananatis*.

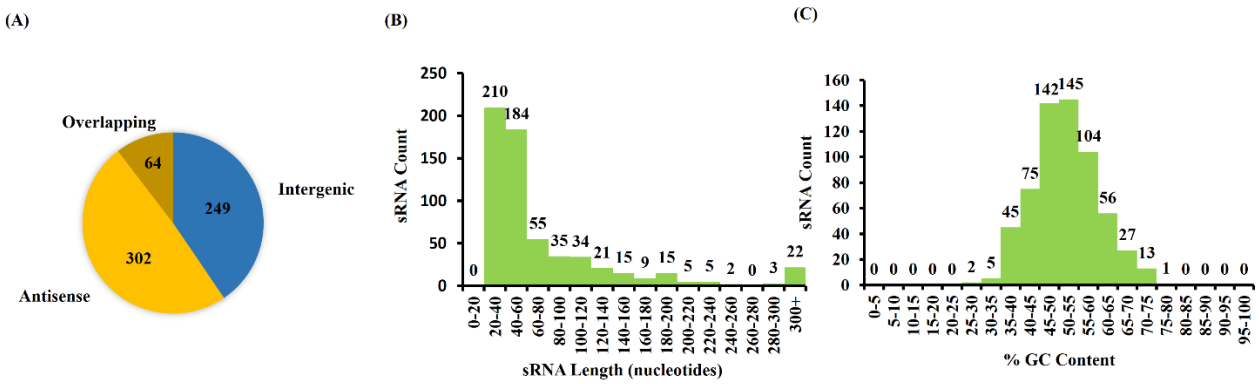

Figure 2.5 Characterization of *Pantoea ananatis* sRNAs (pPAR sRNA). (A) A total of 615 putative *P. ananatis* LMG 2665^{T} sRNAs were classified into 302 antisense, 64 overlappings, 249 intergenic pPAR sRNAs. (B) The mean length of pPAR sRNAs was 66.4 bases with a median of 42 bases. (C) The mean GC content of pPAR SRNAs was 52.3% with a median of 52.2%.

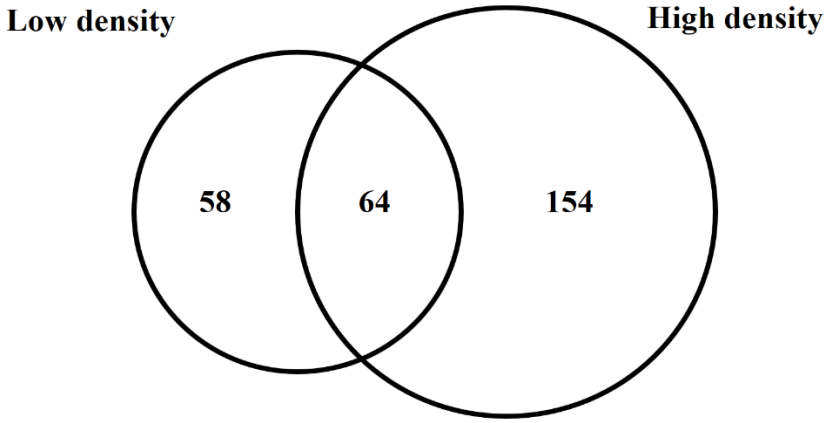

Figure 2.6 Hfq regulates several *Pantoea ananatis* sRNAs (pPAR sRNA). Venn-diagram of differentially-expressed pPAR sRNAs between by the wild-type (WT) and *hfq* mutant (Δ*hfq*) *P. ananatis* LMG 2665^{T} grown *in vitro* at low (OD_{600nm} = 0.2) or high cell density (OD_{600nm} = 0.6).

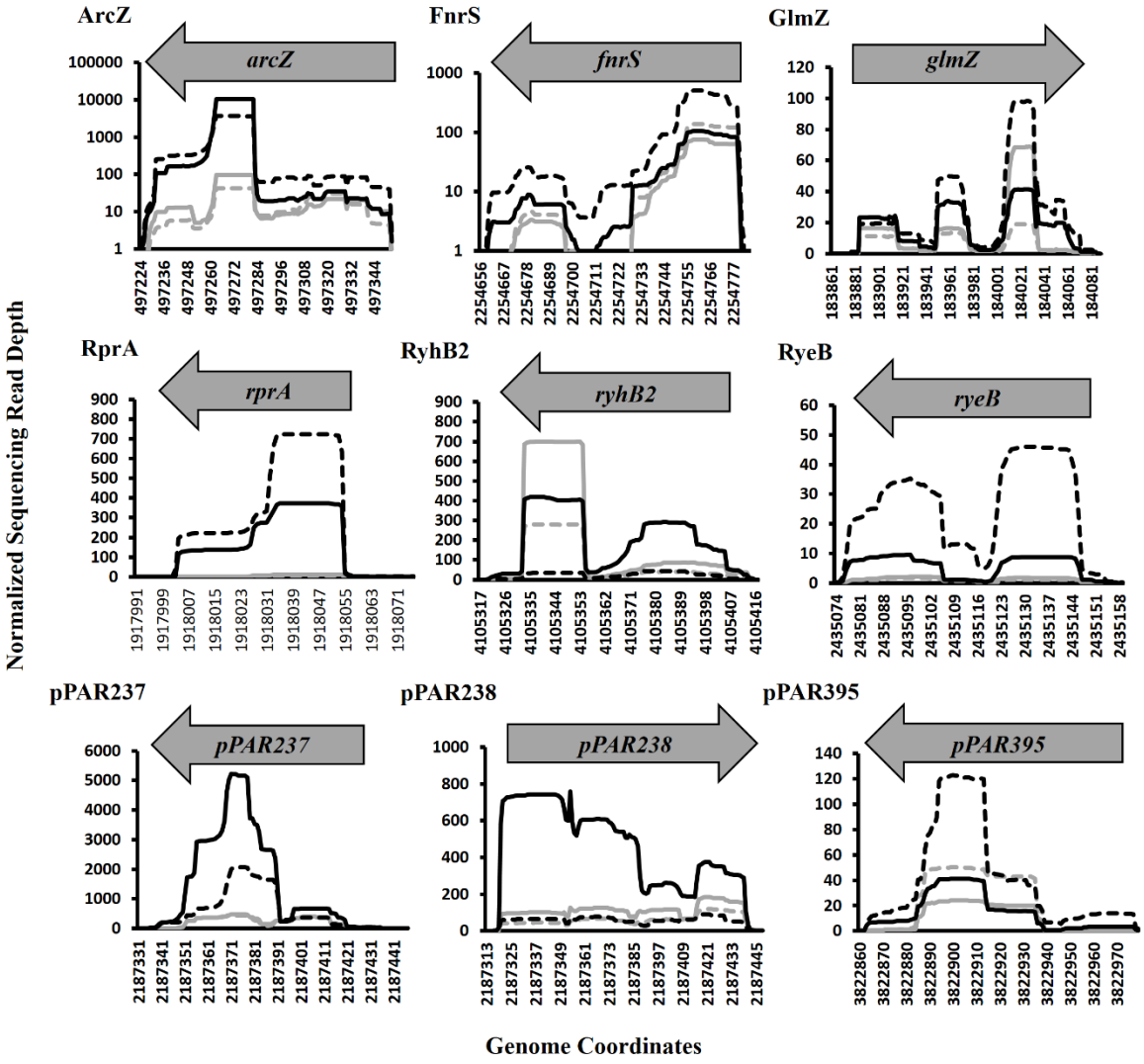

Figure 2.7 Sequencing read depth plots for selected *Pantoea ananatis* sRNAs (pPAR sRNA). Per-base sequencing read depth across the length of sRNAs, normalized to the genome-wide average per-base read depth was plotted for selected *P. ananatis* LMG 2665^{T} sRNAs. Solid black lines represent sRNA sequencing depth in wild-type *P. ananatis* (WT) at low cell density (OD_{600nm} = 0.2) and dashed black lines represent sRNA sequencing depth in WT at high cell density (OD_{600nm} = 0.6). Solid grey lines represent sRNA sequencing depth in *hfq* mutant *P. ananatis* (Δ*hfq*) at low cell density (OD_{600nm} = 0.2) and dashed grey lines represent sRNA sequencing depth in Δ*hfq* at high cell density (OD_{600nm} = 0.6).

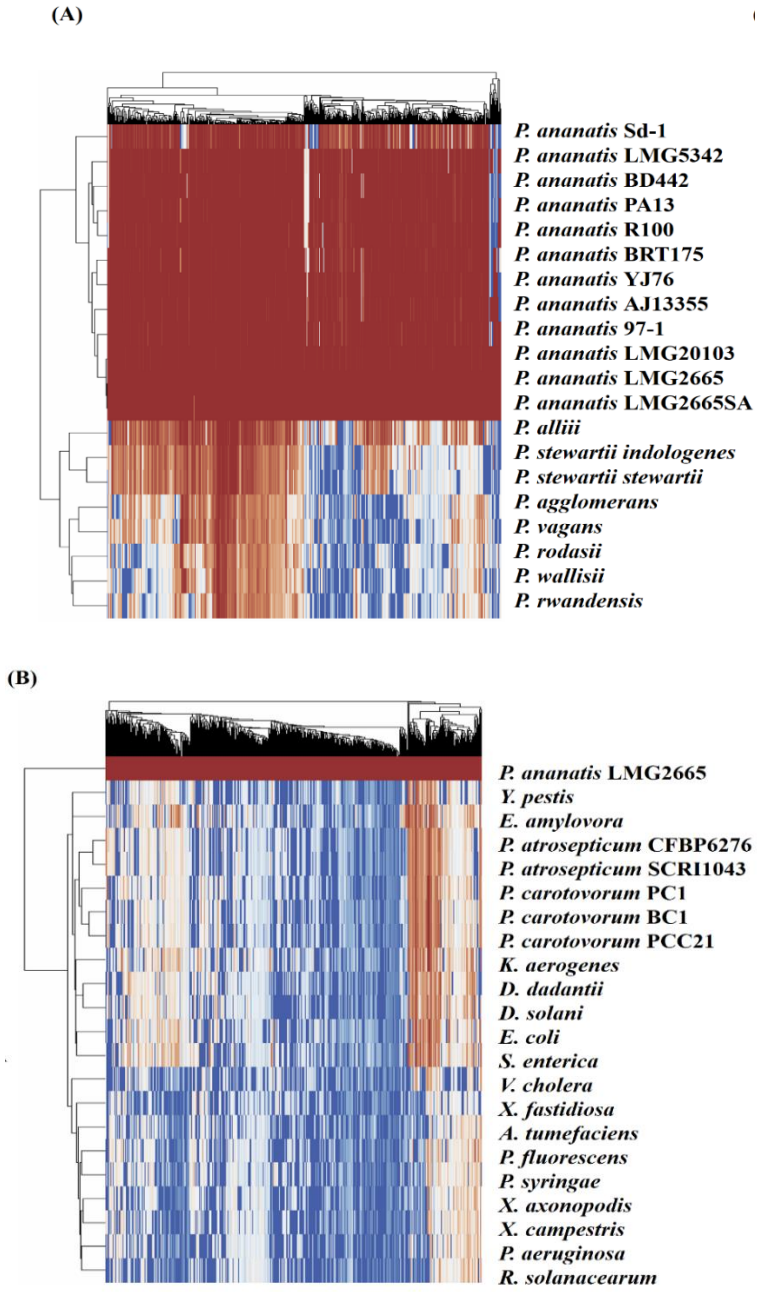

Figure 2.8 Conservation of *Pantoea ananatis* LMG 2665^{T} sRNAs (pPAR sRNAs) in genomes of (A) *Pantoea* species and (B) bacterial species outside of the genus *Pantoea*. BLAST+ was used to query each genome with each pPAR sRNA. Heatmap scale from 0 to 100 represents percent identity between the best BLAST hit and the *P. ananatis* pPAR sRNA sequence from strain LMG 2665. Hierarchical clustering was applied to rows and columns by Euclidean distance with no scaling, and heatmaps (x-axis = pPAR sRNAs, y-axis= sRNAs hit in other *P. ananatis* strain or bacterial species) were generated using ClustVis.

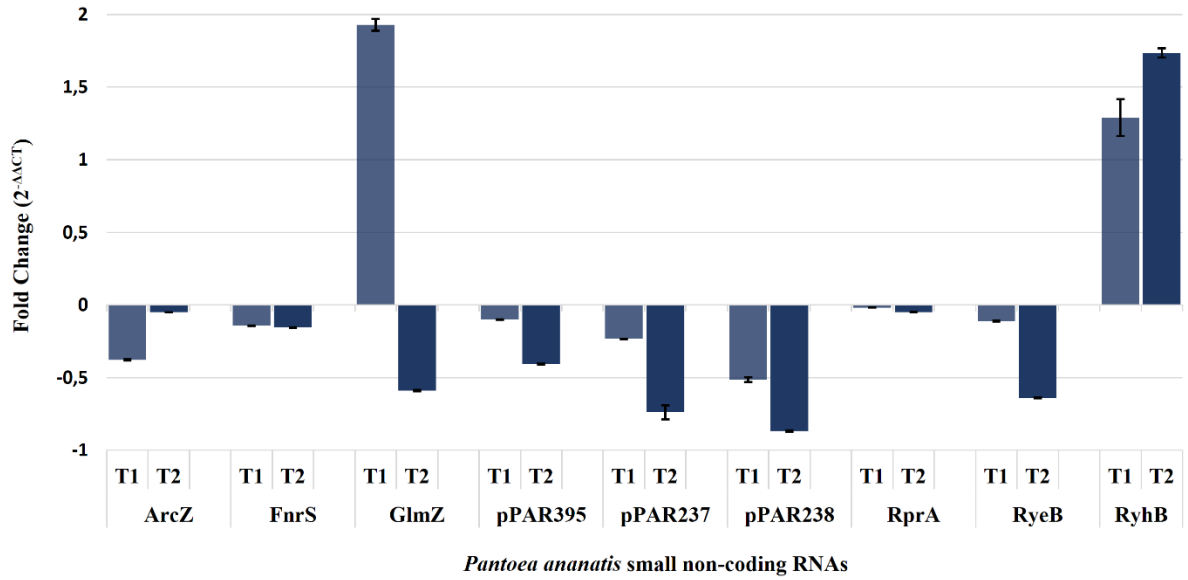

Figure 2.9 Quantification of selected of *Pantoea ananatis* sRNAs (pPAR sRNAs). Transcript levels of a selected set of sRNAs in the *hfq* mutant of *P. ananatis* LMG 2665^{T} (Δ*hfq*) relative to the wild-type (WT) *P. ananatis* LMG 2665^{T} at low (T1; OD_{600nm} = 0.2) and high cell density (T2; OD_{600nm} = 0.6) were quantified using qRT-PCR. The fold change of sRNA expression in Δ*hfq* calibrated by wild-type expression is shown.

S Table 2.1 Summary of sRNA sequencing reads obtained and filtered for use in sRNA identification

Time Point	Strain	Rep	Reads Sequenced	Reads after trimming (%)[a]	Reads mapping (%)[b]	CDS/rRNA/tRNA removed reads	Intergenic/Antisense reads for sRNA identification (%)[c]	Accession number[d]
1	Δ*hfq*	1	12805712	5941160 (46.4)	5071660 (85.4)	4474767	772585 (15.2)	SRX6360880
1	Δ*hfq*	2	15826947	7669898 (48.5)	6547118 (85.4)	6005699	759382 (11.6)	SRX6360881
1	Δ*hfq*	3	16510146	6052015 (36.7)	5186049 (85.7)	4416923	881587 (17.0)	SRX6360882
1	wt	1	14649162	6705591 (45.8)	5514211 (82.2)	4998767	851927 (15.4)	SRX6360883
1	wt	2	13581459	4764989 (35.1)	3960973 (83.1)	3265001	787185 (19.9)	SRX6360884
1	wt	3	11822001	3622119 (30.6)	3054719 (84.3)	2503109	610814 (20.0)	SRX6360885
2	Δ*hfq*	1	17472236	4951444 (28.3)	3972637 (80.2)	3101846	926505 (23.3)	SRX6360886
2	Δ*hfq*	2	14827958	5872626 (39.6)	4789010 (81.5)	4064192	869664 (18.2)	SRX6360887
2	Δ*hfq*	3	13979121	7352684 (52.6)	6036552 (82.1)	5415534	910203 (15.1)	SRX6360878
2	wt	1	13305844	4869024 (36.6)	3962410 (81.4)	3372805	762242 (19.2)	SRX6360879
2	wt	2	13869254	3846989 (27.7)	3182489 (82.7)	2442902	794122 (25.0)	SRX6360876
2	wt	3	13381665	5088389 (38.0)	4250962 (83.5)	3567480	794023 (18.7)	SRX6360877

[a]Percent of initial reads sequenced that passed quality filtering and adapter trimming

[b]Percent of reads mapped out of reads remaining after trimming

[c]Percent of mapped reads that did not map to known coding sequences, rRNAs, or tRNAs

[d]NCBI accession number of raw RNA sequencing data

S Table 2.2 A list of sRNAs identified, their genomic coordinates and selected characteristics

sRNA Locus_tag	sRNA name	Time point	Strand	Start[a]	End[a]	Length (nt)	Position[b]	Antisense to[c]	% GC	RIT[d]	Scaffold ID in LMG2665[e]	Scaffold number[e]	Start[e]	End[e]
pPAR001		1,2	-	21684	21767	83	I		43.4	N	KK328466.1	10	22081	22000
pPAR002		1,2	-	30018	30039	21	A	*glmU*	47.6	N	-	-	-	-
pPAR003		1,2	-	50388	50412	24	A	*yneA*	50.0	N	-	-	-	-
pPAR004		1,2	-	71288	71349	61	A	*ccpA*	44.3	N	KK328466.1	10	71668	71609
pPAR005		1,2	-	76201	76229	28	A	*yiaD*	57.1	N	KK328466.1	10	71668	71609
pPAR006		1,2	-	87409	87502	93	A	*yfcI*	49.5	N	KK328466.1	10	87821	87730
pPAR007		1,2	-	87687	87722	35	A	*yfcI*	54.3	N	KK328466.1	10	88041	88008
pPAR008		1,2	+	88431	88524	93	O	*ibpA*	53.8	N	KK328466.1	10	88751	88842
pPAR009		1,2	+	97939	98052	113	I		51.3	Y	KK328466.1	10	98259	98370
pPAR010		1,2	-	110123	110175	52	O	*glyS*	55.8	N	KK328466.1	10	110493	110443
pPAR011		1,2	+	111021	111048	27	A	*mipA*	66.7	N	-	-	-	-
pPAR012		1,2	-	116256	116314	58	I		51.7	N	KK328466.1	10	116645	116589
pPAR013		1,2	+	117678	117730	52	A	*yibL*	48.1	N	KK328466.1	10	118011	118061
pPAR014		1,2	+	121741	121776	35	I		54.3	N	KK328466.1	10	122074	122107
pPAR015		1,2	+	123660	123693	33	I		51.5	N	KK328466.1	10	123992	124023
pPAR016		1,2	+	127352	127387	35	I		34.3	N	KK328466.1	10	127684	127717
pPAR017		1,2	+	128009	128040	31	A	*spoT*	58.1	N	KK328466.1	10	128381	128410
pPAR018		1,2	-	128746	128785	39	A	*ohrR*	64.1	N	KK328466.1	10	129155	129118
pPAR019		1,2	-	135485	135512	27	A	*cds122*	51.9	N	-	-	-	-
pPAR020		1,2	-	138367	138427	60	I		60.0	N	KK328466.1	10	138802	138744
pPAR021		1,2	-	139112	139154	42	I		31.0	N	KK328466.1	10	139529	139489
pPAR022		1,2	+	156491	156576	85	A	*xynB*	56.5	N	KK328466.1	10	153999	154082
pPAR023		1,2	+	168059	168117	58	I		51.7	N	KK328466.1	10	165559	165615
pPAR024		1,2	+	169651	169680	29	I		55.2	N	KK328466.1	10	167151	167178

pPAR025		1,2	-	174886	174907	21	A	*rffG*	47.6	N	-	-	-	-
pPAR026	*glmZ*	1,2	+	183885	184074	189	I		48.7	Y	KK328466.1	10	181396	181583
pPAR027		1,2	-	188172	188199	27	I		37.0	N	-	-	-	-
pPAR028		1,2	+	188221	188384	163	I		46.0	N	KK328466.1	10	185732	185893
pPAR029		1,2	-	188297	188610	313	O	*cyaA*	48.9	N	KK328466.1	10	186119	185808
pPAR030		1,2	-	188297	188610	313	O	*cyaA*	48.9	N	KK328466.1	10	186119	185808
pPAR031		1,2	-	220549	220610	61	A	*ubiB*	45.9	N	KK328466.1	10	218119	218060
pPAR032		1,2	+	234728	234913	185	I		47.6	N	JFZU01000018.1	15	357	270
pPAR033		1,2	-	234873	234938	65	I		38.5	N	JFZU01000016.1	19	284	346
pPAR034		1,2	-	235982	236023	41	A	*rRNA*	46.3	N	KK328466.1	10	233530	233491
pPAR035		1,2	-	241229	241262	33	A	*murB*	57.6	Y	-	-	-	-
pPAR036		1,2	+	243740	243817	77	I		55.8	N	JFZU01000021.1	22	6183	6258
pPAR037		1,2	+	243957	243998	41	I		61.0	N	-	-	-	-
pPAR038		1,2	+	245370	245988	618	I		55.7	N	JFZU01000016.1	19	27515	26900
pPAR039		1,2	+	245370	245988	618	I		55.7	N	JFZU01000016.1	19	27515	26900
pPAR040		1,2	+	246351	246420	69	I		59.4	N	JFZU01000016.1	19	26535	26472
pPAR041		1,2	-	246423	246452	29	I		37.9	N	JFZU01000022.1	20	1139	1112
pPAR042		1,2	+	249093	249195	102	I		54.9	N	JFZU01000022.1	20	3782	3882
pPAR043		1,2	+	272301	272486	185	I		47.6	N	JFZU01000018.1	15	357	270
pPAR044		1,2	-	272446	272513	67	I		38.8	N	JFZU01000016.1	19	282	346
pPAR045		1,2	-	273555	273595	40	A	*rRNA*	47.5	N	KK328466.1	10	233529	233491
pPAR046		1,2	-	281119	281153	34	A	*metA*	47.1	N	JFZU01000023.1	4	6224	6192
pPAR047		1,2	-	293636	293799	163	A	*metH*	51.5	N	JFZU01000023.1	4	18870	18709
pPAR048		1,2	-	304166	304197	31	O	*lysC*	48.4	N	JFZU01000023.1	4	29267	29238
pPAR049		1,2	-	305607	305645	38	I		55.3	N	JFZU01000023.1	4	30715	30679
pPAR050		1,2	+	314450	314484	34	A	*cds253*	61.8	N	JFZU01000023.1	4	39522	39554
pPAR051		1,2	+	318218	318267	49	I		49.0	N	JFZU01000023.1	4	43290	43337
pPAR052		1,2	+	318391	318427	36	I		44.4	Y	JFZU01000023.1	4	43464	43498

pPAR053		1,2	+	363615	363636	21	A	*sbmA*	57.1	N	-	-	-	-
pPAR054		1,2	+	380043	380093	50	A	*gcd*	58.0	N	JFZU01000023.1	4	104861	104909
pPAR055		1,2	-	398674	398706	32	A	*scrK*	59.4	N	JFZU01000023.1	4	123521	123491
pPAR056		1,2	-	415713	415763	50	I		38.0	N	JFZU01000023.1	4	140578	140530
pPAR057		1,2	-	448295	448329	34	I		44.1	N	JFZU01000023.1	4	173142	173110
pPAR058		1,2	-	454417	454452	35	I		42.9	N	JFZU01000023.1	4	179265	179232
pPAR059		1,2	+	455050	455189	139	I		41.7	N	JFZU01000023.1	4	179865	180002
pPAR060		1,2	+	455050	455189	139	I		41.7	N	JFZU01000023.1	4	179865	180002
pPAR061		1,2	-	458522	458572	50	I		36.0	N	JFZU01000023.1	4	183385	183337
pPAR062		1,2	-	465518	465540	22	I		50.0	N	-	-	-	-
pPAR063	*arcZ*	1,2	-	497228	497409	181	I		44.2	Y	JFZU01000023.1	4	222225	222046
pPAR064		1,2	+	497611	497656	45	I		44.4	N	JFZU01000023.1	4	222429	222472
pPAR065		1,2	+	502410	502486	76	O	*yhbG*	43.4	N	JFZU01000023.1	4	227228	227302
pPAR066		1,2	+	503540	503586	46	A	*yhbN*	54.3	N	JFZU01000023.1	4	228358	228402
pPAR067		1,2	-	510154	510229	75	I		50.7	N	JFZU01000023.1	4	235045	234972
pPAR068		1,2	+	511978	512025	47	A	*sfsB*	46.8	N	JFZU01000023.1	4	236797	236842
pPAR069		1,2	+	518137	518185	48	O	*dacB*	45.8	Y	JFZU01000023.1	4	242956	243002
pPAR070		1,2	-	524426	524461	35	O	*secG*	37.1	N	JFZU01000023.1	4	249278	249245
pPAR071		1,2	-	524817	524931	114	I		50.9	N	JFZU01000023.1	4	249748	249636
pPAR072		1,2	-	525482	525523	41	A	*yhbC*	58.5	N	JFZU01000023.1	4	250341	250302
pPAR073	*psrO*	1,2	-	531910	532014	104	A	*pnp*	52.9	N	JFZU01000023.1	4	256832	256730
pPAR074		1,2	-	583109	583158	49	A	*yjgQ*	55.1	N	JFZU01000023.1	4	308455	308408
pPAR075		1,2	-	597218	597240	22	A	*cds512*	45.5	N	-	-	-	-
pPAR076	*symR*	1,2	+	614941	614966	25	O	*yjiW*	56.0	N	-	-	-	-
pPAR077		1,2	-	657217	657253	36	A	*xylB*	66.7	N	JFZU01000024.1	17	48890	48857
pPAR078		1,2	-	674456	674485	29	A	*cds587*	48.3	N	-	-	-	-
pPAR079		1,2	-	689286	689315	29	I		48.3	N	JFZU01000001.1	9	8810	8783
pPAR080		1,2	-	690626	690676	50	I		44.0	N	JFZU01000001.1	9	10171	10123

pPAR081		1,2	-	690952	691006	54	A	*yohN*	42.6	N	JFZU01000001.1	9	10501	10449
pPAR082		1,2	+	696302	696347	45	I		48.9	N	JFZU01000001.1	9	15799	15842
pPAR083		1,2	-	696416	696492	76	I		50.0	N	JFZU01000001.1	9	15987	15913
pPAR084		1,2	+	740054	740082	28	A	*braG*	64.3	N	JFZU01000001.1	9	15987	15913
pPAR085		1,2	+	742449	742470	21	A	*braD*	52.4	N	-	-	-	-
pPAR086		1,2	+	745380	745417	37	A	*ntaR*	48.6	N	JFZU01000001.1	9	64880	64915
pPAR087		1,2	-	751934	751968	34	A	*cds646*	73.5	N	JFZU01000001.1	9	71466	71434
pPAR088		1,2	-	756425	756615	190	A	*creA*	48.9	N	JFZU01000001.1	9	76113	75925
pPAR089		1,2	-	757569	757673	104	I		41.3	N	JFZU01000001.1	9	77171	77069
pPAR090		1,2	-	757768	757824	56	I		48.2	N	JFZU01000001.1	9	77322	77268
pPAR091		1,2	+	758889	758998	109	I		43.1	Y	JFZU01000001.1	9	78389	78496
pPAR092		1,2	-	765136	765162	26	A	*talB*	61.5	N	-	-	-	-
pPAR093		1,2	-	770128	770156	28	A	*dnaK*	53.6	N	JFZU01000001.1	9	78389	78496
pPAR094		1,2	-	783522	783560	38	A	*carB*	71.1	N	JFZU01000001.1	9	102991	102955
pPAR095		1,2	-	784388	784434	46	A	*carB*	47.8	N	JFZU01000001.1	9	103865	103821
pPAR096		1,2	+	788196	788233	37	A	*cds676*	54.1	N	JFZU01000001.1	9	107630	107665
pPAR097		1,2	+	798490	798535	45	A	*imp*	60.0	N	-	-	-	-
pPAR098		1,2	+	798677	798755	78	A	*imp*	52.6	N	JFZU01000001.1	9	118120	118196
pPAR099		1,2	+	800103	800125	22	A	*cds687*	45.5	N	-	-	-	-
pPAR100		1,2	+	821192	821218	26	I		65.4	N	-	-	-	-
pPAR101		1,2	+	823856	823896	40	A	*leuB*	67.5	N	JFZU01000001.1	9	143298	143336
pPAR102		1,2	-	828855	828889	34	A	*ilvH*	44.1	N	JFZU01000001.1	9	148329	148297
pPAR103		1,2	-	837519	837556	37	A	*mraY*	59.5	N	JFZU01000001.1	9	156996	156961
pPAR104		1,2	-	840295	840327	32	A	*cds717*	40.6	N	JFZU01000001.1	9	159767	159737
pPAR105		1,2	+	885775	885838	63	I		58.7	N	JFZU01000001.1	9	205230	205291
pPAR106		1,2	+	885980	886040	60	I		61.7	N	JFZU01000001.1	9	205435	205493
pPAR107		1,2	+	887347	887382	35	A	*speE*	60.0	N	JFZU01000001.1	9	206802	206835

pPAR108		1,2	+	887870	887904	34	A	*yacC*	58.8	N	JFZU01000001.1	9	207325	207357
pPAR109		1,2	+	894824	894941	117	A	*panD*	50.4	N	JFZU01000001.1	9	214278	214393
pPAR110		1,2	+	914944	915150	206	O	*cds780*	51.0	N	JFZU01000001.1	9	234392	234596
pPAR111		1,2	-	946354	946388	34	A	*dnaE*	55.9	N	JFZU01000001.1	9	265834	265802
pPAR112		1,2	-	948496	948527	31	A	*ldcC*	51.6	N	JFZU01000001.1	9	267973	267944
pPAR113		1,2	-	949212	949235	23	A	*ldcC*	56.5	N	-	-	-	-
pPAR114		1,2	-	949707	949734	27	O	*yaeR*	44.4	N	-	-	-	-
pPAR115		1,2	+	959514	959621	107	I		44.9	N	JFZU01000018.1	15	357	271
pPAR116		1,2	-	959582	959647	65	I		38.5	N	JFZU01000016.1	19	284	346
pPAR117		1,2	+	966630	966659	29	I		51.7	N	JFZU01000002.1	16	1622	1649
pPAR118		1,2	+	972649	972712	63	A	*cds830*	54.0	N	JFZU01000002.1	16	7640	7701
pPAR119		1,2	+	1018139	1018172	33	A	*yafK*	54.5	N	JFZU01000002.1	16	53131	53162
pPAR120		1,2	+	1027162	1027196	34	O	*pepD*	47.1	N	JFZU01000002.1	16	62259	62291
pPAR121		1,2	+	1027437	1027470	33	A	*pepD*	66.7	N	JFZU01000002.1	16	62534	62565
pPAR122		1,2	-	1037650	1037712	62	A	*cds895*	69.4	N	JFZU01000002.1	16	72808	72748
pPAR123		1,2	+	1044754	1044788	34	A	*dhaD*	50.0	N	JFZU01000002.1	16	79851	79883
pPAR124		1,2	+	1062409	1062428	19	I		57.9	N	-	-	-	-
pPAR125		1,2	-	1062943	1062983	40	I		65.0	N	JFZU01000003.1	24	2704	2666
pPAR126		1,2	+	1063231	1063270	39	I		48.7	N	JFZU01000006.1	1	1683	1717
pPAR127		1,2	-	1075568	1075597	29	I		41.4	N	JFZU01000004.1	13	11915	11888
pPAR128		1,2	-	1076039	1076082	43	A	*lldP*	51.2	N	JFZU01000004.1	13	12400	12359
pPAR129		1,2	-	1082037	1082088	51	A	*licC*	37.3	N	JFZU01000004.1	13	18405	18356
pPAR130		1,2	+	1086384	1086477	93	O	*cds933*	49.5	N	JFZU01000004.1	13	22703	22794
pPAR131		1,2	-	1090288	1090338	50	A	*hcaD*	44.0	N	JFZU01000004.1	13	26667	26619
pPAR132		1,2	-	1096985	1097005	20	A	*mak*	50.0	N	-	-	-	-
pPAR133		1,2	-	1128359	1128392	33	I		69.7	N	JFZU01000004.1	13	64718	64687
pPAR134		1,2	-	1128552	1128607	55	A	*thiI*	52.7	N	JFZU01000004.1	13	64933	64880

pPAR135		1,2	+	1143253	1143285	32	I		40.6	N	JFZU01000004.1	13	79579	79609
pPAR136		1,2	+	1148007	1148057	50	I		48.0	N	JFZU01000004.1	13	84333	84381
pPAR137	*Ffs*	1,2	+	1166468	1166603	135	I		60.7	N	JFZU01000004.1	13	102783	102916
pPAR138		1,2	+	1166713	1166782	69	A	*hha*	50.7	N	JFZU01000004.1	13	103028	103095
pPAR139		1,2	-	1168010	1168060	50	I		40.0	N	JFZU01000004.1	13	104373	104325
pPAR140		1,2	-	1176148	1176177	29	A	*acrR*	65.5	N	JFZU01000004.1	13	112488	112461
pPAR141		1,2	-	1189564	1189586	22	A	*ushA*	45.5	N	-	-	-	-
pPAR142		1,2	-	1191395	1191428	33	A	*ntcB*	63.6	N	JFZU01000004.1	13	127738	127707
pPAR143		1,2	+	1192217	1192317	100	O	*ybaP*	42.0	Y	JFZU01000004.1	13	128529	128627
pPAR144		1,2	-	1196018	1196046	28	I		53.6	N	JFZU01000004.1	13	128529	128627
pPAR145		1,2	+	1196641	1196781	140	I		53.6	N	JFZU01000004.1	13	132952	133090
pPAR146		1,2	+	1198572	1198770	198	O	*ybbK*	57.6	N	JFZU01000004.1	13	134883	135079
pPAR147		1,2	+	1213542	1213576	34	I		50.0	N	JFZU01000004.1	13	149855	149887
pPAR148		1,2	+	1243112	1243143	31	A	*ydhS*	64.5	N	JFZU01000006.1	1	21613	21642
pPAR149		1,2	+	1244791	1244827	36	I		58.3	N	JFZU01000006.1	1	23293	23327
pPAR150		1,2	+	1246877	1246903	26	A	*ydeU*	42.3	N	-	-	-	-
pPAR151		1,2	+	1248734	1248784	50	I		48.0	N	JFZU01000006.1	1	27237	27285
pPAR152		1,2	+	1257219	1257313	94	I		45.7	N	JFZU01000006.1	1	45223	45315
pPAR153		1,2	+	1257464	1257514	50	I		60.0	N	JFZU01000006.1	1	45468	45516
pPAR154		1,2	+	1270872	1270923	51	I		41.2	N	JFZU01000006.1	1	58876	58925
pPAR155		1,2	+	1306802	1306953	151	A	*nagA*	52.3	Y	JFZU01000006.1	1	94929	95078
pPAR156		1,2	-	1314028	1314052	24	I		45.8	N	-	-	-	-
pPAR157		1,2	+	1314108	1314153	45	I		57.8	N	JFZU01000006.1	1	102233	102276
pPAR158		1,2	-	1384575	1384611	36	A	*uvrB*	61.1	N	JFZU01000006.1	1	172735	172701
pPAR159		1,2	-	1395985	1396035	50	A	*dusC*	52.0	N	JFZU01000006.1	1	184160	184112
pPAR160		1,2	-	1423232	1423257	25	A	*ydcN*	52.0	N	-	-	-	-
pPAR161		1,2	-	1431994	1432029	35	A	*gudP*	37.1	N	JFZU01000006.1	1	220157	220124
pPAR162		1,2	-	1452891	1453335	444	O	*ompX*	54.7	N	JFZU01000006.1	1	243379	242939
pPAR163		1,2	-	1459840	1459884	44	I		59.1	N	JFZU01000006.1	1	249929	249887

pPAR164		1,2	+	1479783	1479827	44	A	*ybjL*	59.1	N	JFZU01000006.1	1	269831	269873
pPAR165		1,2	-	1480479	1480511	32	I		53.1	Y	JFZU01000006.1	1	270556	270526
pPAR166		1,2	+	1484502	1484527	25	I		40.0	N	-	-	-	-
pPAR167		1,2	+	1502302	1502657	355	O	*cspD*	46.2	N	JFZU01000006.1	1	292352	292705
pPAR168		1,2	+	1502302	1502657	355	O	*cspD*	46.2	N	JFZU01000006.1	1	292352	292705
pPAR169		1,2	-	1502837	1502898	61	A	*clpS*	39.3	N	JFZU01000006.1	1	292946	292887
pPAR170		1,2	+	1511707	1511808	101	I		47.5	N	JFZU01000006.1	1	301757	301856
pPAR171		1,2	-	1520862	1521011	149	O	*ycaD*	55.0	N	JFZU01000006.1	1	311058	310911
pPAR172		1,2	-	1536621	1536650	29	A	*msbA*	48.3	N	-	-	-	-
pPAR173		1,2	-	1566804	1566847	43	A	*cds1378*	53.5	N	JFZU01000006.1	1	356880	356839
pPAR174		1,2	-	1577465	1577490	25	A	*cds1386*	48.0	N	-	-	-	-
pPAR175		1,2	+	1592616	1592666	50	A	*yccW*	64.0	N	JFZU01000006.1	1	382652	382700
pPAR176		1,2	-	1613795	1613829	34	I		35.3	N	-	-	-	-
pPAR177		1,2	-	1616264	1616371	107	I		43.0	N	JFZU01000006.1	1	406375	406270
pPAR178		1,2	+	1623254	1623302	48	A	*cds1435*	66.7	N	JFZU01000006.1	1	413260	413306
pPAR179		1,2	-	1636284	1636303	19	A	*yceA*	42.1	N	-	-	-	-
pPAR180		1,2	+	1640399	1640486	87	O	*cds1451*	48.3	N	JFZU01000006.1	1	430393	430478
pPAR181		1,2	-	1667162	1667243	81	A	*yceD*	53.1	N	JFZU01000006.1	1	457231	457152
pPAR182		1,2	-	1671353	1671475	122	A	*fabG*	54.9	N	JFZU01000006.1	1	461462	461342
pPAR183		1,2	-	1671535	1671586	51	A	*acpP*	39.2	N	JFZU01000006.1	1	461573	461524
pPAR184		1,2	-	1706868	1706902	34	A	*icd*	50.0	Y	JFZU01000006.1	1	496900	496868
pPAR185		1,2	-	1718609	1718698	89	A	*uidR*	46.1	N	JFZU01000006.1	1	509288	509201
pPAR186		1,2	+	1719774	1719820	46	I		65.2	N	JFZU01000006.1	1	510366	510410
pPAR187		1,2	-	1729391	1729438	47	A	*yegV*	61.7	N	JFZU01000006.1	1	520098	520053
pPAR188		1,2	-	1736691	1736744	53	A	*mltE*	73.6	N	JFZU01000006.1	1	527404	527353
pPAR189		1,2	+	1738186	1738217	31	A	*deoR*	38.7	N	-	-	-	-
pPAR190		1,2	+	1742349	1742394	45	A	*ynaI*	62.2	N	-	-	-	-

pPAR191		1,2	+	1781610	1781639	29	I		51.7	N	-	-	-	-
pPAR192		1,2	-	1781795	1781842	47	I		72.3	N	JFZU01000006.1	1	570757	570712
pPAR193		1,2	-	1790241	1790277	36	I		52.8	N	-	-	-	-
pPAR194		1,2	-	1794250	1794295	45	A	*cds1592*	51.1	N	JFZU01000006.1	1	561443	561486
pPAR195		1,2	-	1801467	1801494	27	I		51.9	N	-	-	-	-
pPAR196		1,2	-	1808196	1808227	31	A	*yveA*	58.1	N	JFZU01000006.1	1	596852	596823
pPAR197		1,2	-	1816693	1816727	34	A	*vdcC*	55.9	N	JFZU01000006.1	1	604881	604849
pPAR198		1,2	-	1817502	1817548	46	O	*vdcC*	39.1	N	JFZU01000006.1	1	605702	605658
pPAR199		1,2	-	1820623	1820673	50	I		40.0	N	JFZU01000006.1	1	608827	608779
pPAR200		1,2	-	1821960	1821992	32	A	*xylE*	53.1	N	JFZU01000006.1	1	610146	610116
pPAR201		1,2	+	1856570	1856604	34	I		61.8	N	JFZU01000007.1	5	33175	33207
pPAR202		1,2	-	1858181	1858230	49	I		57.1	N	JFZU01000007.1	5	34833	34786
pPAR203		1,2	-	1883817	1883859	42	A	*astB*	66.7	N	JFZU01000007.1	5	60463	60423
pPAR204		1,2	-	1900966	1901000	34	A	*thrS*	61.8	Y	JFZU01000007.1	5	77616	77584
pPAR205	*rprA*	1,2	-	1918007	1918133	126	I		40.5	Y	JFZU01000007.1	5	94754	94630
pPAR206		1,2	-	1921969	1922645	676	A	*ydiJ*	56.5	N	JFZU01000007.1	5	99266	98592
pPAR207		1,2	-	1923537	1923619	82	O	*sufA*	47.6	N	JFZU01000007.1	5	100240	100160
pPAR208		1,2	+	1936663	1936699	36	A	*cfa*	50.0	N	JFZU01000007.1	5	113276	113310
pPAR209		1,2	+	1936855	1936924	69	I		63.8	N	JFZU01000007.1	5	113468	113535
pPAR210		1,2	+	1937768	1937793	25	A	*ydhC*	68.0	N	-	-	-	-
pPAR211		1,2	+	1955916	1955956	40	I		50.0	N	JFZU01000007.1	5	132531	132569
pPAR212		1,2	+	1958431	1958475	44	A	*glgX*	43.2	N	JFZU01000007.1	5	135046	135088
pPAR213		1,2	+	1963784	1963883	99	I		54.5	N	JFZU01000007.1	5	140399	140496
pPAR214		1,2	+	1973541	1973570	29	A	*cds1761*	58.6	N	JFZU01000007.1	5	150155	150182
pPAR215		1,2	-	1981298	1981342	44	I		52.3	N	JFZU01000007.1	5	157961	157919
pPAR216		1,2	+	1986788	1986838	50	A	*tppB*	54.0	N	-	-	-	-
pPAR217		1,2	+	2005274	2005324	50	I		42.0	N	JFZU01000007.1	5	182168	182216
pPAR218		1,2	-	2008519	2008625	106	A	*yhcD*	54.7	N	JFZU01000007.1	5	185517	185413

pPAR219		1,2	-	2011684	2011727	43	A	*cds1800*	51.2	N	JFZU01000007.1	5	188621	188580
pPAR220		1,2	-	2016937	2016975	38	A	*yjeP*	42.1	N	-	-	-	-
pPAR221		1,2	+	2022885	2022929	44	A	*gabT*	61.4	N	JFZU01000007.1	5	200300	200342
pPAR222		1,2	+	2056211	2056285	74	I		47.3	N	JFZU01000007.1	5	233627	233699
pPAR223		1,2	+	2069994	2070021	27	A	*yncD*	59.3	N	-	-	-	-
pPAR224		1,2	-	2075557	2075613	56	A	*pqqB*	55.4	N	JFZU01000007.1	5	253035	252981
pPAR225		1,2	-	2088930	2088993	63	I		55.6	N	JFZU01000007.1	5	266416	266355
pPAR226		1,2	-	2094988	2095030	42	A	*rbsA*	59.5	N	-	-	-	-
pPAR227		1,2	-	2096492	2096522	30	A	*rbsC*	46.7	N	JFZU01000007.1	5	273945	273917
pPAR228		1,2	+	2106379	2106412	33	A	*lacA*	57.6	N	JFZU01000007.1	5	284020	284051
pPAR229		1,2	+	2108491	2108522	31	A	*cds1886*	61.3	N	JFZU01000007.1	5	286134	286163
pPAR230		1,2	-	2125878	2125942	64	A	*phoA*	48.4	N	JFZU01000007.1	5	303584	303522
pPAR231		1,2	+	2136378	2136451	73	A	*cds1915*	53.4	N	JFZU01000007.1	5	314019	314090
pPAR232		1,2	-	2150287	2150312	25	A	*ydeP*	60.0	N	-	-	-	-
pPAR233		1,2	-	2152780	2152801	21	I		52.4	N	-	-	-	-
pPAR234		1,2	+	2161514	2161560	46	A	*cds1934*	58.7	N	JFZU01000008.1	14	25361	25405
pPAR235		1,2	+	2175449	2175480	31	A	*tcp*	54.8	N	JFZU01000008.1	14	39295	39324
pPAR236		1,2	+	2185685	2185737	52	I		50.0	N	JFZU01000008.1	14	49510	49560
pPAR237		1,2	-	2187335	2187526	191	I		44.5	Y	JFZU01000008.1	14	51351	51162
pPAR238		1,2	+	2187321	2187467	146	I		46.6	N	JFZU01000008.1	14	51148	51292
pPAR239		1,2	+	2195727	2195775	48	A	*yqeB*	64.6	N	JFZU01000008.1	14	59554	59600
pPAR240		1,2	-	2215561	2215611	50	A	*sotB*	54.0	N	JFZU01000008.1	14	79418	79370
pPAR241		1,2	-	2226977	2227034	57	I		50.9	Y	JFZU01000008.1	14	90834	90779
pPAR242		1,2	+	2237033	2237085	52	A	*cds1997*	42.3	N	JFZU01000008.1	14	100835	100885
pPAR243		1,2	+	2246240	2246274	34	A	*hrpA*	61.8	N	JFZU01000008.1	14	110039	110070
pPAR244		1,2	-	2254366	2254399	33	A	*ydaO*	60.6	N	JFZU01000008.1	14	118194	118163

pPAR245	*fnrS*	1,2	-	2254671	2254792	121	I		42.1	Y	JFZU01000008.1	14	118587	118468
pPAR246		1,2	-	2267249	2267331	82	I		58.5	Y	JFZU01000017.1	11	87009	86982
pPAR247		1,2	+	2267292	2267395	103	I		43.7	N	JFZU01000008.1	14	131088	131189
pPAR248		1,2	-	2272137	2272166	29	A	*sapD*	51.7	N	JFZU01000008.1	14	135956	135929
pPAR249		1,2	-	2297821	2298115	294	I		42.5	N	JFZU01000009.1	8	30211	29919
pPAR250		1,2	-	2298626	2298685	59	I		42.4	N	JFZU01000009.1	8	30781	30724
pPAR251		1,2	-	2318729	2318761	32	A	*trpA*	71.9	N	JFZU01000009.1	8	50858	50828
pPAR252		1,2	+	2334130	2334162	32	I		62.5	N	JFZU01000009.1	8	66222	66252
pPAR253		1,2	+	2345226	2345257	31	A	*ychK*	64.5	N	JFZU01000009.1	8	77320	77348
pPAR254		1,2	+	2349596	2349641	45	A	*topB*	57.8	N	JFZU01000009.1	8	81849	81892
pPAR255		1,2	-	2354807	2354857	50	A	*pncA*	54.0	N	JFZU01000009.1	8	87107	87059
pPAR256		1,2	+	2356048	2356089	41	I		39.0	N	-	-	-	-
pPAR257		1,2	+	2356164	2356207	43	I		58.1	N	JFZU01000009.1	8	88416	88457
pPAR258		1,2	-	2398329	2398476	147	O	*cspC*	40.8	N	JFZU01000009.1	8	130741	130596
pPAR259		1,2	-	2419496	2419559	63	O	*betB*	49.2	N	JFZU01000009.1	8	151823	151762
pPAR260		1,2	+	2421408	2421487	79	I		44.3	N	JFZU01000009.1	8	153674	153751
pPAR261		1,2	+	2439197	2439235	38	A	*ptrB*	50.0	N	JFZU01000009.1	8	171424	171460
pPAR262		1,2	-	2445884	2445918	34	I		55.9	N	JFZU01000009.1	8	178144	178112
pPAR263		1,2	+	2451765	2451968	203	A	*znuA*	48.3	Y	JFZU01000009.1	8	183993	184194
pPAR264		1,2	+	2468378	2468407	29	I		48.3	N	JFZU01000009.1	8	200606	200633
pPAR265		1,2	+	2478252	2478379	127	O	*cheR*	50.4	N	JFZU01000009.1	8	210480	210605
pPAR266		1,2	+	2484276	2484326	50	A	*cds2229*	50.0	N	JFZU01000009.1	8	216505	216553
pPAR267		1,2	-	2507613	2507677	64	I		50.0	N	JFZU01000009.1	8	240074	240012
pPAR268		1,2	-	2514732	2514751	19	A	*putA*	52.6	N	-	-	-	-
pPAR269		1,2	-	2530628	2530652	24	A	*cds2269*	58.3	N	-	-	-	-
pPAR270		1,2	+	2531651	2531733	82	A	*cds2270*	47.6	N	JFZU01000009.1	8	264066	264146
pPAR271		1,2	+	2539511	2539554	43	A	*cds2276*	53.5	N	JFZU01000009.1	8	271928	271969

pPAR272		1,2	+	2542760	2542790	30	A	*cds2279*	56.7	N	JFZU01000009.1	8	275177	275205
pPAR273		1,2	+	2547331	2547362	31	A	*cds2280*	38.7	N	JFZU01000009.1	8	279748	279777
pPAR274		1,2	+	2550448	2550483	35	I		37.1	N	JFZU01000009.1	8	282865	282898
pPAR275		1,2	-	2556847	2556880	33	O	*fliS*	48.5	N	JFZU01000010.1	18	2552	2521
pPAR276		1,2	-	2580795	2580835	40	A	*cds2317*	42.5	N	JFZU01000010.1	18	26506	26468
pPAR277		1,2	+	2588147	2588252	105	I		45.7	N	JFZU01000010.1	18	33820	33922
pPAR278		1,2	-	2589792	2589887	95	A	*yeeI*	55.8	N	JFZU01000010.1	18	35557	35464
pPAR279		1,2	+	2590392	2590439	47	I		53.2	N	JFZU01000010.1	18	36145	36190
pPAR280		1,2	+	2605074	2605124	50	A	*ybgG*	58.0	N	JFZU01000010.1	18	50834	50882
pPAR281		1,2	-	2609994	2610066	72	I		61.1	N	JFZU01000010.1	18	57258	57188
pPAR282		1,2	-	2635130	2635232	102	I		39.2	N	JFZU01000012.1	7	19556	19456
pPAR283		1,2	+	2644935	2644994	59	A	*cds2374*	54.2	N	JFZU01000012.1	7	29262	29319
pPAR284		1,2	-	2647080	2647136	56	I		41.1	N	JFZU01000012.1	7	31461	31407
pPAR285		1,2	+	2702175	2702331	156	A	*mocB*	48.7	N	JFZU01000012.1	7	86824	86978
pPAR286		1,2	+	2703432	2703730	298	I		47.0	N	JFZU01000010.1	18	35732	35838
pPAR287		1,2	+	2750610	2750660	50	I		46.0	Y	JFZU01000012.1	7	135339	135387
pPAR288		1,2	+	2780323	2780348	25	I		48.0	N	-	-	-	-
pPAR289		1,2	+	2797035	2797081	46	I		52.2	N	JFZU01000012.1	7	176340	176384
pPAR290		1,2	-	2811295	2811321	26	A	*mdtB*	76.9	N	-	-	-	-
pPAR291		1,2	-	2821244	2821276	32	A	*yegS*	62.5	N	JFZU01000012.1	7	200587	200557
pPAR292		1,2	-	2822674	2822713	39	A	*ydfI*	53.8	N	JFZU01000012.1	7	202024	201987
pPAR293		1,2	-	2830306	2830333	27	A	*cds2534*	59.3	N	-	-	-	-
pPAR294		1,2	-	2842877	2842967	90	I		57.8	N	JFZU01000012.1	7	231672	231584
pPAR295		1,2	+	2853965	2854079	114	I		44.7	N	JFZU01000012.1	7	242671	242783
pPAR296		1,2	-	2856010	2856063	53	A	*yeiH*	54.7	N	JFZU01000012.1	7	244764	244716
pPAR297		1,2	-	2869861	2869911	50	O	*yeiP*	54.0	N	JFZU01000012.1	7	259697	259649

pPAR298		1,2	+	2872012	2872040	28	I		42.9	N	JFZU01000012.1	7	259697	259649
pPAR299		1,2	-	2872803	2872834	31	I		45.2	N	-	-	-	-
pPAR300		1,2	+	2888720	2888764	44	O	*cds2586*	52.3	N	JFZU01000013.1	3	8657	8699
pPAR301		1,2	+	2898498	2898537	39	I		56.4	N	JFZU01000013.1	3	18437	18474
pPAR302		1,2	-	2902105	2902132	27	A	*exbB*	63.0	N	-	-	-	-
pPAR303		1,2	+	2906513	2906563	50	I		50.0	N	JFZU01000013.1	3	26451	26499
pPAR304		1,2	+	2908850	2908900	50	A	*yojI*	70.0	N	JFZU01000013.1	3	28788	28836
pPAR305		1,2	+	2911509	2911554	45	A	*apbE*	60.0	N	JFZU01000013.1	3	31447	31490
pPAR306		1,2	+	2912954	2913012	58	A	*ompC*	41.4	N	JFZU01000002.1	16	66649	66702
pPAR307		1,2	+	2914323	2914402	79	I		39.2	Y	JFZU01000013.1	3	34261	34339
pPAR308		1,2	+	2914690	2914754	64	A	*lktD*	50.0	N	JFZU01000013.1	3	34629	34691
pPAR309		1,2	+	2952557	2952583	26	I		46.2	N	-	-	-	-
pPAR310		1,2	-	2971470	2971599	129	I		39.5	N	JFZU01000013.1	3	91734	91607
pPAR311		1,2	-	2972996	2973181	185	I		48.6	N	JFZU01000013.1	3	93316	93133
pPAR312		1,2	-	2975504	2975560	56	A	*yfbR*	55.4	N	JFZU01000013.1	3	95695	95641
pPAR313		1,2	-	2977642	2977673	31	I		45.2	N	JFZU01000013.1	3	97808	97779
pPAR314		1,2	-	2977759	2978148	389	O	*ackA*	47.6	N	JFZU01000013.1	3	98283	97896
pPAR315		1,2	-	2977759	2978148	389	O	*ackA*	47.6	N	JFZU01000013.1	3	98283	97896
pPAR316		1,2	-	2984475	2984498	23	A	*puuE*	56.5	N	-	-	-	-
pPAR317		1,2	-	3000103	3000133	30	I		50.0	N	JFZU01000013.1	3	122254	122226
pPAR318		1,2	+	3007535	3007567	32	A	*truA*	59.4	N	JFZU01000013.1	3	129658	129688
pPAR319		1,2	-	3045967	3045996	29	I		27.6	N	JFZU01000013.1	3	168116	168089
pPAR320		1,2	+	3047431	3047455	24	I		37.5	N	-	-	-	-
pPAR321		1,2	-	3047635	3047662	27	I		48.1	N	-	-	-	-
pPAR322		1,2	+	3052311	3052361	50	A	*malE*	52.0	N	JFZU01000013.1	3	174432	174480
pPAR323		1,2	+	3078017	3078064	47	I		66.0	N	JFZU01000013.1	3	200138	200183
pPAR324		1,2	-	3080772	3080806	34	A	*ypdB*	44.1	N	JFZU01000013.1	3	202928	202896
pPAR325		1,2	-	3088078	3088140	62	I		46.8	N	JFZU01000013.1	3	210262	210202

pPAR326		1,2	-	3088400	3088590	190	A	*nupC*	49.5	N	JFZU01000013.1	3	210712	210524
pPAR327		1,2	-	3089572	3089596	24	I		62.5	N	-	-	-	-
pPAR328		1,2	+	3090999	3091020	21	I		52.4	N	-	-	-	-
pPAR329		1,2	-	3092261	3092289	28	A	*yfeC*	46.4	N	JFZU01000013.1	3	210712	210524
pPAR330		1,2	-	3095161	3095223	62	I		37.1	Y	JFZU01000013.1	3	217188	217128
pPAR331		1,2	-	3122307	3122893	586	O	*tktB*	59.2	N	JFZU01000013.1	3	244859	244275
pPAR332		1,2	-	3146708	3146885	177	I		46.3	Y	JFZU01000013.1	3	268849	268674
pPAR333		1,2	+	3207668	3207699	31	A	*qumA*	45.2	N	JFZU01000013.1	3	325115	325144
pPAR334		1,2	-	3208594	3208626	32	I		56.3	N	JFZU01000013.1	3	326072	326042
pPAR335		1,2	+	3209096	3209143	47	A	*engA*	57.4	N	JFZU01000013.1	3	326544	326589
pPAR336		1,2	+	3214855	3214879	24	A	*yfgA*	54.2	N	-	-	-	-
pPAR337		1,2	-	3235861	3235937	76	A	*csiE*	51.3	Y	JFZU01000013.1	3	353358	353284
pPAR338		1,2	+	3238962	3238991	29	A	*glyA1*	58.6	N	JFZU01000013.1	3	356386	356413
pPAR339		1,2	+	3243947	3243977	30	A	*yfhK*	50.0	N	JFZU01000013.1	3	361372	361400
pPAR340	*glmY*	1,2	-	3245122	3245276	154	I		51.3	N	JFZU01000013.1	3	362699	362547
pPAR341		1,2	-	3257494	3257538	44	I		45.5	N	JFZU01000013.1	3	374948	374906
pPAR342		1,2	-	3267429	3267619	190	O	*srmB*	50.5	N	JFZU01000013.1	3	385029	384841
pPAR343	*ssrA*	1,2	+	3274707	3274936	229	I		53.7	Y	JFZU01000013.1	3	436616	436651
pPAR344		1,2	-	3309493	3309542	49	A	*fecE*	42.9	N	JFZU01000013.1	3	455124	455077
pPAR345		1,2	+	3335859	3335962	103	O	*cds2977*	44.7	Y	JFZU01000013.1	3	482764	482866
pPAR346		1,2	-	3341101	3341330	229	I		51.1	N	JFZU01000013.1	3	488226	487999
pPAR347		1,2	-	3342013	3342064	51	A	*dppA*	68.6	N	JFZU01000013.1	3	488960	488911
pPAR348		1,2	-	3350692	3351173	481	O	*ygaM*	53.0	N	JFZU01000013.1	3	498069	497590
pPAR349		1,2	-	3350692	3351173	481	O	*ygaM*	53.0	N	JFZU01000013.1	3	498069	497590
pPAR350		1,2	-	3361149	3361201	52	A	*emrA*	51.9	N	JFZU01000013.1	3	508097	508047
pPAR351		1,2	+	3381129	3381255	126	I		46.0	N	JFZU01000018.1	15	251	357
pPAR352		1,2	-	3381204	3381400	196	I		51.0	N	JFZU01000018.1	15	510	460
pPAR353	*ryfD*	1,2	+	3384054	3384108	54	A	*clpB*	44.4	N	JFZU01000015.1	2	2752	2804

pPAR354		1,2	+	3384204	3384239	35	I		51.4	N	JFZU01000015.1	2	2902	2935
pPAR355	*micA*	1,2	+	3399326	3399497	171	O	*gshA*	49.1	N	JFZU01000015.1	2	18025	18194
pPAR356		1,2	+	3402396	3402446	50	I		50.0	N	JFZU01000015.1	2	21101	21149
pPAR357		1,2	-	3412750	3412774	24	A	*mutS*	45.8	N	-	-	-	-
pPAR358		1,2	+	3417364	3417407	43	O	*nlpD*	53.5	N	JFZU01000015.1	2	36337	36378
pPAR359		1,2	+	3454200	3454327	127	A	*rumA*	64.6	N	JFZU01000015.1	2	71946	72071
pPAR360		1,2	+	3458563	3458597	34	A	*garR*	70.6	N	JFZU01000015.1	2	76309	76341
pPAR361	*csrB*	1,2	-	3468194	3468435	241	I		54.4	N	JFZU01000015.1	2	86179	85940
pPAR362	*csrB*	1,2	-	3468194	3468435	241	I		54.4	N	JFZU01000015.1	2	86179	85940
pPAR363		1,2	-	3469435	3469524	89	A	*queF*	52.8	N	JFZU01000015.1	2	87268	87181
pPAR364	*gcvB*	1,2	+	3475041	3475225	184	I		40.8	Y	JFZU01000015.1	2	92787	92969
pPAR365		1,2	+	3475516	3475566	50	I		54.0	N	JFZU01000015.1	2	93263	93311
pPAR366		1,2	+	3491908	3491966	58	A	*ptrA*	65.5	N	JFZU01000015.1	2	109793	109846
pPAR367		1,2	-	3505014	3505042	28	A	*ygdR*	50.0	Y	JFZU01000015.1	2	109793	109846
pPAR368		1,2	+	3517636	3517681	45	I		35.6	N	JFZU01000015.1	2	135521	135563
pPAR369		1,2	-	3555499	3555541	42	A	*glvR*	52.4	N	JFZU01000015.1	2	139376	139336
pPAR370	*ssrS*	1,2	+	3568049	3568139	90	I		54.4	N	JFZU01000015.1	2	151886	151972
pPAR371		1,2	+	3569932	3569968	36	A	*serA*	61.1	N	JFZU01000015.1	2	153769	153803
pPAR372		1,2	+	3580932	3580966	34	A	*tktA*	58.8	N	JFZU01000015.1	2	164769	164801
pPAR373		1,2	+	3584177	3584205	28	A	*speA*	42.9	N	JFZU01000015.1	2	164769	164801
pPAR374		1,2	+	3586159	3586209	50	I		54.0	N	JFZU01000015.1	2	169995	170043
pPAR375		1,2	+	3633735	3633782	47	A	*ydaM*	55.3	N	JFZU01000015.1	2	217566	217611
pPAR376		1,2	-	3637753	3637800	47	A	*cds3265*	42.6	N	JFZU01000015.1	2	221630	221585
pPAR377		1,2	-	3642823	3642986	163	A	*cds3269*	54.6	N	JFZU01000015.1	2	226729	226568
pPAR378		1,2	-	3645948	3645973	25	I		60.0	N	-	-	-	-
pPAR379		1,2	+	3656196	3656245	49	I		42.9	N	JFZU01000015.1	2	237464	237511
pPAR380		1,2	-	3658221	3658271	50	I		40.0	N	JFZU01000015.1	2	239537	239489
pPAR381		1,2	+	3665555	3665579	24	A	*leuC*	41.7	N	-	-	-	-

pPAR382		1,2	+	3666656	3666706	50	A	*leuA2*	54.0	N	JFZU01000015.1	2	247925	247973
pPAR383		1,2	+	3669964	3669997	33	I		57.6	N	JFZU01000015.1	2	251233	251264
pPAR384		1,2	-	3670461	3670511	50	I		46.0	N	JFZU01000015.1	2	251778	251730
pPAR385		1,2	+	3677380	3677425	45	A	*mrdA*	57.8	N	JFZU01000015.1	2	258649	258692
pPAR386		1,2	+	3691649	3691679	30	A	*yicI*	60.0	N	JFZU01000015.1	2	272918	272946
pPAR387		1,2	+	3712567	3712611	44	A	*ydcR*	63.6	N	JFZU01000015.1	2	293838	293880
pPAR388		1,2	+	3747994	3748044	50	A	*plsC*	56.0	Y	JFZU01000015.1	2	329261	329309
pPAR389		1,2	-	3751915	3751943	28	A	*licR*	50.0	N	JFZU01000015.1	2	329261	329309
pPAR390		1,2	-	3763482	3763683	201	A	*tolC*	54.2	N	JFZU01000015.1	2	344954	344755
pPAR391		1,2	-	3775254	3775282	28	I		53.6	N	JFZU01000015.1	2	344954	344755
pPAR392		1,2	+	3796183	3796288	105	A	*cds3408*	41.9	N	JFZU01000015.1	2	378903	379006
pPAR393		1,2	-	3814227	3814256	29	I		62.1	N	JFZU01000015.1	2	396974	396947
pPAR394		1,2	-	3822243	3822284	41	I		61.0	Y	JFZU01000015.1	2	404983	404947
pPAR395		1,2	-	3822866	3822977	111	I		45.9	Y	JFZU01000015.1	2	405680	405571
pPAR396		1,2	+	3825965	3826011	46	A	*cds3440*	58.7	N	JFZU01000015.1	2	408675	408719
pPAR397		1,2	+	3826209	3826260	51	I		33.3	N	JFZU01000015.1	2	408919	408967
pPAR398		1,2	-	3851921	3851968	47	I		59.6	N	JFZU01000015.1	2	434677	434632
pPAR399	*rnpB*	1,2	-	3866834	3867171	337	I		60.2	N	JFZU01000015.1	2	449883	449547
pPAR400		1,2	+	3874674	3874714	40	A	*licR*	55.0	N	JFZU01000015.1	2	457388	457426
pPAR401		1,2	-	3912338	3912371	33	A	*ytfJ*	42.4	N	JFZU01000015.1	2	495084	495053
pPAR402		1,2	+	3912724	3912754	30	A	*cysQ*	53.3	N	JFZU01000015.1	2	495439	495467
pPAR403		1,2	+	3928163	3928399	236	A	*yjeB*	53.0	N	JFZU01000015.1	2	510878	511112
pPAR404		1,2	+	3929664	3929700	36	A	*purA*	55.6	Y	JFZU01000015.1	2	512379	512413
pPAR405		1,2	+	3930211	3930262	51	O	*yjeT*	54.9	N	JFZU01000015.1	2	512926	512974
pPAR406		1,2	+	3934507	3934631	124	O	*hfq*	44.4	N	JFZU01000015.1	2	517222	517344
pPAR407		1,2	-	3942661	3942866	205	I		55.1	N	JFZU01000006.1	1	401549	401603
pPAR408		1,2	-	3949516	3949647	131	I		51.1	N	JFZU01000015.1	2	532478	532349
pPAR409		1,2	-	3949864	3950330	466	I		51.3	N	JFZU01000015.1	2	533161	532697

pPAR410		1,2	-	3952437	3952621	184	O	*yhcN*	53.3	N	JFZU01000015.1	2	535452	535270
pPAR411		1,2	+	3953279	3953329	50	A	*yfcI*	46.0	N	JFZU01000015.1	2	536112	536160
pPAR412		1,2	+	3958652	3958713	61	A	*aaeX*	54.1	N	JFZU01000015.1	2	541485	541544
pPAR413		1,2	+	3961051	3961091	40	A	*tldD*	72.5	N	JFZU01000015.1	2	543884	543922
pPAR414		1,2	+	3981376	3981481	105	I		53.3	N	JFZU01000015.1	2	564208	564311
pPAR415		1,2	+	3981651	3981692	41	I		41.5	N	JFZU01000015.1	2	564483	564522
pPAR416		1,2	+	3986433	3986454	21	I		42.9	N	-	-	-	-
pPAR417		1,2	-	4001073	4001117	44	O	*trkA*	43.2	N	JFZU01000016.1	19	9399	9357
pPAR418		1,2	+	4001816	4001864	48	O	*yhdL*	41.7	Y	JFZU01000016.1	19	10100	10146
pPAR419		1,2	+	4005576	4005610	34	A	*secY*	44.1	N	JFZU01000016.1	19	13861	13893
pPAR420		1,2	+	4005725	4005757	32	A	*secY*	40.6	N	JFZU01000016.1	19	14010	14040
pPAR421		1,2	+	4009824	4010048	224	A	*rplE*	52.2	N	JFZU01000016.1	19	18109	18331
pPAR422		1,2	+	4010692	4010736	44	A	*rplN*	63.6	N	JFZU01000016.1	19	18977	19019
pPAR423		1,2	-	4030405	4030455	50	A	*yheS*	48.0	N	JFZU01000017.1	11	12292	12244
pPAR424		1,2	+	4039482	4039512	30	I		56.7	N	JFZU01000017.1	11	21321	21349
pPAR425		1,2	-	4039650	4039695	45	A	*crp*	46.7	N	JFZU01000017.1	11	21532	21489
pPAR426		1,2	+	4062247	4062309	62	I		41.9	N	JFZU01000017.1	11	44086	44146
pPAR427		1,2	-	4064524	4064554	30	A	*yrfF*	40.0	N	JFZU01000017.1	11	46391	46363
pPAR428		1,2	-	4071466	4071491	25	I		64.0	N	-	-	-	-
pPAR429		1,2	-	4098919	4099238	319	I		52.0	N	JFZU01000017.1	11	80866	80556
pPAR430		1,2	+	4098951	4099324	373	I		49.3	N	JFZU01000017.1	11	80588	80952
pPAR431		1,2	+	4098951	4099324	373	I		49.3	N	JFZU01000017.1	11	80588	80952
pPAR432		1,2	-	4098919	4099238	319	I		52.0	N	JFZU01000017.1	11	80866	80556
pPAR433	*ryhB*	1,2	-	4105322	4105419	97	I		48.5	Y	JFZU01000008.1	14	131095	131068
pPAR434		1,2	-	4128085	4128113	28	A	*zntA*	57.1	N	-	-	-	-
pPAR435		1,2	-	4134759	4134785	26	I		50.0	N	-	-	-	-
pPAR436		1,2	-	4151618	4151753	135	O	*hemB*	51.9	N	JFZU01000017.1	11	133323	133190
pPAR437		1,2	-	4167553	4167660	107	O	*uspA*	54.2	N	JFZU01000017.1	11	149230	149125
pPAR438		1,2	-	4174328	4174358	30	A	*gor*	53.3	N	JFZU01000017.1	11	155928	155900

pPAR439		1,2	-	4175149	4175203	54	A	*gor*	51.9	N	JFZU01000017.1	11	156773	156721
pPAR440		1,2	+	4201912	4201957	45	I		60.0	N	JFZU01000017.1	11	183485	183528
pPAR441		1,2	+	4213277	4213327	50	I		44.0	N	JFZU01000017.1	11	194851	194899
pPAR442		1,2	-	4239633	4239719	86	I		38.4	Y	JFZU01000017.1	11	221293	221209
pPAR443		1,2	+	4248548	4248686	138	I		49.3	N	JFZU01000018.1	15	254	357
pPAR444		1,2	-	4248620	4248776	156	I		47.4	N	JFZU01000018.1	15	357	326
pPAR445		1,2	-	4251846	4251956	110	O	*trmA*	51.8	N	JFZU01000018.1	15	3661	3553
pPAR446		1,2	-	4254474	4254498	24	A	*sthA*	50.0	N	-	-	-	-
pPAR447		1,2	+	4256795	4256882	87	I		54.0	Y	JFZU01000018.1	15	8501	8586
pPAR448		1,2	+	4261334	4261458	124	A	*argC*	54.0	N	JFZU01000018.1	15	13040	13162
pPAR449		1,2	+	4270396	4270456	60	A	*metL*	73.3	N	JFZU01000018.1	15	22103	22161
pPAR450		1,2	-	4281365	4281794	429	O	*glpF*	50.6	N	JFZU01000018.1	15	33502	33075
pPAR451		1,2	-	4288008	4288046	38	A	*yiiQ*	50.0	N	JFZU01000018.1	15	39754	39718
pPAR452		1,2	+	4294503	4294551	48	A	*cpxP*	56.3	N	JFZU01000018.1	15	46203	46249
pPAR453		1,2	+	4298420	4298444	24	A	*cysE*	50.0	N	-	-	-	-
pPAR454		1,2	-	4308555	4308590	35	A	*rfaC*	45.7	N	JFZU01000018.1	15	60288	60255
pPAR455		1,2	-	4309940	4309973	33	A	*wcaL*	39.4	N	JFZU01000018.1	15	61671	61640
pPAR456		1,2	+	4315772	4315859	87	O	*rfaF*	47.1	N	JFZU01000018.1	15	67476	67561
pPAR457		1,2	-	4330842	4330892	50	O	*yicC*	44.0	Y	JFZU01000018.1	15	82590	82546
pPAR458		1,2	+	4348047	4348092	45	I		42.2	N	JFZU01000018.1	15	87466	87509
pPAR459		1,2	+	4349103	4349150	47	I		63.8	N	JFZU01000018.1	15	88522	88567
pPAR460		1,2	-	4366040	4366070	30	I		46.7	N	JFZU01000018.1	15	105488	105460
pPAR461		1,2	-	4367104	4367132	28	A	*glnA*	39.3	N	JFZU01000018.1	15	105488	105460
pPAR462		1,2	-	4370287	4370417	130	A	*ntrC*	61.5	N	JFZU01000018.1	15	109835	109707
pPAR463		1,2	-	4372873	4372966	93	I		49.5	Y	JFZU01000018.1	15	112384	112293
pPAR464	*spf*	1,2	-	4373881	4373992	111	I		45.9	Y	JFZU01000018.1	15	113411	113302
pPAR465		1,2	-	4377144	4377170	26	I		42.3	N	-	-	-	-
pPAR466		1,2	+	4377953	4378021	68	A	*dsbA*	47.1	N	JFZU01000018.1	15	117373	117439
pPAR467		1,2	+	4384013	4384079	66	I		47.0	N	KK328466.1	10	235061	234997

pPAR468		1,2	+	4385952	4386091	139	I		47.5	N	JFZU01000018.1	15	253	357
pPAR469		1,2	-	4386026	4386222	196	I		50.0	N	JFZU01000018.1	15	511	327
pPAR470		1,2	-	4388229	4388352	123	O	*yebG*	54.5	Y	JFZU01000025.1	6	117245	117366
pPAR471		1,2	-	4388441	4388502	61	I		45.9	N	JFZU01000025.1	6	117095	117154
pPAR472		1,2	-	4389608	4389639	31	A	*tcp*	38.7	N	JFZU01000025.1	6	115958	115987
pPAR473		1,2	-	4390805	4390943	138	A	*tcp*	54.3	N	JFZU01000025.1	6	114654	114790
pPAR474		1,2	+	4405233	4405276	43	A	*putP*	41.9	N	JFZU01000025.1	6	100369	100328
pPAR475		1,2	-	4413679	4413706	27	I		40.7	N	-	-	-	-
pPAR476		1,2	-	4419368	4419398	30	A	*pagO*	40.0	N	JFZU01000025.1	6	86205	86233
pPAR477		1,2	-	4421545	4421570	25	A	*tsr*	76.0	N	-	-	-	-
pPAR478		1,2	+	4442620	4442700	80	I		48.8	N	JFZU01000025.1	6	62982	62904
pPAR479		1,2	-	4457282	4457307	25	I		56.0	Y	-	-	-	-
pPAR480		1,2	-	4471539	4471597	58	I		43.1	N	JFZU01000025.1	6	38498	38552
pPAR481		1,2	-	4484716	4484747	31	A	*yliB*	35.5	N	JFZU01000025.1	6	25343	25372
pPAR482		1,2	+	4492821	4492859	38	I		57.9	N	JFZU01000025.1	6	17267	17231
pPAR483		1,2	-	4497070	4497096	26	A	*iolH*	42.3	N	-	-	-	-
pPAR484		1,2	+	4508389	4508419	30	I		53.3	N	JFZU01000025.1	6	1694	1666
pPAR485		1,2	+	4508823	4508872	49	I		44.9	N	JFZU01000025.1	6	1260	1213
pPAR486		1,2	+	4509007	4509057	50	A	*cre*	50.0	N	JFZU01000014.1	12	171862	171814
pPAR487		1,2	+	4510021	4510045	24	I		54.2	N	-	-	-	-
pPAR488		1,2	+	4531263	4531311	48	A	*dsbD*	54.2	N	JFZU01000025.1	6	260899	260853
pPAR489		1,2	+	4542396	4542446	50	I		58.0	N	-	-	-	-
pPAR490		1,2	-	4552607	4552715	108	I		37.0	N	JFZU01000025.1	6	239442	239548
pPAR491		1,2	+	4570086	4570150	64	I		39.1	N	JFZU01000025.1	6	222072	222010
pPAR492		1,2	+	4633072	4633099	27	A	*thiF*	63.0	N	-	-	-	-
pPAR493		1,2	-	4637173	4637255	82	A	*ydcN*	56.1	N	JFZU01000025.1	6	185557	185637
pPAR494		1,2	+	4642131	4642173	42	I		45.2	N	JFZU01000025.1	6	180679	180639
pPAR495		1,2	-	4646432	4646474	42	O	*repA*	52.4	N	JFZU01000025.1	6	176338	176378
pPAR496		1,2	+	4647276	4647319	43	I		53.5	N	JFZU01000025.1	6	175533	175492

pPAR497		1,2	-	4651376	4651412	36	I		44.4	N	JFZU01000025.1	6	171391	171425
pPAR498		1,2	-	4681084	4681134	50	O	*ycgF*	50.0	N	JFZU01000025.1	6	141652	141700
pPAR499		1,2	-	4689491	4689655	164	A	*ascG*	50.0	N	JFZU01000025.1	6	133092	133254
pPAR500		1,2	-	4694407	4694433	26	I		57.7	N	-	-	-	-
pPAR501		1,2	+	4697062	4697135	73	I		53.4	N	JFZU01000025.1	6	125683	125612
pPAR502		1,2	-	4700178	4700211	33	I		39.4	N	-	-	-	-
pPAR503		1,2	-	4700743	4700779	36	I		38.9	N	-	-	-	-
pPAR504		1,2	-	4702565	4702590	25	A	*fhuE*	44.0	N	-	-	-	-
pPAR505		1	-	21997	22028	31	I		35.5	N	KK328466.1	10	22342	22313
pPAR506		1	+	69465	69498	33	A	*celB*	54.5	N	KK328466.1	10	69786	69817
pPAR507		1	-	111481	111504	23	I		52.2	N	-	-	-	-
pPAR508		1	-	116400	116431	31	O	*ybjX*	29.0	N	KK328466.1	10	116762	116733
pPAR509		1	+	122956	123006	50	I		56.0	Y	KK328466.1	10	123288	123336
pPAR510		1	-	132080	132109	29	I		37.9	N	KK328466.1	10	132483	132456
pPAR511		1	-	132823	132844	21	A	*dppA*	71.4	Y	-	-	-	-
pPAR512		1	-	160615	160639	24	A	*yhjG*	54.2	N	-	-	-	-
pPAR513		1	-	190695	190726	31	A	*cyaA*	51.6	N	KK328466.1	10	188235	188206
pPAR514		1	-	224692	224714	22	I		50.0	N	-	-	-	-
pPAR515		1	+	250400	250422	22	I		72.7	N	-	-	-	-
pPAR516		1	-	280899	281010	111	A	*metA*	49.5	N	JFZU01000023.1	4	6081	5972
pPAR517		1	-	329405	329451	46	I		45.7	N	-	-	-	-
pPAR518		1	-	362549	362662	113	I		55.8	N	JFZU01000023.1	4	87479	87368
pPAR519		1	+	368297	368335	38	A	*yyaJ*	50.0	N	JFZU01000023.1	4	93116	93152
pPAR520		1	-	382323	382353	30	I		50.0	N	JFZU01000023.1	4	107169	107141
pPAR521		1	+	392904	392975	71	A	*yeaU*	59.2	Y	JFZU01000023.1	4	117721	117790
pPAR522		1	+	458098	458151	53	I		47.2	N	JFZU01000023.1	4	182913	182964
pPAR523		1	+	476525	476629	104	A	*yjeK*	61.5	N	JFZU01000023.1	4	201341	201443
pPAR524		1	-	476891	476919	28	A	*efp*	53.6	N	JFZU01000023.1	4	201341	201443
pPAR525		1	-	477597	477633	36	I		36.1	Y	JFZU01000023.1	4	202447	202413

pPAR526		1	-	484946	484966	20	A	*rpsI*	50.0	N	-	-	-	-
pPAR527		1	+	501048	501076	28	A	*rpoN*	57.1	N	JFZU01000023.1	4	202447	202413
pPAR528		1	-	689566	689587	21	A	*ampC*	52.4	N	-	-	-	-
pPAR529		1	+	694328	694352	24	A	*mdoB*	45.8	N	-	-	-	-
pPAR530		1	+	706157	706383	226	O	*tRNA*	52.2	N	KK328466.1	10	180555	180490
pPAR531		1	-	714617	714642	25	A	*yqeI*	44.0	N	-	-	-	-
pPAR532		1	+	730476	730516	40	I		20.0	N	-	-	-	-
pPAR533		1	+	737491	737635	144	A	*foxA*	55.6	N	JFZU01000001.1	9	56992	57134
pPAR534		1	+	797263	797288	25	A	*imp*	64.0	N	-	-	-	-
pPAR535		1	+	809520	809548	28	A	*tbpA*	53.6	Y	JFZU01000001.1	9	56992	57134
pPAR536		1	+	826046	826074	28	I		42.9	N	JFZU01000001.1	9	56992	57134
pPAR537		1	+	826540	826575	35	I		54.3	N	JFZU01000001.1	9	145982	146015
pPAR538		1	-	829834	829871	37	A	*fruR*	51.4	N	-	-	-	-
pPAR539		1	+	853720	853811	91	A	*coaE*	54.9	N	JFZU01000001.1	9	173163	173252
pPAR540		1	+	859083	859127	44	A	*nadC*	54.5	N	JFZU01000001.1	9	178526	178568
pPAR541		1	-	869125	869194	69	O	*aceE*	46.4	N	JFZU01000001.1	9	188633	188566
pPAR542		1	+	892158	892253	95	A	*can*	57.9	N	JFZU01000001.1	9	211613	211706
pPAR543		1	+	892552	892640	88	A	*can*	62.5	N	JFZU01000001.1	9	212007	212093
pPAR544		1	+	900462	900550	88	A	*sfsA*	59.1	Y	JFZU01000001.1	9	219916	220002
pPAR545		1	+	913681	913745	64	A	*hemL*	54.7	N	JFZU01000001.1	9	233129	233191
pPAR546		1	-	948176	948206	30	A	*ldcC*	56.7	N	JFZU01000001.1	9	267652	267624
pPAR547		1	+	983734	983768	34	A	*fliY*	58.8	N	JFZU01000002.1	16	18726	18758
pPAR548		1	+	1007656	1007684	28	A	*yafV*	60.7	N	JFZU01000002.1	16	18726	18758
pPAR549		1	+	1045192	1045236	44	I		50.0	N	JFZU01000002.1	16	80289	80331
pPAR550		1	-	1110202	1110246	44	I		50.0	N	JFZU01000004.1	13	46572	46530
pPAR551		1	+	1110468	1110570	102	A	*agp*	58.8	N	JFZU01000004.1	13	46796	46896
pPAR552		1	-	1150770	1150790	20	A	*lon*	65.0	N	-	-	-	-
pPAR553		1	+	1208686	1208765	79	I		46.8	N	JFZU01000004.1	13	144998	145075
pPAR554		1	+	1267955	1267984	29	I		48.3	N	-	-	-	-

pPAR555		1	+	1316077	1316237	160	I		45.0	N	JFZU01000006.1	1	104202	104360
pPAR556		1	+	1385847	1385897	50	I		58.0	N	JFZU01000006.1	1	173974	174022
pPAR557		1	-	1520576	1520735	159	A	*ycaD*	57.2	N	JFZU01000006.1	1	310782	310625
pPAR558		1	+	1525462	1525572	110	I		36.4	N	JFZU01000006.1	1	315511	315619
pPAR559		1	-	1530203	1530237	34	I		44.1	N	JFZU01000006.1	1	320284	320252
pPAR560		1	-	1665016	1665077	61	I		57.4	N	JFZU01000006.1	1	455065	455006
pPAR561		1	+	1719592	1719659	67	I		52.2	N	JFZU01000006.1	1	510184	510249
pPAR562		1	+	1791105	1791127	22	A	*tar*	63.6	N	-	-	-	-
pPAR563		1	-	1844197	1844225	28	A	*kdsA*	71.4	N	JFZU01000006.1	1	510184	510249
pPAR564		1	+	1877571	1877641	70	I		52.9	N	JFZU01000007.1	5	54177	54245
pPAR565		1	+	1878994	1879041	47	I		51.1	N	JFZU01000007.1	5	55600	55645
pPAR566		1	-	1885501	1885529	28	A	*astE*	53.6	N	JFZU01000007.1	5	55600	55645
pPAR567		1	-	1978388	1978444	56	A	*cds1766*	55.4	N	JFZU01000007.1	5	155056	155002
pPAR568		1	-	2004739	2004763	24	I		20.8	N	-	-	-	-
pPAR569		1	+	2190764	2190789	25	A	*cds1958*	68.0	N	-	-	-	-
pPAR570		1	-	2202083	2202115	32	A	*ydfG*	62.5	N	JFZU01000008.1	14	65941	65911
pPAR571		1	+	2221801	2221834	33	I		45.5	N	JFZU01000008.1	14	85610	85641
pPAR572		1	+	2246777	2246803	26	I		57.7	N	-	-	-	-
pPAR573		1	+	2293880	2293926	46	A	*pgpB*	65.2	N	JFZU01000009.1	8	25977	26021
pPAR574		1	-	2322328	2322412	84	A	*yciA*	45.2	N	JFZU01000009.1	8	54508	54426
pPAR575		1	-	2322487	2322519	32	O	*yciA*	50.0	N	JFZU01000009.1	8	54615	54585
pPAR576		1	+	2376566	2376596	30	I		53.3	N	JFZU01000009.1	8	108819	108847
pPAR577		1	-	2378746	2378771	25	O	*minD*	52.0	N	-	-	-	-
pPAR578		1	-	2393594	2393618	24	I		45.8	N	-	-	-	-
pPAR579		1	+	2444603	2444633	30	I		63.3	N	JFZU01000009.1	8	176831	176859
pPAR580		1	-	2527908	2527928	20	I		75.0	N	-	-	-	-
pPAR581		1	-	2538871	2538914	43	I		30.2	N	JFZU01000009.1	8	271330	271289
pPAR582		1	+	2552244	2552278	34	I		35.3	Y	JFZU01000009.1	8	284662	284694

pPAR583		1	-	2610794	2610811	17	I		29.4	N	-	-	-	-
pPAR584		1	+	2667169	2667320	151	I		53.0	N	JFZU01000012.1	7	51537	51686
pPAR585		1	+	2675263	2675289	26	A	*ycdL*	61.5	N	-	-	-	-
pPAR586		1	+	2754255	2754281	26	I		65.4	N	-	-	-	-
pPAR587		1	+	2778600	2778622	22	A	*galE*	50.0	N	-	-	-	-
pPAR588		1	-	2849684	2849723	39	A	*yeiG*	48.7	N	JFZU01000012.1	7	238428	238391
pPAR589		1	-	2855860	2855896	36	A	*yeiH*	66.7	N	JFZU01000012.1	7	244600	244566
pPAR590		1	-	2886291	2886321	30	A	*yejL*	60.0	Y	JFZU01000012.1	7	276107	276079
pPAR591		1	+	3005194	3005224	30	A	*folC*	53.3	N	-	-	-	-
pPAR592		1	+	3063537	3063566	29	A	*papC*	62.1	N	JFZU01000013.1	3	185658	185685
pPAR593		1	+	3081505	3081552	47	A	*glk*	59.6	N	JFZU01000013.1	3	203629	203674
pPAR594		1	-	3137705	3137731	26	A	*rbsK*	57.7	N	-	-	-	-
pPAR595		1	+	3166328	3166374	46	A	*cysW*	54.3	N	JFZU01000013.1	3	288294	288338
pPAR596		1	+	3248228	3248253	25	A	*purL*	64.0	N	-	-	-	-
pPAR597		1	+	3256515	3256590	75	A	*era*	57.3	N	JFZU01000013.1	3	373939	374012
pPAR598		1	+	3402041	3402053	12	I		58.3	N	-	-	-	-
pPAR599		1	+	3402526	3402942	416	O	*tRNA*	53.1	N	JFZU01000015.1	2	21231	21290
pPAR600		1	-	3619491	3619636	145	I		49.0	N	JFZU01000015.1	2	203464	203321
pPAR601		1	+	3704250	3704279	29	A	*yecS*	55.2	N	-	-	-	-
pPAR602		1	-	3728249	3728278	29	A	*cds3343*	65.5	N	JFZU01000015.1	2	309544	309517
pPAR603	*sroG*	1	-	3768794	3768820	26	I		53.8	N	-	-	-	-
pPAR604		1	+	3775153	3775182	29	I		48.3	N	JFZU01000015.1	2	356428	356455
pPAR605		1	+	3827763	3827791	28	A	*tcp*	57.1	N	JFZU01000015.1	2	356428	356455
pPAR606		1	-	3858551	3858601	50	A	*cds3469*	38.0	N	JFZU01000015.1	2	441310	441262
pPAR607		1	-	3921227	3921262	35	A	*tsr*	60.0	N	JFZU01000015.1	2	503979	503946
pPAR608		1	+	3962774	3962823	49	A	*yhdP*	67.3	Y	JFZU01000015.1	2	545607	545654
pPAR609		1	+	3966220	3966270	50	A	*cafA*	64.0	N	JFZU01000015.1	2	549053	549101
pPAR610		1	-	3970396	3970441	45	I		40.0	N	JFZU01000015.1	2	553272	553229

pPAR611		1	+	3992007	3992144	137	I		48.2	N	JFZU01000018.1	15	252	357
pPAR612		1	-	3992081	3992235	154	I		48.7	N	JFZU01000018.1	15	357	326
pPAR613		1	+	4010830	4010998	168	O	*rplN*	52.4	N	JFZU01000016.1	19	19115	19281
pPAR614		1	-	4016708	4016727	19	A	*tapD*	68.4	N	-	-	-	-
pPAR615		1	+	4027358	4027383	25	A	*kefB*	52.0	N	-	-	-	-
pPAR616		1	+	4045321	4045365	44	A	*ppiA*	54.5	N	JFZU01000017.1	11	27160	27202
pPAR617		1	+	4049619	4049670	51	A	*trpS*	58.8	N	JFZU01000017.1	11	31458	31507
pPAR618		1	-	4062388	4062405	17	I		64.7	N	-	-	-	-
pPAR619		1	+	4079220	4079269	49	A	*malQ*	63.3	N	JFZU01000017.1	11	61058	61105
pPAR620		1	+	4082769	4082817	48	A	*malP*	60.4	N	JFZU01000017.1	11	64607	64653
pPAR621		1	-	4142788	4142813	25	A	*yicE*	52.0	N	-	-	-	-
pPAR622		1	+	4215179	4215199	20	A	*yfiK*	65.0	N	-	-	-	-
pPAR623		1	-	4252047	4252078	31	A	*trmA*	54.8	N	JFZU01000018.1	15	3783	3754
pPAR624		1	+	4259380	4259415	35	A	*argG*	54.3	N	JFZU01000018.1	15	11086	11119
pPAR625		1	-	4263059	4263087	28	O	*ppc*	50.0	N	JFZU01000018.1	15	11086	11119
pPAR626		1	+	4293304	4293392	88	I		46.6	Y	JFZU01000018.1	15	45014	45100
pPAR627		1	+	4315209	4315238	29	A	*rfaF*	65.5	N	JFZU01000018.1	15	66913	66940
pPAR628		1	+	4386232	4386282	50	I		64.0	N	JFZU01000025.1	6	119364	119316
pPAR629		1	-	4399184	4399203	19	I		42.1	N	-	-	-	-
pPAR630		1	+	4407867	4407913	46	I		47.8	N	JFZU01000025.1	6	97735	97691
pPAR631		1	+	4418111	4418135	24	A	*lumQ*	66.7	N	-	-	-	-
pPAR632		1	+	4459587	4459632	45	A	*zwf2*	53.3	Y	JFZU01000025.1	6	50505	50462
pPAR633		1	+	4498553	4498578	25	A	*sardH*	64.0	N	-	-	-	-
pPAR634		1	-	4673747	4673797	50	A	*lip-1*	62.0	N	JFZU01000025.1	6	148991	149039
pPAR635		2	-	21824	21897	73	I		46.6	N	KK328466.1	10	22211	22143
pPAR636		2	-	48729	48748	19	I		68.4	N	-	-	-	-
pPAR637		2	-	50286	50313	27	A	*yneA*	44.4	N	-	-	-	-
pPAR638		2	+	58679	58728	49	I		65.3	Y	KK328466.1	10	58993	59040

pPAR639		2	-	59173	59226	53	I		41.5	N	KK328466.1	10	59538	59487
pPAR640		2	-	102026	102047	21	I		57.1	N	-	-	-	-
pPAR641		2	+	112485	112513	28	A	*yibF*	71.4	N	KK328466.1	10	59538	59487
pPAR642		2	-	116116	116179	63	O	*sodA*	55.6	Y	KK328466.1	10	116486	116425
pPAR643		2	-	123677	124128	451	I		46.3	N	KK328466.1	10	124458	124009
pPAR644		2	+	127097	127183	86	I		45.3	N	KK328466.1	10	127429	127513
pPAR645		2	-	127164	127368	204	I		37.7	N	KK328466.1	10	127698	127496
pPAR646		2	-	127557	127580	23	I		47.8	N	-	-	-	-
pPAR647		2	-	128493	128529	36	A	*ohrR*	44.4	N	KK328466.1	10	128899	128865
pPAR648		2	-	220373	220400	27	A	*ubiB*	51.9	N	-	-	-	-
pPAR649		2	-	249541	249562	21	A	*rplJ*	57.1	N	-	-	-	-
pPAR650		2	-	250584	250626	42	A	*rpoB*	33.3	N	JFZU01000022.1	20	5313	5273
pPAR651		2	+	329993	330021	28	A	*uvrA*	64.3	N	JFZU01000022.1	20	5313	5273
pPAR652		2	-	344064	344092	28	A	*yjcD*	53.6	N	-	-	-	-
pPAR653		2	-	463204	463235	31	I		41.9	N	JFZU01000023.1	4	188048	188019
pPAR654		2	-	463594	463620	26	I		38.5	N	-	-	-	-
pPAR655		2	-	483977	484014	37	I		40.5	N	-	-	-	-
pPAR656		2	-	497626	497669	43	I		53.5	N	JFZU01000023.1	4	222485	222444
pPAR657		2	-	543482	543527	45	A	*yraR*	68.9	N	-	-	-	-
pPAR658		2	+	585636	585684	48	O	*vat*	64.6	N	-	-	-	-
pPAR659		2	+	593344	593391	47	A	*rbsK*	61.7	N	JFZU01000023.1	4	318644	318689
pPAR660		2	-	635004	635031	27	A	*cds547*	48.1	N	-	-	-	-
pPAR661		2	-	649089	649204	115	A	*acpT*	64.3	N	JFZU01000024.1	17	40843	40730
pPAR662		2	-	715162	715185	23	A	*cds621*	39.1	N	-	-	-	-
pPAR663		2	+	723823	723871	48	A	*yjjK*	50.0	N	JFZU01000001.1	9	43322	43368
pPAR664		2	-	760811	760838	27	A	*thrA*	51.9	N	-	-	-	-
pPAR665	*tpke11*	2	-	770761	770778	17	I		58.8	N	-	-	-	-
pPAR666		2	-	789978	790043	65	I		43.1	N	JFZU01000001.1	9	109475	109412

pPAR667		2	+	812084	812142	58	O	*yabN*	53.4	Y	JFZU01000001.1	9	131528	131584
pPAR668		2	-	848578	848602	24	I		45.8	N	-	-	-	-
pPAR669		2	-	879785	879812	27	A	*kdgT 1*	63.0	N	-	-	-	-
pPAR670		2	-	893848	893879	31	A	*yadH*	54.8	N	JFZU01000001.1	9	213332	213303
pPAR671		2	+	899182	899212	30	A	*gluQ*	66.7	N	JFZU01000001.1	9	218636	218664
pPAR672		2	+	901371	901405	34	A	*ligT*	70.6	N	-	-	-	-
pPAR673		2	-	914392	914432	40	O	*yadR*	47.5	N	JFZU01000001.1	9	233878	233840
pPAR674		2	-	917244	917363	119	A	*cds78 3*	47.9	N	JFZU01000001.1	9	236809	236695
pPAR675		2	-	931679	931709	30	A	*dxr*	53.3	N	JFZU01000001.1	9	251155	251127
pPAR676		2	-	965102	965122	20	I		55.0	N	-	-	-	-
pPAR677		2	+	993811	993872	61	A	*cds85 4*	50.8	N	JFZU01000002.1	16	28803	28862
pPAR678		2	-	1010269	1010294	25	A	*cds87 1*	52.0	N	-	-	-	-
pPAR679		2	+	1035446	1035471	25	I		52.0	Y	-	-	-	-
pPAR680		2	+	1036530	1036573	43	I		39.5	N	JFZU01000002.1	16	71627	71668
pPAR681		2	+	1080785	1080815	30	I		66.7	N	JFZU01000004.1	13	17104	17132
pPAR682		2	+	1097597	1097625	28	A	*sbcC*	53.6	N	JFZU01000004.1	13	17104	17132
pPAR683		2	+	1124850	1124871	21	A	*yajO*	42.9	N	-	-	-	-
pPAR684		2	+	1127151	1127187	36	A	*ispA*	50.0	N	JFZU01000004.1	13	63479	63513
pPAR685		2	+	1171258	1171292	34	I		52.9	N	JFZU01000004.1	13	107573	107605
pPAR686		2	+	1176606	1176683	77	O	*ybaM*	53.2	N	JFZU01000004.1	13	112919	112994
pPAR687		2	+	1191907	1191929	22	A	*ybaK*	59.1	N	-	-	-	-
pPAR688		2	-	1232418	1232440	22	A	*oppA*	54.5	N	-	-	-	-
pPAR689		2	+	1270628	1270678	50	A	*eutG*	68.0	N	JFZU01000006.1	1	58632	58680
pPAR690		2	+	1273006	1273063	57	A	*cds11 11*	66.7	N	JFZU01000006.1	1	61021	61075
pPAR691		2	-	1274938	1274969	31	A	*phnO*	48.4	N	JFZU01000006.1	1	63037	63008

pPAR692		2	-	1327199	1327226	27	A	*cds1165*	59.3	N	-	-	-	-
pPAR693		2	+	1330409	1330446	37	A	*gltA*	59.5	N	JFZU01000006.1	1	118535	118570
pPAR694		2	+	1341139	1341182	43	I		41.9	N	JFZU01000006.1	1	129266	129307
pPAR695		2	-	1384476	1384505	29	A	*uvrB*	62.1	N	JFZU01000006.1	1	172629	172602
pPAR696		2	+	1402345	1402371	26	A	*cds1238*	53.8	N	-	-	-	-
pPAR697		2	-	1436985	1437126	141	A	*hutC*	58.2	N	JFZU01000006.1	1	225254	225115
pPAR698		2	-	1468982	1469012	30	A	*yliB*	63.3	N	JFZU01000006.1	1	259057	259029
pPAR699		2	-	1501874	1501915	41	A	*ybjD*	56.1	Y	JFZU01000006.1	1	291963	291924
pPAR700		2	+	1579444	1579465	21	A	*fabA*	57.1	N	-	-	-	-
pPAR701		2	-	1608251	1608306	55	O	*uvrY*	52.7	N	JFZU01000006.1	1	398310	398257
pPAR702		2	+	1712543	1712568	25	A	*hifC*	40.0	N	-	-	-	-
pPAR703		2	-	1718411	1718465	54	I		59.3	N	JFZU01000006.1	1	509055	509003
pPAR704		2	-	1746468	1746489	21	A	*ycdW*	71.4	N	-	-	-	-
pPAR705		2	-	1779369	1779399	30	A	*cds1581*	63.3	N	JFZU01000006.1	1	568311	568283
pPAR706		2	+	1800600	1800643	43	A	*yaeR*	41.9	N	JFZU01000006.1	1	580946	580987
pPAR707		2	+	1832752	1832778	26	A	*engD*	76.9	N	-	-	-	-
pPAR708		2	-	1834538	1834563	25	I		52.0	N	-	-	-	-
pPAR709		2	+	1835027	1835144	117	A	*yedQ*	59.0	N	JFZU01000007.1	5	11633	11748
pPAR710		2	+	1836200	1836223	23	I		47.8	N	-	-	-	-
pPAR711		2	-	1897496	1897678	182	A	*yniB*	57.7	N	JFZU01000007.1	5	74294	74114
pPAR712		2	-	1927080	1927107	27	A	*sufD*	63.0	N	-	-	-	-
pPAR713		2	-	1941724	1941752	28	A	*ydhD*	50.0	N	JFZU01000007.1	5	74294	74114
pPAR714		2	-	2049786	2049816	30	A	*cds1835*	60.0	Y	JFZU01000007.1	5	227230	227202
pPAR715		2	+	2051738	2051757	19	I		52.6	N	-	-	-	-
pPAR716		2	+	2073296	2073328	32	A	*leuA*	50.0	N	JFZU01000007.1	5	250720	250750
pPAR717		2	-	2096766	2096793	27	A	*rpiR*	44.4	N	-	-	-	-
pPAR718		2	+	2127363	2127468	105	A	*malG*	50.5	N	JFZU01000007.1	5	305006	305109

pPAR719		2	-	2171734	2171781	47	I		51.1	Y	JFZU01000008.1	14	35626	35581
pPAR720		2	-	2213290	2213318	28	I		53.6	N	JFZU01000008.1	14	35626	35581
pPAR721		2	-	2227480	2227561	81	A	*ydcI*	54.3	N	JFZU01000008.1	14	91361	91282
pPAR722		2	+	2255738	2255766	28	A	*ydaN*	64.3	N	JFZU01000008.1	14	91361	91282
pPAR723		2	-	2335373	2335399	26	O	*adhE*	50.0	N	-	-	-	-
pPAR724		2	+	2341919	2341964	45	A	*udg*	71.1	Y	JFZU01000009.1	8	74013	74056
pPAR725		2	+	2343204	2343245	41	I		41.5	N	JFZU01000009.1	8	75298	75337
pPAR726		2	-	2353498	2353521	23	I		73.9	Y	-	-	-	-
pPAR727		2	+	2360189	2360270	81	I		39.5	N	JFZU01000009.1	8	92441	92520
pPAR728		2	-	2368777	2368801	24	A	*cmlA*	58.3	N	-	-	-	-
pPAR729		2	-	2368942	2369021	79	A	*cmlA*	69.6	N	JFZU01000009.1	8	101272	101195
pPAR730		2	+	2373767	2373787	20	A	*fadR*	50.0	N	-	-	-	-
pPAR731		2	-	2398787	2398810	23	I		26.1	N	-	-	-	-
pPAR732	*ryeB/sdsR*	2	-	2435078	2435148	70	I		48.6	Y	JFZU01000009.1	8	167372	167304
pPAR733		2	+	2465315	2465343	28	I		50.0	N	-	-	-	-
pPAR734		2	-	2502080	2502109	29	A	*cds2244*	58.6	N	JFZU01000009.1	8	234504	234477
pPAR735		2	-	2529163	2529196	33	A	*rfbC*	60.6	N	JFZU01000009.1	8	261610	261579
pPAR736		2	-	2575491	2575514	23	A	*rcsA*	47.8	N	-	-	-	-
pPAR737		2	-	2586541	2586599	58	A	*tsr*	75.9	N	JFZU01000010.1	18	32270	32214
pPAR738		2	+	2598739	2598772	33	A	*cds2341*	60.6	N	JFZU01000010.1	18	44500	44531
pPAR739		2	-	2634923	2634972	49	I		49.0	N	JFZU01000012.1	7	19296	19249
pPAR740		2	+	2723324	2723348	24	A	*rhaT*	79.2	N	-	-	-	-
pPAR741		2	+	2727597	2727627	30	A	*cds2448*	40.0	N	JFZU01000012.1	7	112326	112354
pPAR742		2	-	2749243	2749293	50	A	*puuB*	46.0	N	JFZU01000012.1	7	134020	133972
pPAR743		2	+	2788223	2788242	19	A	*wcaA*	52.6	N	-	-	-	-
pPAR744		2	-	2823873	2823891	18	A	*ydfH*	66.7	N	-	-	-	-
pPAR745		2	+	2842907	2842984	77	I		53.2	N	JFZU01000012.1	7	231614	231689

pPAR746		2	-	2902295	2902325	30	A	*exbD*	46.7	N	JFZU01000013.1	3	22262	22234
pPAR747		2	+	2915172	2915202	30	A	*lktD*	63.3	N	-	-	-	-
pPAR748		2	-	3067833	3067864	31	I		48.4	N	JFZU01000013.1	3	189983	189954
pPAR749		2	-	3121960	3122014	54	A	*tktB*	51.9	N	JFZU01000013.1	3	243980	243928
pPAR750		2	-	3184783	3184814	31	A	*ppx*	45.2	N	-	-	-	-
pPAR751		2	-	3204478	3204501	23	A	*prt1*	56.5	N	-	-	-	-
pPAR752		2	+	3226953	3226976	23	A	*sseB*	69.6	N	-	-	-	-
pPAR753		2	+	3227632	3227667	35	A	*pepB*	65.7	N	JFZU01000013.1	3	345087	345120
pPAR754		2	+	3232957	3232986	29	A	*cds2875*	51.7	N	JFZU01000013.1	3	350380	350407
pPAR755		2	-	3302946	3302965	19	O	*mhpC*	47.4	N	-	-	-	-
pPAR756		2	-	3346115	3346138	23	A	*oppF*	69.6	N	-	-	-	-
pPAR757		2	+	3375878	3375899	21	I		57.1	N	-	-	-	-
pPAR758		2	-	3612509	3612525	16	I		56.3	N	-	-	-	-
pPAR759		2	+	3619152	3619183	31	O	*yqjH*	61.3	N	JFZU01000015.1	2	202982	203011
pPAR760		2	-	3646616	3646643	27	I		51.9	N	-	-	-	-
pPAR761		2	+	3658183	3658214	31	I		58.1	N	JFZU01000015.1	2	239451	239480
pPAR762		2	-	3674383	3674416	33	A	*cds3297*	48.5	N	JFZU01000015.1	2	255683	255652
pPAR763		2	+	3703628	3703674	46	A	*gluA*	47.8	N	JFZU01000015.1	2	284898	284942
pPAR764		2	+	3716345	3716382	37	I		37.8	N	JFZU01000015.1	2	297617	297652
pPAR765		2	-	3763787	3763821	34	A	*tolC*	50.0	Y	JFZU01000015.1	2	345092	345060
pPAR766		2	+	3779585	3779618	33	A	*gcp*	63.6	N	JFZU01000015.1	2	360860	360891
pPAR767		2	-	3807915	3807943	28	I		75.0	N	JFZU01000015.1	2	360860	360891
pPAR768		2	+	3816958	3816985	27	I		48.1	N	-	-	-	-
pPAR769		2	-	3817021	3817047	26	I		26.9	N	-	-	-	-
pPAR770		2	-	3873323	3873605	282	A	*yhaJ*	59.6	N	JFZU01000015.1	2	456317	456037
pPAR771		2	+	3902205	3902234	29	A	*cds3512*	62.1	N	JFZU01000015.1	2	484920	484947
pPAR772		2	-	3922733	3922814	81	O	*tsr*	48.1	N	JFZU01000015.1	2	505531	505452

pPAR773		2	-	3922906	3923056	150	A	*yjfO*	67.3	N	JFZU01000015.1	2	505773	505625
pPAR774		2	-	3951781	3951806	25	I		60.0	N	-	-	-	-
pPAR775		2	-	3952282	3952380	98	A	*yhcN*	57.1	N	JFZU01000015.1	2	535211	535115
pPAR776		2	+	3986687	3986708	21	I		57.1	N	-	-	-	-
pPAR777		2	-	4037744	4037773	29	A	*yheU*	48.3	N	JFZU01000017.1	11	19610	19583
pPAR778		2	-	4046703	4046818	115	A	*tsgA*	56.5	N	JFZU01000017.1	11	28655	28542
pPAR779		2	-	4064206	4064239	33	A	*yrfF*	63.6	N	JFZU01000017.1	11	46076	46045
pPAR780		2	+	4094103	4094281	178	A	*glgC*	55.6	N	JFZU01000017.1	11	75740	75916
pPAR781		2	+	4115716	4115745	29	A	*livM*	72.4	N	JFZU01000017.1	11	97345	97372
pPAR782		2	-	4136325	4136384	59	A	*iolE*	59.3	N	JFZU01000017.1	11	117954	117897
pPAR783		2	-	4142145	4142181	36	A	*yicE*	44.4	N	JFZU01000017.1	11	123750	123716
pPAR784		2	-	4225292	4225311	19	A	*aapJ*	36.8	N	-	-	-	-
pPAR785		2	-	4227916	4227952	36	O	*argH 2*	38.9	N	JFZU01000017.1	11	209524	209490
pPAR786		2	+	4243298	4243319	21	I		57.1	N	-	-	-	-
pPAR787		2	+	4292470	4292547	77	A	*fieF*	53.2	N	JFZU01000018.1	15	44180	44255
pPAR788		2	-	4302819	4302996	177	A	*yibQ*	52.0	N	JFZU01000018.1	15	54694	54519
pPAR789		2	-	4310328	4310350	22	A	*rfaL*	45.5	N	-	-	-	-
pPAR790		2	+	4345120	4345149	29	I		65.5	N	JFZU01000018.1	15	84515	84542
pPAR791		2	+	4392435	4392457	22	I		45.5	N	-	-	-	-
pPAR792		2	+	4405628	4405651	23	I		56.5	N	-	-	-	-
pPAR793		2	-	4420191	4420213	22	I		45.5	Y	-	-	-	-
pPAR794		2	+	4442485	4442508	23	I		39.1	N	-	-	-	-
pPAR795		2	+	4465967	4465984	17	A	*yoaF*	58.8	N	-	-	-	-
pPAR796		2	-	4502685	4502709	24	I		62.5	Y	-	-	-	-
pPAR797		2	-	4508266	4508286	20	I		55.0	N	-	-	-	-
pPAR798		2	-	4508748	4508784	36	I		36.1	N	JFZU01000025.1	6	1301	1335
pPAR799		2	-	4510008	4510067	59	I		45.8	N	JFZU01000014.1	12	170804	170861
pPAR800		2	+	4548781	4548802	21	I		71.4	N	-	-	-	-

pPAR801		2	-	4558604	4558623	19	A	*ddc*	63.2	N	-	-	-	-
pPAR802		2	-	4565243	4565355	112	A	*dcuR*	56.3	N	JFZU01000025.1	6	226804	226914
pPAR803		2	-	4620180	4620223	43	I		41.9	N	JFZU01000025.1	6	202589	202630
pPAR804		2	-	4620922	4620951	29	I		55.2	N	JFZU01000025.1	6	201861	201888
pPAR805		2	+	4654503	4654523	20	A	*yjgF*	60.0	N	-	-	-	-
pPAR806		2	+	4657102	4657123	21	A	*ymgB*	52.4	N	-	-	-	-
pPAR807		2	+	4699705	4699725	20	A	*hns*	75.0	N	-	-	-	-
pPAR808		2	-	4702378	4702409	31	A	*fhuE*	38.7	N	-	-	-	-

[a]Start and End based on LMG 20103 genome

[b]Classification of sRNA based on its position. **A**: Antisence; **I**: Intergenic and **O**: Overlapping

[c]Gene on opposite strand of sRNA if sRNA is A or O

[d]Presence of rho-independent terminator using computational prediction. **N**: No and **Y**: Yes

[e]Start, End, Scaffold ID and Scaffold number based on LMG 2665 genome

*** This table has been modified to fit the text. The original S2 table can be found online at https://www.frontiersin.org/articles/10.3389/fmicb.2019.02075/full#supplementary-material**

S Table 2.3 A list of sRNAs that has significant abundance difference between wild-type and *hfq* mutant strains of *Pantoea ananatis*

sRNA Locus	LOG_2(Δ*hfq*/wt) Timepoint 1	LOG_2(Δ*hfq*/wt) Timepoint 2	code[a]
pPAR510	-6.31	-1.89	T1
pPAR777	-	-6.25	T1 T2
pPAR205	-4.56	-6.02	T1 T2
pPAR063	-5.78	-4.74	T1 T2
pPAR406	-5.60	-5.64	T1 T2
pPAR675	-3.79	-5.39	T1 T2
pPAR645	0.81	-5.15	T2
pPAR694	-3.73	-5.00	T1 T2
pPAR677	-2.39	-4.32	T1 T2
pPAR643	1.01	-4.23	T2
pPAR319	-3.07	-4.12	T1 T2
pPAR732	-1.86	-3.99	T1 T2
pPAR021	-3.87	-2.74	T1 T2
pPAR720	-1.45	-3.85	T2
pPAR639	-1.31	-3.69	T2
pPAR143	-1.29	-3.66	T2
pPAR785	-0.97	-3.55	T2
pPAR458	-3.52	-2.80	T1 T2
pPAR764	-1.12	-3.52	T2
pPAR638	-2.38	-3.50	T1 T2
pPAR537	-3.41	-0.52	T1
pPAR242	-2.85	-3.35	T1 T2
pPAR464	-3.29	-0.48	T1
pPAR175	-3.21	-1.58	T1
pPAR311	-2.59	-3.18	T1 T2
pPAR070	-3.03	-2.44	T1 T2
pPAR680	-3.02	-2.87	T1 T2
pPAR719	-1.16	-2.99	T2
pPAR584	-2.96	-0.49	T1
pPAR697	-0.06	-2.92	T2
pPAR397	-2.24	-2.91	T1 T2
pPAR690	0.00	-2.90	T2
pPAR739	-2.89	-2.44	T1 T2
pPAR244	-2.25	-2.84	T1 T2
pPAR282	-2.35	-2.77	T1 T2
pPAR154	0.79	-2.69	T2
pPAR748	-0.61	-2.64	T2
pPAR466	-2.63	-2.62	T1 T2

pPAR127	-2.60	-2.06	T1 T2
pPAR016	-1.29	-2.55	T1 T2
pPAR237	-2.52	-0.99	T1
pPAR593	-2.52	0.89	T1
pPAR052	-2.50	-0.64	T1
pPAR709	-0.06	-2.50	T2
pPAR227	-2.49	-1.65	T1 T2
pPAR329	-2.16	-2.45	T1 T2
pPAR151	-0.84	-2.44	T2
pPAR284	-2.15	-2.36	T1 T2
pPAR296	-1.61	-2.35	T1 T2
pPAR682	1.03	-2.34	T2
pPAR083	-1.15	-2.26	T2
pPAR455	-2.20	-2.22	T1 T2
pPAR474	-0.75	-2.22	T2
pPAR161	-2.21	-1.58	T1 T2
pPAR017	-0.81	-2.17	T2
pPAR635	-0.19	-2.07	T2
pPAR159	-2.02	-1.17	T1
pPAR686	0.00	-2.02	T2
pPAR470	-2.00	-0.51	T1
pPAR199	-1.97	-0.48	T1
pPAR157	-1.63	-1.94	T1 T2
pPAR395	-1.14	-1.91	T2
pPAR644	0.18	-1.89	T2
pPAR725	-0.73	-1.88	T2
pPAR417	-0.79	-1.88	T2
pPAR520	-1.88	-0.69	T1
pPAR718	1.15	-1.86	T2
pPAR379	-1.44	-1.85	T1 T2
pPAR163	-0.99	-1.84	T2
pPAR716	0.74	-1.82	T2
pPAR071	0.02	-1.82	T2
pPAR653	-0.31	-1.80	T2
pPAR460	-0.44	-1.78	T2
pPAR144	-1.63	-1.78	T1 T2
pPAR771	-1.78	-1.43	T1 T2
pPAR478	-0.59	-1.77	T2
pPAR365	0.15	-1.75	T2
pPAR623	-1.71	-0.65	T1
pPAR266	-0.88	-1.71	T2
pPAR211	-0.40	-1.70	T2

pPAR681	0.55	-1.66	T2
pPAR345	-1.08	-1.65	T1 T2
pPAR289	-1.50	-1.63	T1 T2
pPAR389	-0.95	-1.62	T2
pPAR247	-1.61	-0.29	T1
pPAR667	1.00	-1.60	T2
pPAR473	-1.60	-0.77	T1
pPAR445	-0.60	-1.58	T2
pPAR616	-1.57	0.41	T1
pPAR773	0.51	-1.57	T2
pPAR177	-1.55	-0.17	T1
pPAR471	-1.55	-0.19	T1
pPAR200	-1.55	-1.43	T1 T2
pPAR396	-1.54	-1.05	T1 T2
pPAR047	-0.85	-1.54	T2
pPAR264	-0.28	-1.52	T2
pPAR254	0.04	-1.51	T2
pPAR238	-1.50	0.78	T1
pPAR026	0.14	-1.46	T2
pPAR198	0.32	-1.46	T2
pPAR558	-1.45	-0.28	T1
pPAR333	-0.96	-1.44	T2
pPAR041	-1.42	-0.96	T1
pPAR129	1.18	-1.41	T2
pPAR086	-0.60	-1.40	T2
pPAR400	-0.64	-1.39	T2
pPAR402	-0.37	-1.38	T2
pPAR452	-0.36	-1.35	T2
pPAR015	-0.35	-1.33	T2
pPAR134	0.26	-1.31	T2
pPAR252	-0.38	-1.30	T2
pPAR241	-1.30	0.36	T1
pPAR408	0.97	-1.29	T2
pPAR088	-1.29	0.50	T1
pPAR353	0.29	-1.29	T2
pPAR457	-1.28	-0.56	T1
pPAR287	-1.26	0.22	T1
pPAR770	1.03	-1.26	T2
pPAR231	0.25	-1.26	T2
pPAR131	-0.51	-1.25	T2
pPAR007	-0.10	-1.24	T2
pPAR595	-1.24	-0.69	T1

pPAR339	-0.24	-1.23	T2
pPAR772	0.48	-1.23	T2
pPAR245	-0.19	-1.22	T2
pPAR790	-0.59	-1.22	T2
pPAR248	0.22	-1.21	T2
pPAR722	1.03	-1.21	T2
pPAR046	-0.14	-1.20	T2
pPAR103	-1.00	-1.20	T2
pPAR283	0.21	-1.19	T2
pPAR213	-0.95	-1.19	T2
pPAR331	-0.11	-1.17	T2
pPAR727	-0.67	-1.16	T2
pPAR485	0.92	-1.16	T2
pPAR499	0.13	-1.15	T2
pPAR222	-1.15	2.67	T1 T2
pPAR579	-1.15	2.39	T1 T2
pPAR279	-1.12	-0.08	T1
pPAR292	1.13	-1.11	T1 T2
pPAR201	1.26	-1.08	T1 T2
pPAR073	-1.08	0.85	T1
pPAR215	-0.41	-1.07	T2
pPAR480	-1.06	0.49	T1
pPAR295	-0.23	-1.00	T2
pPAR285	0.58	0.96	T2
pPAR069	0.64	0.99	T2
pPAR031	0.67	1.02	T2
pPAR042	-0.32	1.04	T2
pPAR550	-1.05	1.04	T2
pPAR304	1.06	0.59	T1
pPAR313	0.92	1.06	T2
pPAR181	-0.05	1.07	T2
pPAR051	0.22	1.08	T2
pPAR405	1.08	0.06	T1
pPAR271	-0.78	1.09	T2
pPAR081	0.58	1.14	T2
pPAR137	0.18	1.20	T2
pPAR450	0.92	1.22	T2
pPAR556	1.04	1.23	T2
pPAR555	0.20	1.23	T2
pPAR597	0.11	1.24	T2
pPAR346	1.12	1.26	T1 T2
pPAR332	1.27	0.79	T1

pPAR183	1.28	0.87	T1
pPAR098	-0.73	1.30	T2
pPAR410	1.32	0.01	T1
pPAR257	0.48	1.33	T2
pPAR061	-0.88	1.36	T2
pPAR575	0.55	1.36	T2
pPAR420	0.19	1.38	T2
pPAR162	1.38	0.45	T1
pPAR323	1.32	1.39	T2
pPAR182	1.39	0.58	T1
pPAR387	1.40	0.10	T1
pPAR301	0.44	1.40	T2
pPAR120	-0.45	1.42	T2
pPAR590	0.01	1.42	T2
pPAR265	1.43	0.21	T1
pPAR153	1.43	-0.09	T1
pPAR077	-0.65	1.43	T2
pPAR110	1.44	0.48	T1
pPAR600	0.78	1.44	T2
pPAR390	0.04	1.45	T2
pPAR456	1.04	1.45	T1 T2
pPAR399	1.45	1.01	T1 T2
pPAR608	0.34	1.46	T2
pPAR735	1.46	1.14	T1 T2
pPAR122	0.03	1.48	T2
pPAR524	0.42	1.49	T2
pPAR102	0.63	1.51	T2
pPAR589	0.49	1.52	T2
pPAR366	1.53	1.04	T1 T2
pPAR109	1.53	0.08	T1
pPAR484	1.54	0.82	T1
pPAR055	0.12	1.56	T2
pPAR766	1.57	0.02	T1
pPAR068	1.00	1.58	T2
pPAR326	0.09	1.61	T2
pPAR506	0.89	1.61	T2
pPAR564	1.62	1.59	T1 T2
pPAR337	1.13	1.64	T1 T2
pPAR641	0.77	1.65	T2
pPAR695	1.67	-0.55	T1
pPAR008	0.92	1.71	T2
pPAR551	0.74	1.71	T2

pPAR358	1.71	0.94	T1
pPAR802	1.73	-0.28	T1
pPAR659	1.18	1.75	T2
pPAR355	1.75	1.29	T1 T2
pPAR440	1.46	1.76	T1 T2
pPAR341	0.30	1.77	T2
pPAR650	1.78	-0.17	T1
pPAR343	1.79	1.04	T1
pPAR775	1.80	0.31	T1
pPAR738	1.80	-0.27	T1
pPAR255	1.81	1.39	T1 T2
pPAR516	0.84	1.82	T2
pPAR541	-0.08	1.82	T2
pPAR338	0.64	1.83	T2
pPAR753	1.85	-0.94	T1
pPAR546	0.31	1.85	T2
pPAR374	-0.78	1.86	T2
pPAR009	0.52	1.86	T2
pPAR392	0.59	1.87	T2
pPAR699	1.87	-0.63	T1
pPAR394	1.16	1.87	T2
pPAR535	0.59	1.89	T2
pPAR613	-0.19	1.90	T2
pPAR571	-0.60	1.91	T2
pPAR609	0.36	1.97	T2
pPAR372	1.22	2.00	T2
pPAR495	2.01	2.05	T1 T2
pPAR476	2.06	1.57	T1 T2
pPAR619	1.52	2.06	T2
pPAR469	1.36	2.07	T1 T2
pPAR202	0.72	2.08	T2
pPAR737	2.08	-0.80	T1
pPAR439	0.90	2.09	T2
pPAR599	0.46	2.10	T2
pPAR013	2.13	0.36	T1
pPAR742	2.16	0.16	T1
pPAR543	0.99	2.17	T2
pPAR549	0.91	2.20	T2
pPAR090	0.36	2.22	T2
pPAR401	0.75	2.22	T2
pPAR022	1.88	2.24	T1 T2
pPAR765	2.26	-0.27	T1

pPAR155	1.10	2.26	T1 T2
pPAR588	1.28	2.32	T1 T2
pPAR094	0.60	2.33	T2
pPAR207	1.09	2.33	T1 T2
pPAR557	-0.82	2.33	T2
pPAR581	-0.86	2.36	T2
pPAR407	2.41	0.93	T1
pPAR522	-1.90	2.48	T2
pPAR714	2.50	1.52	T1 T2
pPAR235	0.13	2.50	T2
pPAR610	0.44	2.53	T2
pPAR661	2.59	0.88	T1
pPAR273	0.79	2.66	T2
pPAR246	0.56	2.66	T2
pPAR433	0.52	2.74	T2
pPAR624	0.05	2.88	T2
pPAR421	0.21	3.08	T2
pPAR547	-0.15	3.11	T2
pPAR196	1.81	3.12	T1 T2
pPAR251	0.56	3.24	T2
pPAR206	1.19	3.36	T1 T2
pPAR604	2.41	3.37	T1 T2
pPAR628	0.73	3.47	T2
pPAR542	0.80	3.53	T2
pPAR340	-0.26	3.86	T2
pPAR724	3.97	2.98	T1 T2
pPAR530	-0.59	4.04	T2
pPAR307	3.27	5.82	T1 T2

[a]T1 and T2 denote significant (adjusted $P<0.05$) difference between *hfq* mutant and wild-type at timepoint 1 or timepoint 2, respectively.

S Table 2.4 A list of predicted targets of selected sRNAs

mRNA target prediction of sRNA FnrS									
Rank	**Gene**	**Product**	**Locus tag**	**Energy**	**P value**	**sRNA_ start[a]**	**sRNA_ stop[a]**	**mRNA_ start[b]**	**mRNA _stop[b]**
1	*yjjL*	MFS transporter	PANA_3801	-15.17	0.001	18	35	-21	-6
2	*yhdX*	Amino acid ABC transporter permease	PANA_3579	-14.95	0.001	17	34	2	20
3	*aaeB*	P-hydroxybenzoic acid efflux pump subunit AaeB	PANA_3556	-14.76	0.001	19	31	-57	-45
4	*gcvP*	Aminomethyl-transferring glycine dehydrogenase	PANA_3187	-13.75	0.002	1	17	-5	12
5	*rapA*	RNA polymerase-associated protein RapA	PANA_0689	-13.24	0.003	16	31	-59	-45
6	*trpS*	Tryptophanyl-tRNA synthetase	PANA_3662	-13.06	0.004	15	32	4	20
7	*yccA*	FtsH protease modulator YccA, binds to the HflBKC complex which modulates FtsH activity	PANA_1406	-13.03	0.004	26	37	-65	-54
8	*ydcN*	Helix-turn-helix transcriptional regulator	PANA_4179	-12.58	0.005	18	32	7	20
9	*yddW*	Glycoside hydrolase family 10 protein	PANA_1922	-12.37	0.006	22	34	5	17
10	*argR*	Transcriptional regulator ArgR	PANA_3549	-12.34	0.006	12	32	2	20
11	-	NUDIX domain-containing protein	PANA_1928	-12.17	0.007	41	57	-15	2
12	-	Hypothetical protein	PANA_1758	-12.08	0.007	57	73	-71	-54
13	*ydfG*	Bifunctional NADP-dependent 3-hydroxy acid dehydrogenase/3-hydroxypropionate dehydrogenase YdfG	PANA_1965	-12.05	0.007	19	38	-3	17
14	*ygbK*	four-carbon acid sugar kinase family protein, type III effector Hrp-dependent outers YgbK	PANA_0751	-11.87	0.008	16	31	-71	-57
15	*yniA*	Fructosamine-3-kinase	PANA_1691	-11.68	0.009	11	25	-51	-38
16	*cybB*	B-type di-heme cytochrome with a major alpha-absorption peak at 561 nm and a minor peak at 555 nm	PANA_1979	-11.62	0.009	19	33	-59	-45
17	*fliY*	Cystine ABC transporter substrate-binding protein	PANA_2261	-11.41	0.011	24	36	-69	-57
18	*yejM*	Inner membrane protein YejM	PANA_2581	-11.4	0.011	19	33	-39	-24
19	*pyrD*	quinone-dependent dihydroorotate dehydrogenase	PANA_1381	-11.19	0.012	10	25	-29	-15
20	*pcm*	Protein-L-isoaspartate O-methyltransferase	PANA_3044	-11.18	0.012	86	99	6	19
21	*ompF*	Outer membrane protein F precursor	PANA_1371	-11.17	0.012	22	39	3	20
22	-	Hypothetical protein	PANA_3819	-11.15	0.013	24	38	3	20

23	*amsK*	Amylovoran biosynthesis glycosyltransferase (exopolysaccaride/glycan biosynthesis)	PANA_2496	-11.14	0.013	39	58	-56	-38
24	-	Phosphatase PAP2 family protein	PANA_2511	-10.98	0.014	17	31	-79	-64
25	*amsG*	phosphatase PAP2 family protein (exopolysaccaride/glycan biosynthesis)	PANA_2506	-10.91	0.014	66	85	-10	8
26	*yihD*	DUF1040 family protein	PANA_3958	-10.5	0.018	12	26	7	20
27	*aldA*	Aldehyde dehydrogenase	PANA_0984	-10.49	0.018	17	33	2	19
28	*gltA*	Glutamate synthase	PANA_0418	-9.72	0.027	21	35	-41	-26
29	*tcp*	Methyl-accepting chemotaxis protein	PANA_3965	-9.55	0.029	86	101	-8	7
30	*yidC*	Membrane protein insertase YidC	PANA_0093	-9.45	0.03	19	38	1	20
31	*ydcO*	Benzoate/H(+) symporter BenE family transporter	PANA_1845	-9.39	0.031	12	32	-75	-55
32	*mrp*	Iron-sulfur cluster carrier protein ApbC	PANA_2532	-9.38	0.031	24	39	1	17
33	-	Steryl acetyl hydrolase	PANA_1594	-9.3	0.033	15	27	-21	-10
34	*yiaJ*	IclR family transcriptional regulator	PANA_0370	-9.29	0.033	42	54	-6	7
35	*yccU*	CoA-binding Protein YccU	PANA_1401	-9.25	0.033	17	32	-64	-51
36	*yghB*	Inner membrane protein YghB	PANA_3353	-9.24	0.033	40	54	-69	-55
37	*phoU*	Phosphate signaling complex protein PhoU	PANA_0036	-9.11	0.035	91	99	-68	-60
38	*ygeA*	Aspartate/glutamate racemase	PANA_4083	-8.94	0.038	21	32	-59	-48
39	*ampG*	Muropeptide MFS transporter AmpG	PANA_0992	-8.9	0.039	16	35	-64	-48
40	*yeiB*	Hypothetical protein	PANA_2543	-8.86	0.039	18	32	2	16
41	*htpX*	Protease HtpX	PANA_2156	-8.85	0.04	7	23	-80	-62
42	*yihS*	Sulfoquinovose isomerase	PANA_3495	-8.76	0.041	20	36	-14	3
43	*yyaJ*	MFS transporter	PANA_0303	-8.69	0.043	19	38	-75	-59
44	-	Hypothetical protein	PANA_1899	-8.6	0.044	22	40	-22	-2
45	*ydhK*	Fusaric Acid Resistance Protein	PANA_1741	-8.53	0.045	11	28	-68	-49
46	*ydhD*	Grx4 family monothiol glutaredoxin	PANA_1732	-8.5	0.046	1	11	-13	-2
47	*yedA*	Transporter drug/metabolite exporter permease family protein	PANA_1411	-8.47	0.046	1	17	-64	-47
48	*sppA*	Signal peptide peptidase SppA	PANA_2104	-8.29	0.05	29	43	-5	10

***Locus tag of *Pantoea ananatis* LMG20103**
[a]Start and End position based on sRNA sequence

[b]Start and End position based on mRNAposition

mRNA target prediction of sRNA GlmZ									
Rank	**Gene**	**Product**	**Locus tag**	**Energy**	**Pvalue**	**sRNA_ start[a]**	**sRNA_ stop[a]**	**mRNA_ start[b]**	**mRNA _stop[b]**
1	*ydgJ*	Oxidoreductase Gfo/Idh/MocA Family	PANA_1829	-15.88	0	5	16	-4	8
2	*ada*	AraC family transcriptional regulator	PANA_0276	-14.88	0.001	6	21	-4	11
3	*znuC*	Zinc ABC transporter ATP-binding protein ZnuC	PANA_2198	-14.21	0.001	44	60	-58	-42
4	*yaaU*	MFS transporter	PANA_1933	-14	0.002	1	15	-68	-53
5	*kdpF*	K(+)-transporting ATPase subunit F	PANA_3791	-13.5	0.003	33	51	-12	8
6	*fba*	Fructose bisphosphate aldolase	PANA_3364	-13.42	0.003	23	36	-80	-68
7	*phoP*	Two-component system response regulator PhoP	PANA_1512	-12.66	0.005	48	65	-80	-65
8	*yagG*	MFS transporter	PANA_1085	-12.49	0.005	8	22	-77	-62
9	*yceG*	Aminodeoxychorismate Lyase, cell division protein	PANA_1487	-11.99	0.008	25	42	-1	16
10	*ynfL*	LysR family transcriptional regulator	PANA_1976	-11.97	0.008	52	61	12	20
11	*yjjA*	Glycoprotein/Receptor	PANA_0518	-11.65	0.009	27	38	-32	-20
12	*emrA*	Multidrug resistance/export protein	PANA_2738	-10.75	0.016	56	64	-76	-68
13	-	Hypothetical protein	PANA_3172	-10.33	0.02	53	64	-66	-55
14	*yajO*	Aldo/keto reductase	PANA_0375	-10.25	0.021	24	38	-77	-62
15	*ydjR*	HutD family protein, hypothetical protein	PANA_1267	-10.05	0.023	23	37	-54	-42
16	*yedY*	protein-methionine-sulfoxide reductase catalytic subunit	PANA_3568	-9.9	0.025	24	42	-69	-51
17	*mrdA*	Penicillin-binding protein 2	PANA_3297	-9.84	0.025	26	42	-51	-36
18	-	Hypothetical protein	PANA_2733	-9.79	0.026	52	61	-59	-50
19	-	DUF943 family protein	PANA_3930	-9.36	0.032	26	40	-17	-3
20	-	Hypothetical protein	PANA_2292	-9.29	0.033	21	40	-11	8
21	*ybjL*	Transporter protein	PANA_1307	-9.25	0.033	52	63	-14	-3
22	*gdhA*	Glutamate dehydrogenase	PANA_3966	-9.21	0.034	45	59	-53	-38
23	*yjbQ*	YjbQ family protein	PANA_0268	-9.18	0.034	42	55	-73	-59

24	-	Hypothetical protein	PANA_1541	-9.15	0.035	10	21	-62	-51
25	*dnaQ*	DNA polymerase III epsilon subunit	PANA_0830	-8.98	0.038	1	20	-7	12
26	*ygbI*	DeoR/GlpR transcriptional regulator	PANA_2460	-8.78	0.041	8	21	-4	11
27	*cinB*	Alpha/beta hydrolase	PANA_2842	-8.68	0.043	18	31	-21	-8
28	*araF*	Arabinose ABC transporter substrate-binding protein	PANA_1825	-8.67	0.043	1	16	-11	5
29	*pncA*	Bifunctional nicotinamidase/pyrazinamidase	PANA_2106	-8.65	0.043	18	35	-15	1
30	*yfeR*	LysR family transcriptional regulator	PANA_2756	-8.57	0.045	52	63	10	20
31	*cndP 1*	Glutamate carboxypeptidase-like protein 2 precursor	PANA_3275	-8.56	0.045	17	35	-10	8
32	*rbsB*	D-ribose-binding periplasmic protein precursor	PANA_1667	-8.46	0.047	56	64	2	10
33	*crr*	PTS glucose transporter subunit IIA	PANA_2765	-8.44	0.047	56	64	-53	-45
34	*yqjC*	DUF1090 domain-containing protein	PANA_3461	-8.31	0.05	24	38	-7	8

***Locus tag of *Pantoea ananatis* LMG20103**
[a]Start and End position based on sRNA sequence
[b]Start and End position based on mRNAposition

mRNA target prediction of sRNA pPAR 237									
Rank	**Gene**	**Product**	**Locus tag**	**Energy**	**Pvalue**	**sRNA_ start[a]**	**sRNA_ stop[a]**	**mRNA_ start[b]**	**mRNA _stop[b]**
1	*ycbX*	MOSC domain-containing protein	PANA_1383	-17.81	0	10	22	7	19
2	*perM*	Putative permease	PANA_2810	-16.89	0	7	20	-63	-50
3	*arnA*	Bifunctional polymyxin resistance ArnA protein (UDP-4-amino-4-deoxy-L-arabinose)	PANA_4004	-16.47	0	92	109	-77	-59
4	-	Putative haloacid dehalogenase type II	PANA_2414	-15.47	0	4	15	-30	-19
5	-	Putative ABC-Type Sugar Transport System Periplasmic protein	PANA_0367	-14.71	0.001	114	129	-22	-6
6	*yohF*	SDR family oxidoreductase	PANA_1240	-13.7	0.002	97	110	-76	-64
7	*amiC*	N-acetylmuramoyl-L-alanine amidase	PANA_0644	-13.48	0.003	136	152	-56	-41
8	-	Hypothetical protein	PANA_0579	-13.18	0.003	114	130	-24	-7
9	*msrB*	Peptide-methionine (R)-S-oxide reductase	PANA_2109	-13.04	0.004	44	62	-26	-8
10	*ppa*	Inorganic pyrophosphatase	PANA_3069	-12.56	0.005	7	26	-58	-40

11	*pqqB*	Pyrroloquinoline quinone biosynthesis protein	PANA_1854	-12.55	0.005	143	159	-55	-42
12	*pitA*	Inorganic phosphate transporter	PANA_3764	-12.54	0.005	8	25	-47	-31
13	*sfcA*	NAD-dependent malic enzyme	PANA_2537	-12.5	0.005	92	108	-79	-61
14	*csgA*	SDR family oxidoreductase	PANA_3752	-11.95	0.008	91	108	-78	-61
15	-	Hypothetical protein	PANA_0007	-11.8	0.009	92	108	-60	-44
16	*malE*	Maltose/maltodextrin ABC transporter substrate-binding protein	PANA_1911	-11.7	0.009	134	150	-80	-64
17	*foxA*	TonB-dependent siderophore receptor	PANA_4210	-11.55	0.01	45	65	-68	-49
18	*yieN*	ATPase RavA	PANA_0013	-11.47	0.01	8	22	-77	-62
19	*proW*	Glycine betaine/L-proline transport system permease	PANA_0589	-11.46	0.011	4	17	-54	-41
20	*holE*	DNA polymerase III subunit theta	PANA_2185	-11.29	0.012	135	154	-16	5
21	*mprA*	DNA-binding transcriptional repressor of microcin B17 synthesis and multidrug efflux; negative regulator of the multidrug operon emrAB	PANA_2997	-11.25	0.012	141	155	-56	-41
22	*hifC*	Outer membrane usher protein HifC precursor	PANA_1522	-10.99	0.014	114	129	-25	-9
23	*yjeF*	Bifunctional ADP-dependent NAD(P)H-hydrate dehydratase/NAD(P)H-hydrate epimerase	PANA_3542	-10.79	0.015	143	161	-80	-61
24	*X*	Tail protein X	PANA_3416	-10.57	0.017	8	27	-80	-62
25	*glnS*	Glutamine-tRNA ligase	PANA_1149	-10.5	0.018	136	152	-21	-3
26	*cex*	Putative exoglucanase/xylanase precursor	PANA_0376	-10.44	0.019	148	164	-49	-32
27	*ygjE*	DASS family sodium-coupled anion symporter, putative tartrate carrier	PANA_4118	-10.42	0.019	62	74	-45	-33
28	*yhhQ*	7-cyano-7-deazaguanine/7-aminomethyl-7-deazaguanine transporter	PANA_3732	-10.19	0.021	111	131	-74	-55
29	*crr*	PTS glucose transporter subunit IIA	PANA_2765	-10.18	0.021	70	81	-36	-25
30	*mcpB*	PAS domain S-box protein, methyl accepting chemotaxis protein	PANA_3263	-9.9	0.025	134	145	-56	-45
31	*gabD*	NAD-dependent succinate-semialdehyde dehydrogenase	PANA_3555	-9.8	0.026	149	161	-41	-29
32	-	Hypothetical protein	PANA_1424	-9.78	0.026	91	107	-47	-31
33	*yobA*	Copper homeostasis periplasmic binding protein	PANA_2184	-9.6	0.028	64	78	-80	-67
34	-	Putative glycoside hydrolase family 127 protein	PANA_2811	-9.59	0.028	142	160	-63	-45
35	-	Hypothetical protein	PANA_1526	-9.38	0.031	120	133	-28	-15
36	*ppdA*	Prepilin peptidase dependent protein A precursor	PANA_3113	-9.37	0.031	126	139	-80	-68

37	*tssM*	Type VI secretion system membrane subunit TssM	PANA_1655	-9.34	0.032	4	18	-44	-30
38	*tcp*	Methyl-accepting chemotaxis citrate transducer	PANA_3261	-9.26	0.033	110	125	-15	1
39	*yckA*	Probable amino-acid ABC transporter permease	PANA_4057	-8.62	0.044	114	133	-27	-8
40	-	Acireductone synthase	PANA_0872	-8.49	0.046	127	142	-80	-64
41	-	DUF2474 domain-containing protein	PANA_3244	-8.39	0.048	136	151	2	19
42	*frr*	Ribosome recycling factor	PANA_0795	-8.32	0.049	138	148	-33	-23

***Locus tag of Pantoea ananatis LMG20103**
[a]Start and End position based on sRNA sequence
[b]Start and End position based on mRNAposition

mRNA target prediction of sRNA pPAR 238									
Rank	**Gene**	**Product**	**Locus tag**	**Energy**	**Pvalue**	**sRNA_ start[a]**	**sRNA_ stop[a]**	**mRNA _start[b]**	**mRNA _stop[b]**
1	*yohF*	SDR family oxidoreductase	PANA_1240	-20.09	0	96	110	-77	-63
2	*tauA*	Taurine ABC transporter substrate-binding protein	PANA_3646	-16.68	0	91	109	-32	-15
3	*yafD*	Endonuclease/exonuclease/phosphatase family protein	PANA_0825	-16.21	0	98	109	8	19
4	-	Hypothetical protein	PANA_3279	-15.7	0	92	107	-80	-67
5	*fliF*	Flagellar M-ring protein	PANA_2295	-14.09	0.002	15	27	-68	-56
6	*uvrD*	DNA helicase II	PANA_0169	-13.58	0.002	91	104	-74	-61
7	*lldR*	Putative L-lactate dehydrogenase operon regulatory protein	PANA_0924	-13.24	0.003	50	65	-21	-5
8	-	Hypothetical protein	PANA_1542	-13.08	0.004	97	111	-50	-36
9	*lolA*	Outer membrane lipoprotein chaperone	PANA_1342	-12.81	0.004	26	41	-59	-45
10	*ycaD*	MFS-type transporter protein	PANA_1345	-12.48	0.005	27	39	2	15
11	*atpD*	F0F1 ATP synthase subunit beta	PANA_0027	-12.44	0.006	92	105	-62	-49
12	*yeeO*	EmmdR/YeeO family multidrug/toxin efflux MATE transporter	PANA_2374	-11.61	0.01	97	109	8	20
13	*yjhB*	MFS transporter	PANA_0037	-11.24	0.012	91	108	-59	-42
14	*mltB*	membrane-bound lytic murein transglycosylase B; catalyzes the cleavage of the glycosidic bonds between N-acetylmuramic acid and N-acetylglucosamine in peptidoglycan	PANA_3038	-10.97	0.014	45	60	-32	-18
15	*rpe*	Ribulose-phosphate 3-epimerase	PANA_3664	-10.41	0.019	95	110	-47	-31

16	*glgX*	Glycogen debranching protein Glg	PANA_1750	-10.31	0.02	16	26	-58	-48
17	*yohK*	CidB/LrgB family autolysis modulator	PANA_2535	-10.29	0.02	21	41	-72	-52
18	*yfcI*	Putative transposase, Rpn family recombination-promoting nuclease	PANA_4113	-9.9	0.025	15	31	-22	-5
19	*sgcQ*	Photosystem I Assembly BtpA	PANA_0511	-9.85	0.025	95	109	-52	-39
20	*yncC*	GntR family transcriptional regulator	PANA_0840	-9.82	0.025	15	33	-68	-49
21	*yncD*	TonB-dependent receptor	PANA_1849	-9.75	0.026	27	44	-26	-11
22	*pdxJ*	Pyridoxine 5'-phosphate synthase	PANA_2890	-9.71	0.027	25	39	-65	-51
23	*sfcA*	NAD-dependent malic enzyme	PANA_2537	-9.6	0.028	92	107	-79	-61
24	*gabD*	NAD-dependent succinate-semialdehyde	PANA_2416	-9.42	0.031	67	77	-76	-66
25	*yibD*	Glycosyltransferase	PANA_3891	-9.4	0.031	68	78	-65	-55
26	-	Hypothetical membrane protein	PANA_0559	-9.35	0.032	91	107	-23	-5
27	*uidR*	TetR/AcrR family transcriptional regulator (repressor)	PANA_1528	-9.3	0.033	103	118	-15	1
28	-	Hypothetical protein	PANA_3292	-9.27	0.033	64	75	-52	-41
29	*mltC*	Membrane-bound lytic murein transglycosylase C	PANA_3237	-9.26	0.033	15	30	-27	-12
30	*yedX*	Hydroxyisourate hydrolase	PANA_0867	-9.21	0.034	53	70	-13	4
31	*pntB*	Re/Si-specific NAD(P)(+) transhydrogenase subunit beta	PANA_1994	-9.1	0.036	93	104	-73	-62
32	*yibF*	Glutathione S-transferase	PANA_0104	-9.09	0.036	50	61	-19	-8
33	*ygjO*	23S rRNA (guanine(1835)-N(2))-methyltransferase	PANA_3449	-9.02	0.037	101	114	-39	-26
34	*yeeI*	Inner Membrane Protein; Mlc anti-repressor, regulates ptsG by binding and inactivating Mlc	PANA_2326	-8.9	0.039	92	104	-18	-6
35	*cex*	Putative exoglucanase/xylanase precursor	PANA_0376	-8.65	0.043	22	36	-46	-32
36	*apt*	Adenine phosphoribosyltransferase	PANA_1027	-8.35	0.049	45	59	-5	9
37	*coaBC*	bifunctional phosphopantothenoylcysteine decarboxylase/phosphopantothenate-cysteine ligase CoaBC	PANA_3905	-8.32	0.049	51	70	-26	-6

***Locus tag of *Pantoea ananatis* LMG20103**
[a]Start and End position based on sRNA sequence
[b]Start and End position based on mRNAposition

mRNA target prediction of sRNA pPAR 395									
Rank	**Gene**	**Product**	**Locus tag**	**Energy**	**P value**	**sRNA_ start[a]**	**sRNA _stop[a]**	**mRNA _start[b]**	**mRNA _stop[b]**
1	*yicJ*	Inner membrane symporter, MFS transporter	PANA_2812	-14.86	0.001	36	54	-8	11
2	-	Hypothetical protein	PANA_2514	-14.62	0.001	86	97	8	20
3	-	Hypothetical protein	PANA_1112	-13.7	0.002	69	81	-80	-67
4	*aqpZ*	Aquaporin Z	PANA_2219	-13.5	0.003	84	96	-49	-37
5	*yibQ*	Periplasmic protein, divergent polysaccharide deacetylase family protein	PANA_3883	-13.3	0.003	8	23	2	17
6	*thiI*	Thiamine biosynthesis protein	PANA_0979	-13.12	0.003	84	96	-76	-63
7	*perM*	Putative permease	PANA_2810	-13.01	0.004	86	95	-59	-50
8	*sardH*	Sarcosine dehydrogenase, mitochondrial precursor	PANA_1939	-12.98	0.004	86	99	-2	12
9	*mocC*	TIM barrel protein	PANA_1626	-12.57	0.005	86	99	-74	-60
10	*codA*	Cytosine deaminase	PANA_3661	-12.4	0.006	86	94	7	15
11	*arcA*	Two-component system response regulator, aerobic respiration control protein	PANA_0653	-12.3	0.006	84	95	8	20
12	*yedQ*	GGDEF domain-containing protein	PANA_1637	-12	0.007	84	97	-16	-3
13	*qseC*	Two-component system sensor histidine kinase	PANA_0011	-11.62	0.01	86	95	-44	-35
14	*nhaA*	Na+/H+ antiporter	PANA_0665	-11.35	0.011	78	96	1	20
15	*nikB*	ABC transporter permease	PANA_4182	-10.9	0.015	83	96	-59	-47
16	*dsdC*	LysR family transcriptional regulator, HTH-type transcriptional regulator DsdC	PANA_0854	-10.82	0.015	86	99	-2	12
17	*sirA*	Sulfurtransferase TusA	PANA_3731	-10.67	0.016	1	16	-20	-5
18	*glnQ*	Glutamine ABC transporter ATP-binding protein	PANA_1280	-10.65	0.017	83	96	-31	-19
19	*pleD*	GGDEF domain-containing response regulator protein	PANA_3296	-10.56	0.018	84	98	-2	13
20	*yedD*	Lipoprotein	PANA_2286	-10.55	0.018	84	96	-66	-52
21	-	Hypothetical protein	PANA_3340	-10.54	0.018	68	76	-47	-39
22	*nudH*	RNA pyrophosphohydrolase	PANA_3117	-10.48	0.018	84	96	-80	-69
23	*copA*	Copper-exporting P-type ATPase CopA	PANA_1042	-10.47	0.018	84	95	-28	-17
24	*sapF*	Peptide ABC transporter ATP-binding protein	PANA_2034	-10.41	0.019	82	96	-37	-24

25	*rbsB*	Sugar ABC transporter substrate-binding protein	PANA_0509	-10.31	0.02	84	97	-32	-20
26	*nagE*	PTS N-acetylglucosamine transporter subunit, phosphoenolpyruvate-dependent sugar phosphotransferase system	PANA_1148	-10.31	0.02	68	83	-15	-1
27	*phoR*	Phosphate regulon sensor histidine kinase part of the two-component phosphate regulatory system phoR/phoB	PANA_0954	-10.1	0.022	84	97	-28	-16
28	*htpX*	Protease HtpX	PANA_2156	-9.99	0.023	87	95	-69	-61
29	*xynB*	Alpha/beta hydrolase	PANA_0136	-9.87	0.025	29	43	-22	-8
30	*fliP*	Flagellar type III secretion system pore protein	PANA_2305	-9.82	0.026	86	94	-77	-69
31	*rne*	Ribonuclease E	PANA_1475	-9.8	0.026	84	98	-48	-34
32	-	Nucleotidyltransferase	PANA_2751	-9.45	0.03	84	95	-56	-44
33	*ygaM*	DUF883 family protein	PANA_2988	-9.31	0.032	74	94	-22	-4
34	*rph*	Ribonuclease PH	PANA_3909	-9.29	0.033	64	72	-14	-6
35	*yeiB*	DUF418 family protein, hypothetical protein	PANA_2543	-9.2	0.034	82	96	1	18
36	*xerC*	Tyrosine recombinase XerC	PANA_0167	-9.02	0.037	65	77	-79	-66
37	*qor*	Quinone oxidoreductase	PANA_0263	-8.99	0.037	80	94	-58	-44
38	-	Hypothetical protein	PANA_2126	-8.94	0.038	84	94	-27	-17
39	*fbaA*	Ketose 1,6-bisphosphate aldolase	PANA_2380	-8.74	0.042	86	94	-57	-49
40	*yhiR*	23S rRNA (adenine(2030)-N(6))-methyltransferase	PANA_3769	-8.74	0.042	68	76	-51	-43
41	*yccX*	acylphosphatase	PANA_1404	-8.69	0.042	29	39	-20	-10
42	*rof*	Rho-binding antiterminator, suppresses temperature-sensitive mutations in essential genes by modulating rho-dependent transcription termination	PANA_0814	-8.68	0.043	53	64	-51	-40
43	-	Hypothetical protein	PANA_2734	-8.61	0.044	33	52	-6	14
44	-	Terminase small subunit	PANA_1063	-8.6	0.044	21	35	-58	-44
45	*tsx*	Nucleoside-specific channel-forming protein Tsx	PANA_0306	-8.55	0.045	29	45	-31	-14
46	*yeiR*	GTP-binding protein	PANA_4184	-8.53	0.045	27	43	-79	-63
47	*cynX*	MFS transporter	PANA_0922	-8.48	0.046	30	44	-76	-62
48	*npdA*	NAD-dependent protein deacylase	PANA_1508	-8.39	0.048	82	96	1	16

***Locus tag of *Pantoea ananatis* LMG20103**
[a]Start and End position based on sRNA sequence
[b]Start and End position based on mRNAposition

S Table 2.5 A custom python script compiled for bioinformatic analyses of sRNA sequencing data

Genic_filter.py

```
##SAM file genic filter

#import
threading
#import Queue
import sys

#Parse and store CDS sequences from annotation file
annotfile='ref/GCA_000025405.2_ASM2540v1_geno
mic.gff' aFile=open(annotfile,'r')

outfile_name="sfilt_"+sys.arg
v[1]
outfile=open(outfile_name,'w')
plus_CDS={}
minus_CDS={
} for liner in
aFile:
        liner=liner.rstrip()
        if liner.startswith("#"):
                skip=True
                #skip comments/headers
        else:
  splat=liner.split("\t") #print splat
  if splat[2]=="CDS" or splat[2]=="tRNA" or splat[2]=='rRNA': if
          splat[6]=="+":
                  #Add to + strand list of features
                  >>>>> Remove promoters and terminators too.<<<<<<<<<
                          for n in range(int(splat[3])-
                                  120,int(splat[4])+120):
                                  plus_CDS[n]='+'
                  elif splat[6]=="-":
                          #Add to - strand list of features
                          for n in range(int(splat[3])-
                                  120,int(splat[4])+120):
                                  minus_CDS[n]='-'

samfile=sys.argv[1
] #Parse sam file:
file=open(samfile,'
r')
s_plus_CDS=set(plus_CDS.keys(
))
```

```
s_minus_CDS=set(minus_CDS.k
eys()) total_sam_lines=0
kept=0
removed=0
unmapped=0
for line in
file:
        line=line.rstrip()
        if line.startswith("@"):
                skip=True

                outfile.write("%s\n"%li
                ne) #re-print sam
        else    headers
        :
                total_sam_lines+=1
                #line=line.rstrip()
                cutup=line.split()
                location=int(cutup[3
                ]) if cutup[1]=='4':
                        #skip all unmapped
                        reads unmapped+=1
                elif cutup[1]=='16':

                        if location in
                                s_minus_CDS:
                                removed+=1
                        else:
                                outfile.write("%s\n"%li
                                ne) kept+=1
                elif cutup[1]=='0':

                        if location in s_plus_CDS:
                                removed+=1
                        else:
                                #print
                                line
                                kept+=1
outfile.close(                  outfile.write("%s\n"%line)
)

print("%s reads in sam
file"%total_sam_lines) print("%s were
unmapped"%unmapped)
print("%s mapped to CDS regions and were removed"%removed)
print("%s mapped to intergenic regions or antisense regions and were kept"%kept)
```

Peak_ID.py

```
'''
read sam file
        go through genomic positions
        compute depth > one set for + strand, another for - strand

Analyze depth > one strand at a time
        estimate background using a sliding window
        ID peaks that are at least 50 bases long X-fold above background across entire length >>
test different levels

        output peak start and end, depth, background



'''
samfile=""
sam_file=open(samfile,'
r')


#initialize Dictionaries



bases=0
plus_depth={}
minus_depth=
{}
GenomeLength=4703372
for i in
        range(1,GenomeLength
        +1): plus_depth[i]=0
        minus_depth[i]=0
for line in sam_file:
        line=line.rstrip()
        if line.startswith("@"):
                ignore=True
        else:
                columns=line.split()
                bases=bases+len(columns[
                9]) if columns[1]=='4':
                        unmapped=Tru
                e     elif
                columns[1]=='0':
                        #plus_strand
```

```
                        for x in
                                range(int(columns[3]),int(columns[3])+len(column
                                s[9])): if x<=GenomeLength:
                                        plus_depth[x]+=1
                                else:
plus_depth[x-GenomeLength]+=1
                elif columns[1]=='16':
                        #minus_strand
                        for x in
                                range(int(columns[3]),int(columns[3])+len(column
                                s[9])): if x<=GenomeLength:
                                        minus_depth[x]+=1
                                else:
                                        minus_depth[x-GenomeLength]+=1

#print bases
#print bases/GenomeLength
Gbackground=float(bases)/GenomeLen
gth windowWidth=1000
stepSize=1
ratio_Threshold=
10 pos=1
#Peak finding
fpeakLength=
0
rpeakLength=
0
#set initial Forward
background #fsum=0
#for x in range(1,1000):
#
        fsum+=plus_depth[
x]
#fbackground=fsum/1000

#set initial minus
background #rsum=0
#for x in range(1,1000):
#
        rsum+=minus_depth[
x] #rbackground=rsum/1000

#outfile=open("zzz_F_test_N.txt",'
w') #Print Headers:
#for file in samfile_list:
#
        outfile.write("%s\t"%fi
```

```
le) #outfile.write("\n")

while pos<GenomeLength:
        #fbackground=fbackground-(plus_depth[pos-
        1]/1000)+(plus_depth[pos+1000]/1000) #rbackground=rbackground-
        (minus_depth[pos-1]/1000)+(minus_depth[pos+1000]/1000) if
        (plus_depth[pos]/Gbackground)>ratio_Threshold:
                fpeakLength+=1
        else:
                if fpeakLength>=10:# and fpeakLength<50:
                        print "+\t%s\t%s\t%s\t%s"%(pos-fpeakLength,pos-1,plus_depth[pos-
fpeakLength],plus_depth[pos-1])
                fpeakLength=0
        if (minus_depth[pos]/Gbackground)>ratio_Threshold:

                gth+=1
        else
        :       if rpeakLength>=10:# and rpeakLength<50:
                                print "-\t%s\t%s\t%s\t%s"%(pos-rpeakLength,pos-
                                                1,minus_depth[pos-
  rpeakLen
rpeakLength],minus_depth[pos-1])
                rpeakLength=0
        #outfile.write("%s\t"%(po
        s)) #index=0
        #for dict in f_depth_files:
        #
                outfile.write("%s\t"%(dict[pos]/(float(library_size[index])/GenomeLe
        ngth))) #       index+=1
        #outfile.write("\n")
        pos+=1
#outfile.close()
```

MergeList.py

```
#Merge lists of putative sRNAs

infile1=open("list1.txt",'
r')
infile2=open("list2.txt",'
r')


time1=[
]
time2=[
]
for line1 in infile1:
        line1=line1.rstrip()
        time1.append(line
        1)
for line2 in infile2:
        line2=line2.rstrip()
        time2.append(line
        2)
count=0
newList=
[]
for entry1 in time1:
        entry1Limits=(int(entry1.split("\t")[2]),int(entry1.split("\t"
        )[3])) for entry2 in time2:
                entry2Limits=(int(entry2.split("\t")[2]),int(entry2.split("\t")[3]))

                if entry1.split("\t")[1]==entry2.split("\t")[1]:

                        if entry1Limits[0] in range(entry2Limits[0],entry2Limits[1]) or
entry1Limits[1] in range(entry2Limits[0],entry2Limits[1]):
                                #print entry1+"\n"+entry2+"\n\n"

        newList.append("1,2\t%s\t%s\t%s"%(entry1.split("\t")[1],min(entry1Limits[0],entry1Lim
its[1],en try2Limits[0],entry2Limits[1]),
max(entry1Limits[0],entry1Limits[1],entry2Limits[0],entry2Limits[1])))
                                count+=1

count1=0
newNewList
=[]
for entry1 in time1:
        entry1Limits=(int(entry1.split("\t")[2]),int(entry1.split("\t"
        )[3])) found=False
```

```
        for entryNew in newList:
                entryNewLimits=(int(entryNew.split("\t")[2]),int(entryNew.split("\t")[3]))

                if entry1.split("\t")[1]==entryNew.split("\t")[1]:
                        if entry1Limits[0] in
range(entryNewLimits[0],entryNewLimits[1]) or entry1Limits[1] in
range(entryNewLimits[0],entryNewLimits[1]):
                                found=True

        if found:

                skip=True
                #already in newList
        else
        :       newNewList.append(entry
                1) count1+=1

count2=0
for entry2 in time2:
        entry2Limits=(int(entry2.split("\t")[2]),int(entry2.split("\t"
        )[3])) found=False
        for entryNew in newList:
                entryNewLimits=(int(entryNew.split("\t")[2]),int(entryNew.split("\t")[3]))

                if entry2.split("\t")[1]==entryNew.split("\t")[1]:
                        if entry2Limits[0] in
range(entryNewLimits[0],entryNewLimits[1]) or entry2Limits[1] in
range(entryNewLimits[0],entryNewLimits[1]):
                                found=True

        if found:
                skip=True
                #already in newList
        else:
                newNewList.append(entry
                2) count2+=1
for new in newList:
        print

new print

"\n\n\n"

for newnew in
        newNewList:
        print newnew
```

```
print "%s found in both
timepoints"%count print "%s found in
timepoint 1 only"%count1 print "%s
found in timepoint 2 only"%count2
```

RI_term.py

```
def char_count(string,
        character):
        count=0
        for char in string:
                if char in character:
                        count+=1

        return count


genome=open("../gina/genomes/GCA_000025405.2_ASM2540v1_ge


nomic.fa",'r') genome_seq="
for line in genome:
        line=line.rstrip()
        if line.startswith(">"):
                id=line.strip(">")
        else:
                genome_seq=genome_seq+line

i=0

#list of
poly-T
polyT
=[]
while i<len(genome_seq)-8:
        if "TTTTTT" in
                genome_seq[i:i+8]:#,"T")>
                =6: polyT.append((i,i+8))
        i+=1
newPoly
T=[]
previous
T=(0,0)
for Ti in
polyT:
        if Ti[0] in
                range(previousT[0],previo
                usT[1]): skip=True
        else:
                newPolyT.append(Ti)
        previousT=Ti

newNewPolyT=[]
for entry in newPolyT:
        #print entry
```

```
        if char_count(genome_seq[entry[0]-
                4:entry[0]+2],"GC")>3:
                newNewPolyT.append(entry)
#print len(newPolyT)

newNewNewPolyT=[]
for candidate in newNewPolyT:
        if char_count(genome_seq[candidate[0]-
                23:candidate[0]+2],"GC")>12:
                newNewNewPolyT.append(candidate)
print "%s TTTTTTs found on DNA strand"%len(newPolyT)
print "of these, %s had 4 GCs in the last 6 bases before the poly-
T"%len(newNewPolyT) print "of these, %s had more than 50 percent GC
in the last 25 bases before the poly- T"%len(newNewNewPolyT)


annotation_file=open("../gina/genomes/GCA_000025405.2_ASM2540v1_gen
omic.gff",'r') gene_ends=[]
for line in annotation_file:
        line=line.rstrip()
        if line.startswith("#"):
                ignore=True #comment
        else:
                columns=line.split("\t")
                if columns[2]=="CDS" or columns[2]=="rRNA" or
                        columns[2]=="tRNA": if columns[6]=="+":
                                gene_ends.append(int(columns[4]))
sRNA_file=open("NmergeL
ist.txt",'r') sRNA_ends=[]
for line in sRNA_file:
        line=line.rstrip(
        )
        columns=line.s
        plit("\t") if
        columns[1]=="
        +":
                sRNA_ends.append(int(columns[3]))


gene_associated=[]
for cand in
        newNewNewP
        olyT: for end in
        gene_ends:
                if (cand[1]-6)-end > 0 and (cand[1]-6)-
                        end < 120:
                        gene_associated.append(cand)

sRNA_associated=[]
for cand2 in
```

```
        newNewNewPol
        yT: for endS in
        sRNA_ends:
                if (cand2[1]-6)-endS >0 and (cand2[1]-6)-
                        endS < 80:
                        sRNA_associated.append(cand2)
                        print cand2
print "%s gene_associated putative Rho-independent terminator
sites"%len(gene_associated) print "%s sRNA_associated putative Rho-
independent terminator sites"%len(sRNA_associated)
```

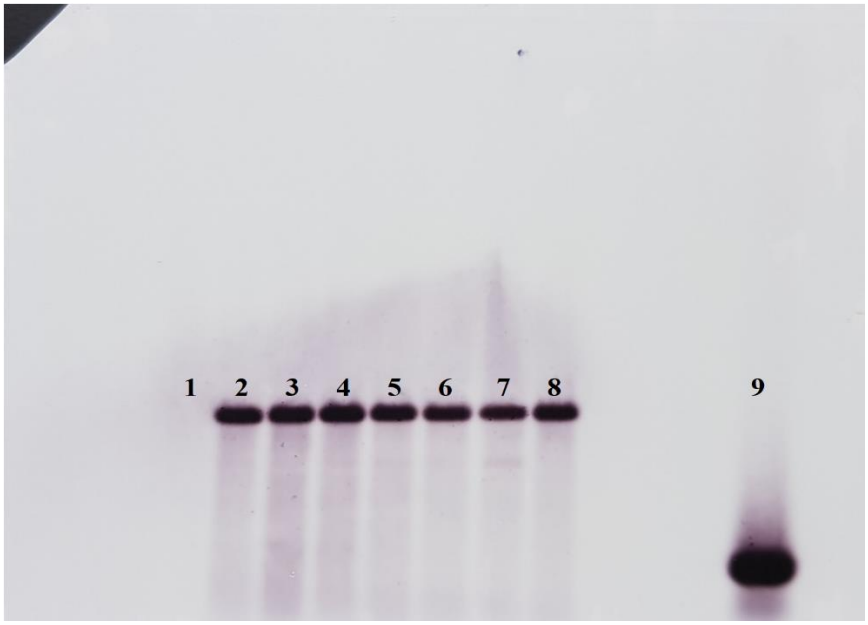

S Figure 2.1 Southern blot validation of *hfq* knock-out mutation in *Pantoea ananatis*. Genomic DNA of the wild-type (WT) and *hfq* mutant (Δ*hfq*) strains of *P. ananatis* LMG 2665^{T} digested with EcoRI and HindIII restriction enzymes was hybridized to a DIG-labelled probe (a partial amplicon of kanamycin resistance gene). Positive detection of the antibiotic marker was observed in the Δ*hfq* strains of *P. ananatis* LMG 2665^{T} (lane 2 to 8). WT of *P. ananatis* LMG 2665^{T} DNA was used as a negative control (lane 1) whereas unlabelled probe was used as a positive control (lane 9).

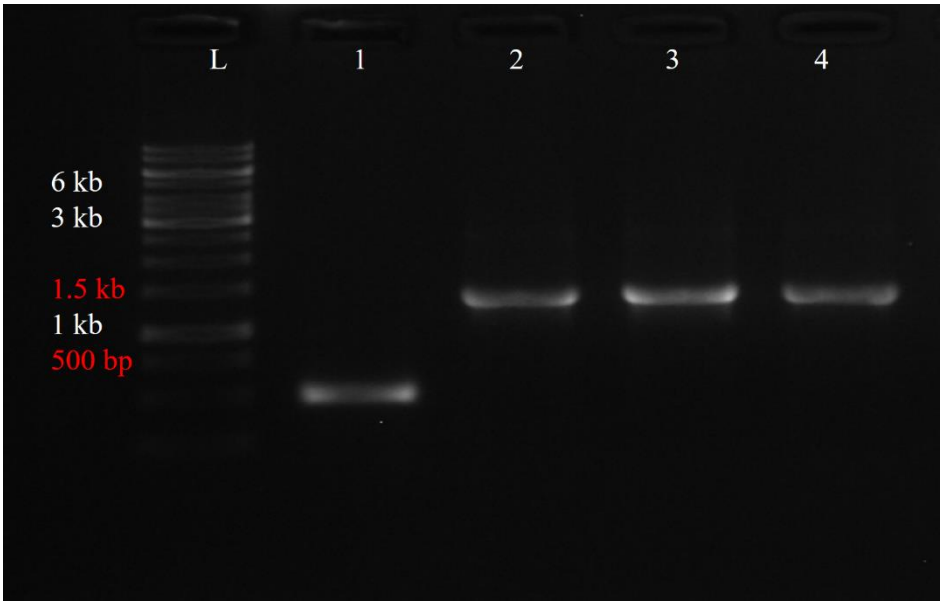

S Figure 2.2 Colony PCR verification of *hfq* knock-out mutation in *Pantoea ananatis*. A colony PCR confirmation of insertion of kanamycin resistance gene in the *hfq* gene region using Test primers (Table 2.2) *hfq* mutant (Δ*hfq*) strains of *P. ananatis* LMG 2665^{T}. L represents a molecular ladder and the sizes of its prominent bands 1 kilo basepairs (kb), 3 kb and 6kb are indicated below. A wild-type (WT) colony of *P. ananatis* LMG 2665^{T} was used as a negative control (lane 1; 500 bp). Insertion of kanamycin resistance marker is shown in colony PCRs of *hfq* mutant (Δ*hfq*) strains of *P. ananatis* LMG 2665^{T} (lane 2, 3 and 4; 1.5 kb).

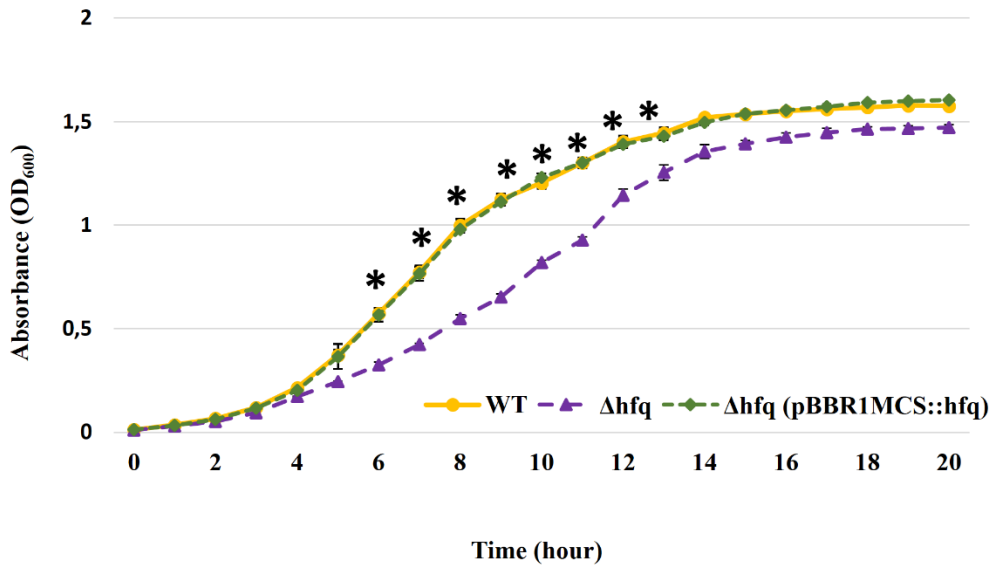

S Figure 2.3 *In vitro* growth assay. Growths of wild-type (WT), *hfq* mutant (Δ*hfq*) and *hfq* complementing (Δ*hfq* pBBR1MCS::*hfq*) strains of *Pantoea ananatis* LMG 2665^{T} in LB broth at 28°C. The growth was monitored for 20 h at optical density 600nm (OD_{600}) and the mean OD_{600} readings of the three replicates for each *P. ananatis* LMG 2665^{T} strains were plotted. Solid line (yellow) represent WT, dashed line (purple) Δ*hfq* and dotted line (green) Δ*hfq* pBBR1MCS::*hfq*. Asterisks denote significance differences (P<0.05) in the absorbance of Δ*hfq* relative to WT *P. ananatis* LMG 2665^{T}.

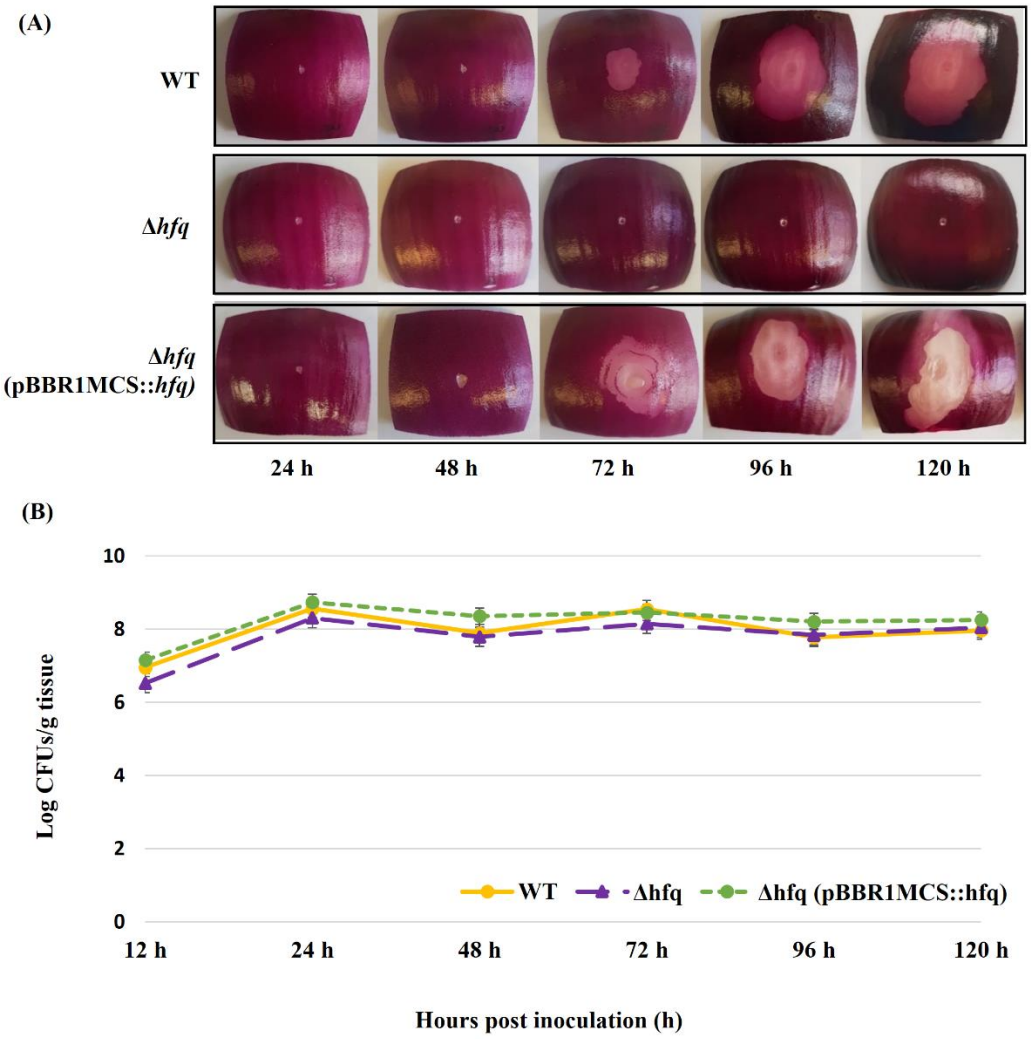

S Figure 2.4 *In planta* growth assay. (A) Disease progression in onion scales inoculated with wild-type (WT), *hfq* mutant (Δ*hfq*) and *hfq* complementing (Δ*hfq* (pBBR1MCS::*hfq*) strains of *P. ananatis* LMG 2665^{T}, and incubated for 5 days post inoculation (dpi). (B) *In planta* populations of WT, Δ*hfq* and Δ*hfq* (pBBR1MCS::*hfq*) strains of *P. ananatis* LMG 2665^{T} in onion scales measured for 5 dpi. The mean CFUs of three replicates for each strain from two independent experiments were plotted. Solid line (yellow) represents WT, dashed line (purple) Δ*hfq* and dotted line (green) Δ*hfq* (pBBR1MCS::*hfq*).

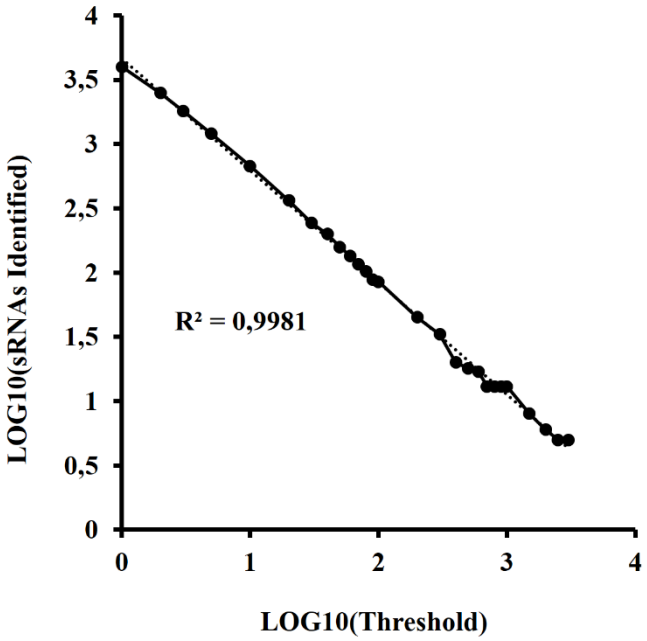

S Figure 2.5 Logarithmic plot of the number of putative small RNAs (sRNAs) identified in *Pantoea ananatis* LMG 2665^{T} (pPAR sRNA) as a function of the threshold selected for calling sRNAs. This was generated by calling putative sRNAs across a range of thresholds using the custom script (see script.pdf in section peak_ID.py)

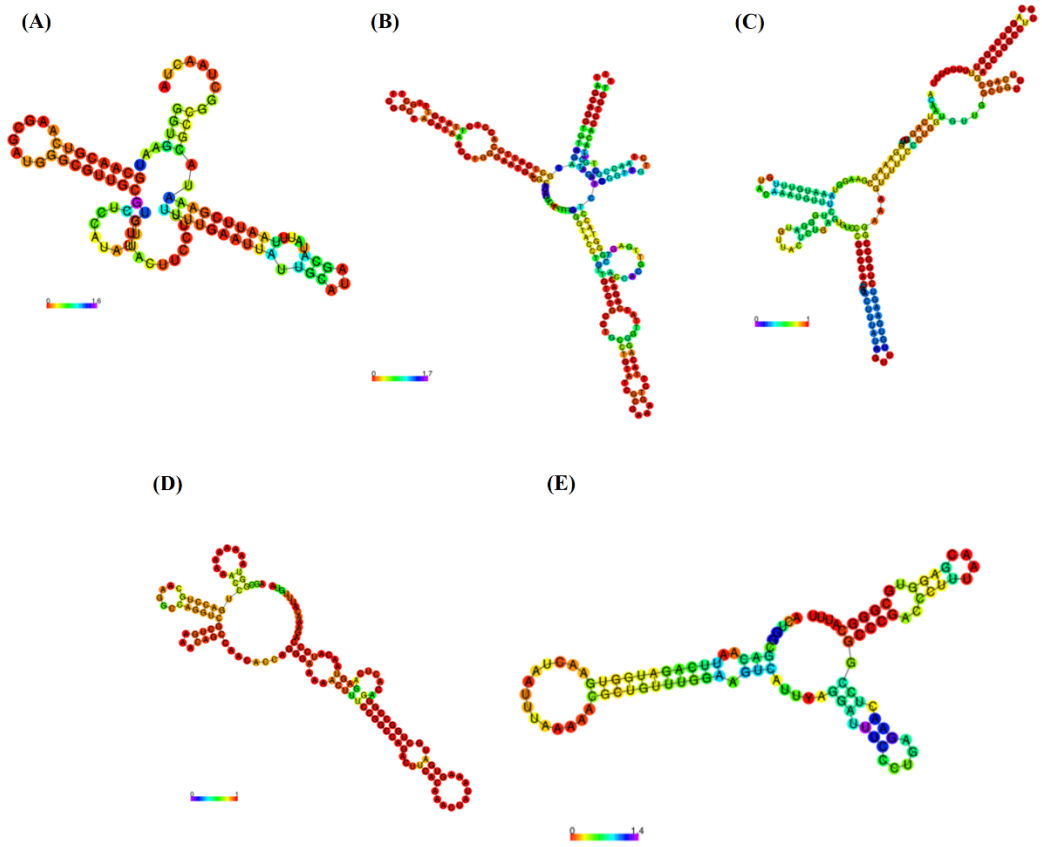

S Figure 2.6 *In silico* prediction of selected *Pantoea ananatis* sRNAs (pPAR sRNA) secondary structure. Secondary structures of *P. ananatis* LMG 2665^{T} sRNAs (A) FnrS, (B) GlmZ, (C) pPAR 237, (D) pPAR 238 and (E) pPAR 395 were predicted based on a minimum free energy model provided by RNAfold (http://rna.tbi.univie.ac.at).

(A)

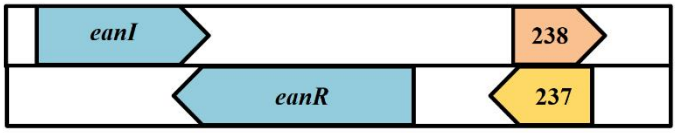

(B)

```
                1                     23
                |                     |
          5'-           U   A   C    AGAUG...GAA-3'
              UCAGGGAGAA UUU CCG CCA
              :||||||:|| :|| ||| |||
              GGUCCCUUUU GAA GGC GGU
3'-UUU...GUUGU           U   A   C    CUGAA...ACA-5'
             |                        |
             123                      100
```

(C)

```
            39                                                          90
            |                                                           |
5'-AUG...CGGAU    U     CUU    A       AAG                      GG   GU     GUACG...UAG-3'
             ACGC UCAGA   ACAU  CAGAGA              UUAUCUUCGUUU   CA  CCUGA
             ||:| |||||   ||||  ||||:|              |||:||||||:||   ||  |||||
             UGUG AGUCU   UGUA  GUCUUU              AAUGGAAGCGAA   GU  GGACU
3'-UUU...GGCCC          CAU    GG      GUAAACAUGUUUGUA            AGG  GU     AACA-5'
            |                                                           |
            68                                                          4
```

(D)

```
              77         87
              |          |
5'-CUU...GAGAA           CCAAG...GAU-3'
               UUUUACCGC
               |||||||||
               AAAAUGGCG
3'-AUG...AAAAA           A-5'
              |          |
              11         1
```

S Figure 2.7 Putative interaction of pPAR237 and pPAR238 to *ean*IR in *Pantoea ananatis* LMG 2665^{T}. (A) Location of pPAR237 and pPAR238. *In silico* predicted interaction of pPAR237 (red) to *ean*IR (black): (B) *ean*I upstream sequence (Energy: -8.62323 kcal/mol; hybridization Energy: -23.5). (C) *ean*R coding sequence (Energy: -13.63700 kcal/mol, hybridization Energy: -39.4) and (D) i*n silico* predicted interaction of pPAR238 (red) to *ean*I (black) upstream sequence (Energy: -7.83954 kcal/mol, hybridization energy: -12.0).

CHAPTER THREE

3.1 CONCLUDING SUMMARY

Since the sequencing of the first *P. ananatis*' genome (De Maayer *et al*., 2010), our understanding of this bacterium has improved significantly. The strains of *P. ananatis* have been predicted to have an 'open' pan-genome that harbours a significant portion of accessory genes whose functions are largely unknown. Within pan-genome, some genes were predicted to encode proteins that were restricted to animal-, insect- and plant-associated bacteria (De Maayer *et al*., 2014), thereby contributing to the versatility of *P. ananatis* as a pathogen of diverse hosts. Examination of the publicly available *P. ananatis* genome sequences also led to *in silico* characterization of genetic elements such as Integrative Conjugative Elements of *Pantoea ananatis* (ICE*Pan*). The products of the genes found on this island are suggested to participate in antibiosis, stress-response and functional diversification of *P. ananatis* (De Maayer *et al*., 2015). Furthermore, a plasmid-borne Onion Virulence Region (OVR) was described from onion pathogenic strains of *P. ananatis* whose products have been predicted to contribute to detoxification of the necrotic onion tissue environment (Stice *et al*., 2018).

Subsequently, the functionality of genes encoding virulence traits identified from the genome sequencing was experimentally determined. These include motility (Weller-Stuart *et al*., 2016), type 6 secretion system (Shyntum *et al*., 2015) and quorum-sensing (Sibanda *et al*., 2016). Mutagenesis of the genes needed for the normal functioning of these factors led to attenuated virulence in onion plants, indicating that they are all likely to be necessary for pathogenicity and fitness of *P. ananatis*. A genomic island strongly associated with onion pathogenic *P. ananatis* strains, initially discovered by Professor Takikawa's lab and named *P*antoea *a*nanatis specific virulence locus (PASVIL) Tomita *et al*., (2016) was subsequently described as 'HiVir' by Asselin *et al*. in 2018. Approximately, 18 ORFs are found on this island whose protein products have been predicted to catalyse phosphonate biosynthesis and other molecules. Among these ORFs, deletion mutation of a gene *pepM* (encoding phosphoenol pyruvate mutase) lead to virulence attenuation in onion plant, (Asselin *et al.* 2018). Furthermore, introduction of this island into a non-pathogenic *P. ananatis* strain rendered this strain pathogenicity in tobacco, onion and rice, (personal communication with Professor Takikawa). However, in latter's case, more ORFs than just *pepM* were confirmed indispensable for the acquisition of pathogenicity in *P. ananatis*. Understanding the functional roles of these indispensable genes or their products *in planta* condition would likely to help unravelling *P. ananatis* virulence mechanisms in diverse host plants.

Except for PASVIL/HiVir, most of *P. ananatis* virulence traits studied are conserved features in both pathogenic and non-pathogenic strains, making determination of pathogenicity in *P. ananatis,* solely based on the presence of these traits, difficult. In a comparative genomic study conducted by Sheibani-Tezerji *et al*., (2015) subtle genetic differences between the maize plant beneficial, commensal and pathogenic strains of *P. ananatis* were found. Besides the observed differences in the distribution of mobile elements and the type 6 secretion system gene clusters found in these strains, the authors have suggested that regulation of gene expression in response to plant host or environment may determine the phenotype of the bacterium.

Trans-encoded sRNAs are post-transcriptional regulators of genes which together with concerted action of Hfq, enhance or repress the translation of target transcripts (Vogel and Luisi, 2011). The sRNA-Hfq regulation of their targets results in the rapid rewiring of global cellular processes consequently leading to adaptive response and/or virulence in bacterial pathogens (Papenfort and Vogel, 2014; Holmqvist and Wagner, 2017). The work of this thesis thus aimed to investigate the role of Hfq in motility, biofilm formation, QS-autoinducer molecule (AHL) production and pathogenicity in *P. ananatis* and to identify a group of trans-encoded sRNAs that are dependent on Hfq. The results of this study showed that the deletion of the *P. ananatis hfq* had a pleiotropic effect on the aforementioned virulence factors. For example, motility and pathogenicity of *hfq* mutant *P. ananatis* were attenuated and a significant reduction in AHL production and biofilm formation was observed. The complementation of this mutation restored these phenotypes to that of the wild-type which indicates that *hfq* is important for functioning of these factors.

The sequencing of sRNA transcriptomes of both the wild-type and *hfq* mutant *P. ananatis* strains revealed a large number of putative sRNAs expressed from the inter- and intra-genic regions as well as the antisense strand of the coding regions of *P. ananatis* genome. Of these, 276 putative sRNAs were differentially expressed in the absence of *hfq*. Using bioinformatics tools, these candidates were further screened for the set of Hfq-dependent sRNA characteristics previously determined by Zeng and Sundin, (2014). The results identified known Hfq-dependent enterobacterial as well as novel *P. ananatis* sRNAs which suggest that *P. ananatis* sRNAs are also likely to be Hfq-dependent. Indeed, experimental gene expression of a subset of these sRNAs in *hfq* mutant measured against that of the wild-type showed a decrease in their abundances without *hfq*, with exception of GlmZ and RyhB, which was in agreement with their sequencing read depth plots. The 5’ rapid amplification of cDNA ends (5’ RACE) analysis was able to retrieve the full sequence of sRNAs FnrS, GlmZ, pPAR237, pPAR238 and pPAR395

whose *in silico* predicted targets included virulence-related genes encoding enzymes needed for degradation of the plant cell wall and biosynthesis of ‘amylovoran’-like exopolysaccharide.

The outcomes of this study revealed the presence of post-transcriptional regulators that were previously undescribed in *P. ananatis* and provided experimental evidence for Hfq as a global virulence regulator of this bacterium.

3.2 RECOMMENDATIONS FOR FUTURE STUDIES

The pleiotropic effects caused by *hfq* mutation in *P. ananatis* certainly suggest functional importance of this protein in AHL production, biofilm formation, motility and pathogenicity. However, it is unclear how this mutation affects each system. A small- and mRNA transcriptome profiling will reveal complete sets of RNAs that are affected by the loss of *hfq* gene. As sRNA samples are prepared in such a way to select for RNA molecules that are sized less than 500 nt, a majority of protein-coding transcripts are excluded from deep-sequencing. Thus, having identities of differentially regulated protein-coding genes as well as sRNAs may provide a clue as to which sRNAs are dedicated to regulating such genes or systems. Secondly, the total sRNA identified in this study could be further screened for the presence ORF using a bioinformatics approach such as DiSCO-Bac (Friedman *et al*., 2017). This search may yield putative sRNAs that are encoded into small peptides and perform dual function as a RNA binder or a repressor/toxin. Thirdly, determining functionality of sRNAs identified in this study will further enhance our understanding of their regulatory roles in modulating virulence factors. This part of work would entail mutagenesis of sRNA genes and characterizing the phenotypes of the sRNA-null mutants. Interestingly, for some sRNAs, such as ArcZ and OmrB in *E. coli*, overexpression of these sRNAs resulted in hypermotility and not only their inactivation (De Lay and Gottesman, 2012). Lastly, the sRNA regulation of computationally predicted targets can be experimentally validated. This can be done by making use of the translational fusion construct containing the target gene fused with a reporter gene such as GFP (green fluorescent protein). The relative GFP fluorescence intensity measured from the sRNA mutant and the wild-type strains represents the relative target gene expression under the absence and presence of the sRNA, respectively.

To capture populations of sRNAs involved in the virulence of plant host, sequencing of these sRNAs originating from *in planta* RNA extraction would be ideal. However, this approach is currently limited by a number of technical difficulties. As sRNAs are short and vulnerable to ribonucleases, extracting sufficient quantity and decent quality sRNAs from plant material may be challenging. Moreover, RNA extracted from plant material would mostly comprise of the host (plant) RNAs and significantly less of bacterial RNAs thereby requiring high sequencing depth. However, with the advent of technology, dual RNA-sequencing of both the host and pathogen may become available at a reduced cost which will allow capturing of the interactive dialogue between the host and pathogen at transcriptome levels.

The functional roles of other RNA chaperones remain to be elucidated. The genome of *P. ananatis* LMG 2665 possesses copies of both RNA binding proteins CsrA (homolog RsmA) and ProQ. According to Smirnov *et al*. (2016), these RNA-binding proteins (RBP) are functionally related to different classes of sRNAs. However, some sRNAs are shared between the RBPs (Holmqvist, 2013) and this could explain why in the absence of global regulators such as Hfq, *P. ananatis* was still able to survive.

3.3 REFERENCES

Asselin, J.E., Bonasera, J.M. and Beer, S.V. (2018) Center rot of onion (*Allium cepa*) caused by *Pantoea ananatis* requires *pepM*, a predicted phosphonate-related gene. *Mol. Plant Microbe-Interact.* doi: 10.1094/MPMI-04-18-0077-R.

De Lay, N. and Gottesman, S. (2012) A complex network of small non-coding RNAs regulate motility in *Escherichia coli*. *Mol. Microbiol*, 86, 524–538. doi: 10.1111/j.1365-2958.2012.08209.x. doi: 10.1111/j.1365-2958.2012.08209.x

De Maayer, P., Chan, W.Y, Rubagotti, Venter, S.N., Toth, I.K., Birch, P.R.J. and Coutinho, T.A. (2014) Analysis of the *Pantoea ananatis* pan-genome reveals factors underlying its ability to colonize and interact with plant, insect and vertebrate hosts. *BMC Genomics*, 15,404. doi: 10.1186/1471-2164-15-404

De Maayer, P., Chan, W.Y., Martin, D.A., Blom, J., Venter, S.N., Duffy, B., Cowan, D.A., Smits, T.H.M. and Coutinho, T.A. (2015) Integrative conjugative elements of the *ICEPan* family play a potential role in *Pantoea ananatis* ecological diversification and antibiosis. *Front. Microbiol*, 6, 576. doi: 10.3389/fmicb.2015.00576

De Maayer, P., Chan, W.Y., Venter, S.N., Toth, I.K., Birch, P.R.J., Joubert, F. and Coutinho. T.A. (2010) Genome Announcement: Genome sequence of *Pantoea ananatis* LMG20103, the causative agent of *Eucalyptus* blight and dieback. *J. Bacteriol*, 192, 2936-2937. doi: 10.1128/JB.00060-10

Friedman, R.C., Kalkhof, S., Doppelt-Azeroua, O., Mueller, S.A., Chovancová, M., von Bergen, M. and Schwikowski, B. (2017) Common and phylogenetically widespread coding for peptides by bacterial small RNAs. *BMC Genomics*, 18, 553. doi: 10.1186/s12864-017-3932-y

Holmqvist, E. (2013) A small RNA serving both the Hfq and CsrA regulons. *Genes Dev*, 27, 1073-1078. doi: 10.1101/gad.220178.113

Holmqvist, E. and Wagner, E.G.H. (2017) Impact of bacterial sRNAs in stress responses. *Biochem. Soc. T*, 45, 1203-1212. doi: 10.1042/BST20160363

Papenfort, K. and Vogel, J. (2014) Small RNA functions in carbon metabolism and virulence of enteric pathogens. *Front. Cell. Infec. Microbiol*, 4, 1–12. doi: 10.3389/fcimb.2014.00091

Sheibani-Tezerji, R., Naveed, M., Jehl, M-A., Sessitsch, A., Rattei, T. and Mitter, B. (2015) The genomes of closely related *Pantoea ananatis* maize seed endophytes having different effects on the host plant differ in secretion system genes and mobile genetic elements. *Front. Microbiol*, 6, 1–16. doi: 10.3389/fmicb.2015.00440

Shyntum, D.Y., Theron, J., Venter, S.N., Moleleki, L.N., Toth, I. K. and Coutinho, T. A. (2015). *Pantoea ananatis* utilizes a type VI secretion system for pathogenesis and bacterial competition. *Mol. Plant-Microbe Interact*, 28, 420-431. doi: 10.1094/MPMI-07-14-0219-R

Sibanda, S., Theron, J., Shyntum, D.Y., Moleleki, L.N. and Coutinho, T.A. (2016) Characterization of two LuxI/R homologs in *Pantoea ananatis* LMG 2665^{T}. *Can. J. Microbiol*, 62, 893-903. doi: 10.1139/cjm-2016-0143

Smirnov, A., Forstner, K.U., Holmqvist, E., Otto, A., Gunster, R., Becher, D., Reinhardt, R. and Vogel, J. (2016) Grad-seq guides the discovery of ProQ as a major small RNA-binding protein. *Proc. Natl. Acad. Sci. USA*, 113, 11591-11596. doi: 10.1073/pnas.1609981113

Stice, S.P., Stumpf, D.S., Gitaitis, R.D. Kvitko, B.H. and Dutta, B. (2018) *Pantoea ananatis* genetic diversity analysis reveals limited genomic diversity as well as accessory genes correlated with onion pathogenicity. *Front. Microbiol*, 9, 1–18. doi: 10.3389/fmicb.2018.00184

Tomita, S., Kubota, Y., Kido, K., Kido, K. and Takikawa, Y. (2016) '*Pantoea ananatis* Group III を用いた PASVIL 領域の調査' *Phytopathol. Soc. J*, Okayama, 21 – 23 March.

Vogel, J. and Luisi, B.F. (2011) Hfq and its constellation of RNA. *Nat. Rev. Microbiol, 9*, 578. doi: 10.1038/nrmicro2615

Weller-Stuart, T., Toth, I., De Maayer, P. and Coutinho, T.A. (2016) Swimming and twitching motility are essential for attachment and virulence of *Pantoea ananatis* in onion seedlings. *Mol. Plant Pathol*, 18, 734-745. doi: 10.1111/mpp.12432

Zeng, Q. and Sundin, G.W. (2014) Genome-wide identification of Hfq-regulated small RNAs in the fire blight pathogen *Erwinia amylovora* discovered small RNAs with virulence regulatory function. *BMC Genomics*, 15, 414. doi: 10.1186/1471-2164-15-414

SUMMARY

Functional characterisation of Hfq and identification of Hfq-dependent sRNAs in *Pantoea ananatis*

The trans-encoded small RNAs (sRNAs) are novel gene expression regulators in bacteria. In response to external stimuli, sRNAs rapidly modulate the expression of genes at the post-transcriptional level to allow bacteria to reprogram its cellular environment for survival and fitness. These regulatory actions of sRNAs are chaperoned by the indispensable RNA-binding protein, Hfq, that stabilizes sRNAs and facilitates the base-pairing between the sRNA and target mRNA. The functional role of this protein in a broad-host-range phytopathogen *P. ananatis* was determined by constructing an *hfq*-null mutant strain of *P. ananatis* LMG 2665^{T}. Overall, deletion of the *hfq* gene in *P. ananatis* had a negative effect on motility, biofilm formation, production of quorum sensing autoinducer molecule and pathogenicity of the bacterium, suggesting a collective involvement of Hfq in above-mentioned physiological processes.

To identify trans-encoded sRNAs that are dependent on Hfq, strand-specific sRNA sequencing was conducted on total RNA extracted from both the wild-type and *hfq* mutant strains of *P. ananatis* at low (OD_{600} = 0.2) and high (OD_{600} = 0.6) cell-density conditions. The resulting sRNA transcriptome data were computationally screened for putative sRNAs by applying known sRNA characteristics. The filtering yielded 615 putative sRNAs (302 antisense sRNAs, 249 intergenic sRNAs and 64 gene-overlapping sRNAs). Of these sRNAs, 276 candidate sRNAs were differentially regulated by the loss of *hfq* (low cell condition = 58, high cell condition = 154 and both cell conditions = 64). Among 276 differentially regulated sRNA candidates, 41 were positive for Rho-independent terminator sequences, which included enterobacteria-conserved Hfq-dependent sRNAs such as ArcZ, FnrS, GlmZ, RprA, RyeB, RyhB, RyhB2, Spot42, SsrA as well as 16 novel *P. ananatis* sRNAs. Of the 41, the expression profile of nine sRNAs determined by sequencing depth plots and quantitative PCR (qRT-PCR) showed that the abundances of these sRNAs were negatively affected by the absence of the *P. ananatis hfq* gene, supporting their dependency on Hfq. In addition, computationally predicted target genes of selected sRNAs, whose full-length sequence was determined by 5' rapid amplification of cDNA ends (5' RACE) analysis, included those involved in the synthesis of exopolysaccharide, cell wall degrading enzyme and type 6 secretion system. The result

suggests possible sRNA-regulation of virulence-related genes. Future works will focus on determining the functional roles of sRNAs and experimentally validating the predicted targets of these sRNAs. Overall, the findings of the current work highlight the importance of Hfq as a global virulence regulator in *P. ananatis* and identified previously uncharacterized sRNAs that possibly play essential roles in regulating bacterium's adaptive responses.